PHOTOVOLTAIC POTENTIAL AND PERFORMANCE EVALUATION STUDIES IN INDIA AND THE UK

T. GEORGITSIOTI

PhD

2015

PHOTOVOLTAIC POTENTIAL AND PERFORMANCE EVALUATION STUDIES IN INDIA AND THE UK

TATIANI GEORGITSIOTI

A thesis submitted in partial fulfilment of the requirements of the University of Northumbria at Newcastle for the degree of Doctor of Philosophy

Research undertaken in the Faculty of Engineering and Environment

November 2015

Abstract

The research expresses the PV potential in the UK and India by examining the performance and the cost of domestic grid-connected PV systems. Further, crystalline systems and two thin film system technologies (amorphous silicon and copper indium gallium diselenide), which are installed at a site in India, are examined in order to validate the simulated outputs compared to the systems' field performance and to compare the behaviour of the different module technologies under the harsh climatic conditions of India.

The aim of this study was to evaluate the PV system performance and to develop methods for expressing the PV systems lifetime energy generation and the levelized cost of energy (LCOE) in both countries as a function of location or other influencing parameters.

In the beginning the study presents the UK and India climates and the solar databases with their limitations. Further, it discusses the simulation outputs and the annual energy predictions for the UK and India. It also presents the UK and India PV markets and their policies and the LCOE equation, which was formed, and the methodology used for the LCOE calculations. It discusses the LCOE results and presents indicative lifetime CO_2 (carbon dioxide) emissions savings for the researched locations. Continuing, this study presents the model formed for the lifetime energy prediction and annual energy assessment based on PV system degradation and uncertainty factors. Finally, it summarises the technical and economic outputs of this research, by expressing the PV potentials in the UK and India.

Even for these two countries, which are significantly different in respect to their solar resource, the PV systems may produce similar amounts of energy during their lifetime for reasonable assumptions of degradation rates and uncertainty levels. An uncertainty in the energy output makes the economic viability uncertain. Hence, the investor should be aware of the energy prediction risks, especially in investments where a minimum rate of return is specified. The intermediate lifetime energy range is 60,000-70,000 kWh for the UK while is between 70,000-100,000 kWh for India. The cost per kWh of a domestic PV system in India (range: 0.07-0.13 £/kWh) is lower than in the UK (range: 0.11-0.17 £/kWh) by considering only the net PV cost. However, it is more profitable with the current policies to install a domestic PV system in the UK rather than India. This shows that India has to reconsider its incentive policies for the domestic PV system deployment.

List of Contents

List of Tables

List of Figures

List of Abbreviations

a-Si: Amorphous Silicon

BOS: Balance of System

CdTe: Cadmium Telluride

CERC: Central Electricity Regulatory Commission

CIGS: Copper Indium Gallium Diselenide

CIS: Copper Indium Selenide

CM-SAF: Climate Monitoring Satellite Application Facility

c-Si: Crystalline Silicon

DAS: Data Acquisition System

DCR: Domestic Content Requirement

DECC: Department of Energy and Climate Change

EPSRC: Engineering and Physical Sciences Research Council

ESRA: European Solar Radiation Atlas

EVA: Ethylene Vinyl Acetate

FiT: Feed-in Tariffs

GBI: Generation Based Incentive

GHG: Greenhouse Gas

Glass AR: Anti-reflective Coating of the Glass

HIT: Heterojunction with Intrinsic Thin Layer

IAM: Incident Angle Modifier

IEA: International Energy Agency

IIT Kanpur: Indian Institute of Technology in Kanpur

IMD: India Meteorological Department

IPCC: International Panel on Climate Change

j-box: Junction Box

JNNSM: Jawaharlal Nehru National Solar Mission

JRC: Joint Research Centre

LCOE: Levelized Cost of Energy

LID: Light-Induced Degradation

MCS: Micro Certification Scheme

MNRE: Ministry of New and Renewable Energy

mono-Si: Mono-crystalline Silicon

MPP: Maximum Power Point

multi-Si: Multi-crystalline Silicon

NAPCC: National Action Plan on Climate Change

NASA-SSE: Surface Meteorological and Solar Energy Programme

nc-Si/a-Si: Microcrystalline (Type of silicon cell consisting of a nanocrystalline layer and an amorphous layer.)

NISE: National Institute of Solar Energy

NOC: Nominal Operating Conditions

NPV: Net Present Value

NREL: National Renewable Energy Laboratory

NSM: National Solar Mission

NVVN: NTPC VidyutVyapar Nigam

Ofgem: Office of Gas and Electricity Markets

PC: Personal Computer

PEUC: Prosumer Electricity Unit Cost

PID: Potential Induced Degradation

PPAs: Power Purchase Agreements

PV: Photovoltaic

PVGIS: Photovoltaic Geographical Information System

PVPS: Photovoltaic Power Systems Programme

REC: Renewable Energy Certificate

RES: Renewable Energy Sources

RO: Renewables Obligation

ROCs: Renewables Obligation Certificates

RPO: Renewable Purchase Obligation

RPSSGP: Rooftop PV and Small Solar Power Generation Program

SAM: System Advisor Model

SERC: State Electricity Regulatory Commission

SERE: Solar Energy Research Enclave

STAPP: Stability and Performance of Photovoltaic

STC: Standard Test Conditions

T&D: Transmission and Distribution

TF: Transposition Factor

UNFCCC: United Nations Framework Convention on Climate Change

VGF: Viability Gap Funding

WRDC: World Radiation Data Centre

List of Symbols

ΔP_m: Measurement Uncertainty

ΔP_{max}: Module Tolerance of Manufacture

AC: Annualised Cost

Am: Tropical Monsoon Climate

Aw: Tropical Wet and Dry Climate

B: Annual Variability of the Standard Deviation Expressed in kWh

b: Annual Variability Rate of the Standard Deviation

b_0: Parameter Used in the "ASHRAE" Model

BSh: Warm Semi-arid Climate

C: Cost

C_0: Investment Cost

Cfa: Humid Subtropical Climate

Cfb: Temperate Oceanic Climate

Cfc: Cool Oceanic Climate

C_n: Costs of the System in Year *n*

CO_2: Carbon Dioxide

CRF: Capital Recovery Factor

CU: Combined Uncertainty

D: Annual Degradation Rate

d: Annual Discount Rate

DiffHor: Diffuse Horizontal Irradiation (Energy density of sunlight)

E: Energy Output

E_0: Energy Output in the First Year

E1: Local PV Energy Consumed Annually

E2: PV Energy Exported into the Grid Annually

E3: Energy Imported from the Grid Annually

E_{DC}: DC Energy Output

Electr.C: Retail Electricity Cost

$E_{n,min}$: Minimum Annual Energy in Year n

E_n: Energy Produced by the System in Year *n*

Export.T: Export Tariff

FF: Fill Factor

F_{IAM}: Incident Angle Modifier Factor

FIT1: Feed in Tariff for Local Consumption

FIT2: Feed in Tariff for Energy Exported into the Grid

G: Irradiance (Power density of sunlight)

Gamma: Diode Quality Factor

Gener.T: Generation Tariff

G_i: Instant Irradiance (Power density of sunlight)

GlobHor: Global Horizontal Irradiation (Energy density of sunlight)

GlobInc: Global Inclined Irradiation (Energy density of sunlight)

i: Annual Inflation Rate

I: Current

I_{MPP}: Maximum Power Current

Inv.RC: Inverter Replacement Cost

I_o: Inverse Saturation Current

I_{ph}: Photocurrent

IR: Annual Interest Rate

I_{SC}: Short Circuit Current

i_θ : Incidence Angle on the Plane

k: Boltzmann's Constant

N: Project Lifetime

N_C: Number of Cells in Series

p(E): Probability Density Function of Energy

P_{AC}: AC Power

P_{DC}: DC Power

P_{INV}: Inverter Nominal Power

P_m: Measured Module Power

P_{max}: Maximum Power Rating

P_{PV}: PV Array Power

PR: Performance Ratio

P_T: Theoretical Power

q: Charge of the Electron

R: Ohmic Resistance

R_S: Series Resistance

R_{SH}: Parallel Resistance

T: Temperature

T_{amb}: Ambient Temperature

TASC: Total Annualised System Cost

T_C: Effective Temperature of the Cells

TEC: Total Energy Consumed

T_i: Instant Temperature

U: Combined Uncertainty Factor

U_C: Constant Component of the Thermal Loss Factor

U_T: Thermal Loss Factor

U_V: Proportional to the Wind Velocity Component of the Thermal Loss Factor

V: Voltage

V_{MPP}: Maximum Power Voltage

V_{OC}: Open Circuit Voltage

WindVel: Wind Velocity

x: Nominal Discount Rate

Y_A: Array Yield

Y_f: Specific Yield

Y_r: Reference Yield

α: Absorption Coefficient of Solar Irradiation

η: Inverter Efficiency

η_{EURO}: Euro Efficiency

η_{PV}: PV Module Efficiency According to the Operating Conditions

μ(t): Mean Annual Energy Function of Time

μ: Mean Annual Energy

σ(t): Standard Deviation Function of Time

σ: Standard Deviation

σ_0: Standard Deviation in the First Year

List of Publications

Journal Papers

- “Near-Term Economic Benefits from Grid-Connected Residential PV Systems”, Energy, April 2014 (Gobind Pillai, Ghanim Putrus, Tatiani Georgitsioti & Nicola Pearsall)
- “The Simplified Levelised Cost of the Domestic PV Energy in the UK: The Importance of the Feed-in Tariff Scheme”, IET Renewable Power Generation, invited revised version of PVSAT-9 paper, July 2014 (Tatiani Georgitsioti, Nicola Pearsall & Ian Forbes)
- “Short-term Performance Variations of Different PV System Technologies under the Humid Subtropical Climate of Kanpur in India”, IET Renewable Power Generation, invited revised version of PVSAT-10 paper, July 2015 (Tatiani Georgitsioti, Gobind Pillai, Nicola Pearsall, Ghanim Putrus, Ian Forbes & Raghubir Anand)

Journal Papers to Be Submitted

- “PV system potentials in India and the UK: A combined model for lifetime energy prediction and annual energy assessment”, (Tatiani Georgitsioti, Nicola Pearsall & Ian Forbes) in preparation
- “Economic Potential of the Domestic PV Market in India and the Current Status” (Tatiani Georgitsioti, Nicola Pearsall & Ian Forbes) in preparation

Conference Papers

- “The Simplified Levelised Cost of the Domestic PV Energy in the UK: The Importance of the Feed-in Tariff Scheme”, PVSAT-9, UK Solar Energy Society, Swansea, April 2013 (Tatiani Georgitsioti, Nicola Pearsall & Ian Forbes)

- "Role of Routine Visual Inspection in Performance Monitoring of Photovoltaic (PV) Systems", International Conference on Energy Efficient LED Lighting and Solar PhotoVoltaic Systems at Indian Institute of Technology, Kanpur, March 2014. (Gobind Pillai, Raghubir Anand, Nicola Pearsall, Ghanim Putrus, Tatiani Georgitsioti, Ian Forbes, Pon Perumal & Shivam Srivastava)

- “Short-term Performance Variations of Different PV System Technologies under the Humid Subtropical Climate of Kanpur in India”, PVSAT-10, UK Solar Energy Society, Loughborough, April 2014 (Tatiani Georgitsioti, Nicola Pearsall, Raghubir Anand, Gobind Pillai, Pon Perumal, Ian Forbes, Shivam Srivastava & Deepak Sahu)

- “PV system potentials in India and the UK: A combined model for lifetime energy prediction and annual energy assessment”, 29th EU PVSEC, Amsterdam, Holland, September 2014, (Tatiani Georgitsioti, Nicola Pearsall & Ian Forbes)

- “Economic Potential of the Domestic PV Market in India and the Current Status” PVSAT-11, UK Solar Energy Society, Leeds, April 2015 (Tatiani Georgitsioti, Nicola Pearsall & Ian Forbes)

Acknowledgements

First of all, I would like to thank my principal supervisor, Prof. Nicola Pearsall, for her invaluable assistance and inspiring guidance during these years. She has the ability to resolve any difficult issue that I have faced during my research. Additionally, she inspired me regarding my work and provided me with extra motivation in times that were difficult for me. Secondly, I would like to thank my second supervisor, Dr. Ian Forbes, for his guidance, support and understanding. Thirdly, I would like to thank Prof. Ghanim Putrus, not only for his support but also because he was the person who informed me about this PhD opportunity. Moreover, I would like to thank Dr. Thomas Huld, who was the external advisor of this research and he provided me with the PVGIS solar data for India ahead of their release. I would also like to thank all the STAPP project partners, especially those from the UK and particularly Ms. Dan Wu, Dr. Raghubir Anand from the IIT Kanpur in India for our collaboration, Dr. Rani Chinnappa Naidu, and the EPSRC and Northumbria University for the studentship and financial support.

In addition, I would like to express my gratitude to my parents and all my friends (old and new) without whose moral support I would not have been able to conduct this research. Special thanks to Dr. Gobind Gopalakrishna Pillai, who was my PhD colleague and we became close friends during these years. The quality of his character, his generosity and his immediate assistance made me to lose count on how many times he has supported me. The same stands for my close friend Foteini Kyriakopoulou for her endless support in all the difficulties that I faced during my last year of my studies. Last but not least, I would like to thank my partner Nikolaos Georgakopoulos, who was there for me and stood by my side from the very beginning.

Finally, I would like to dedicate this thesis to the memory of my beloved grandmother and grandaunt…

Tatiani Georgitsioti

Declaration

I declare that the work contained in this thesis has not been submitted for any other award and that it is all my own work. I also confirm that this fully acknowledges opinions, ideas and contributions from the work of others. This work was done in collaboration with the academic partners of the UK-India Stability and Performance of Photovoltaic project funded by Research Councils UK (RCUK) Energy Programme in the UK (contract no: EP/H040331/1) and the Department of Science and Technology (DST) in India.

The project was assessed by the Faculty Ethics Committee at the beginning of the project and it was approved in April 2012.

I declare that the Word Count of this Thesis is 42,132 words

Name: Tatiani Georgitsioti

Signature:

Date: November 2015

Chapter 1: Introduction

This research was undertaken as part of the EPSRC (Engineering and Physical Sciences Research Council) funded India-UK collaborative project called Stability and Performance of Photovoltaic (STAPP) [1]. STAPP general objective was the understanding of the stability and lifetime performance of photovoltaic (PV) systems [2].The project involved 9 institutes, 5 from the UK and 4 from India, a number of different industrial partners and research organizations including the Joint Research Centre (JRC) of the European Commission. Dr. Thomas Huld, who works at the JCR, was the external advisor of this specific research and he has provided the solar data for India for this study [3].

1.1 Research background

Taking into account the effect of climate change, the shortage of fossil fuels and the world's growing energy demand, renewable energy sources (RES) are considered to be one of the solutions that can contribute to the reduction of the greenhouse gas emissions and the meeting of energy demand. India's National Action Plan on Climate Change is promoting the renewable energy sources having a total installed capacity of around 26.4 GW at the end of 2012 [4]. This capacity refers to grid-connected renewable applications excluding large hydro plants. In addition according to the data released by the Ministry of New and Renewable Energy (MNRE) of India, 69.5% of the total renewable energy capacity is attributed to wind energy, while solar PV contributes around 4% [4]. Regarding solar power, India's National Solar Mission plan states that the installed capacity of solar power could reach 22 GW by 2022 (20 GW of grid-connected and 2 GW of off-grid solar power capacity) [5].

According to the "UK Renewable Energy Roadmap" report published at the end of 2012 by the Department of Energy and Climate Change (DECC), the total installed capacity of RES in the UK has reached 14.4 GW while solar PV provides around 9.7% of the cumulative renewable power capacity [6]. Moreover, the UK National Renewable Energy Action Plan estimates that the solar power capacity will reach 2.68 GW by 2020 [7]. However, this was estimated in 2010, before the full implementation of the Feed-in-

Tariff (FiT) scheme. The cumulative installed PV capacity in the UK had reached 4.46 GW by April 2014 [8] and it reached almost 5 GW by the end of that year [9].

This study concentrates on the performance and the cost-effectiveness of grid-connected PV systems under the various climates of UK and India. Both countries seem to have the potential for PV implementation. At the UK PV national conference (PVSAT-8) in 2012, a study about PV potential in the UK concluded that "20% of current UK electricity generation can be provided by Solar PV using only 0.2% of land area" [10]. In addition, the UK Roadmap reports that the cumulative PV capacity could reach from 7 to 20 GW in 2020, considering 7 GW as the lowest limit. On the other hand, India has an abundant solar resource and a huge electricity demand, which indicates that the PV penetration could be supportive to the country's electricity generation [11]. India has an energy deficit attributed to the shortage of coal. Coal supports 57% of the country's energy production and the main exporters (Indonesia, South Africa and Australia) of coal to India have increased their exportation taxes. Hence, nowadays it is more expensive for India to import coal [12]. There are major cities in India, like Trivandrum, where the electricity is scheduled to be cut for at least two hours per day because of the shortage of supply, however the retail cost of electricity is retained relatively low due to the central government subsidiary policies. Below is presented a graph (Figure 1.1) with India's energy supply from 2005 to 2012 (7 years-actual values) and the estimations from 2013 to 2017 (4 years-estimated values), where the deficit can be clearly seen.

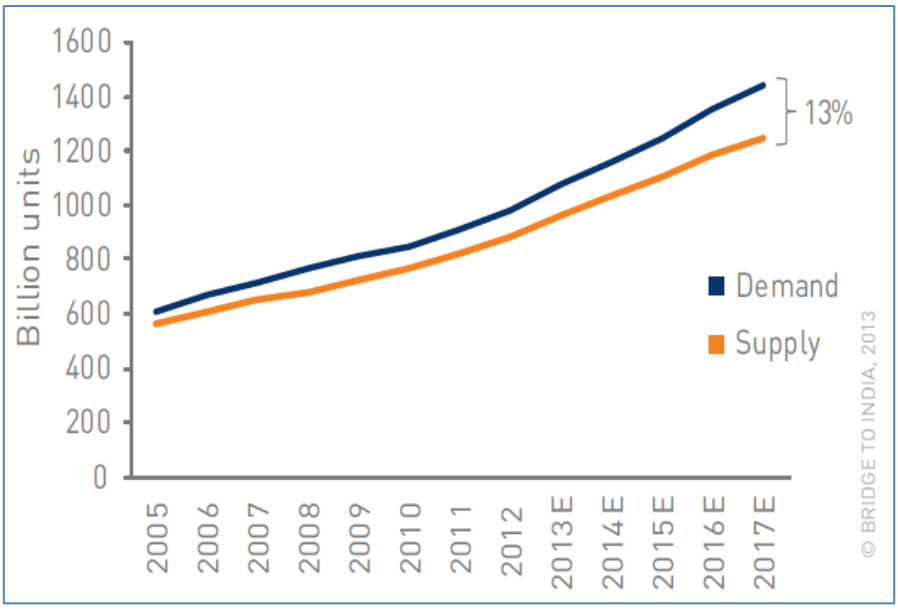

Figure 1.1: India's energy demand and supply, E denotes the estimated values [12]
(y-axis: units of electricity as sold equivalent to 1 kWh per unit)

Generally, there are a variety of aspects that can influence PV system performance: the PV module technology, PV system design (electrical and mechanical), and the climatic conditions valid in the location where the system is installed. Some of the main influencing parameters could be the solar irradiation levels and the ambient temperature of the system's location, the system energy conversion efficiency, the fraction of the reflected sunlight from the module surface, and degradation factors during the system's lifetime [13]. In addition to these parameters, there is also the uncertainty of how these parameters have been measured. Canada Centre for Mineral and Energy Technology uncertainty analysis presented that the combined uncertainty over a PV system's lifetime could be 7.9% for an average modelled energy yield. This value cannot be neglected from PV system performance predictions as it can play a key role in the PV system viability, especially for large scale PV systems [14].

In general, a viable PV system needs to be cost-effective during its lifetime. Nowadays, the most common used parameter for the PV system's economic evaluation is the levelized cost of energy (LCOE). The levelized cost of energy for a PV system depicts the average price paid to generate 1 kWh of electricity during a certain period under the financial parameters valid for the PV system installation in that period. It has the advantage of comparing different energy generation systems while it expresses their cost-effectiveness, this stands under the condition that the same boundary and financial factors are used in each case. LCOE takes into account the total life cycle cost of the system and the total lifetime energy production [15].

Having mentioned the two main aspects (performance and cost) that are influencing PV system viability, this study examined and analysed them, and tried to express the PV system potential as a function of the location. For this purpose, the Photovoltaic Geographical Information System (PVGIS) solar database was used as reference for irradiation and temperature data for India and the UK [16]. Moreover, PVsyst software was used to simulate PV systems and obtain their predicted energy outputs [17].

1.2 Project description

As was stated above, this study concentrates on the PV potential in the UK and India by examining the performance and the cost of grid-connected PV systems. Specifically, the main focus of this study is on multi-crystalline silicon small scale grid-connected PV systems. Further, crystalline silicon systems and two thin film system technologies (amorphous silicon and copper indium gallium diselenide), which are installed at a site in India, were examined in order to validate the simulated outputs compared to the systems' field performance and to compare the behaviour of the different module technologies under the harsh climatic conditions of India.

The aims of this study are:

1) To evaluate the performance of crystalline silicon PV systems under the various climate and operating conditions in India and UK.

2) To develop methods for expressing the PV systems lifetime potential generation and the levelized cost of energy (LCOE) in both countries as a function of location or other influencing parameters.

The objectives of this study are:

- Assess the PVGIS climate database and identify the limitations
- Simulate PV systems with PVGIS and PVsyst simulation packages and identify their treatment of the PV system losses
- Make an economic evaluation for the researched PV systems, including the savings in CO_2 emissions by the produced energy of the systems
- Express the lifetime potential of crystalline silicon PV systems and the LCOE as a function of climate and location
- Evaluate the results in relation to different target groups (i.e. investors, governments, customers, scientists)

1.3 Scope of the research and timeliness

The shortage of the conventional sources of energy and the word's growing energy demand make urgent the need for protection measures. Especially for India, which has an energy deficit, there is a need for a solution that does not exacerbate the climate change. The use of the RES is widely recognized as a compatible measure. Generally, solar energy is considered one of the most important renewable energy sources. Hence, the UK and India governments have announced plans for the implementation of solar energy technologies. On the way to achieve their goals, the STAPP project was established under the India-UK Collaborative Research Initiative in Solar Energy [1]. This research is a part of the STAPP project and its scope was to investigate the potentials of grid-connected PV systems in the UK and India for the deployment of the solar energy in these countries. The specific research is timely addressing the plan of the UK and India governments for solar energy deployment by investigating the PV potential of small scale PV systems. The technical and economic potential of the two countries are expressed through a comprehensive analysis of the uncertainties included in these predictions. An accessible way to determine the best implementation routes for the PV systems is provided.

1.4 Work done

Namely, the work that has been made is the following:

1) Assess PVGIS solar database
2) Study PV system simulation software capabilities (PVsyst & PVGIS)
3) Investigate PV system simulation software outputs for a specific module technology (crystalline silicon)
4) Research the UK and India PV markets and their supporting mechanisms
5) Study the main economic parameters and the LCOE
6) Form an LCOE equation based on the UK PV market policy and calculate the LCOE for residential PV systems in the UK

7) Adjust the UK LCOE equation to the Indian PV market and calculate the LCOE for residential PV systems in India

8) Make indicative calculations for the carbon dioxide (CO_2) emission savings based on the PV system energy production

9) Analyse near-term economic of domestic PV systems in the UK and India (in co-operation with Gobind Pillai-PhD student of the STAPP project)

10) Study the basic concepts for the use of statistical analysis, uncertainty error calculations

11) Analyse field data from a research PV plant in India to identify the short-term performance variations of different PV module technologies

12) Study the degradation factors that influence the PV systems lifetime energy yield

13) Form a model based on the PV system degradation and uncertainty of the energy prediction in order to predict the lifetime energy of a PV system

14) Express the PV systems potentials in the UK and India for multi-crystalline module technology

Moreover, the literature review that has been conducted relates to all the above subjects, so it is presented throughout the thesis and not as a separate section.

1.5 Thesis structure

This research is divided in two main areas: the PV systems performance evaluation and the PV systems economic evaluation. Chapter 2 and 3 present the performance evaluation and express the PV system potential in regards to their annual energy and short-term performance. Chapter 4 presents the economic evaluation for the researched PV systems and expresses their potentials taking into account their finance. Chapter 5 combines the technical and economic outputs of this research and expresses the lifetime PV potentials in the UK and India. More analytically, Chapter 2 presents the UK and India climates, the PVGIS solar database and its limitations, and other available solar databases. Further, it presents the PV simulation software packages used in this research and their treatment to the system losses. Finally, it discusses the simulation outputs and the annual energy predictions for the UK and

India. Chapter 3 presents the short-term performance variations for the different PV module technologies installed at a site in India. Also, it discusses the differences between the simulated results to the field PV performance for this specific site. Chapter 4 presents the UK and India PV markets and their policies. Moreover, it presents the LCOE equation, which was formed, and the methodology used for the LCOE calculations. Finally, it discusses the LCOE results and presents indicative lifetime CO_2 emissions calculations for the researched locations. Chapter 5 presents the model formed for the lifetime energy prediction based on the PV system degradation factors and the uncertainty of the energy prediction. Finally, Chapter 6 presents the main conclusions that have been drawn and future recommendations for research. It also expresses analytically the original contribution and evaluates the results of this work.

Briefly, the originality of this research is based on four main parts:

- The assessment of the performance variations of different PV system technologies in a harsh Indian environment.
- The calculation of the LCOE parameter for the domestic PV system deployment and cost-effective planning, especially in India.
- The development of a generic model on the lifetime energy prediction and annual energy assessment.
- The expression of the combined PV potential (technical, economic and environmental) as a function of the location within and between the two countries

Chapter 2: Climatic Conditions and PV Energy Prediction

Chapter 2 starts by describing the climatic conditions in India and the UK. Continuing, it presents the study regarding the PVGIS assessment and the available solar databases. Finally, it includes a description of the PV system simulation software used for this study and discusses the results obtained by the simulations.

2.1 Climatic conditions

India is a large country and extends from around 8 to 37 degrees North from the equator (latitude) and between 68 to 97 degrees East (longitude) [18]. Its land area is 973,190 km^2 [19] and for this reason India has a variety of climates. On the other hand, the UK is a relatively small country characterised mainly by one type of climate with some geographical variations due to the proximity to the sea (land area=241,930 km^2, latitude range≈50 to 58 North in degrees, longitude range≈8 West to 1.7 East in degrees [19, 20]).

2.1.1 Climate of India

The Indian climatic condition range is vast. The climate is tropical in the south and becomes alpine in the Himalayan north, where regions with high altitude receive persistent snowfall during winters. The climate of India is formed by the southwest monsoon, which is considered as the most important influence, as it controls the annual rainfall. The monsoon season is from June to September and about 75% of the annual rain falls in that period of the year. The monsoon is mainly created by the combination of two weather features. Firstly, by the dry and cold air during winter, which is originated from the northern latitudes having a northeast direction, and secondly by the intense heat of summer, where the northern regions have high temperatures and consequently a moist wind is formed over the oceans producing a reverse wind flow over the region [21].

It can be said that the rainfall pattern over India approximately reflects the different climatic regions, which vary from a humid climate in the northeast (about 180 days rainfall in a year), to an arid climate in Rajasthan (20 days rainfall in a year). For example, the average annual rainfall at Mausiram in the Meghalaya is around 11,410 mm while in western Rajasthan it is less than 130 mm. The average annual rainfall in India is 1,182.8 mm while during the monsoon season the average rainfall is 877.2 mm. This means that the average annual rainfall contribution by the monsoon season is 74.2%. Table 2.1 shows the average rainfall percentage contribution for each month of the monsoon season across whole India. Regarding the pre (March, April and May) and post (October, November and December) monsoon season, the contribution of the rainfall is almost the same, around 11% [21].

Table 2.1: Average rainfall percentage contribution during the monsoon season [21]

Monsoon Season	Percentage contribution of the average annual rainfall (%)
June	13.8
July	24.2
August	21.2
September	14.2

Apart from the rainfall variations, India has strong temperature variations as well. In general, the average temperature during winter is around 10°C while in summer it is around 32°C. The seasonal temperature variation over India is presented in Appendix A. Below are presented two maps of India, originated by the India Meteorological Department (IMD), to help the reader to better understand the locations referred to in this analysis. The first map is the political map of India while the second shows the meteorological regions of India.

Figure 2.1: Political map of India [22]

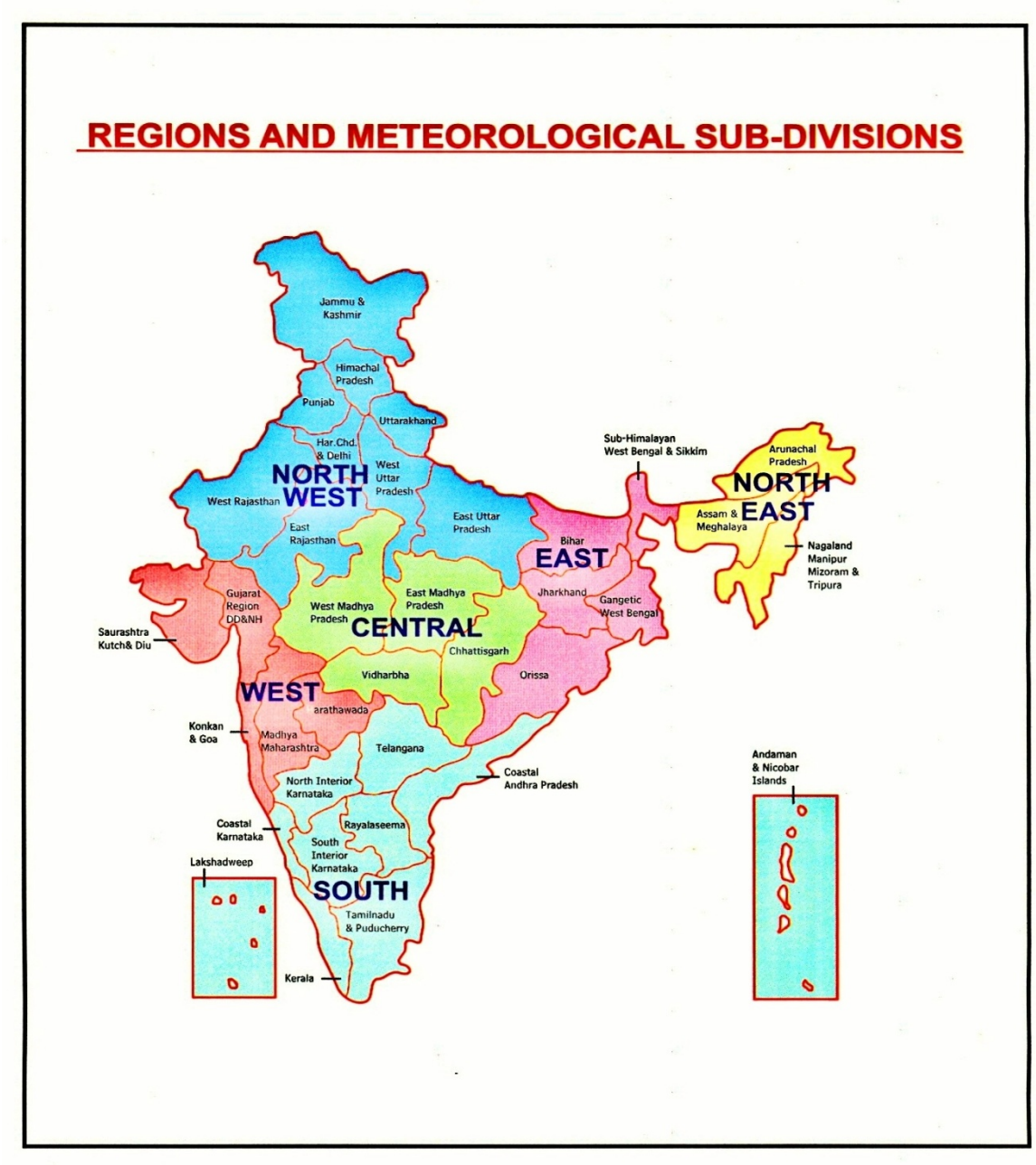

Figure 2.2: Regions of India [22]

The months of January and February have been categorised as the winter season by the IMD. However, for the northwestern parts of India, December can also be considered as a winter month. The winter in India has clear sky, light northerly winds, low humidity and relatively low temperature (average minimum temperatures around 10°C in the northern plains to 22°C in the southern parts). The rains during winter mostly happen in the states of Tamil Nadu and Kerala in the south and in the western Himalayas and the extreme northeastern parts.

The months of March, April and May are considered as the pre-monsoon season or summer. The temperature increases during March and April, with an average daily temperature around 30-35°C and with a maximum temperature reaching around 45°C by the end of May and early June in the north and northwest regions of India. This season is characterised by a big variation in the daily temperature between daylight and night hours (more than 15°C difference in certain locations), by cyclonic storms (northeast and northwest) and thunderstorms in some parts of India (northeast-central-extreme southwest), and by "hot and dry winds accompanied with dust winds blow usually over the plains of northwest India" [21].

As has already been discussed, the months from June to September are considered as the monsoon season. However, for a particular location the actual monsoon period is between the onset and withdrawal dates of the monsoon. Generally the monsoon period can vary from less than 75 days (West Rajasthan) to more than 120 days (southwest of India). It starts from the southwest coast of India on the 1st of June and by the middle of July has covered the whole country [21]. As an example, below is a map showing the withdrawal dates of the monsoon in India in 2013 [23].

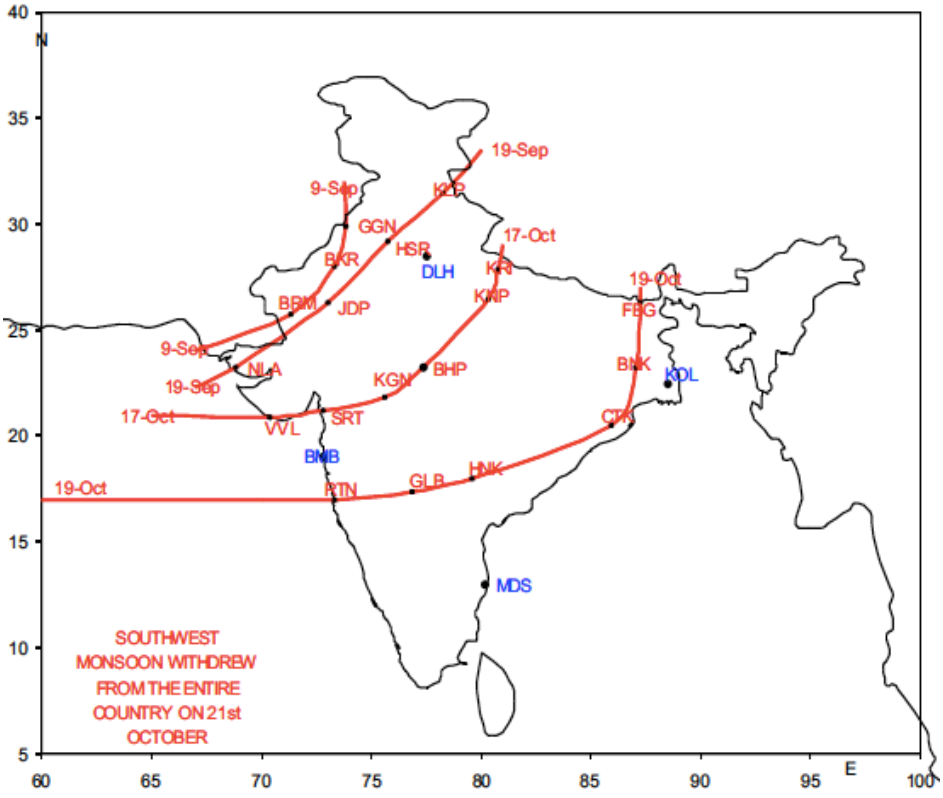

Figure 2.3: Withdrawal of the southwest monsoon in 2013 [23]

Finally, the months of October, November and December are considered as the post-monsoon season. This season is characterised by northeast winds all over India, “decrease in humidity levels and clear skies over most parts of north and central India after mid-October” [21]. However, the precipitation during these months in the south parts of India can reach about 35% of their annual total precipitation. Namely, these parts are Tamil Nadu, coastal Andhra Pradesh, Kerala and south interior Karnataka. Moreover, the south coastal regions of India experience strong winds, heavy rainfall and storm surges. The average daily temperatures decrease during this period from around 38°C in October to 28°C in November for the northwest parts of the country [21].

Since India is a large country, its climate is divided in different climatic zones. Generally, Köppen climate classification is an empirical vegetation-based climate classification system. Köppen has divided the various climates into five main types symbolized by the capital letters A, B, C, D, and E. All the types apart from type B have been categorised by temperature criteria. However, type B is more dependent on how dry the vegetation is, rather than the temperature. Moreover, all the types are subdivided into subtypes, using additional letters to define them. Köppen’s classification is widely used and there are also modified versions of Köppen’s system, made by other climatologists based on their experience [24].

According to the Köppen-Geiger classification, the eastern part of India and the west coast is classified as a tropical wet and dry climate (**Aw** climate). Aw climate has mean temperatures above 18°C for all the months of the year and a dry winter. The precipitation in the driest month is less than 60 mm. The southern part of India is classified as a tropical monsoon climate (**Am** climate), which is a tropical rainforest climate with monsoon rains and average monthly temperatures above 18°C. Central and northwest India have a warm semi-arid climate (**BSh** climate). This climate has an annual average temperature above 18°C and is considered as dry steppe climate. Finally, the north and mountainous parts have a humid subtropical climate (**Cfa** climate). Cfa climate is a humid climate with the warmest month temperature to be above 22°C and the precipitation distribution to be relatively uniform throughout the year [24-26].

2.1.2 Climate of the UK

As was mentioned, the UK is a relatively small country. Hence, the UK climate is not as diverse as the Indian climate. However, the latitude of the UK is much higher than India, so leading to lower sun angles and greater variations in day length. The main influence in the UK climate is the Gulf Stream, which results in a temperate maritime climate over the country. The north of England has an average annual rainfall more than 1,600 mm while the central and southern locations have less than 800 mm. Moreover, the average annual rainfall in the north of England (1,600 mm) is higher than the average of India (1,182.8 mm). The winter period in the UK is from December to February and the average monthly temperature is between 3 to 6°C. On the other hand, in the summer months of July and August the average temperature is between 16 and 21°C. Further, the rainfalls in the UK are throughout the year, but the weather can sometimes have rapid changes, especially during autumn and winter. This is due to the strong Atlantic low-pressure systems that can bring gales, heavy rain, showers or even thunderstorms. Moreover, the climate in Scotland is similar to England's climate but with generally lower temperatures than the rest of the UK. Generally, the British weather has moderate winters and cool summers. Usually, there are no extreme seasonal variations, although in the Scottish Highlands and in mountainous areas the winters can be harsh with gales and heavy rainfall [27].

Below are presented two maps and a table showing annual average weather data from 1981 to 2010. Regarding the maps, Figure 2.4 shows the annual average rainfall and Figure 2.5 the annual average daily temperature from 1981 to 2010. Note that the average data are available for official Met Office stations only and the sunshine averages are not available for all stations [28].

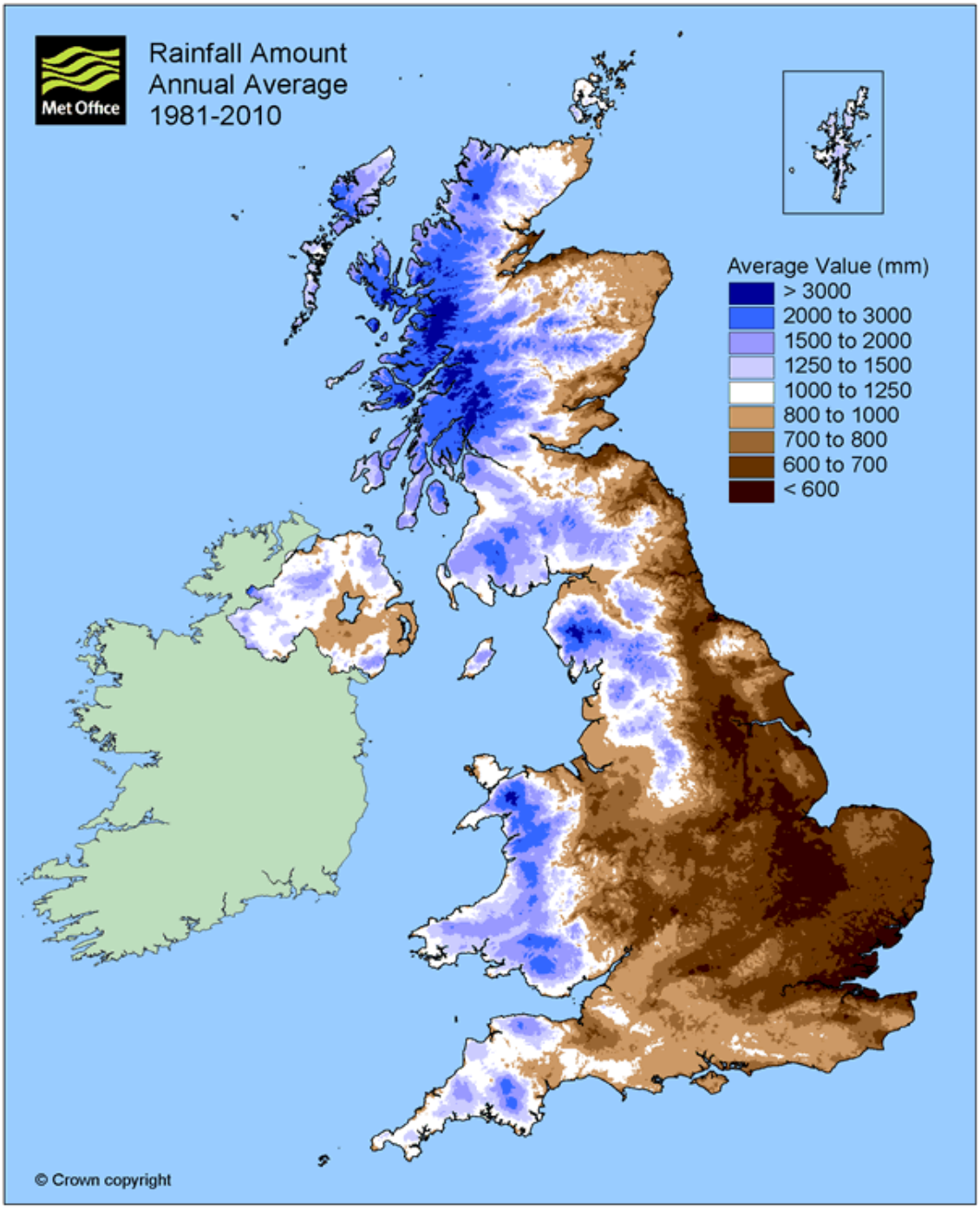

Figure 2.4: UK annual average rainfall [28]

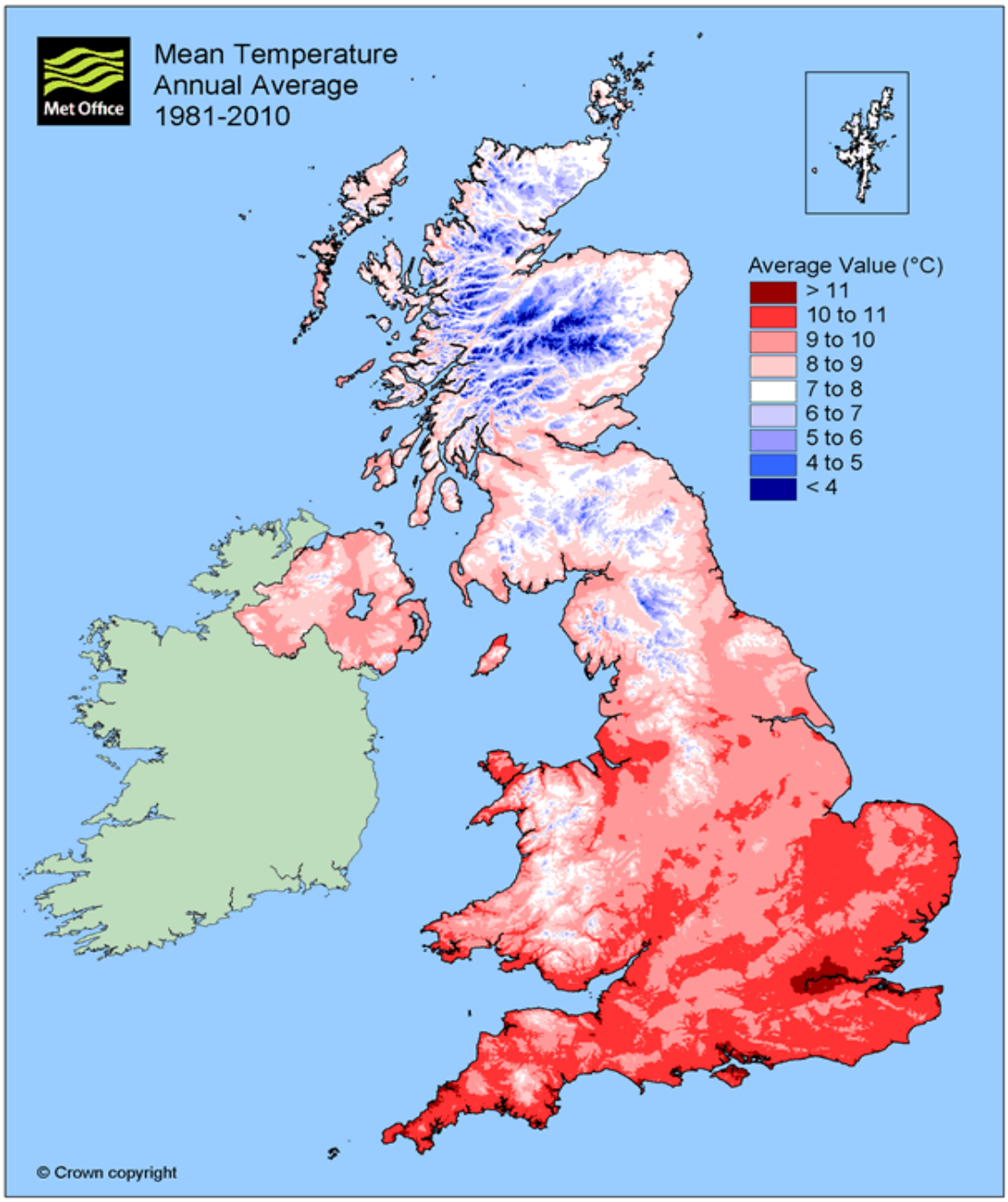

Figure 2.5: UK annual average daily temperature [28]

Table 2.2: Annual average values of the UK climate from 1981 to 2010 [28]

UK (1981-2010)	Max. Temp. (°C)	Min. Temp. (°C)	Sunshine (hours)	Rainfall (mm)	Days of rainfall>=1mm (days)	Days of air frost (days)
Annual Average	12.4	5.3	1372.8	1154.0	156.2	54.6

According to the Köppen-Geiger classification, the climate of England is a temperate oceanic climate (**Cfb** climate) while the mountainous areas in Wales and Scotland have a cool oceanic climate (**Cfc** climate). The Cfc climate is similar to Cfb, but the monthly average temperature is above 10°C for less than four months per year. The Cfb climate is moderate humid climate with monthly average temperature above 10°C for four or more months per year and the warmest month's temperature lower than 22°C [24, 26, 27].

2.1.3 Climatic factors

The climate could be characterised by certain factors such as the solar irradiation, ambient temperature, air humidity, precipitation, wind speed and direction, and sky condition. The solar irradiation is measured in Wh/m^2 and varies according to the location (geographical co-ordinates), the season, the time of the day and the atmospheric conditions. The ambient temperature is dependent on the location, the solar irradiation, the wind, and the presence of water. The air humidity is the amount of moisture in the air and it is often expressed as relative humidity. Relative humidity is expressed as a percentage and its definition is the ratio of the water vapour mass in a certain volume of moist air to the water vapour mass in the same volume of saturated air, at a given temperature. The relative humidity varies during the day and the season and with the location. It is also dependent on the ambient temperature. For example, it reduces at midday when the temperature usually increases while it increases at dawn when the temperature is at its lowest. However, there are areas with high humidity levels and high temperatures as well. Further, "in areas with high humidity levels, the transmission of solar radiation is reduced because of atmospheric absorption and scattering" [29]. The precipitation includes water in the form of rain, snow, hail or dew and it is measured in millimetres (mm). The wind can be determined as the movement of air due to the difference of atmospheric pressure. It is "caused by differential heating of land and water mass on the earth's surface by solar radiation and rotation of earth" [29]. Finally, the sky condition is referred to the level of cloud cover in the sky and it is measured in okta. Generally, the irradiation increases under clear sky conditions while it decreases due to cloud cover, for example, in the monsoon season [29].

2.2 Solar data

Having defined the climatic factors and described the climatic variability of the two countries, this part of the research concentrates on the solar data. The two main climatic factors that affect the PV systems performance are the solar irradiation and the ambient temperature and for this reason the choice of the solar data play a key role in the PV energy prediction. In this research, the PVGIS solar database was chosen as the input for the PV energy prediction. Generally, PVGIS provides a map-based record of solar energy resource and evaluation of the electricity generation from photovoltaic systems in Europe, Africa, and South-West Asia. One of the two architects of PVGIS is Thomas Huld who was the external advisor of this specific research, and he has provided this research with the PVGIS solar data for India ahead of their release in the PVGIS web site [3]. The PVGIS solar database was studied to establish its reliability compared to other available solar data sources and identify its limitations.

2.2.1 PVGIS solar databases

PVGIS provides two solar databases for Europe, the classic and the climate SAF. The classic PVGIS solar database is based on data from the European Solar Radiation Atlas. It includes data from 560 different ground weather stations across Europe, during the period of 1981 to 1990. The disadvantages of the PVGIS classic database are:

1) The data collected are old, so the solar irradiation values may not be representative of the current conditions.
2) The mathematical interpolation used for acquiring data between the stations is subject to uncertainties.
3) The density of stations varies across Europe, so the uncertainty can be very high in areas with few stations.
4) Large areas that have only one station or have a station placed in a location that is not representative of the area can face significant measurement errors.

The new PVGIS solar database has been calculated from solar radiation data made available by the Climate Monitoring Satellite Application Facility (CM-SAF). The solar radiation values have been estimated from satellite images. The data are over the period 1998 to 2011, so they are not subject to major climate changes. The CM-SAF data has been tested extensively against high-quality ground measurements and the overall local error for the whole year is less than 5%. The disadvantages of PVGIS CM-SAF database are:

1) The pixel size in the satellite images is about 3-5 km; so smaller features such as narrow mountain valleys cannot be resolved.
2) The computer algorithm that calculates the solar radiation on the ground may have difficulties to distinguish the difference between snow and clouds.
3) When the sun's altitude is very low, the calculation from the satellite data becomes very difficult.

Moreover, for the Mediterranean Basin, Africa and South-West Asia PVGIS also provides two solar databases: the Helioclim-1 and the CM-SAF. HelioClim-1 database consists of daily sums of global horizontal irradiation calculated from Meteosat Prime images by the Heliosat 2 method. The values represent the period of 1985-2004 and "the original calculation is 15 arc-minutes, or about 28 km right below the satellite (at the equator, 0 degrees West)" [16]. It is obvious that even though the data are not very old the spatial resolution is too low; hence the uncertainty could be very high [16].

2.2.2 Solar data sources

This section presents the most popular solar databases, which provide monthly average data and can also be imported into PVsyst simulation software. PVsyst software is analytically discussed in the following section (Section 2.3). The reason of this study was to compare the different solar data sources with PVGIS solar data. Namely, these databases are: Meteonorm [30], World Radiation Data Centre [31], NASA-SSE [32], SolarGIS iMaps [33], and RETScreen [34].

Meteonorm software gives average monthly irradiance data from 1200 weather stations during the period of 1960-1991. Moreover, in version 6 of Meteonorm, data are also provided for the period of 1981-2000.

World Radiation Data Centre (WRDC) gives average monthly irradiance data from 1195 sites in the world, during the period of 1964-1993. However, many of the data are averaged only for a few years and not throughout the whole period. In addition, WRDC database does not include temperature data.

NASA-SSE (Surface Meteorological and Solar Energy Programme) has satellite monthly data for a grid of 111 km x 111 km covering the whole world, for the period 1983-1993. It is noticed, that the data are quite old and the spatial resolution is low.

SolarGIS iMaps provides average monthly data of solar radiation and air temperature for Europe, Africa, and Middle East. The data are regularly revised and developed from Meteosat MSG data. Their spatial resolution is about 4 x 5 km at mid latitudes and 3 km at the sub-satellite point [33].

RETScreen Canadian software provides a complete database for any location in the world. It uses the best available data at each location from about 20 sources; the main ones are the WRDC and the NASA.

Table 2.3 presents a summary of the meteorological databases available with importing tool in PVsyst software [17].

Table 2.3: Summary of meteorological databases [17]

Database	Region	Values	Source	Period	Variables	Availability	PVsyst import
Meteonorm	Worldwide	Monthly	**1'700 Terr. stations** Interpolations	**1960-1991** averages V 6.0: 1995-2005 (optional)	GlobH Temp. Wind Others	Software	Direct by file (300 *stations* in PVsyst DB)
Meteonorm	Worldwide	Hourly	**Synthetic** generation	idem	GH, DH, TA VindVel	Software	Direct by file
Satellight	Europe	Hourly	**Meteosat** Any pixel of about 5x7 km²	5 years **1996-2000**	GlobH no temper.	Web free	Direct by file
US TMY2/3	USA	Hourly	NREL, **1020 stations** Typical Meteo Years	**1991-2005** (samples)	GH, DH, TA WindVel	Web free	Direct by file
EPW	Canada	Hourly	CWEC, **72 stations** Typical Meteo Years	**1953-1995** (samples)	GH, DH, TA WindVel	Web free	Direct by file
ISM-EMPA	Switzerland	Hourly	22 stations **Design Ref. Years**	**1981-1990** (samples)	GH, DH, TA WindVel	Included in PVsyst	Included in database
Helioclim - 3 (SoDa)	Europe Africa	Hourly	**Meteosat**	**from 02/2004** **=> today**	GlobH no temper.	Web restricted 2005 free	Direct by copy/paste
NASA-SSE	Worldwide	Monthly	Satellites 1°x1° cells (111 km)	**1983-1993** averages	GlobH Temp	Web free	Direct
WRDC	Worldwide	Hourly Daily Monthly	1195 stations	**1964-1993** (each)	GlobH no temper.	Web free	Direct by copy/paste
PVGIS-ESRA	Europe Africa S-W Asia	Monthly	**Europe**: 566 stations Interp. 1x1 km² **Africa**: Meteosat (Helioclim-1 database)	**1981-1990** averages 1985-2004	GlobH Temp. Linke turbidity	Web free	Direct by copy/paste
Helioclim - 1 (SoDa)	Europe Africa	Monthly	**Meteosat** 50x50 km²	**1985-2005** (each year)	GlobH no temper.	Web restricted 1985-89 free	Direct by copy/paste
RETScreen	Worldwide	Monthly	Compil. 20 sources incl. WRDC - NASA	**1961-1990** (averages)	GlobH, TA WindVel	Software, free	Direct by copy/paste

In general, some of the sources like NASA-SSE, ESRA (European Solar Radiation Atlas) and NREL (National Renewable Energy Laboratory) are providing data with global or continental coverage; however their spatial resolution is relatively low (i.e. 40 km x 40 km for NREL data). “Strongly varying elevation gradients combined with terrain shadowing can cause significant local irradiance fluctuations” [16]. Hence, it has been concluded that the main solar database for this research will be the PVGIS CM-SAF database as it is a free access, recently revised source with fairly uniform land coverage and good spatial resolution (pixel size 3-5 km).

2.3 PV simulation software

There are many well-developed software programs, which calculate the PV system energy output taking into account various parameters. Hence, there is no need for this specific research to develop algorithms for the PV energy calculations. PVsyst software is one of the most well-known programs for its detailed PV system design and simulation. It uses the Meteonorm solar database but also provides the choice to import solar data from other databases as well, such as the ones discussed above (NASA worldwide, RETScreen worldwide, PVGIS etc.). Furthermore, it has a variety of modules and inverters that can be used for the PV system design and gives the choice to import the technical data of any module and/or inverter that is currently on the market [17]. For the above reasons PVsyst software has been chosen for the PV system simulations and consequently for the annual energy prediction. However, a comparison between the PVsyst and the PVGIS simulation software was made in order to identify the differences in their outputs and their treatment to the systems losses. An additional reason for the aforementioned comparison was to establish the value of the annual PV energy prediction between two simulation tools, when the same solar database is used.

Generally, the inputs and outputs of the software have to be identified in order to gain a clear view for the analysis of the obtained results. The following sections present the most important inputs and the outputs of these two software packages for grid-connected PV system simulations.

2.3.1 Grid-connected PV systems: Annual energy estimation by PVGIS software

PVGIS inputs are the following [16]:

1) Radiation database: the software gives the option to choose between two solar databases in most of the locations (classic and CM-SAF for Europe and Helioclim-1 and CM-SAF for Africa).

2) PV technology: it gives the option to choose from the following module technologies: crystalline silicon, copper indium selenide (CIS), cadmium

telluride (CdTe), and other. Generally, five families of materials are used in PV modules manufacture: 1. mono-crystalline silicon, 2. multi-crystalline silicon, 3. amorphous silicon, 4. cadmium telluride and 5. copper indium selenide. Hence, PVGIS is considering mono and multi crystalline modules as one category and it gives the opportunity to simulate four out of five general categories.

3) Installed peak PV power (kW) of the system

4) Estimated system losses (%): this choice takes into account all system losses except for the reflection losses by the array and the temperature losses of the PV system. Usually, it has a default number of 14% but that can be changed.

5) Mounting position of the system: free standing and building integrated

6) Tilt angle and azimuth angle: it gives the opportunity to choose any tilt and azimuth angle for the designed system or to choose the optimum tilt and azimuth angle proposed by the software.

7) Tracking options: vertical axis, inclined axis, and two axes

8) Horizon: PVGIS includes a database of the horizon height around each point of the chosen area with a resolution of 90 meters. In this way, the PV performance calculations take into account the effects of the far shading on the PV array by mountains and hills. Near shading effects by trees or buildings are not included, although the software gives the possibility to upload a file with the horizon height if it is known.

PVGIS outputs are the following [16]:

1) Location (latitude, longitude, elevation): although the location can be considered as an input since the site has to be chosen before the simulation, after the simulation PVGIS provides analytically the site parameters.

2) Estimated losses due to temperature (%)

3) Estimated loss due to angular reflectance effects (%)

4) Combined PV system losses (%)

5) Electricity production (kWh)

6) Global irradiation (kWh/m^2)

7) Graphs (energy output, in-plane irradiation, outline of horizon)

2.3.2 Grid-connected PV systems: Annual energy estimation by PVsyst software

PVsyst inputs are the following [17]:

1) Geographical location and meteo data (see section 2.2.2 for discussion of the data sources)
2) Albedo value (default value 0.2 for an urban environment)
3) Array operating temperatures: PVsyst uses default values but it also gives the choice to change them, these parameters are used for the design and are not involved in the simulation.
4) Orientation and field type of the array (fixed or tracking mounted)
5) Horizon and diffuse factor (the amount of the diffuse irradiation contributing in the simulation results): PVsyst does not include any horizon database like PVGIS but it gives the opportunity to the user to import a horizon file. For the diffuse factor its default value is 1.
6) Near shading (no shading, linear shading, according to the module strings)
7) System electrical design (choice of modules and inverters)

PVsyst outputs are the following [17]:

1) Specific energy production (kWh/kW/year)
2) Normalized energy production (kWh/kW/day)
3) Performance ratio
4) Analytical collection losses and system losses
5) Array and system efficiencies
6) Electricity production values (kWh)
7) Global irradiation values (kWh/m^2)
8) Diffuse and albedo factors
9) Various graphs and tables.

2.3.3 PVGIS and PVsyst calculations and losses treatment

Having identified the inputs and the outputs of the two software packages, another aspect that has to be examined is how the software calculates the outputs and what losses are included in their PV system performance calculations. This aspect is presented in this section and it is important for the analysis of the simulation results.

PVsyst annual energy calculations contain the following steps:

(1) The software makes a correction of the horizontal global irradiation to the global incident irradiation on the collector plane.

(2) It makes the correction for the IAM (incident angle modifier) factor (F_{IAM}) on the global irradiance to calculate the effective irradiance on the collectors. In practice this loss refers to the transmission and reflections of the incident irradiance that falls on the PV array. In PVsyst, this loss is calculated by the "ASHRAE" model, which depends only on the parameter b_0. For crystalline modules the default value used is $b_0 = 0.05$.

$F_{IAM} = 1 - b_0 \times (1/\cos(i_\theta) - 1)$, where i_θ = incidence angle on the plane (2.1)

(3) It makes the conversion of the irradiance to the PV system generated kWh depending on the module efficiency at the STC (standard test conditions); array nominal energy at STC efficiency.

(4) It takes into account the following losses and gives the array virtual energy at MPP (maximum power point).

- PV loss due to irradiance level: The efficiency of the array is defined at the STC (1000 W/m²), but is decreasing with irradiance according to the PV standard model.

- PV loss due to temperature: The thermal behaviour of the array is computed at each simulation step, by a thermal model. This model determines an energy balance between the ambient temperature and the cell temperature due to incidence irradiance. The model is presented in the equation 2.2 below:

$$U_T \times (T_{cell} - T_{amb}) = \alpha \times G_i \times (1 - \eta_{PV}) \quad (2.2)$$

where α is the absorption coefficient of solar irradiation, η_{PV} is the PV module efficiency according to the operating conditions and U_T is the thermal loss factor. U_T can be divided into a constant component (U_C) and a factor proportional to the wind velocity (U_V) (Equation 2.3).

$$U_T = U_C + U_V \times v \ (W/m^2*k), \text{ where } v = \text{wind velocity (m/s)} \quad (2.3)$$

This factor is dependent on the mounting position of the modules and its default value in the software is U_T= 20 W/m²*k. Hence, the thermal model used by PVsyst establishes the instantaneous operating temperature, which is then used by the PV modules modelling.

- Soiling loss: According to PVsyst, the soiling effect is almost negligible in middle-climate residential areas. However, it may become significant in industrial environments, desert climates and areas with snow effects. The default value for the soiling loss by the software is 3% and its use is optional in the simulation.

- Module quality loss: This parameter expresses the matching of the real module performance to the manufacturer's specification. The default value is half the lower tolerance of the chosen module.

- Module/array mismatch loss: The real modules in the array do not present the same I/V characteristics compare to the manufacturers specification. In PVsyst this loss acts as a constant loss during the simulation and is divided into two default values; the first one is the energy loss at MPP (maximum power point) and the second one is a loss factor for fixed voltage operation.

- Ohmic wiring loss: The loss between the available power from the modules and the power at the terminals of the array is caused by the ohmic wiring resistance (R) and is equal to R x I^2 (where I is the current). The software has a default system wiring loss of 1.5% by respect to the STC.

(5) Continuing its calculations, PVsyst takes into account the following losses and it gives the available energy at inverter output (energy injected into the grid).

- Inverter loss during operation (efficiency)
- Inverter loss over nominal inverter power
- Inverter loss due to power threshold
- Inverter loss over nominal inverter voltage
- Inverter loss due to voltage threshold

It can be noticed that PVsyst is a complicated simulation tool as it takes into account many aspects in order to predict the system's energy output. Moreover, there are some extra features that can be used in PVsyst simulation such as the partial shading [17]. On the other hand, PVGIS energy calculations are more simplified than PVsyst. The model for the power output of the PV system in PVGIS depends only on the module temperature and the in-plane irradiance [13]. Moreover, as regards the losses, PVGIS takes into account only 3 kinds of losses; the losses due to temperature, the losses due to the angular reflectance and the combined system losses [16]. Table 2.4 presents the main input parameters that were kept constant in PVsyst and PVGIS software for all the simulation sets. It also shows the differences in the default parameters between PVsyst version 5.3.1, which is used in this research, and PVsyst version 6.2.2 (latest version at the time of writing).

Table 2.4: Main simulation input parameters

PVsyst Version 5.3.1						
Thermal loss factor	Wiring ohmic loss at STC	Module efficiency loss	Power loss at MPP	Loss at fixed voltage	Soiling loss	IAM loss ASHRAE model b_0
20 (W/m^2)*k	1.5%	1.5%	2%	4%	3%	0.05
PVsyst Version 6.2.2						
20 (W/m^2)*k	1.5%	1.5%	1%	2%	3%	0.05
PVGIS Version 4						
PV technology	Installed peak power		Estimated system losses		Optimum tilt angle	Optimum orientation
Crystalline silicon	3 kW	10 kW	14%		Proposed by the software	

It has been observed that some of the default loss parameters in PVsyst have been reduced, resulting to a higher annual energy prediction than before [17]. However, the main influence to their different energy prediction is due to the transposition model. The transposition model calculates the incident irradiance on a tilted plane from the horizontal irradiance. Generally, PVsyst has two transposition models, the Hay's model and the Perez model. In the older version, Hay's model was the default model while now it is the Perez model. Hay's model has the advantage of producing good results even when the knowledge of the diffuse irradiation component is not very precise. On the other hand, the Perez model requires well-measured data and is more sensitive to a realistic determination of the diffuse irradiation than Hay's model [17]. Therefore, for this research, Hay's model and version 5.3.1 have been chosen for the system simulations, since the solar data have been acquired by satellite measurements with an associated uncertainty as discussed in Section 2.2.

2.4 System design and simulation choices

This research aims to express the grid-connected PV system potentials in the UK and India, so an optimum system design in respect to orientation, tilt angle and inverter/array capacity ratio was chosen for the PV system simulations. The default horizon was used and near shading has not been included. Variations in either of these assumptions would be likely to reduce the annual energy output. Another reason for optimizing the PV design was to compare the PVGIS and PVsyst software considering their system losses. As was mentioned in the previous section, PVsyst software is much more detailed than PVGIS regarding its inputs and outputs, so an optimally

designed system can make the system parameter comparison more straightforward than any other design.

Various sets of simulations have been made during this research. The simulations included locations in Europe and India in order to capture a wide range of latitudes and consequently the diversity of the irradiation and temperature values in all these locations. A medium-scale PV system (10 kW) with an optimum design was simulated for capital cities around Europe while a domestic (3 kW) optimally designed PV system was simulated in cities around the UK and India. The PVGIS solar data for India had not been obtained at the beginning of this research. Hence, the medium-scale (10 kW) system and the locations around Europe have been chosen as a trial comparison between the two software packages to identify their outputs by using the same solar database. The chosen module technology was crystalline silicon, which is the oldest and most well developed PV technology. Crystalline silicon cells have a market share of 80-90% in the global PV market manufacturing [35]. Moreover, after PV market survey took place, the multi-crystalline 250 W modules of Sharp and SMA inverters (Sunny Boy 2500HF and 3000HF, Sunny Tripower 8000TL) were chosen [36-38]. The Sharp module manufacturer was in the top 10 manufacturers in the global PV market sales while SMA was the first PV inverter manufacturer during the last years [39, 40]. In addition, both companies have distributers in India and the UK. The main technical characteristics of the module and the inverters are presented in Appendix B.

Table 2.5: Simulation sets summary

Simulation Sets Summary						
Simulation Set	**No of Locations**	**Latitude Range (degrees)**	**System size (kW)**	**Simulation Software**	**Solar data**	**Modification of optimum tilt angle**
Capitals of Europe 1	16	35-57	10	PVsyst& PVGIS	PVGIS CM-SAF	No
Capitals of Europe 2	16	35-57	10	PVsyst	Meteonorm	No
Capitals of Europe 3	4	35-49	10	PVsyst& PVGIS	PVGIS CM-SAF	Yes
UK cities 1	20	50-57	3	PVsyst& PVGIS	PVGIS CM-SAF	No
UK cities 2	4	50.8-56.5	3	PVsyst& PVGIS	PVGIS CM-SAF	Yes
Indian Cities 1	22	8.5-34	3	PVsyst	RETscreen	No
Indian Cities 2	4	13-28.5	3	PVsyst	Meteonorm	No
Indian Cities 3	36	8.5-34	3	PVsyst	PVGIS CM-SAF	No

Three simulation sets were performed for the capitals of Europe each time changing a different parameter. Two simulation sets were made for the UK cities and three for the Indian cities. More specifically, 16 locations in Europe have been chosen in order to compare both the outputs between PVGIS and PVSyst software using the same solar database, and PVsyst outputs using different solar sources. The latitude range of these locations is from around 35 to 57 degrees North. The simulation sets for the UK cities was made using PVGIS CM-SAF solar data. These sets present the energy output predictions for domestic (3 kW) PV systems for 20 cities around UK by PVGIS and PVSyst. It also presents a comparison between the software outputs using PVGIS solar data (latitude range ≈50-57 degrees North). Since PVGIS software was not yet available for India, the simulation sets for the Indian cities were made only in PVSyst software using solar data from RETScreen, PVGIS CM-SAF and Meteonorm solar sources. These sets were made for small scale (3 kW) PV systems as for the UK sets in order to compare the outputs between the two countries. The 3 kW size was chosen because the average installed capacity of the residential PV systems in the UK was 3.1 kW for the period of 1 April 2011 to 31 March 2012 [41] while India has a limited deployment on small scale grid-connected PV systems. Table 2.5 summarises all the simulation sets and their input parameters.

UK and India locations were initially chosen from the solar irradiation maps of the UK and India provided by SolarGIS iMaps (Appendix C) [33]. Hence, the initial number of locations in the UK was 20 and in India 22. However, the chosen Indian locations increased from 22 to 36 in order to have a major or capital city from each state and union territory of India. Moreover, the Indian solar data from PVGIS CM-SAF were acquired in the middle of this research, so the initial 22 Indian locations were simulated using RETScreen solar database, which was the best available choice for India.

2.5 Annual energy prediction and simulation results

This section presents the main results from all the simulation sets and the annual energy prediction, by PVsyst, for all the locations in the UK and India using the PVGIS CM-SAF data [42, 43]. Moreover, PVsyst outputs for the locations of New Delhi and London are analytically discussed. Two main comparisons have taken place about the simulated annual energy output; the first one was made between the two software using the same solar database (PVGIS CM-SAF) and the second one was made using only PVsyst software with imported solar data from different sources. These comparisons demonstrate how important it is for the annual energy prediction to compare PV simulation software and different locations using the same solar data source.

2.5.1 PVGIS vs. PVsyst

The parameters that are available in PVGIS software are compared to the respective parameters in PVsyst. The main results from the simulation sets regarding the two software packages are:

1. PVGIS and PVsyst have different methods for calculating the PV system's temperature and reflection losses. PVsyst reflection losses are always greater than PVGIS with a mean percentage difference around 11% based on PVGIS. However, for southern climates the percentage difference becomes higher (maximum value 20.83%, at Nicosia, Cyprus). Regarding temperature losses, PVGIS losses are usually much greater than PVsyst with a mean percentage difference around 30% based on PVGIS.

Especially in northern latitudes like the UK, the mean percentage difference reaches 46% (Figure 2.6). However, for southern climates PVsyst temperature losses tend to agree with PVGIS values (Figure 2.7). Moreover, PVsyst temperature losses are greater for sites with high irradiation and temperature levels like many Indian cities (Figure 2.8). The x-axis in Figures 2.6 and 2.7 show the relevant cities for each set in decreasing latitude order. Figure 2.6 shows that the temperature losses increase by moving from the north to the south of the UK. However, there is a drop in the temperature losses for the location of Cardiff indicating that the annual average ambient temperature is lower than other locations in the south of the UK. This drop is smaller for PVGIS temperature losses than for PVsyst temperature losses demonstrating the different calculating methods of the two software packages since the temperature data that have been used are the same in both cases.

2. They propose different optimum tilt angle between 1-5 degrees difference, even if they use the same solar data (PVsyst had consistently lower tilt angle than PVGIS in the researched locations). However, in the UK simulation set where the optimum tilt angle of PVGIS was used in PVsyst and vice versa, it was shown that the annual energy output stays the same for both suggested optimum tilt angles. Moreover, the UK results were similar to those for a set of cities in southern Europe, which was investigated to establish the influence of low latitudes. Hence, differences between 1-5 degrees in the tilt angle do not give much difference in predicted output when this difference is around the optimum tilt angle.

3. They propose different optimum azimuth angles due to the fact that PVGIS simulations take into account the horizon shading and PVSyst does not. However, the absolute difference is only 0-2 degrees in the due south orientation and does not play an important role for the system energy outputs.

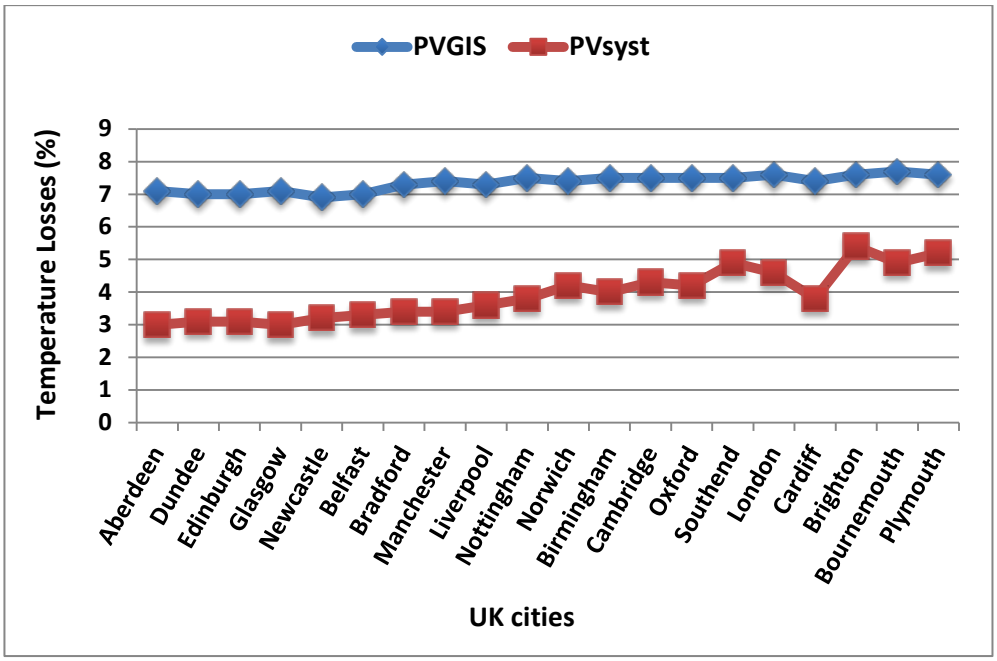

Figure 2.6: Comparison of PVGIS and PVsyst temperature losses for the UK cities

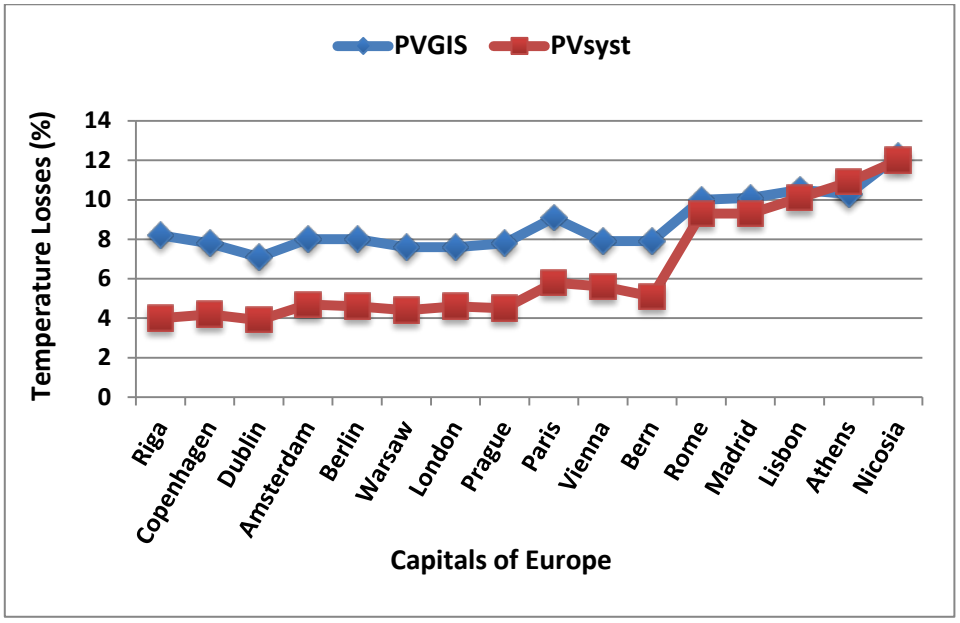

Figure 2.7: Comparison of PVGIS and PVsyst temperature losses for the capitals of Europe

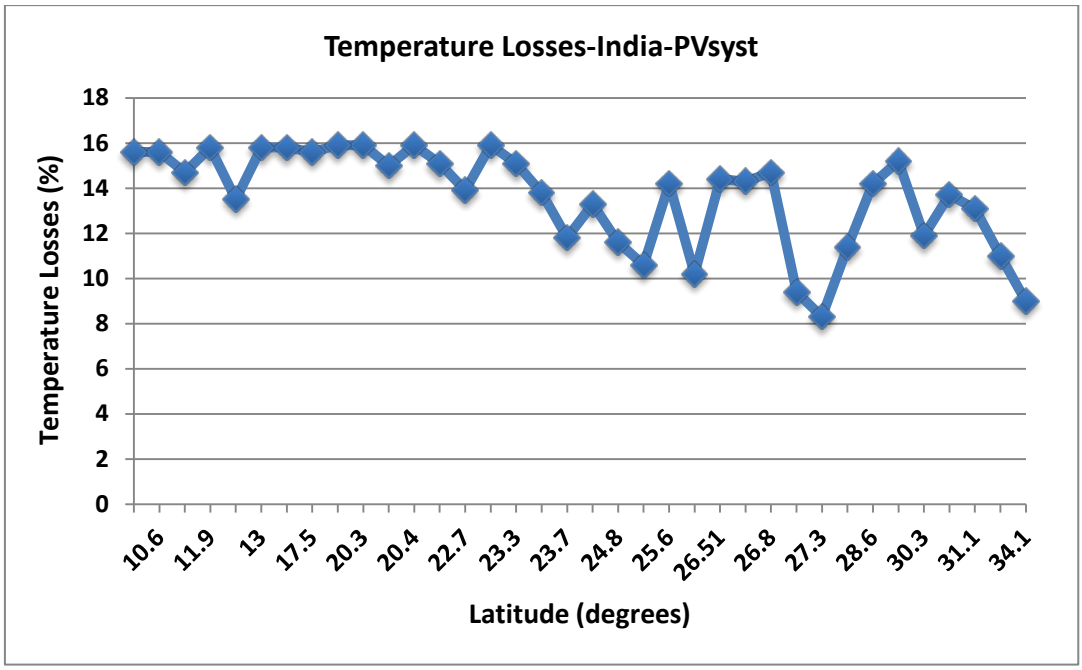

Figure 2.8: PVsyst temperature losses for the cities of India

4. The “Other Losses”, which present all the system losses except for the temperature and the reflection losses in PVGIS, have a default number of 14%. However, in PVsyst the other losses have a range of 12.7-18.1% that corresponds to a latitude range from 8.5 to 57 degrees North. It is noticed that for northern climates the other losses in PVSyst have greater values than the ones they get for southern climates, however for the case of India their mean value is 14.7%.

5. The combined PV system losses of PVGIS and PVSyst have a mean percentage difference of 5.1% for the capitals of Europe and 2.7% for the UK cities based on PVGIS. Hence, the mean annual performance ratio (PR) values of the two software programs are quite close. Table 2.6 shows the mean PR values of these sets.

Table 2.6: Mean PR values from the simulations in PVsyst and PVGIS

Simulations Sets	Performance Ratio (%)
Capitals of Europe	PVGIS: 76.3
Capitals of Europe	PVsyst: 77.5
UK cities	PVGIS: 77.4
UK cities	PVsyst: 76.8

From the above results, it can be concluded that even though PVGIS and PVsyst calculate and/or assume different parameters, their annual PR is quite similar, hence their annual energy output is very similar as well. This stands only for the case for which they use the same solar data (PVGIS CM-SAF) and for an optimally designed PV system. Their annual energy percentage difference range is between 0.05-2.2% based on PVGIS.

2.5.2 PVsyst energy using different solar databases

When different solar sources are used in a PV simulation program, even if all the other parameters stay constant, the annual energy prediction differs. Hence, this section presents the annual energy percentage difference, which was studied by importing different solar data sources into PVsyst software. Figure 2.9 shows this difference for the capitals of Europe simulation set (16 locations). CM-SAF and Meteonorm solar sources were used in this set.

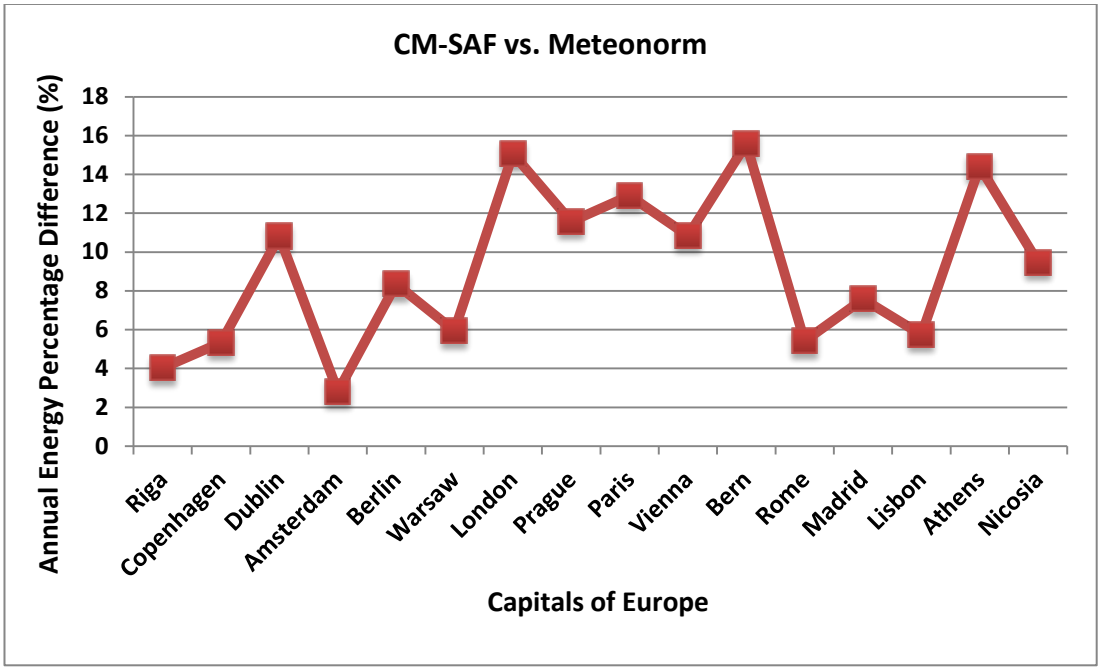

Figure 2.9: CM-SAF vs. Meteonorm for the capitals of Europe (PVsyst energy prediction)

It is observed that the CM-SAF source gives a higher annual energy prediction than Meteonorm, since all the values in Figure 2.9 are positive. Their annual energy percentage difference ranges from 2.81% (Amsterdam) to 15.57% (Bern). A similar

graph is presented below for 22 cities in India (Figure 2.10). In this graph, negative and positive values of the energy percentage difference are observed. CM-SAF and RETScreen databases have been used here, and the negative values show that the RETScreen database gives higher energy output than the CM-SAF in three locations; Chandigarh, Dehra Dun, and Jaipur. However, it is noticed that for the cities of Nangal, Chandigarh and Jaipur, RETScreen and CM-SAF give similar annual energy output (around ± 1% difference). The annual energy percentage difference for the cities of India ranges from around 0% (Nangal) to 15% (Hyderabad).

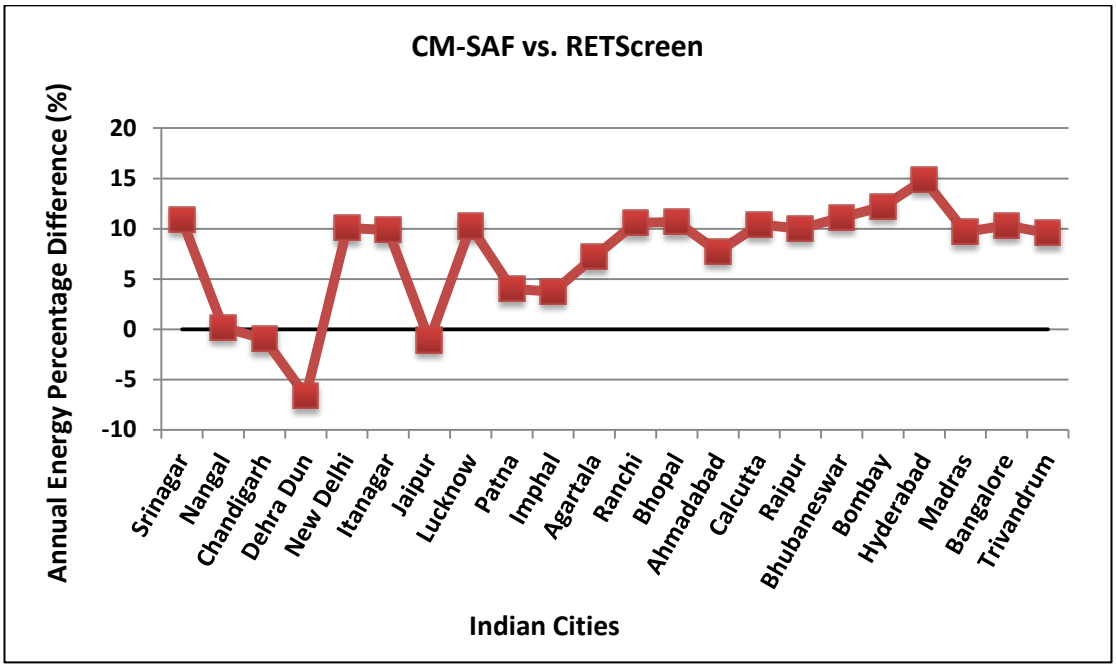

Figure 2.10: CM-SAF vs. RETScreen for the cities of India (PVsyst energy prediction)

Figure 2.11 presents the annual energy prediction by PVsyst software from both solar sources for all 22 cities in India. Moreover, Tables 2.7 and 2.8 present a more analytical comparison between the solar sources for four locations in India. From the tables, it is observed that the main influence in the energy difference is the solar irradiation. However, when there is a difference in the PR, it is mostly attributed to the temperature data of the location since all the other parameters have been kept constant for the simulation. It is obvious that the influence of the temperature on the energy prediction is much smaller than the irradiation according to the specific solar sources. A negative value in the PR difference means that the PV system losses are greater when CM-SAF is used rather than Meteonorm or RETScreen solar sources.

When there is a negative PR difference value, the difference in the annual energy is reduced compared to the inclined irradiation difference and vice versa.

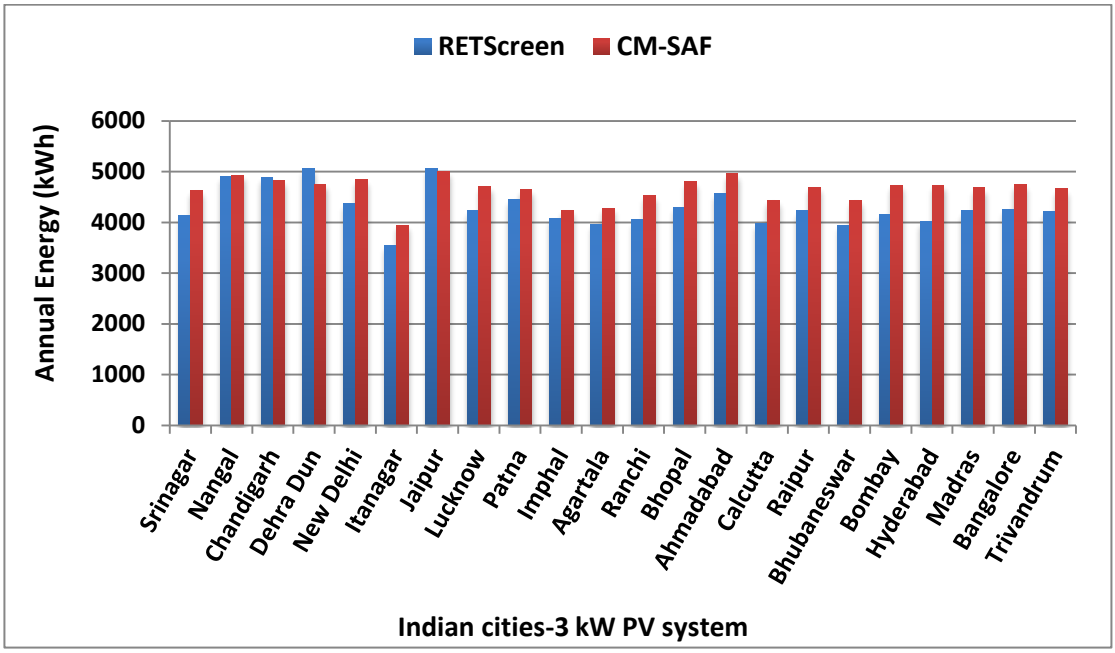

Figure 2.11: PVsyst energy prediction for the cities of India (using two solar sources)

Table 2.7: Differences between CM-SAF and Meteonorm for four sites in India

PVGIS CM-SAF vs. Meteonorm			
Indian cities-4 locations Percentage Difference based on PVGIS	Inclined Irradiation Difference (%)	Annual Energy Difference (%)	PR Difference (%)
New Delhi	3.32	3.30	0.00
Calcutta	10.02	10.68	0.70
Bombay	14.01	13.55	-0.57
Madras	8.20	8.49	0.29

Table 2.8: Differences between CM-SAF and RETScreen for four sites in India

PVGIS CM-SAF vs. RETScreen			
Indian cities-4 locations Percentage Difference based on PVGIS	Inclined Irradiation Difference (%)	Annual Energy Difference (%)	PR Difference (%)
New Delhi	10.08	10.08	0.00
Calcutta	9.59	10.41	0.84
Bombay	12.60	12.20	-0.43
Madras	9.54	9.69	0.14

From all the above, it can be concluded that the same solar database must be used for the comparison of different locations even when the same simulation tool is used and that the choice of the solar database must be carefully considered since it can give up to 15% more in the annual energy prediction for a specific location.

2.5.3 Annual energy prediction in the UK and India

This section presents the annual energy prediction of a 3 kW PV system for 20 cities in the UK and 36 cities in India using the CM-SAF database in PVsyst software. Further, it gives an analytical description of the simulated results for the capital cities of London and New Delhi. Tables with irradiation, energy output, performance ratio, optimum tilt angle, latitude and climate classification for the case of India are presented in Appendixes D and E for all 56 locations.

Figures 2.12 and 2.13 show the annual specific production, the annual inclined and horizontal irradiation for the cities in the UK and India respectively. The specific production is the kWh produced by the PV system divided by the system installed capacity for a certain time period. For the UK, it ranges from 820 to 1100 kWh/kW per year while for India the lowest value of the specific production is 1180 kWh/kW and the highest is 1670 kWh/kW per year. Observing the two graphs, it is noticed that the gain from the conversion of the horizontal irradiation to the inclined irradiation on the collector plane is much greater for the UK than for India. This is due to the transposition factor (TF), which is the ratio of the global incident irradiation on the collector plane to the global horizontal irradiation and indicates how much more irradiation the system will receive compared to the horizontal irradiation with respect to its tilt and azimuth angle [15]. Since the azimuth angle is the same for all the locations (due south), the optimum tilt angle for northern latitudes is much higher than for Indian latitudes. Hence, for the southern cities in India the gain is very small with the minimum gain to be only 20 kWh/m^2 per year for 8.5 degrees latitude. Generally, the optimum tilt angle should be chosen according to the latitude, the climatic condition and the influence of the surroundings of the PV installation [44].

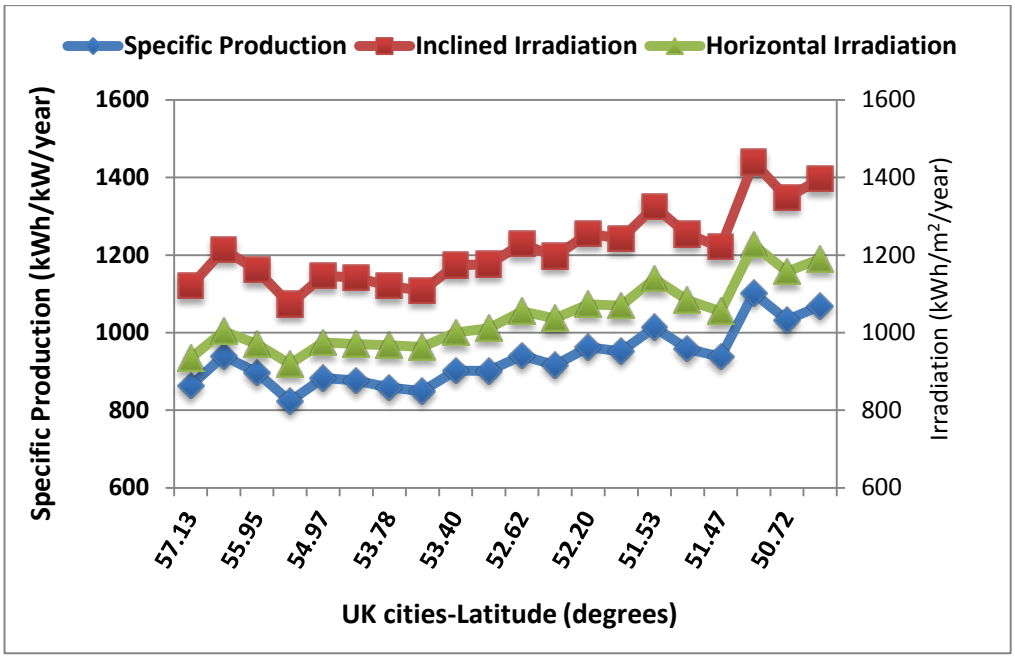

Figure 2.12: Annual irradiation and specific production for the UK cities

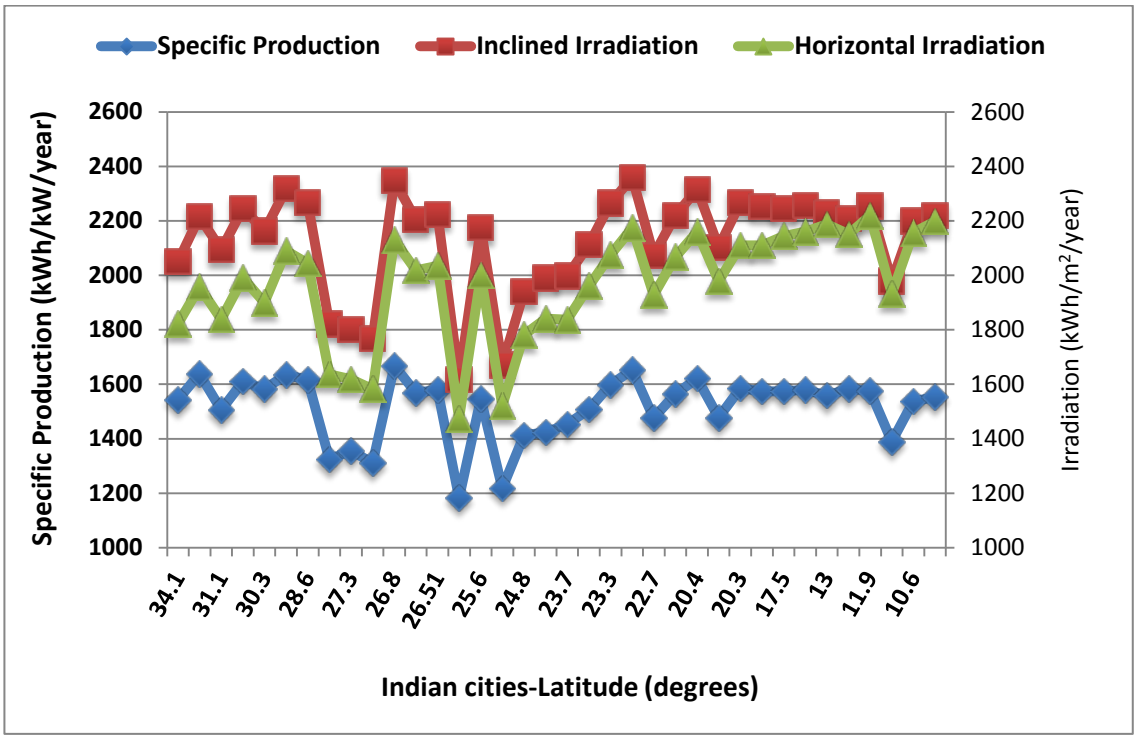

Figure 2.13: Annual irradiation and specific production for the cities of India

Figures 2.14 shows the annual energy of a 3 kW PV system for the cities in the UK while Figures 2.15 and 2.16 show the annual energy for the cities in India by adding a climate and a regional classification respectively. Comparing the energy output of the

same 3 kW PV system in India and the UK, the annual energy for the UK is in the range of 2500-3300 kWh while for India is 3500-5000 kWh. These values are for an optimally designed PV system and the different outputs for the two countries are mainly due to the insolation levels. From Figure 2.14, it can be observed that there is a slight rise of the annual energy output when moving from northern to southern cities of the UK, which is in accordance with the UK climate. However, the same observation cannot be made for India (Figure 2.15) as it has a variety of climates. As is shown in Figure 2.15, the majority of the cities are under the humid subtropical climate (**Cfa**). However, there is not a strong correlation between the climate and the irradiation as it can be observed from the annual energy values and this is due to the fact that the climate classifications are mostly dependent on average temperatures and precipitation levels for a location. On the other hand, there is some correlation between the irradiation and the regional classification (Figure 2.16). Especially, the northeast part of India gives lower values of the annual energy compared to the majority of the cities in the other regions.

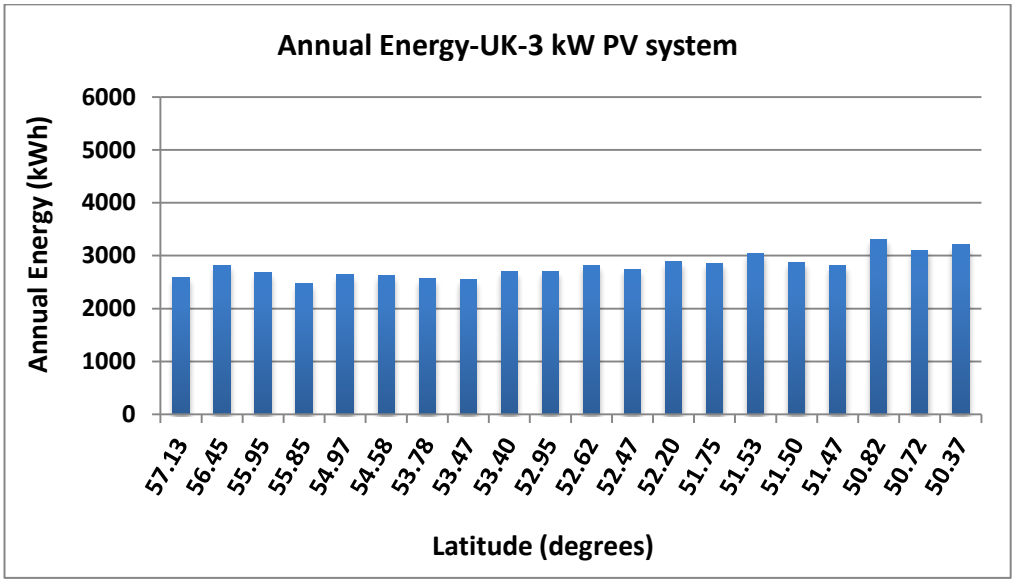

Figure 2.14: PVsyst energy prediction for the cities of the UK (3 kW system)

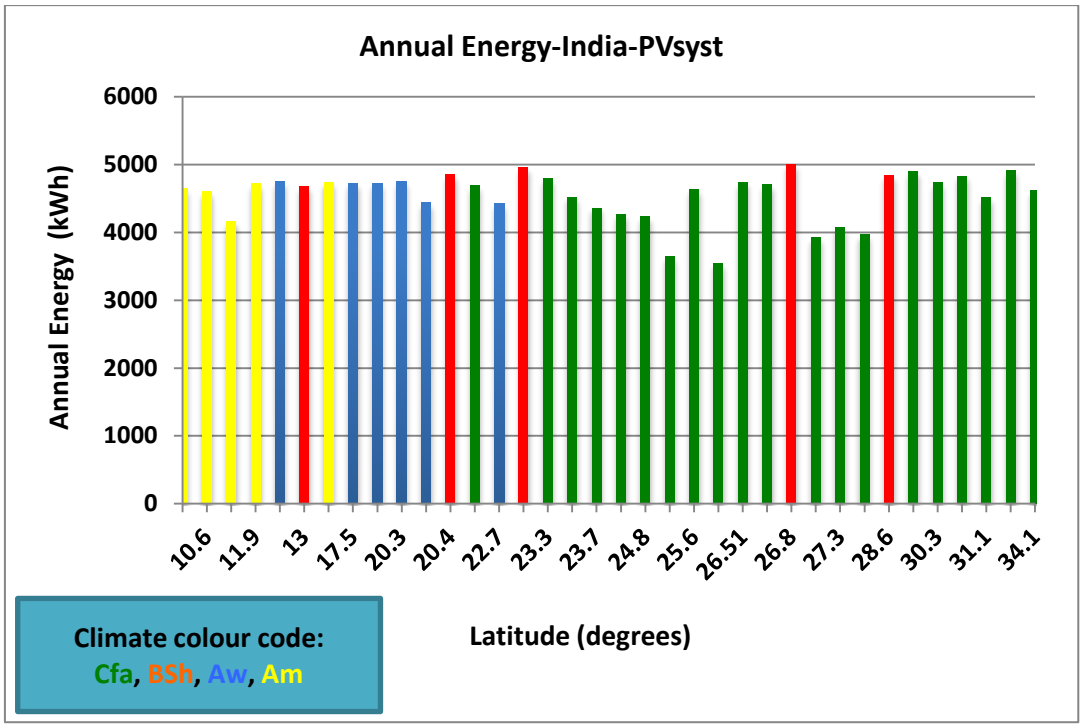

Figure 2.15: PVsyst energy prediction for the cities of India (climate classification)

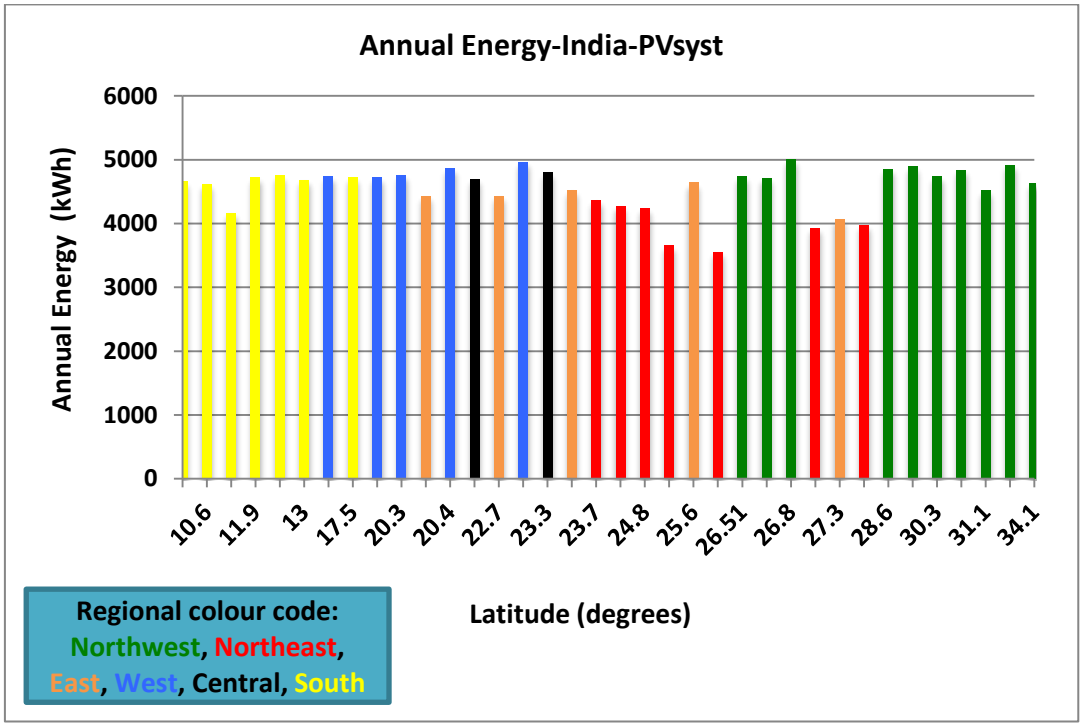

Figure 2.16: PVsyst energy prediction for the cities of India (regional classification)

Apart from the annual energy variation of the two countries, the seasonal energy variation can be seen in Figure 2.17 in accordance with their climatic characteristics.

By examining the monthly energy variations between London and New Delhi, it is clearly shown that the worst-case month for New Delhi is in July, the month of the monsoon season. As was mentioned in Section 2.1.1, the average annual rainfall contribution by the monsoon season is 74.2%. Hence, the PV energy production is lower during the monsoon than the other seasons. Moreover, in areas with intense dust accumulation in India, the PV production will be reduced during the other seasons if the systems are not cleaned. It is noticed that the worst-case months for New Delhi have similar energy output to the best-case months of London, which are during the summer period of the UK. Tables 2.9 and 2.10 present analytically the imported solar data and the simulation outputs of the monthly inclined irradiation (GlobInc), energy output (E) and the PR for these locations. Note that the irradiation data for all the locations in India are long-term monthly averaged data from CM-SAF database. The global horizontal irradiation (GlobHor) has been calculated from satellite data for the periods 2000-2005 and 2007-2011 while the diffuse horizontal irradiation (DiffHor) has been calculated for the same period based on the global and beam irradiation measurements. The temperature values (T_{amb}) are long-term monthly averages from 1990 to 2009 while the wind data (WindVel) are from 2005 to 2009 [3]. Wind data are not available for the UK cities since the CM-SAF solar data have been taken from the PVGIS web page [16].

Table 2.11 presents the distribution of the annual energy gains and losses for the 3 kW system in London and New Delhi, expressed in percentage (%). Even though the system in New Delhi has 5% more annual loss compared to the one in London, their annual energy output has almost 2000 kWh difference (London≈2800 kWh, New Delhi≈4800 kWh). This is due the difference in their irradiation levels. Hence, even if a system performs better in one location than another, it does not mean that the energy output will be higher. It can be said that as module energy output is dependent on the climatic conditions of the location, where this output is measured [45], the same could be considered for a PV system, especially like the ones presented here, which are identical but they are simulated in different climates. Moreover, it is known that the energy output of identical systems with similar performance is proportional to the inclined irradiation at the different locations according to equation 2.4.

$$E = PR \times P_{max} \times GlobInc \quad (2.4)$$

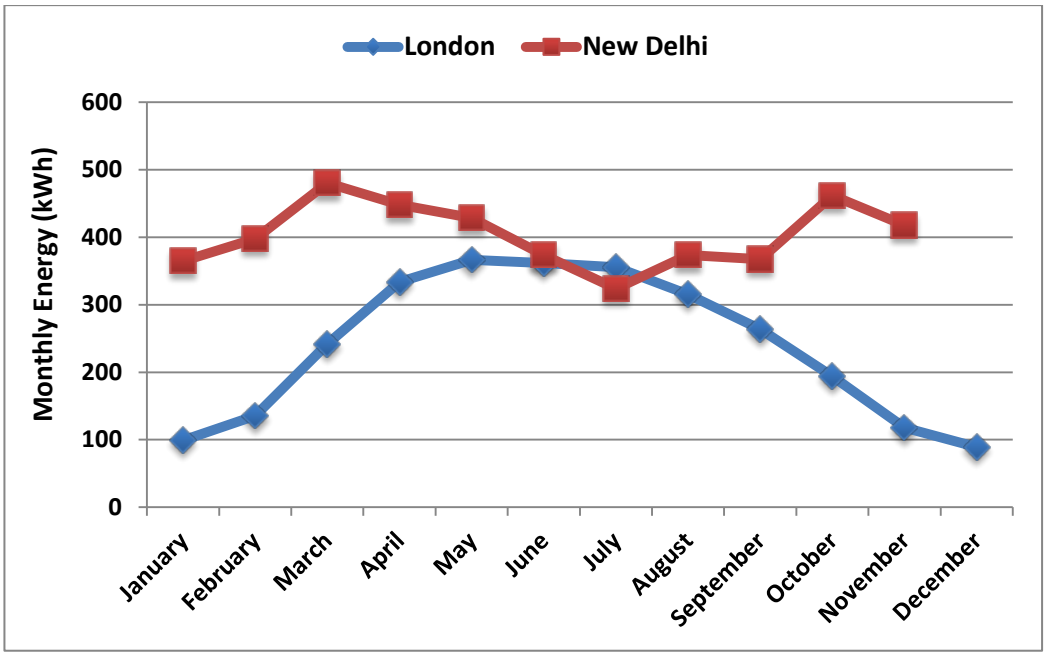

Figure 2.17: PVsyst monthly energy prediction for London and New Delhi 3 kW system)

Table 2.9: Imported solar data and the simulation outputs for London

London	PVGIS CM-SAF solar data			PVsyst simulation results		
3 kW System	GlobHor	DiffHor	T_{amb}	GlobInc	E	PR
	(kWh/m²)	(kWh/m²)	(°C)	(kWh/m²)	(kWh)	
January	24.1	15.91	5.2	42.4	99.0	0.78
February	37.5	23.61	5.8	57.2	135.4	0.79
March	80.0	46.40	7.2	102.7	242.0	0.79
April	125.1	62.60	9.3	142.3	333.9	0.78
May	157.5	85.00	12.6	159.2	366.5	0.77
June	165.0	87.50	15.6	160.0	361.6	0.75
July	161.8	89.01	17.8	160.0	355.5	0.74
August	132.4	72.80	18.2	140.9	315.4	0.75
September	95.7	52.60	15.6	116.4	263.6	0.76
October	57.7	32.90	12.2	83.6	193.7	0.77
November	29.7	18.41	8.1	50.5	118.2	0.78
December	19.3	12.71	5.4	38.4	89.0	0.77
Year	1085.8	599.45	11.1	1253.6	2873.7	0.76

Table 2.10: Imported solar data and the simulation outputs for New Delhi

New Delhi	PVGIS CM-SAF solar data				PVsyst simulation results		
3 kW System	GlobHor	DiffHor	T_{amb}	WindVel	GlobInc	E	PR
	(kWh/m²)	(kWh/m²)	(°C)	(m/s)	(kWh/m²)	(kWh)	
January	115.6	49.3	13.5	2.70	158.6	364.8	0.77
February	136.9	34.7	16.9	2.80	179.2	397.8	0.74
March	193.8	45.3	22.4	2.60	223.0	480.2	0.72
April	215.7	74.1	28.8	2.80	216.0	448.0	0.69
May	230.3	68.2	32.9	2.70	210.8	428.9	0.68
June	206.4	81.9	33.0	2.90	183.2	373.5	0.68
July	169.3	106.0	30.4	2.50	156.3	324.0	0.69
August	185.4	88.4	29.2	2.30	178.7	373.7	0.70
September	164.7	64.5	28.3	2.30	174.9	367.6	0.70
October	172.4	41.2	25.4	2.30	215.8	461.9	0.71
November	134.7	39.9	19.9	2.40	189.8	417.6	0.73
December	119.4	33.8	15.0	2.60	181.3	413.4	0.76
Year	2044.6	727.3	24.7	2.60	2267.5	4851.3	0.71

Finally, regarding the gains and losses in Table 2.11, the global incident irradiation on the collector plane is the only parameter, which increases the energy output of the system with respect to the horizontal irradiation. It presents the gain in irradiation over what would have been received on a horizontal plane. As was mentioned, London's gain is greater than New Delhi due to the TF. The array soiling loss, module quality loss and module-array mismatch loss are the same for all the simulations since these parameters have been kept constant (default values in PVsyst for the specific system design). The temperature loss is more than triple for New Delhi compare to London, which is reasonable by considering the ambient temperature values of the two locations (Tables 2.9 and 2.10).

Table 2.11: Annual energy gains and losses for the 3 kW system in London and New Delhi

Distribution of the annual energy gains and losses	London	New Delhi
Global incident on collector's plane	15.5%	10.9%
IAM factor on global	-3.1%	-2.9%
PV loss due to irradiance level	-6.0%	-3.1%
PV loss due to temperature	-4.6%	-14.2%
Array soiling loss	-3.2%	-3.2%
Module quality loss	-1.6%	-1.6%
Module array mismatch loss	-2.2%	-2.2%
Ohmic wiring loss	-0.8%	-1.1%
Inverter loss during operation (efficiency)	-4.9%	-4.2%
Inverter loss due to power threshold	-0.1%	0.0%
Total Losses	**-24.0%**	**-29.0%**

To summarise, this chapter establishes the basis for the expression of the domestic PV potential in both countries, which is the main aim of this thesis. The variation of the technical and economic potential relies on the validity of the original energy output estimate. This chapter has investigated the limits of this estimate. It has also provided the reader with the general knowledge of the climatic conditions of the two countries and how the PV system simulation software interprets this knowledge to give the annual energy estimation. The following chapter (Chapter 3) will validate further this estimate by presenting a case study in an Indian climate and by revealing the limits of harsh environment. Finally, the economic and technical models presented in Chapters 4 and 5 are based on the annual PV energy prediction that was presented here.

Chapter 3: Performance Assessment

This chapter examines the short-term performance variations of different PV technologies under the humid subtropical climate of Kanpur in India. The reason behind this study is to identify the PV system operating conditions under the harsh Indian environment and to validate the simulation results for this specific site by comparing them to the field measurements that have been acquired. Hence, a description of the studied systems is presented and their results are analysed. Moreover, this chapter presents the main PV performance characteristics and field performance studies that have been reported in the literature. Finally, it discusses some of the limitations of the PV simulation software.

3.1 PV performance characteristics

The different PV module technologies have different performance characteristics due to their material structure. As was mentioned in Chapter 2 (Section 2.3.1) there are five families of materials in PV module manufacturing [13]. However, a general division in PV module technologies is between the crystalline and thin film technologies. Mono-crystalline silicon (mono-Si) and multi-crystalline silicon (multi-Si) belong to the crystalline technologies (c-Si) while amorphous silicon (a-Si), cadmium telluride (CdTe) and copper indium selenide (CIS) belong to the thin film technologies. In general, the most expensive and the most efficient PV cells till now are the mono-crystalline silicon due to their fabricating procedures. The manufacturing procedure for a multi-crystalline PV cell is less demanding so their manufacturing cost is lower than a mono-crystalline cell. Furthermore, thin film modules are still developing and promising lower manufacturing cost and better efficiency [46].

3.1.1 PV module and inverter main parameters

In general, PV module and array parameters are measured under *Standard Test Conditions* (STC): 1000 W/m^2 irradiance, 25°C cell temperature, Air Mass= 1.5 global spectrum and/or *Nominal Operating Conditions* (NOC): 800 W/m^2 irradiance, 20°C ambient temperature and average wind speed of 1 m/s with an open rack mounted

module in an open circuit electrical state. The above ratings provide some information that allows the comparison among the different types of modules. However, in real world conditions many external parameters affect the amount of solar irradiance that a module can receive. These parameters can be affected by the different weather conditions (i.e. airborne dust, water vapour, temperature and air pollution) and by the different irradiation levels that are depended on the seasonal variations and the location of the system. For example, the output voltage of a module will deteriorate at high temperatures, so a module operates better at low temperatures. Nordmann and Clavadetscher report that the PV module temperature rises above ambient temperature around 20°C to 52°C at 1000 W/m^2 [47]. The major electrical parameters that can be found in a PV module datasheet are: the maximum power rating (P_{max}), the open circuit voltage (V_{OC}), the maximum power voltage (V_{MPP}), the short circuit current (I_{SC}), and the maximum power current (I_{MPP}). These parameters are temperature dependent, so they are accompanied with the respective temperature coefficients for the power, the voltage and the current [48].

The Fill Factor (FF) measures the quality of a solar cell and/or module. It is calculated by comparing the maximum power to the theoretical power (P_T). P_T is referred to the output power of both short circuit current and open circuit voltage. Furthermore, FF could be interpreted in a graph as the ratio of the rectangular sections (Figure 3.1). As the I-V curve is more square-like the fill factor is becoming larger. Fill factor could also be represented as a ratio and its typical value range is from 0.5 to 0.85.

For an ideal cell, series resistance (R_S) would be zero and parallel resistance (R_{SH}) would be infinite. So, R_{SH} would not allow the current flow to change directions while R_S would not contribute further to voltage drop. In a real solar cell model if R_S is increased and R_{SH} is decreased, the maximum power and the fill factor will drop as shown in Figure 3.2 V_{OC} will be reduced, when R_{SH} has a major decrease. Moreover, the extreme increase of R_S can decrease I_{SC} [49].

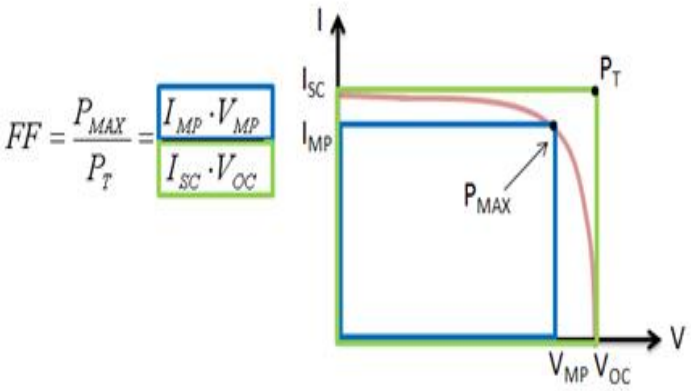

Figure 3.1: The Fill Factor of the I-V Curve [49]

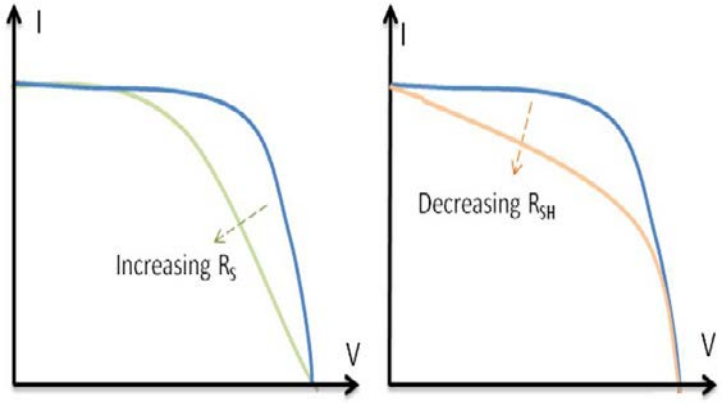

Figure 3.2: Effect of Diverging R_S and R_{SH} from Ideality [49]

The inverters are used for the conversion of the DC voltage that the PV array produces to the AC voltage that is used for the loads and the grid. The inverter is connected to the array and the supply network, its output signal should match with the voltage, the frequency and the power quality limits of the network [50]. The main inverter parameters are: the rated DC and AC power, the maximum power point (MPP) voltage range, the maximum DC/AC current and voltage and the rated DC/AC current and voltage. The most important characteristic of an inverter is its efficiency. The inverter efficiency is the ratio of the AC power output to the DC power input:

$$\eta = P_{AC} / P_{DC} \quad (3.1)$$

Moreover, "Euro η" efficiency was defined in order to make the comparison between different types of inverters that they operate under the European climatic conditions [23]. Specific parameters, which are called energetic weightings, have to be identified to take into account different load conditions of the inverter. Six outputs at different efficiencies are used to calculate the Euro efficiency given by the formula:

$$\eta_{EURO} = 0.03\times\eta_{5\%} + 0.06\times\eta_{10\%} + 0.13\times\eta_{20\%} + 0.1\times\eta_{30\%} + 0.48\times\eta_{50\%} + 0.2\times\eta_{100\%} \qquad (3.2)$$

In a nominal case the $\eta_{100\%}$ gives the efficiency. This makes the inverter nominal power to match with the PV array power ($P_{PV} = P_{INV}$). For a 20% operating time of one year (0.2 x $\eta_{100\%}$) a 100% inverter load is taken. At half array power, the Euro efficiency is assumed for 48% of the operating time (0.48 x $\eta_{50\%}$). The other parameters to calculate the Euro efficiency are determined in a similar way [51]. The operating conditions under which a PV inverter was requested to operate for the calculation of the parameters of the "Euro η" efficiency correspond to a middle-European climate (in-plane irradiance and module temperature) and to a fixed mounted system [52]. Below are presented two figures, which show the I-V curve and the power curve of the selected module for this research under different irradiation levels, and the efficiency curve of the selected inverter for the Indian locations according to the manufacturer specifications.

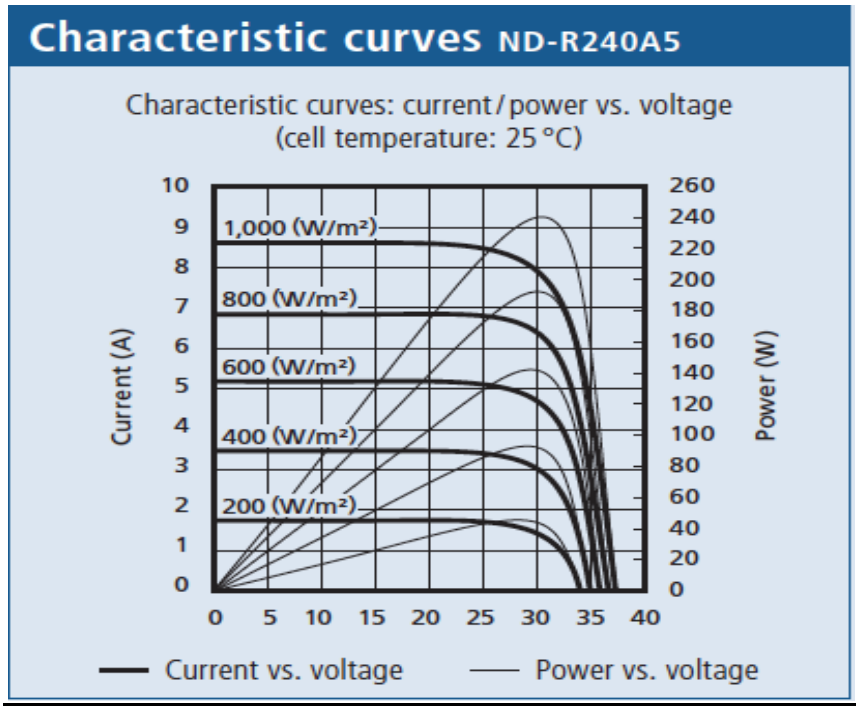

Figure 3.3: Module I-V and power curve [36]

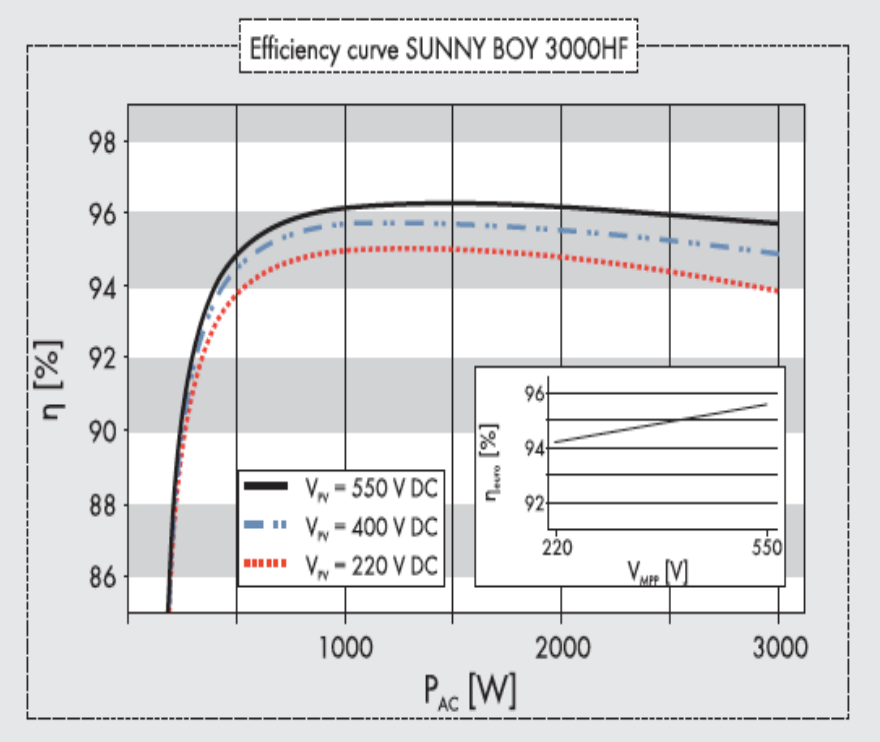

Figure 3.4: Inverter efficiency curve [37]

3.1.2 Main characteristics of PV technologies

The general characteristic for all the module technologies is that their current and voltage are dependent on the irradiance and temperature levels. More analytically, the module current is directly dependent on the irradiance while the module voltage has a logarithmic dependence, although it does not have as much variation as the current with the irradiance variations [51, 53]. The module temperature affects the operating voltage (i.e. increases at low temperatures and decreases at high temperatures) while the current might increase slightly at high temperatures [51]. Technology-wise, crystalline silicon (c-Si) modules usually have low V_{OC} and high I_{SC} values while thin film modules typically have high V_{OC} and low I_{SC} [54]. Finally, regarding the resistances of a module, it is has been observed that a high R_S reduces its FF at high irradiance levels, while a low R_{SH} reduces its FF at low irradiance levels [53]. Hence, modules with low R_{SH} will give lower power output than expected in low irradiation levels while modules with high R_S will give lower power output than expected in high irradiation levels [55].

Regarding the differences between the crystalline and thin film module technologies, apart from their efficiency difference, they vary in terms of irradiance and temperature dependence, shading tolerance and spectral sensitivity.

Generally, thin film cells have larger band gaps than crystalline cells and for this reason thin film modules lose less power at high temperatures than crystalline modules. The temperature power coefficient of the a-Si modules can even take positive values at low irradiances. However, the temperature power coefficient of CIS modules is not that much smaller than that of c-Si modules. This is because CIS has a band gap that is similar to silicon. Typical power temperature coefficient range for a-Si =-0.1 to -0.3%/°C while for CIS=-0.33 to -0.6%/°C. Further, thin film modules have greater shading tolerance compare to crystalline due to stripe-shaped individual cells. Hence, thin film technologies might constitute a better solution for building integrated PV systems since it is more difficult to achieve good ventilation or minimum shading in this type of installations. Nevertheless, thin film technologies have a flatter I-V curve resulting in a lower fill factor than the crystalline modules. For example, the FF range for a-Si modules is between 0.56 to 0.61 while for CIS and c-Si modules is 0.64 to 0.70 and 0.75 to 0.85 respectively.

Thin film cells absorb visible light with short and medium wavelengths better than crystalline cells [51]. This spectral sensitivity of thin film cells enables them to use low solar irradiance more efficiently (low light conditions, diffuse radiation-cloudiness). Thin film efficiency might increase at low incident angles of the sunlight and/or high air mass values while crystalline efficiency drops. Figure 3.5 depicts the relevance of the solar cell material to the solar radiation spectrum. Moreover, thin films might have a slightly higher efficiency at low light levels (+2 to +8% relative has been claimed [56]) due to their series resistance, which is higher compared to the c-Si. Consequently, thin films have higher connection losses, which limit their STC efficiencies at high irradiation levels [57]. On the other hand, R_{SH} has an inversely proportional relationship with the irradiance; it increases as the irradiance decreases. During the last years, the P_{max}-Irradiance linearity of modules has been improved, so the low light level performance has increased partly due to the better control of R_{SH}. Hence, thin film modules do not have as high an efficiency gain at low light level as they used to have, compared to c-Si modules [56].

Finally, for a-Si modules, the light-induced degradation effect, known as the Wronski effect, causes an initial performance decrease during the first 6-12 months of their operation, and then they are stabilized. In addition, reversible degradation occurs during winter, but the high temperatures reverse this in summer (seasonal annealing effect). Hence, the efficiency of the a-Si fluctuates during the year and can be particularly high during summer [51]. However, the seasonal efficiency changes can be distinguished from long-term degradation [58]. Moreover, in a study regarding copper indium gallium diselenide (CIGS) module technology, an increase in CIGS power output was observed when it was exposed to sunlight, a light-induced annealing effect. CIGS has relatively high efficiency compared to other thin film module technologies and lower temperature power coefficient compared to c-Si technologies but a more complicated manufacturing process than other technologies, so high manufacturing cost [53].

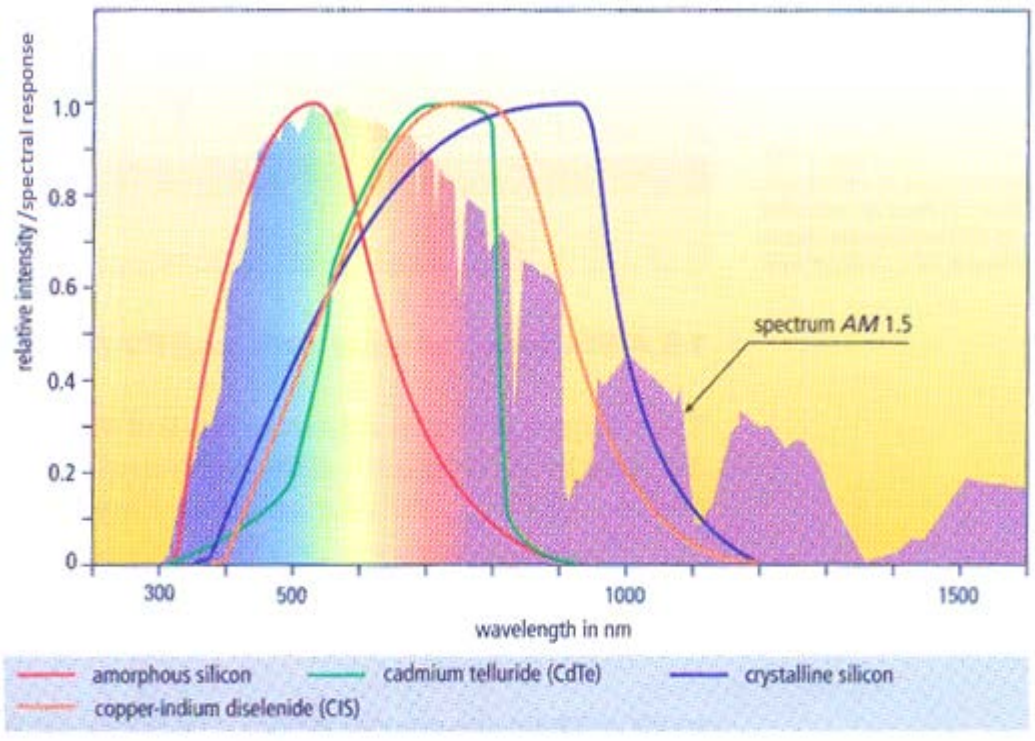

Figure 3.5: Solar spectrum and PV technologies [51]
(the solid lines represent the normalised spectral response of the PV technologies)

3.1.3 PV system performance parameters

The performance of the various PV systems is usually compared using their specific yield and performance ratio parameters. The specific yield (Y_f) is the energy output (E) divided by the rated power (P_{max}) of the installed PV array (Equation 3.3). It defines the number of hours that the PV array needs to operate at its maximum power in order to provide the same amount of energy and is often expressed as the annual energy output per kW. The units are hours or kWh/kW, with the latter to be more preferable because it describes the quantities that are used to define the parameter. Since the Y_f normalizes the energy produced with respect to the system size, this parameter is used to compare the produced energy of PV systems with different sizes, designs, or technologies. Furthermore, Y_f is dependent on the solar resource; it varies in accordance with the irradiation. Hence, if the comparison is made for different locations or time periods, it will not be accurate because solar irradiation is varying [59, 60]. Some performance studies in European climates have shown that the different PV technologies have similar specific yield within an experimental error of ±5% [57].

$$Y_f = \frac{E}{P_{max}} \quad \text{(kWh/kW) or (hours)} \tag{3.3}$$

According to Sutterluetiet et al, energy yields can be different due to technical and commercial reasons and the technical way to ensure a high energy yield is to optimize the combination of the main loss factors as described in Table 3.1 [58].

Table 3.1: Key parameters for maximising energy yield kWh/kW [58]

Parameter	**Comments**
P_{max} nominal / P_{max} nameplate	High from positive binning tolerances from manufacturers
Site selection	High insolation site (kWh/m^2/y)
Good array orientation	Tilt near latitude towards equator for best yields
Low T_{module} with proper ventilation	From better thermal module design and/or free ventilation
Minimal shadowing	Try for no shading in spring to autumn day hours, if impossible string array to minimize total loss
Good module stability	Many guarantees are <20% drop P_{max} in 25 years. Predictable (long-term) degradation during lifetime.
Clean modules	Minimise soiling but compare the cost of cleaning and possible damage vs. lost energy yield
Electrical parameters	
Normalized I_{SC}	Low dirt value, good array coating
Normalized R shunt (nR_{SH})	Good high R shunt will minimize losses at low light levels nR_{SH}>90%
Normalized R series (nR_S)	Good low R series will minimize losses at high light levels nR_S>85%
Normalized V_{OC}	Good temperature V_{OC} coefficient, low T_{module}
Spectral correction	Maximise absorption of each junction and match multi-junctions for best site specific yield
Other	Proper Monitoring equipment and field performance validation

The performance ratio (PR) is the final PV system yield (Y_f) divided by the reference yield (Y_r) (Equation 3.4), where Y_r is the system output for an ideal system and its numerical value is equal to the PV total in-plane irradiance divided by the reference irradiance. PR does not indicate the solar resource variations because of its definition and it is a dimensionless value. It describes the overall effect of system losses on the rated output due to the inverter inefficiency, wiring mismatch and general losses included in the system conversion efficiency. It also includes the losses from the PV module temperature, the partial use of irradiance due to the reflection from the module front surface, the soiling or the snow on the modules, the system downtime, and component failures [59].

$$PR = \frac{Y_f}{Y_r} \text{ (dimensionless)} \quad (3.4)$$

These loss mechanisms can be divided into two categories: module technology dependent and balance of system (BOS) dependent. The module technology could include losses based on the actual / nameplate power (P_{max}) ratio, stability (particularly for thin film technologies), module mismatch, and high module temperature effects. The BOS losses could be due to inverter downtime and low light level performance, wiring losses, shading, and soiling losses [61]. Usually, the system losses cannot "be differentiated from poor module characteristics such as degradation or fall off at low light levels, high temperatures or diffuse light unless there is a much more detailed analysis of the performance" [62]. However, the PR values are usually referred to a monthly or to an annual base. In case they are calculated for shorter periods, like weekly or daily base, they can also contribute to the identification of losses due to component failures. Moreover, due to the losses from the PV module temperature, PR values are usually higher in winter than in summer. In addition, if the PV module soiling is seasonal, it may also have an impact to the PR values from summer to winter. Generally, if the yearly values of the PR are continually decreasing, this indicates a permanent loss in the performance of the system (i.e. degradation). In this case, the system may require some technical changes in order to solve the issues that have appeared [59].

As was discussed, the PR and the Y_f are important parameters for the PV system performance validation. However, there are uncertainties associated with the variability of modules from production lines, field measurements (especially irradiance) and the calibration process that the module manufacturer has used. Moreover, these parameters cannot specify the reason behind a performance change. For example, when the PV current drops, it can be due to module mismatch or by overall reduction of shunt resistance etc. [63]. Further, if a string underperforms on a large PV system, it will bring down the average energy output, and by averaging the energy, the yield in high irradiation levels is underestimated [61]. Hence, it would be appropriate to account for the aforementioned facts and clearly state the conditions for performance measurements and/or calculations, when PV performance results are expressed.

3.1.4 PV simulation programs limitations

PV simulation programs have their own limitations regarding the PV performance prediction even if they coincide with energy output [64]. The energy prediction difference between different PV technologies has been found to be more than 5% in some PV simulation programs. A study of five programs has shown that the modelled performance vs. irradiance and temperature differ between themselves, even though they use the same 1-diode equation to fit I-V curves from the manufacturers' datasheets [56]. The reason this occurs might be that the PV simulation program database sometimes does not match with the values for thermal coefficients and low light efficiency changes provided by the manufacturers and measured according to international standards such as EN 50380 and EN 61215. Even if a system performs optimally, it will still have losses. So, if the modelled parameters are not correct, the whole modelling will be inaccurate [57]. For example, the low irradiance data could be separated into two categories; clear sky conditions (red wavelength), which are associated with high angles of incidence and air mass, i.e. early morning or late evening or cloudy conditions (blue wavelength), which are associated "with low angles of incidence and air mass and low beam fraction" [62]. A model may not distinguish this difference of the low irradiance data. Hence, an error of more than 8% has been found in simulation programs that are using incorrect thermal and low light efficiency coefficients. In general, these parameters "have been pessimistic with regards c-Si and maybe optimistic for thin films" [62].

Some PV simulation programs, which use the 1-diode model, base their results on values originating from only one I-V curve without accounting for the module and inverter variability [62]. For example the PVCEC calculator model considers the R_S as constant, whereas the series resistance value can vary strongly with effective irradiance for each I-V curve [54]. Further, PV simulation programs might assume that the light current is directly proportional to irradiance and that the inherent R_S and R_{SH} are not affected by temperature, time, and irradiance; however, this does not apply to all module technologies. Moreover, while the spectral response and seasonal annealing affect the measured energy yield, usually they are not included in the 1-diode model [56]. In a workshop at Sandia National Laboratories in 2010, where different PV designers used various commercial and internal simulation programs to model the same systems, large variations have been found between the modelled results [65]. Additionally, the designers appeared less confident when PV components

were not included in the program database or when they had to assign derating to the input simulation values. It was concluded that one of the biggest influences in order to achieve a good match between the simulation program and the measured data, was the derating of the inputs (many of which are not known exactly) [65]. Hence, the differences in the results among PV programs raise important concerns about their validity. A designer should be familiar with the program deficiencies because their equations have coefficients, which represent fitting parameters for functions with variables that can differ widely between different PV modules [54].

The version of PVsyst software that is used in this study uses the 1-diode model for its predictions and the R_S and R_{SH} are calculated by the software based on the chosen PV module. The 1-diode model equation is given below:

$$I = I_{ph} - I_o[exp(q \times (V + IR_S)/(N_C \times Gamma \times k \times T_C)) - 1] - (V + IR_S)/R_{SH} \quad (3.5)$$

where I= Current supplied by the module (A), V= Voltage at the terminals of the module (V), I_{ph}= Photocurrent (A) proportional to the irradiance G with a correction as function of T_C, I_o= Inverse saturation current, depending on the temperature (A), q= Charge of the electron= 1.602 10^{-19} Coulomb, k= Boltzmann's constant= 1.381 10^{-23} J/K, Gamma= Diode quality factor, normally between 1 and 2, N_C= Number of cells in series, T_C= Effective temperature of the cells (Kelvin).

The parameters Gamma and I_{ph} are also unknown for this model and are assumed by the software. Sometimes I_{ph}, Gamma and R_S do not have a coherent physical meaning. The Gamma value influences the temperature behaviour of the model and the proposed Gamma default values in PVsyst for each technology are the following: mono-Si Gamma= 1.3, multi-Si Gamma= 1.35, a-Si Gamma= 1.4, CIS Gamma= 1.5. However, if the voltage temperature coefficient is specified, the R_S and the Gamma parameters will take realistic values. Further, R_{SH} is specified at reference conditions (GRef, TRef) and it has an exponential behaviour according to the irradiance [17]. It has been found that with the exponential behaviour of R_{SH}, as used by PVsyst, the modelled power values have an uncertainty of around 1.2% of the nominal power in

any conditions over long periods (up to 6 years study) [66]. Moreover, PVsyst does not take into account the seasonal annealing effect [66] and the light-induced degradation effect for the a-Si technology [17]. Its results, when a-Si modules are used, are referred to stabilised module performance.

The results from a study at Geneva University about the comparison of measurement vs. PVsyst modelled power of various PV module technologies showed a range of ±4% difference to the nominal power values [66]. However, these results are limited to this specific location. Additionally, a survey by PHOTON magazine in 2011, comparing 20 PV simulation programs regarding their yield prediction at three different sites showed that the difference of the PVsyst yield prediction to the measured yield was between 0.5 to -6% by considering the mean bias average difference and around 4 to 6% by considering the absolute average difference. In the same survey, PVGIS software had a mean bias average difference range of 3-9% and an absolute average difference range of 4-9% [67].

3.1.5 Field performance studies

The manufacturer specifications for the PV system components alone are not sufficient to accurately predict PV operation under various climatic conditions. Hence, PV field performance monitoring and data analysis are necessary for the better understanding and development of PV system field behaviour [68]. This sub-section presents some environmental and operational factors, which affect the system operation, as well as some studies regarding the system field performance at various sites.

The performance analysis of various system configurations in Ota (Japan) found that south oriented arrays produce around 11-22% more electricity than other array configurations and that PV performance differences could be caused by the type of module (i.e. module manufacturer) and by the PV system design in case of different string voltages. Specifically, in optimally designed systems the PV performance could differ by more than 10% and in non-optimised could reach up to 50%. It was also commented that the appearance, the price and the reliability of a PV system are equally important as the PR for its evaluation [69].

Another study that considered the uncertainty in PV performance parameters for three different sites in Europe showed that the annual PR uncertainty in low irradiance sites could reach 4.5% while for high irradiance sites it is lower (around 2.5% to 3.5%). These uncertainty values were attributed to the environment of the location and the set-up of the instrumentation. It was also noted that field measurement uncertainty had less influence on the performance indicators than the irradiance measurement uncertainty, which was much higher. Even though this study tried to express an upper limit for performance uncertainty, it was acknowledged that they had used conservative estimates [70].

It is known that the measured irradiation values could differ depending on the measuring instrument used due to different angular and spectral responses. An irradiance sensor could give different values from a pyranometer at low light efficiency, as they have different angular responses. Moreover, different sensor types may also give different measurements depending on their spectral responses [55]. For example, in Germany, on an annual average, the irradiation measured by crystalline silicon sensors is 2-4% lower than that measured by pyranometers [71]. Hence, the annual PR of a PV system located in Germany would be higher if it is calculated based on a c-Si sensor measurement. This has to be taken into account when PR values are being compared.

In a study about "*measured low light efficiency vs. irradiance sensor type"* in Arizona the results have shown that the apparent irradiance is up to 18% lower for the solar sensor compared to the pyranometer at low light levels. Hence, the module performance will appear to be 18% worse when the pyranometer values are used for the PR calculations, compared to the solar sensor values. Also, PV modules will have different efficiency vs. irradiance curves at low light conditions depending on their spectral and angular responses although based on the IEC 61853 matrix method the combination of irradiance and temperature values give a single efficiency. Below is presented, as an example, a graph depicting the DC module efficiency / STC vs. irradiance for a c-Si module at IWES in Germany for clear sky (red) and diffuse (blue) conditions. The measured average efficiency vs. irradiance curve of a module depends on the clear sky and diffuse conditions of the location where the module is installed. For example, in desert environments the apparent low light is prevailed by red light performance (lower and nearer to the red curve) but in low irradiation sites it will be

more dependable on the diffuse component, which is prevailed by blue light performance (relatively higher and nearer to the blue curve) [55].

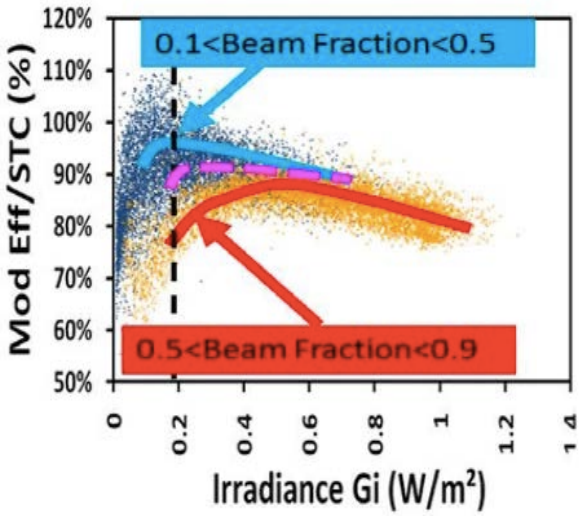

Figure 3.6: DC module efficiency / STC vs. irradiance for a c-Si module at IWES in Germany for clear sky (red) and diffuse (blue) conditions [55]

As was mentioned, both spectral irradiance distribution and temperature influence amorphous silicon module performance while c-Si module performance is mainly influenced by the module temperature. A study in Kusatsu (Japan) on the outdoor performance of a-Si and c-Si modules for the years of 2004 and 2005 demonstrated that the PR of c-Si modules decreased when the module temperature increased and explained the dependence of the output voltage on the module temperature. Further, there were more days with PR above 80% in autumn compared to days in spring, demonstrating the seasonal annealing effect of the a-Si modules. “The recovered performance in summer continued through autumn, demonstrating that a-Si PV modules have a temperature history effect on performance” [72]. The study concluded that the investigation of the outdoor performance of the a-Si modules was more complicated than for c-Si modules due to light-induced degradation and annealing effects. The need for a different evaluation method for a-Si modules from the one used for the c-Si modules was also revealed [72].

A study about the “effects of spectral variation on the device performance of copper indium diselenide and multi-crystalline silicon photovoltaic modules”, at the Department of Physics, Nelson Mandela Metropolitan University, South Africa, showed that both

CIS and multi-Si module have similar behaviour (performance dropped) when the solar spectrum was shifted towards the infrared region. More analytically, the visible region spectrum affects the I_{SC} of the modules more than the infrared region spectrum while the spectrum of the ultraviolet region affects it least. Thus, the decrease of the visible spectrum proportion and the increase of the infrared spectrum proportion in late afternoon spectra cause a decrease in current and consequently a decrease in the system power and efficiency. The infrared radiation is mostly converted as heat to the PV module due to long wavelength photons whose energy is absorbed and converted by a small percentage into current. Moreover, the morning spectra have less infrared radiation compared to the late afternoon spectra. On the other hand, the UV radiation is converted even less to current than the infrared radiation due to the short wavelength of photons [73]. An experimental study for thin film technologies in the UK found that the usable spectral fraction for a-Si ranges from +6% to -9% with respect to the annual average of the global irradiation while CdTe and CIGS had a narrower range of +4 % to -6% and ±1.5% respectively [74].

According to Hamidah et al, field performances of six different grid-connected PV systems installed at Brunei Darussalam, with a nominal power rating of 200 kW each, were analysed following the IEA (International Energy Agency) performance guidelines. The location has a tropical climate with significant insolation fluctuations due to clouds. The field data for mono-Si, multi-Si, a-Si, CIS, microcrystalline (nc-Si/a-Si), and Heterojunction with Intrinsic Thin Layer (HIT) PV technologies were acquired over a one year period. The results were the following [60]:

- CIS system was close enough to its rated performance throughout the year, with the highest efficiency ratio, followed by the a-Si and HIT systems
- a-Si system had the highest array yield and performance ratio, followed by HIT (Array yield: $Y_A = E_{DC} / P_{max}$, where E_{DC} is the array energy output at the DC side.)
- Mono-Si system showed the poorest field performance.

Further, a study conducted under a similar climate in Malaysia for three different PV technologies (mono-Si, multi-Si and a-Si) found that the multi-Si system had the highest PR followed by mono-Si and a-Si systems [75]. However, the results of this study were only for four days, two clear and two cloudy days. On the clear days the c-Si systems had very high PR compared to the a-Si system while in the cloudy days a-

Si had similar PR to the c-Si systems. This is in contrast to the Brunei Darussalam study, which noted that a-Si efficiency was consistent on both clear and cloudy days, while c-Si technology efficiency decreased during cloudy days [60].

Another study about the measured performance parameters of a 1.72 kW mono-Si rooftop grid-connected photovoltaic system in Dublin in Ireland, reported that the annual average daily PR and inverter efficiency were 81.5% and 89.2% respectively (November 2008 to October 2009). Despite the low irradiance levels in Dublin, the average daily specific yield was 2.41 kWh/kW, which was partly attributed to the system design having been optimised with respect to shading, tilt and azimuth angles. The same study also compared the daily specific yield and PR to that reported for a multi-Si system located in Malaga, Spain, which was 3.7 kWh/kW/day and 64.5% respectively. Despite the higher insolation in Malaga, the PR is very low compare to Dublin. This might be due to the high temperatures and their consequent losses in Malaga [76]. It is quite difficult to interpret performance results from different studies, as there are many variables involved in the measurement and calculation procedures. Hence, the more detailed the description of a study, the better the understanding of its results.

In general, it is preferable for the monitoring and the analysis of the PV systems to be made in short time intervals (the shorter the better), because the factors that affect the PV system performance could be identified. A study that presents a model for the performance and fault detection of 27 domestic UK PV systems, which are located in Midlands and Yorkshire regions and recorded in 5-minute intervals, tries to express the effect of faults on the systems performance. The specific model categorises the system faults into four groups. The type of the fault, its category, description and diagnostic method are presented in Table 3.2 [77].

Table 3.2: Description of PV system faults and the four fault categories [77]

Fault	Description	Fault category	Diagnostic method
Component failure	Electricity generation ceases completely due to component failure or breakdown	Sustained zero efficiency fault	Identify faults with zero efficiency (no power output) for long time periods
System isolation – sustained	Electricity generation ceases completely due to the system being isolated (i.e. switched off for maintenance work)		
Inverter shutdown	Electricity generation ceases completely due to a power cut or variation in the grid voltage	Brief zero efficiency fault	Identify faults with zero efficiency (no power output) for short time periods
System isolation – brief	Electricity generation ceases completely due to the system being isolated (i.e. switched off for maintenance work)		
Shading	Solar radiation blocked by external shading objects, i.e. buildings, trees	Shading fault	Identify faults based on the sun positions when the faults occur
Inverter maximum power point (MPP) tracking failure	When MPP tracking causes a significant reduction in efficiency. Also known as 'inverter dropout'	Non-zero efficiency non-shading fault	The faults remaining after the zero efficiency and shading faults have been isolated
Other faults	Other faults that occur, which are not identified as zero efficiency or shading faults		

The results of this study have shown that the systems located in Midlands had an average annual energy loss of 3.6% due to faults while the average annual energy loss for the Yorkshire systems was 18.9%. Hence, the negative influence of the faults to the annual PV production is clearly depicted. Generally, the faults concerning the short durations that a system stops operating could contribute to an annual energy loss up to 23%. Further, the faults regarding the long duration stops of a system and system shading were 58.0% (the maximum annual loss for one system) and 6.9% (7 months of shading for one monitored system) of the annual energy loss respectively [77].

In general, the dust accumulation depends on the dust type, wind speed and direction, humidity, clearness index, last rainfall, the cleaning schedule, the array texture and tilt angle [78, 79]. A paper regarding the performance of a 10 MW PV plant, installed at the

Gujarat Solar Park in India, stressed the influence of the dust on the system performance. The Gujarat environment, where the system is installed, is salty, warm, and humid [79]. The dust reduces the proportion of the insolation that a system could receive due to the scattering of the solar radiation and due to the dust accumulation on the PV array [79, 80]. It is very important, especially for dusty environments, to clean the PV arrays regularly and to take into account the reduction in output due to soiling loss, when a system is studied. Even though the soiling losses in some locations are very low, in other places the soiling losses may contribute up to 70% of the total system losses [71]. The typical estimation of industry regarding the soiling losses is from 1% (in areas of high precipitation) to 4% per year. In a PV soiling experiment conducted in Egypt over a year period, it was found that "the 'one year dusty module' produced 35% lower energy while the 'two month dusty module' produced 25% lower energy compared to the clean module" [53]. An analysis on a grid-connected PV park in Crete in Greece quantified the annual soiling loss to 5.86%, with the winter loss being around 4–5% and the summer soiling loss around 6–7% [53, 78].

Another important factor, which influences the PV system's performance, is the power tolerance of the modules. A common tolerance range for c-Si modules is ±3% while for thin film modules it is ±5%. This uncertainty of the PV modules rated power is due to PV cells power mismatch. Especially for a system, which includes a number of modules, tolerance plays a key role in the field performance evaluation, as the specific yield is used to compare systems installed in the same location. If the tolerance and the uncertainty of the system energy measurement are considered, the total difference between the specific yield of two systems could reach up to 10%. Hence, only with these two uncertainties, it is difficult to achieve an accurate comparison between systems' specific yields [53]. In addition, the mismatch between the modules and the wiring losses of a system contributes at least a 3% loss to the system output power [71].

3.2 IIT Kanpur-Case study

Precise and regular evaluation of PV system performance is vital for the continuing development of the PV industry. During the last 20 years the average PR has been improved from around 0.65 to 0.85 [71]. Apart from the development of the technology, this improvement could also be partly attributed to the PV systems' monitoring. The

main purpose of monitoring is to identify any operational malfunctions. Moreover, a large scale PV system may use monitoring to avoid any economic losses due to operational issues. A detailed monitoring includes, by definition, “an automatic dedicated data acquisition system with a minimum set of parameters to be monitored” [71]. For the manufacturers, performance evaluations indicate the quality of their products. The examination of system performance can also produce important information for future research and can help system installers and customers to evaluate system quality [59]. Finally, operational experience can give an insight into requirements for system maintenance. According to IEA PVPS (Photovoltaic Power Systems Programme) Task 2, the lack of detailed monitoring contributes to the lack of long-term and reliability performance experience. A past (1990s) study in Germany for grid-connected domestic PV systems of 1 to 5 kW found that a statistical failure happened every 4.5 years per system. In these system failures, the percentage contribution of the inverters was 63% while the PV module and BOS were 15% and 22% respectively [71].

This section discusses the short-term performance variations of grid-connected photovoltaic systems installed at a test site at Solar Energy Research Enclave (SERE) of the Indian Institute of Technology in Kanpur (IIT Kanpur), India. This is a new PV research installation built specifically for the purpose of understanding field performance of different PV technologies under Indian conditions. This installation is one of the first in India to have a detailed monitoring system and the analysis takes into account the limited installer experience in the case of sensors and data acquisition systems. The analysis includes three PV system technologies, namely multi-crystalline, copper indium gallium diselenide and amorphous silicon. Kanpur is located in the state of Uttar Pradesh at latitude 26.5 degrees North and has a humid sub-tropical climate. The challenges presented by the operating environment include high ambient temperatures and high levels of dust deposition on the PV array, making regular cleaning essential. Specifically, the Kanpur climate can be classified to tropical wet and dry climates. Normally, weekly cleaning is recommended for moderate dust accumulation and daily cleaning is recommended in the case of intense dust accumulation [78]. In this analysis the main parameters considered to describe the variation in performance of the systems are the PV system final yield and performance ratio, as already discussed in Section 3.1.3 in particular, the difference in yield between fixed and tracking systems is considered for different PV technologies, together with

the operational insights that can be gained from short-term performance ratio variations.

3.2.1 PV systems and monitoring system description

Eight grid-connected PV systems, each of approximately 5 kW rated power, have been installed at the IIT Kanpur, India. The systems are divided into four different PV array technologies: mono-Si, multi-Si, CIGS and a-Si. Each of these technologies is installed on both fixed and tracking structures. The fixed systems are south facing with a tilt angle of 26.5 degrees (same with the latitude angle). The electrical configuration of all the systems is given in Table 3.3.

Table 3.3: IIT Kanpur systems electrical configuration
(* CIGS tracking system has 5 modules less than the fixed system)

System Technology	No of modules	No of modules per string	No of parallel strings	Rated Power	Inverter Type/No of MMPT
a-Si	54	3	18	5.13	HF Transformer/1
multi-Si	22	11	2	5.06	
CIGS*	55/50*	5	11/10*	5.225/4.75*	LF Transformer/1
mono-Si	25	(8+8+9)	3	5.125	HF Transformer/2

Figure 3.7 shows the installation in Kanpur, with the fixed tilt systems in two rows at the front of the compound (to the right hand side of the picture) and the pedestal mounted tracking systems positioned behind them. There are also two small stand-alone arrays positioned to the sides of the fixed systems, but these are not included in this study. The PV systems (based on technology) started operation at different times during 2013. The CIGS systems began operation at the beginning of May, the mono-Si systems at the beginning of July and the a-Si and multi-Si systems at the end of July. Hence, for comparison purposes, the analysis of yield data in this study starts in August 2013. The last data sets considered are for March 2014, although monitoring of the site continues. The analysis of the data from March onwards is not included in this research due to time constraints.

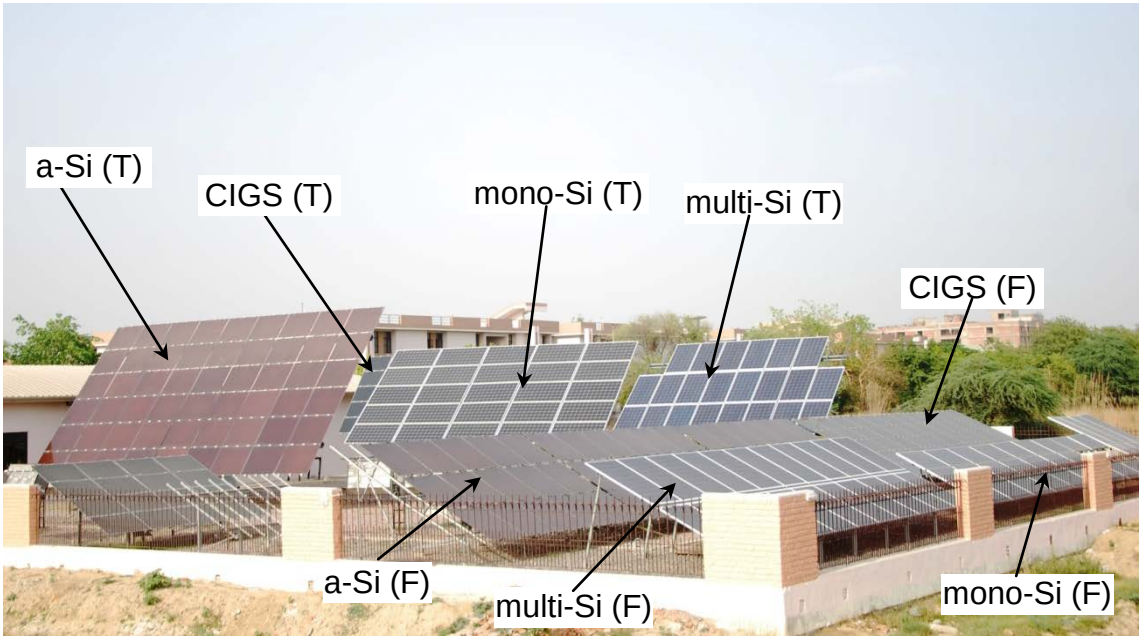

Figure 3.7: The PV systems installed at IIT Kanpur

Daily PR calculations have been made mainly for three months (October, November and February) since due to technical issues there are no weather data before October 2013 and during December 2013. Moreover, useful data were obtained for only 3 out of 31 days in January. These 3 days in January and another 2 days in December have been analysed and their results are integrated in the total sum of the effective days. The term “effective days” defines all the days with a monitoring fraction (MF) ≥ 0.95. Data from periods with a high MF has been chosen for this analysis in order to avoid any misleading results. Table 3.4 presents the number of days considered for the daily PR calculations for each month. Moreover, the last column gives the number of days where ambient temperature readings were available. Finally, the analysis presented here excludes the mono-Si systems due to the small sample of data acquired throughout the analysis period. Nevertheless, an experiment on the effect of the dust in the system efficiency was conducted and focuses specifically on the fixed mono-Si system, because it is the only array technology whose inverter has two MMP trackers. Thus, the effect of the dust, for the specific experiment, was quantified by considering only one string of the mono-Si system, which is directly connected to one MMP tracker. In this way, some of the uncertainties were minimised.

Table 3.4: Effective days for the daily PR calculations

Month	Effective Days (Irradiance measurements)	Effective Days (Temperature measurements)
October	18	18
November	19	19
December	2	2
January	3	3
February	21	8
Total	63	50

Field measurements and weather data are measured through a data acquisition system (DAS) and the data are recorded on a dedicated personal computer (PC). The monitoring system is custom-built for the installation. A software algorithm in National Instruments Labview interfaces the PC with the DAS. Field measurements (voltage, current, and power) are taken at 1-second intervals and then are averaged and recorded at 1-minute intervals. The same procedure is followed for the weather data (normal, horizontal and in-plane irradiance for the fixed and tracking mounted systems, ambient and module temperature, relative humidity, wind speed and wind direction). The sensors and transducers used for monitoring were re-calibrated in December 2013 as a result of offset errors in the measurements. The software algorithm was modified to nullify the offset errors. Hence, the data taken from middle of January onwards are deemed to be improved. Dr. Raghubir Anand, who was an academic project partner in the IIT Kanpur, provided all the data and the information for the monitoring system of the PV systems. This research has analysed the available data, but the staff in Kanpur carried out the design, installation and operation of the monitoring system.

When the PV systems in SERE were installed, there were two pyranometers placed on the a-Si fixed and tracking systems respectively in-plane with the modules. During November 2013, the pyranometer that measures the in-plane irradiation on the tracking systems was transferred temporarily from the tracking to the fixed system in order to correct a calibration error. Hence, the in-plane irradiance values and consequently the performance ratio calculations refer only to the fixed structure PV systems for this period.

A system inspection identified two modules with cracked glass, one each on the CIGS fixed and a-Si tracker systems. This is thought to be due to thermal expansion issues since the cracks are observed to propagate from a fixing point. It is not yet clear whether the damage will affect module performance in the short term, although it could be expected that there will be long-term implications.

The systems are installed on the IIT campus and there is a high level of dust in the atmosphere due to local industry. This requires regular cleaning of the modules to ensure good energy production. Since this is a research installation, all the arrays are cleaned on alternate days during the week. The pyranometers are cleaned less often, giving some uncertainty in the irradiance readings. The module, inverter and pyranometer main specifications of all the grid-connected systems installed at SERE are included in Appendix F.

3.2.2 Difference in energy yield between tracking and fixed PV systems

Generally, the analysis of the energy rating of a system is more complicated than the analysis of its power rating [71]. However, system evaluation based on energy output could be considered more robust than a power-based evaluation [81].

As expected, for all the technologies, the tracking system has a higher energy yield than the fixed system, the relative difference depending on the weather conditions. It has been observed that sometimes, at low irradiation levels, the fixed system production is slightly better than for the tracking systems. This leads to a negative energy percentage difference, with the fixed output as the basis. This can be seen in Figures 3.8 and 3.11, which show the percentage difference in output for the three technologies by day and by the irradiation level respectively during October.

In Figure 3.8, it can be observed that all the technologies follow a similar trend on a day-by-day basis. The lines connecting the data points are included to show this trend and do not express any function or correlation between the values. Further, error bars have been added according to the manufacture tolerance in order to show the uncertainty of the energy difference between the fixed and tracking systems. A few

days in each month show a variation in the trend among the technologies and it is observed that this is due to a difference in the output of the tracking system. For example, on 24th October, the CIGS tracking system yield is greater than that of a-Si and multi-Si tracking systems while the fixed systems have similar energy yields on this day. Particularly, the energy percentage difference of CIGS is around 50% while for the other two technologies is around 20%. On 4th October, all the technologies have a minus energy percentage difference of around 10%. When a negative percentage difference is observed, this occurs on days with low energy yields and so the percentage difference represents a small change in energy, consistent with a combination of measurement accuracy and manufacturer tolerance on module rating. This relative increase in energy output from the fixed systems compare to the tracking may also be a result of the omnidirectional nature of diffuse irradiance.

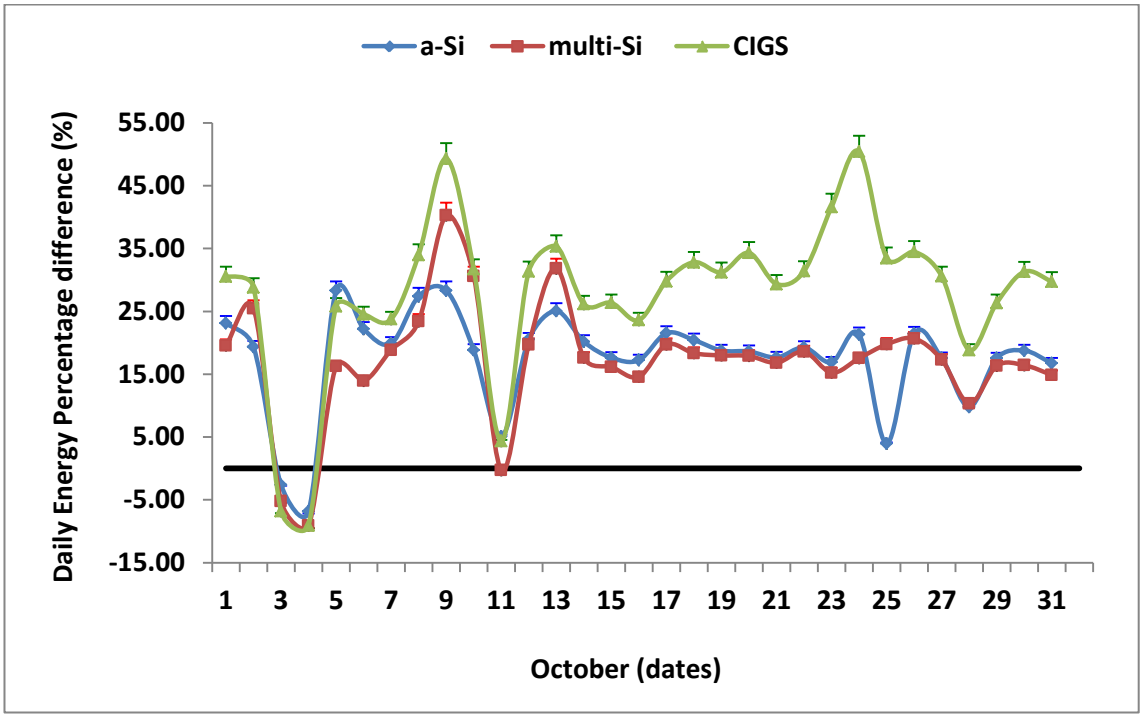

Figure 3.8: Daily percentage energy difference between fixed and tracking systems during October

Table 3.5 shows the specific yield for each technology on these two days. It is observed that on the 4th October even though the energy percentage difference is around -10% for all the technologies, it is a day with low sunlight levels and the fixed PV systems produce slightly more energy than the tracking systems. On the 24th October, CIGS has a much greater energy percentage difference than the other two

technologies, because the CIGS tracking system produces more than the other two tracking systems while the CIGS fixed system has the lowest output compare to the other two fixed systems. This is attributed to shading on the fixed CIGS system by the mono-Si fixed array positioned in front of it and perhaps by the stand-alone system sited on its right side.

Table 3.5: Comparison of specific yield for all the systems on the 4th and 24th of October

Specific Yield	October 4th			October 24th		
	a-Si	multi-Si	CIGS	a-Si	multi-Si	CIGS
	kWh/kW	kWh/kW	kWh/kW	kWh/kW	kWh/kW	kWh/kW
Fixed	0.78	0.82	0.60	4.96	4.75	4.62
Tracking	0.73	0.75	0.54	6.02	5.58	6.94

Figures 3.9 and 3.10 present the specific yield for all the technologies in October for the better understanding of the energy percentage difference values depicted in the Figures 3.8 and 3.11. Again, the lines connecting the data points are included to show the trend of the different technologies.

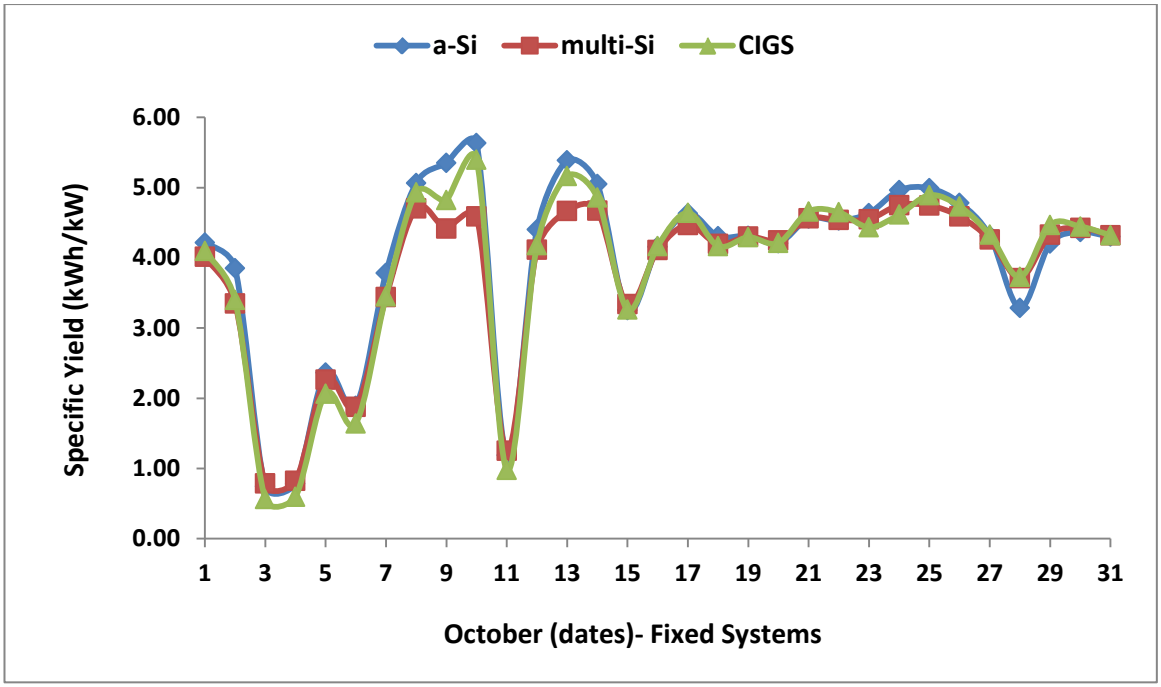

Figure 3.9: Specific yield for the fixed systems in October

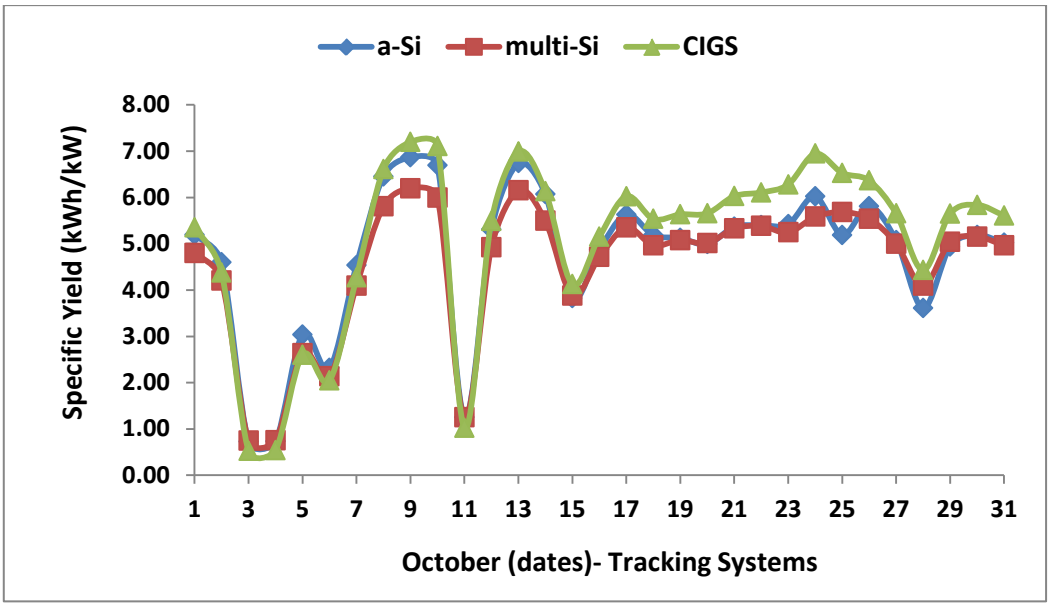

Figure 3.10: Specific yield for the tracking systems in October

Figure 3.11 shows that all the technologies tend to increase their energy percentage difference as the irradiation increases, as would be expected since the percentage of direct irradiation and hence the benefit of tracking also increases. However, the three technologies show differences in rate of change shown by the slopes of the linear fits in the figure.

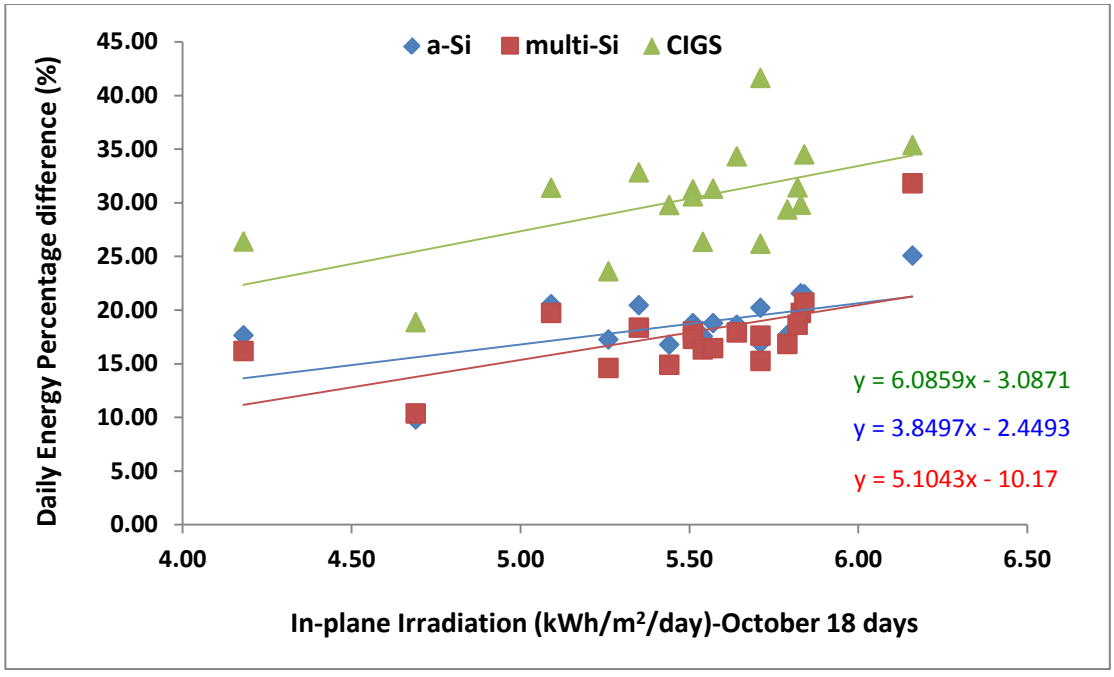

Figure 3.11: Daily percentage energy difference between fixed and tracking structures as a function of daily in-plane irradiation on the fixed structure
(trend line equations for each series are displayed in the respective series colour)

The mean monthly percentage differences are shown in Table 3.6. The mean monthly gain across the whole period for all technologies is 24.08%, but there is significant variation between the three technologies.

Table 3.6: Mean monthly differences between the energy yield of the fixed and tracking structures, expressed as the percentage gain of the tracking compared to the fixed structure

Monthly gain between Tracking and Fixed PV Systems (%)			
	a-Si	multi-Si	CIGS
Aug-13	22.72	19.24	31.96
Sep-13	25.65	28.50	34.02
Oct-13	19.14	19.21	29.76
Nov-13	17.28	16.76	34.48
Dec-13	28.12	15.46	37.58
Jan-14	14.65	10.71	26.21
Feb-14	20.67	16.43	29.45
Mar-14	25.43	20.34	34.24
Mean per technology	21.71	18.33	32.21

There are four possible causes for the difference in behaviour between the technologies. Firstly, different module types have different temperature coefficients. The tracking array will operate at a higher module temperature than the fixed array for most days due to higher irradiance values. The effect on the electrical output will vary depending on the temperature and irradiance. As is observed, the multi-Si array would be expected to have the lowest tracking gain. a-Si would be expected to have a higher gradient of gain with irradiation level, but it is observed to be lower compared to the other technologies, which cannot be explained by the temperature coefficient. Secondly, the close proximity of the installed systems leads to some shading, particularly in the case of the CIGS fixed system, as has been discussed. This leads to a reduced fixed array output and hence an observed higher gain from the unshaded tracking system. Thirdly, the output measurements include the effect of the inverter matching and efficiency, which may differ between technologies. The a-Si and multi-Si systems have the same inverter model whilst the CIGS system has a different inverter model. This aspect requires further investigation to establish its contribution. Finally, the tolerance in module ratings for the different technologies has been considered. The

values in Table 3.6 assume the nominal rating for all modules in both systems. Using the declared manufacturer tolerances, the range of the possible gains is shown in Table 3.7.

Table 3.7: Variation in mean gain as a result of module rating tolerances

Mean gain between tracking and fixed PV systems over all 8 months (%)				
	Minimum Calculated	Nominal Calculated	Maximum Calculated	Nominal Simulated
a-Si	15.91	21.71	27.79	34.20
multi-Si	12.70	18.33	24.25	31.87
CIGS	25.26	31.21	38.83	31.68

The percentage gains shown by the a-Si and multi-Si systems are lower than would be expected for this location according to a system simulation carried out in PVsyst. The same electrical configuration, similar module types (according to the STC) and the PVGIS CM-SAF solar data for Kanpur have been used for the simulations of the three technologies. The module and inverter specifications of all the simulated systems, as long as the input parameters, which have been used for the simulations are included in Appendix G. The simulations gave a monthly gain of around 25%-40% for the same period of the year depending on the month and the technology. The simulated gain shown in Table 3.7 is the mean for the months considered. The CIGS systems results are in line with the PVsyst simulations, but it is known that there is some shading of the fixed system. The temperature data in the simulations has similar values to the measured data, except for December and March when the PVsyst values were 15% and 10% lower respectively, thus lowering the relative tracking gain in practice. The PVsyst irradiation values for October, November, February and March (the months for which sufficient solar data were available) were 18.4-35.8% higher than those measured. This would also result in the relative tracking gain being less in practice compared to the simulation.

3.2.3 PV performance variations

Variations in the daily PR of the PV systems operating in the sub-tropical climate of Kanpur have been examined. As mentioned previously, results are presented only for the fixed systems. Lower PR values are obtained at low irradiation levels, as expected, most likely due to lower inverter efficiency and perhaps some low light level effects at module level. A decrease in the PR of the multi-Si system is also seen at high irradiation levels and is attributed to increased module temperature losses. This is confirmed by examining the dependence of the daily PR on ambient temperature where the multi-Si system shows a decrease at temperatures above 25°C. Neither the a-Si nor the CIGS systems show a noticeable decrease in PR at high ambient temperatures, although they show a greater reduction in PR at low light levels, perhaps due to mismatch with the inverter.

At mid-range irradiation levels, CIGS system has similar PR values to the multi-Si system. Meanwhile, at high and low irradiation levels, CIGS PR values are respectively higher and lower than the multi-Si system. The relatively better performance of CIGS at high irradiation levels is attributed to its lower temperature coefficient. Among the three systems for the analysed period, a-Si has the worst performance since it has the lowest PR values and the difference with the other two systems becomes greater at low and high irradiation levels. The mean daily ambient temperature over the period of these measurements was generally below 25°C, leading to low module temperatures at low irradiance levels and therefore a slower annealing of light-induced defects. Alternatively, the change in performance may be at least partially due to spectral effects [82], although there are no on-site spectral measurements that would allow an assessment of this effect to be made. At high irradiance level, it is likely that the effect is due to a reduction in the electrical efficiency of the module for increasing irradiance. Figures 3.12-3.14 show the calculated daily performance ratio for the multi-Si, CIGS and a-Si fixed systems as a function of daily irradiation.

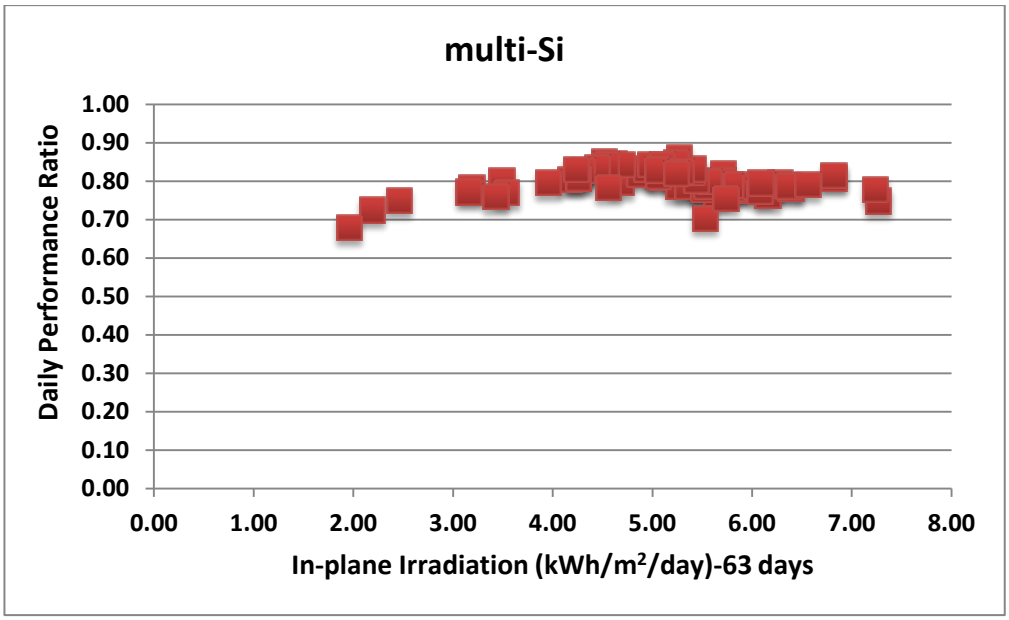

Figure 3.12: Daily performance ratio of multi-Si fixed system vs. daily in-plane irradiation

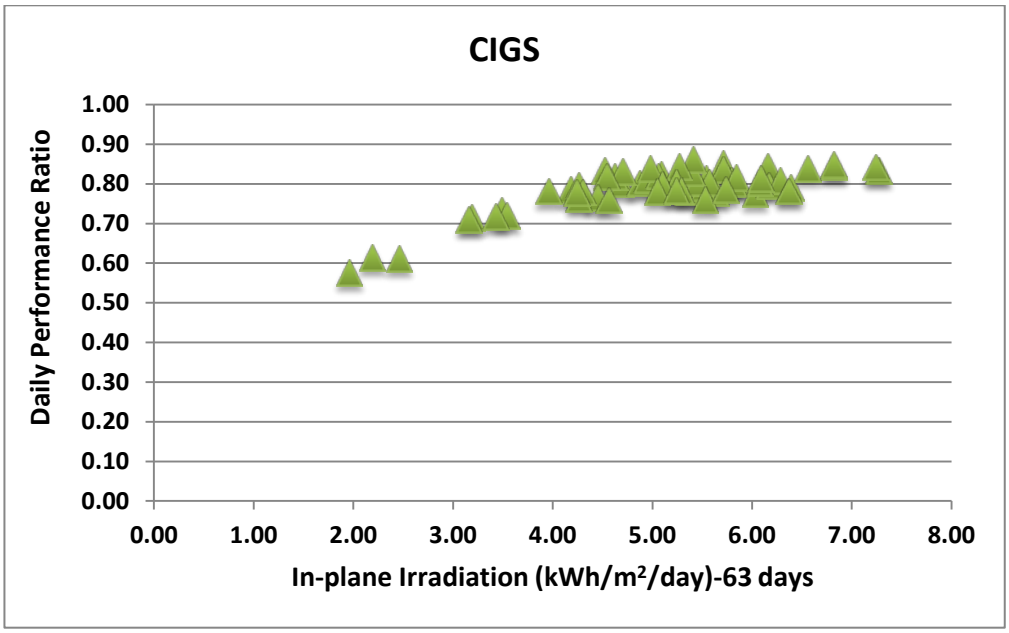

Figure 3.13: Daily performance ratio of CIGS fixed system vs. daily in-plane irradiation

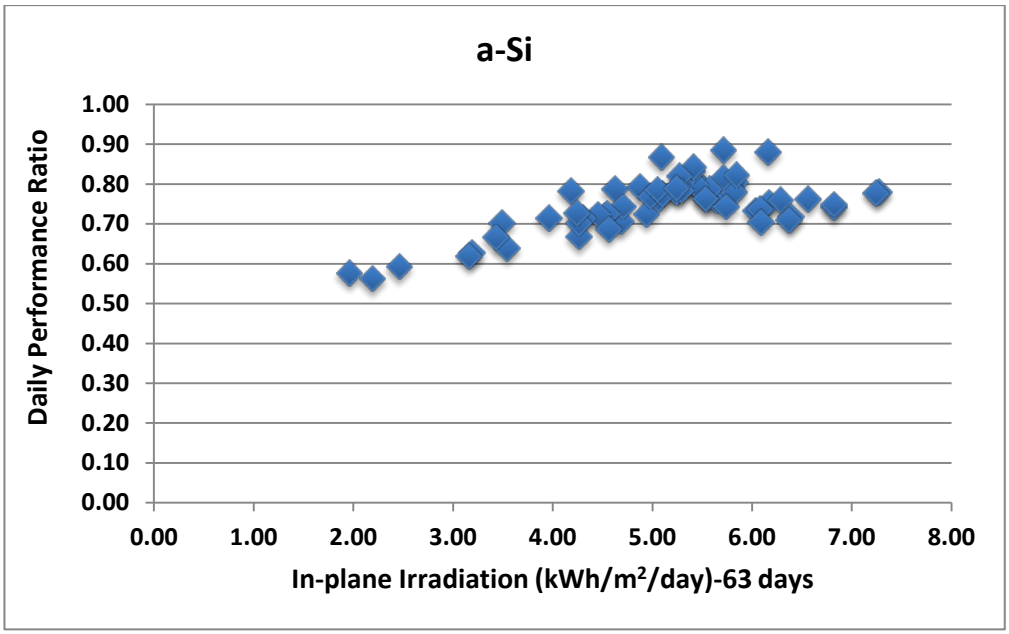

Figure 3.14: Daily performance ratio of a-Si fixed system vs. daily in-plane irradiation

Tables 3.8 and 3.9 below present the in-plane irradiation, ambient temperature, and PR range for all the technologies studied for the relevant months. It also includes the mean PR values from the PVsyst simulations for the same period. During these months the temperature varies by 14°C, which is relatively small, while there is a large range of irradiation values. For the period considered, the mean PR values are very similar to the simulated PR values except for the multi-Si technology, with the simulated value being an underestimate.

Table 3.8: PR range and mean over the studied period plus PVsyst mean PR

	PR a-Si		PR multi-Si		PR CIGS	
	min	max	min	max	min	max
October	0.71	0.88	0.76	0.82	0.78	0.85
November	0.67	0.84	0.81	0.86	0.76	0.86
February	0.53	0.75	0.61	0.78	0.53	0.76
Total mean for all 63 days	0.74		0.78		0.76	
PVsyst mean over the same period	0.75		0.73		0.76	

Table 3.9: Irradiation and temperature ranges over the studied period

	Irradiation (kWh/m^2/day)		Ambient Temperature	
	min	max	min	max
October	4.18	6.16	24.74	27.77
November	4.24	5.41	18.63	26.01
February	1.96	7.27	16.81	20.75
Range for all the effective days	1.96	7.27	14.31	27.77

Figure 3.15 shows the percentage difference between the simulated and the measured values based on the measured values. Particularly, it shows the difference of the in-plane irradiation and the specific yield difference for each technology. The relevant values and their means over these months are included in Table 3.10. Considering the means, it can be clearly seen that the difference in the specific yield is due to the irradiation difference. For these three months, the mean PVsyst irradiation values are around 28% higher. A similar difference is observed in a-Si and CIGS specific yields (around 29% and 27% respectively). Multi-Si system has the smallest yield difference of 21% because the simulated PR value is lower than the measured (Table 3.8). For the studied period, it can be concluded that PVsyst simulations give fair estimates of PR values for both a-Si and CIGS systems while they underestimate the multi-Si system, and that irradiation difference has the greatest influence on the yield difference. However, there is uncertainty associated with the measured values and the fact that the pyranometer was not cleaned as often as the PV arrays. In the latter case, the mean irradiation difference would be smaller and consequently the calculated PR values would be lower.

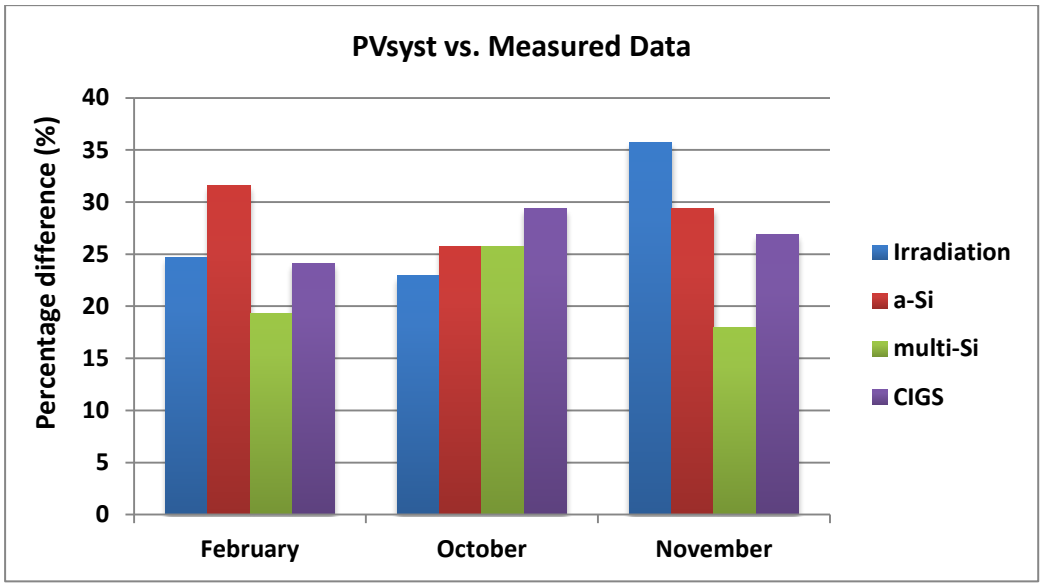

Figure 3.15: PVsyst vs. measured data difference expressed in percentage based on the measured data

Table 3.10: PVsyst vs. measured data difference expressed in percentage based on the measured data

PVsyst vs. Measured data over three months				
		a-Si	multi-Si	CIGS
Month	Irradiation difference (%)	Specific yield difference (%)	Specific yield difference (%)	Specific yield difference (%)
February	24.70	31.62	19.35	24.14
October	22.91	25.75	25.75	29.37
November	35.75	29.39	17.95	26.86
Mean	27.79	28.92	21.01	26.79

3.2.4 Hourly PR variations

This sub-section presents hourly PR results for three selected days in February in order to demonstrate the system performance during the day. More analytically, the days have been chosen based on their irradiance levels (i.e. clear day, partly cloudy and mostly cloudy day).

Figures 3.16-3.18 present the hourly PR for each technology for the selected days. Table 3.11 presents the daily mean ambient temperature and in-plane irradiation. It can be seen that a-Si has poorer performance than the other two technologies on all days. The reduced output of the a-Si array at low and high irradiance values has already been discussed in Section 3.2.3. The CIGS and multi-Si systems have similar performance on the clear and partly cloudy days but on the mostly cloudy day multi-Si performs better. Finally, it is noticed that multi-Si system has the best performance, among all the technologies, during the morning hours when the system starts its operation. The performance difference of multi-Si and CIGS might be attributed to the CIGS inverter threshold and/or the possible shading during the morning hours. Concluding, it can be said that the hourly behaviour for the examined days coincides with the analysis of their daily performance variations presented in Sub-section 3.2.3. A study conducted at Gurgaon (southwest of New Delhi, latitude 28.37° North, longitude 77.04° East) at the Solar Energy Centre of India (now the National Institute of Solar Energy (NISE)) regarding the performance assessment of three different PV array technologies (multi-Si, a-Si and HIT), concluded that in the first year of the array outdoor exposure the HIT had the highest yearly PR followed by a-Si while multi-Si had the poorest performance. However, the experimental facility does not include PV inverters [83]. Hence, the effects of the inverter matching and efficiency to the PV technology performance are not revealed.

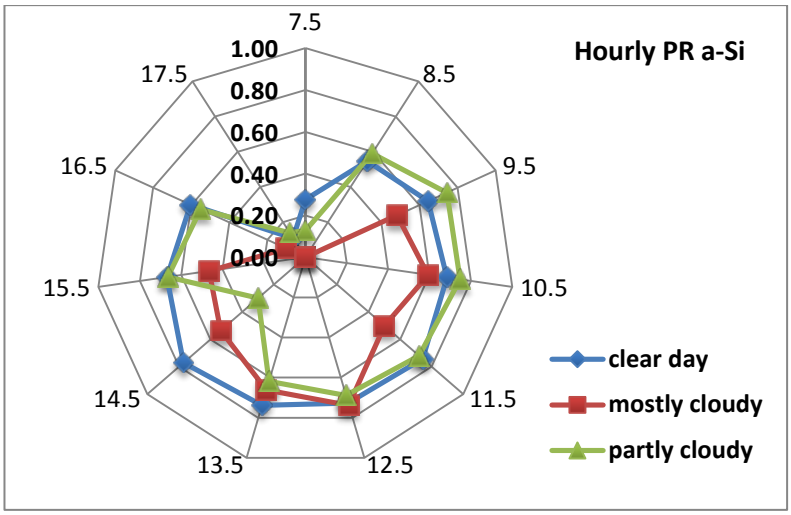

Figure 3.16: Hourly PR for a-Si

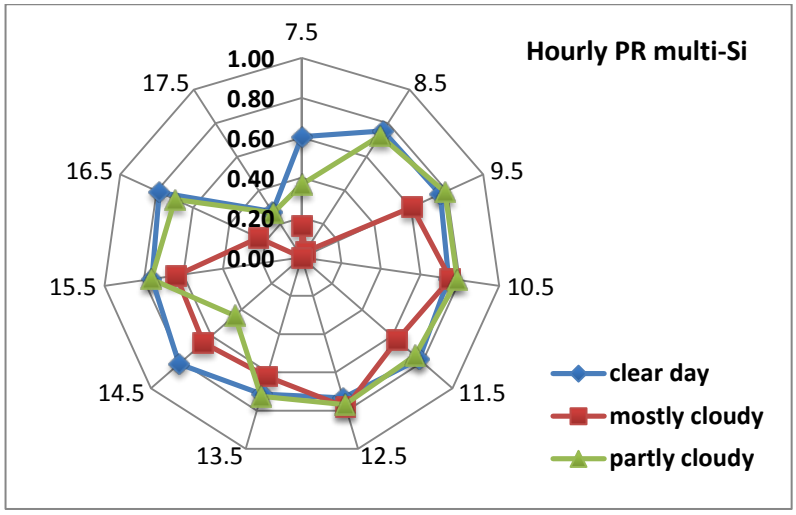

Figure 3.17: Hourly PR for multi-Si

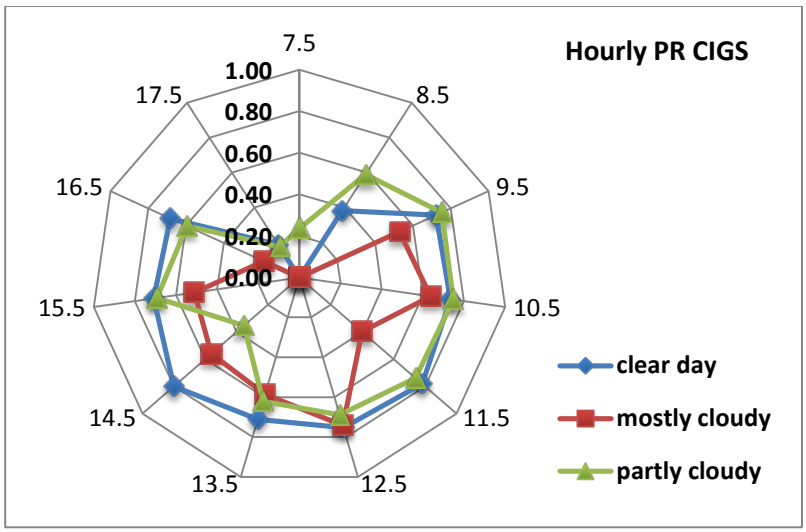

Figure 3.18: Hourly PR for CIGS

Table 3.11: Mean daily irradiation and ambient temperature for the selected days

	Mean Daily Temperature (°C)	Mean Daily Irradiation (kWh/m^2)
Clear Sky	17.90	6.37
Partly Cloudy	19.63	3.43
Cloudy	17.05	1.96

3.2.5 Cleaning experiment

To examine soiling and other non-permanent factors that have an immediate impact on output power, a cleaning experiment was conducted on the fixed PV arrays at SERE. The arrays were cleaned in the morning, allowed two days of dust settling and then cleaned again (on 12th of November 2013). The string current, voltage and power output of all PV systems were recorded along with irradiation and temperature measurements. The pyranometers were not cleaned at the same time as the modules, which should allow the direct effect of the cleaning to be observed. The change in pyranometer soiling during the module cleaning process is assumed to be negligible since the whole cleaning procedure lasts less than an hour.

The effective efficiency, immediately before and after cleaning, was determined for all the strings of the four fixed systems. It was noted that there was some variation in the values obtained at the string level and, in some cases, an apparent reduction in output was observed after cleaning. The electrical configuration of the different arrays has a strong influence on the resulting change in performance, especially where there is performance mismatch between parallel-connected strings [84]. This alters the relative position of the array maximum power point under differing operating conditions and makes direct comparison of before and after readings difficult. The a-Si and CIGS arrays have 18 and 11 strings connected in parallel respectively and, in both cases, significant variation in the current outputs between strings was observed. A possible cause may be relatively heavier soiling of these strings. This is illustrated in Figure 3.19, which shows the variations in string current output for the a-Si array. The string voltages are all equal due to the parallel connection.

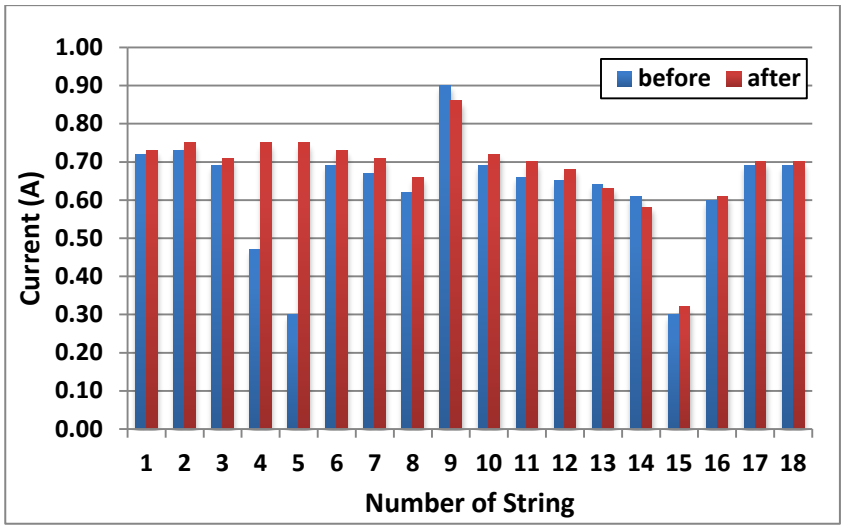

Figure 3.19: a-Si string currents before and after cleaning

It is clear that there is one string with a low current output (String 15) and one with a particularly high output (String 9), but the variation across the strings indicates some mismatch. Similar effects were found from the CIGS array, although with a smaller variation in current levels.

Further analysis was carried out for String 3 of the mono-Si array, since this string of 9 modules is connected to its own maximum power point tracker and thus minimizes the mismatch. There are three factors that affect the increase in efficiency: 1) any change in irradiance between the two measurement times, 2) the cleaning and subsequent increase in irradiance reaching the cells, and 3) the lowering of the module operating temperature due to spraying relatively cool water on the module surface and the subsequent evaporation. The following formulas for the module voltage and current at maximum power point [85] were used:

$$V_{MPP}\,at\,T_i = V_{MPP}\,at\,25\,℃ + [temp.coeff.of\ voltage \times (T_i - 25\,℃)] \quad (3.6)$$

$$I_{MPP}at\,T_i = [I_{MPP}at\,25\,℃ + (temp.coeff.of\ current \times (T_i - 25\,℃))] \times \frac{G_i}{G_{STC}} \quad (3.7)$$

where V_{MPP} and I_{MPP} are the module voltage and current and G_i and T_i are the irradiance and temperature at the instant i.

The module temperatures before and after cleaning were calculated assuming that the impact of irradiance change on V_{MPP} is negligible. The effective irradiance levels reaching the cells before and after cleaning were calculated based on these calculated temperatures and the measured current values. Also, the ideal values of current before and after cleaning, assuming there was no dust and mismatch in the string, were calculated based on the measured irradiance values. The results of these calculations are summarised in Table 3.12. The calculation steps are analytically presented in the Appendix H.

Table 3.12: Results of analysis for string 3 of mono-Si fixed system

	Before	After	Ratio
Measured irradiance (W/m^2)	809.88	834.40	1.03
Measured current (A)	3.88	4.15	1.07
Calculated temperature (°C)	54.37	41.62	0.77
Calculated irradiance (W/m^2)	702.03	754.84	1.08
Calculated current (A)	4.47	4.58	1.02
Percentage difference in current (%)	13.20	9.39	0.71

It was noted that the calculated irradiance values were less than the measured ones. This may be due to uneven dust accumulation or I-V curve mismatches among modules in the string. The after/before ratio of calculated irradiance is higher than that for measured irradiance. This is the impact of cleaning and explains the increase in the measured current post cleaning. As expected, the measured current is closer to the rated current than before cleaning. The percentage difference between measured and calculated currents has been reduced by around 4% post cleaning. Evidently, cleaning increases the current output from the systems. The output power depends on the distribution of the dust [86]. Since the reduction in output with two days of dust accumulation being not so significant, the frequency of cleaning the systems on alternate days was concluded as adequate and it was decided that this cleaning regime would be followed throughout the systems operation period.

Chapter 4: UK and India PV Market and PV Economic Evaluation

Chapter 4 introduces the UK and India PV markets and their policies. It analyses both PV LCOE (Levelized Cost of Energy) and PV economic and financial parameters. Moreover, it presents and discusses the PV LCOE results; the methodology used for the LCOE calculations and the PV economic evaluation for domestic PV systems in the UK and India. Finally, it includes the methodology used for the calculations of the lifetime carbon dioxide (CO_2) emissions savings of the researched PV systems and presents indicative results on the PV system lifetime CO_2 savings.

4.1 UK and India PV markets and their policies

During the last decade PV technology has shown a rapid growth in the global market. The global cumulative capacity of installed PV in 2013 was 138,856 MW compared to 2,635 MW in 2003 [87]. India had a cumulative PV capacity of 1,205 MW in 2012 [88] plus 1,115 MW, which was installed in 2013 [87] equals to 2,320 MW up to the end of 2013. The UK had a cumulative PV capacity of 1,829 MW in 2012 [88] while it reached up to 3,375 MW at the end of 2013 [87]. Further, India has achieved to reach 2.5 GW of utility scale, grid-connected PV cumulative capacity while the total PV installed capacity by June 2014 was around 2.7 GW [89]. By the end of 2014, the UK had reached 5 GW of solar PV installed capacity [9] while India had reached 3 GW [90]. Taking into account the sizes and the solar resource of these two countries, it is obvious that the deployment of PV in India is very small at the moment.

4.1.1 India PV market and policies

India's Jawaharlal Nehru National Solar Mission (JNNSM) was launched in 2010. JNNSM adopted a 3-phase approach for the solar technologies deployment; Phase 1 was until 2012-13, Phase 2 is from 2013 to 2017, and Phase 3 is from 2017 to 2022. The solar capacity targets for each phase are depicted in Table 4.1 below [91].

Table 4.1: Solar capacity targets for each phase in India [91]

Application Segment	Target for Phase I (2010-13)	Target for Phase II (2013-17)*	Target for Phase III (2017-22)*
Solar collectors	7 million square meters (sq m)	15 million sq m	20 million sq m
Off-grid solar applications	200 MW	1,000 MW	2,000 MW
Utility grid power, including roof top	1,000-2,000 MW	4,000-10,000 MW	20,000 MW

Phase 1 was divided in two batches of reverse auctions. The bidding processes included feed-in tariffs (FiT) and long-term power purchase agreements (PPAs) to the selected investors. Table 4.2 summarises the solar capacity of Phase 1 including projects assigned under different schemes and the FiT prices [5].

Table 4.2: Solar capacity of Phase 1 [5]
(exchange rate of 1 Rs= £0.0131, mean rate of Phase 1 (2010-2013) [92]. For example, the CERC tariff for PV in pound sterling for that period would have been £0.23 while the lowest PV tariff would have been £0.14.)

Status of Batch-I							
Schemes		Projects Allotted		Projects Commissioned		CERC tariff (Rs./kWh)	Lowest Tariff discovered (Rs./kWh)
		No	MW	No	MW		
PV projects through NVVN		30	150	25	125	PV – 17.91	PV – 10.95
CSP projects through NVVN		7	470	Schedule to commission by 2013		CSP- 15.31	CSP – 10.49
Migration Scheme	PV	13	54	11	48	-	-
	CSP	3	30	1	2.5		
RPSSGP (PV)		78	98.5	62	76.55	-	-

Status of Batch-II							
Schemes	No	MW	Project Commissioned	Min Rs/KWh	Max Rs/KWh	Avg. tariff Rs/KWh	% Reduction in tariff
PV projects through NVVN	28	350	Schedule to commission by 2013	7.49	9.44	8.77	43%

Generally, there were various incentive schemes in India after the launch of JNNSM. Namely, some of them were: Gujarat Solar Policy Phase 1, Gujarat Solar Policy Phase 2, National Solar Mission (NSM) Batch 1 Phase 1, NSM Batch 2 Phase 1, RPSSGP (Rooftop PV and Small Solar Power Generation Program), Direct RPOs (Renewable

Purchase Obligation) Project, Migration, Generation Based Incentive (GBI), REC (Renewable Energy Certificate) Mechanism, and Demo Project [12]. Specifically for Phase 1, which was completed during 2013, the schemes can be categorised as follows: the Migration, the RPSSGP and the NVVN (NTPC VidyutVyapar Nigam). NVVN is an agency approved by the Indian government in order to fund grid-connected solar power applications. Hence, NSM Batch 1 and Batch 2 projects were selected by NVVN. Batch 1 solar projects were in 2010-11 and their capacity was fixed at 5 MW per project while Batch 2 projects (2012-13) have a minimum capacity of 5 MW up to 20 MW per project. Moreover, the total installed capacity per bidder was limited up to 50 MW. The Migration scheme included solar applications, which started before 2010 in order to give them the opportunity to "migrate" from the former financial arrangements to the schemes proposed by JNNSM. Moreover, the RPSSGP was set for small rooftop plants of capacity less than 2 MW, and it was also assigned under GBI. The GBI equals the difference between the tariff determined by the Central Electricity Regulatory Commission (CERC) or State Electricity Regulatory Commission (SERC) to the base rate of 5.50 Indian Rupees (Rs) per kWh for the financial year of 2010-11 (then is escalated by 3% every year) [5].

In general terms, all the schemes that have been introduced up to date can be sorted in three categories; the schemes under the Central Government of India, the schemes under the individual State Governments and the Renewable Purchase Obligation and Renewable Energy Certificate schemes, which were introduced through the CERC of India for all the renewable energy projects according to the National Action Plan on Climate Change (NAPCC) [93, 94].

Regarding the NAPCC, 15% of India's power has to be generated by renewable energy sources by 2020. Particularly, for solar power the general target is 3% while the SERCs have set individual state targets. The REC mechanism has been introduced in order to fulfil these targets. At the moment, one certificate is provided for every 1,000 kWh of renewable electricity fed into the grid. The obligated entities (utilities, open access buyers of power and large captive power producers) can buy these certificates to fulfil their obligation. So far, this scheme is not successful, since the obligated entities do not always comply with the RPOs and this inadequacy is rarely penalized. Hence, it is possible that this scheme will be revised in the future [93].

Most of the government related incentive schemes have concerned utility-scale grid-connected solar projects in the form of viability gap funding (VGF) or FiT, with the latter preferred by state related schemes as well. The VGF is “a capital subsidy provided to the project developers in order to help them reach a viability threshold at a pre-fixed tariff. The disbursement is linked to performance measures” [93]. Contrary, capital subsidies for rooftop projects or off-grid projects have not been fruitful yet. Finally, tax incentives, such as the accelerated depreciation, have their share in the Indian PV market deployment [93].

Batch 1 of Phase 2 has started and the incentives offered by JNNSM were in VGF form. Moreover, in order to expand the solar market from the utility-scale to medium and small scale projects, JNNSM allocated 50 MW of grid-connected rooftop projects in 2014 while several states “initiated rooftop solar policies and allocations in 2013” [93]. For example, the state of Kerala has initiated a policy for 10,000 rooftop installations of 1 kW each, the state of Gujarat has announced 25 MW of rooftop projects in total, which will be installed in 5 main cities, and the state of Tamil Nadu announced GBI incentives for 50 MW of grid-connected rooftop projects. Further to these, some states have announced plans for net metering policies in order to allow the user to feed power back into the grid. Gujarat state, which is the pioneer state in the solar incentive policies and the first in terms of PV installed capacity, introduced a gross metering policy, according to which all the generated PV electricity is sold to the grid [93]. Specifically for domestic applications, the Ministry of New and Renewable Energy (MNRE) of India has sent a proposal to the Ministry of Finance in order to introduce tax incentives for roof-mounted domestic PV installations. Currently, the owners of such systems do not receive any tax benefits [95]. Finally, 100 MW of PV projects, under the domestic content requirement (DCR) category, are expected to be announced in the near future [93]. DCR policy requires c-Si module technology installations, which is produced by Indian manufacturers. The thin film manufacturing industry in India is still at its infant stage [91].

In addition to solar incentive policies, it should be mentioned that in India the electricity tariffs vary by state and by the type of consumer. A general categorization could be made according to the type of consumer. Hence, commercial consumers such as malls, office spaces, and retail outlets, are paying a commercial tariff around 11 Rs/kWh (exchange rate of 1 Rs= £0.0098, as per September 2014 [96]), which is the

highest tariff among the four categories. Industrial consumers, such as manufacturing facilities, are usually paying the second highest tariff (around 8 Rs/kWh). Residential consumers usually pay around 7 Rs/kWh and agricultural consumers usually receive subsidized tariffs or in certain locations they even receive a full subsidy for their power consumption [12]. The residential segment has the highest energy consumption in India. Hence, the adoption of PV systems will contribute to the grid power deficit. However, as was mentioned above the residential PV market is still at a nascent stage [93].

Concluding, the finance availability is a vital challenge for the Indian solar market that has to be overcome. The two main reasons behind this challenge are the uncertainty of investors regarding the solar market and the lack of knowledge regarding the solar power generation over time. The latter is attributed to the lack of ground solar data and the limited recording of the Indian PV plants. There are many plants in India, which are not performing as expected and there is no clear knowledge on the cause that engendered this operational behaviour [93]. Hence, it is essential for the project developers to concentrate more on the quality of material, the execution, and the maintenance of projects. Further, the recording and the analysis of the data gathered from the PV plants are crucial for acquiring the technical knowledge, which is necessary in order for the expected and the actual PV performance to be compatible. This improvement in the technical knowledge would also influence positively the financial market, as it would provide a more secure investment environment.

4.1.2 UK PV market and policies

The UK solar market has experienced a rapid deployment since 2010. The cumulative installed capacity at the end of 2011 was 875 MW, of which 784 MW was installed in the year [97]. Moreover, UK photovoltaic installation demand continued to rise during 2012, bringing the cumulative PV capacity to 2 GW by early 2013 [98]. However, in January 2011, the UK Government announced an early review of the FiT scheme. On the other hand, in that year (2011) the budget allocated for the Micro Certification Scheme (MCS) by the UK government has been doubled [97]. MCS is an assurance scheme that certifies micro-generation technologies from renewable sources; hence it also includes residential PV systems [99]. The domestic PV FiT rates were reduced from 43.3 p/kWh in 2011 to 14.38 p/kWh (higher rate until 30th of June 2014 [100])

while the tariff lifetime for new installations was reduced from 25 to 20 years [101]. The reduction of the FiT rate affected the timing of installations so as to ensure the highest rate possible is received [97]. Despite the fact that the FiT rates have been reduced, the UK was in the top 10 countries in the world for PV installation demand during 2012 [102] and doubled its annual installed capacity in 2013 becoming one of the main leaders in the European PV market [87]. In addition, Greg Barker, the UK Minister of State for Energy and Climate Change, has stated that he wants "solar energy to provide up to 20 GW of our energy needs by the 2020s" [98]. This represents a significant increase in expectations since the UK National Renewable Energy Action Plan, published in 2010, only estimated a capacity of 2.68 GW in 2020 [103]. Contrary to India's PV market, in which deployment is based on large scale PV systems, the UK is dominated by residential PV systems [104]. However, during 2013 this has started to change and the PV deployment mainly focused on large scale installations [105]. The large scale PV installations have reached 36% of the total solar deployment with a capacity of 1,843 MW by the end of January 2015 [106].

The UK has two main incentive schemes regarding PV systems, the FiT scheme [104] and the Renewables Obligation (RO) scheme [107]. The FiT scheme started in 2010 and had various tariffs depending on the capacity of the PV system and the condition of the building where the system was installed (new build or retrofit) [104]. Currently, there are four main categories based on the PV system capacity. The first three are under the FiT scheme while the fourth is under the RO scheme. Hence, there are feed-in-tariffs for systems up to 4 kW (0.1438 £/kWh), from 4 to 10 kW (0.1303 £/kWh) and from 10 to 50 kW (0.1213 £/kWh). In addition to the generation tariff, there is also an exportation tariff of 0.0638 £/kWh, which is common for all three categories. The aforementioned prices were valid until 30th of June 2014 and the tariff period is 20 years [108]. Note that by the time of the submission of this research the feed-in-tariff for systems up to 4 kW and the exportation tariff have been further reduced to 0.1388 £/kWh and 0.0477 £/kWh respectively (until 31st March 2015) [108].

The Renewables Obligation (RO) scheme was introduced in 2002 in order to provide incentives for the deployment of large scale renewable electricity in the UK [107]. The amount of renewable energy generated by eligible renewable generators is reported monthly to the Office of Gas and Electricity Markets (Ofgem) [109] in order to issue Renewables Obligation Certificates (ROCs) related to the produced amount. By selling

energy to the electricity suppliers, generators are paid for the wholesale electricity cost and the amount of ROCs gathered. ROCs do not have a fixed price, and for this reason their selling price is determined between the supplier and generator. Due to the government financial planning, the value of a ROC for the financial year 2013-14 was set to £42.02 [107]. For the case of PV, the current support (1st of April 2014 until 31st of March 2015) is 1.6 ROCs per MWh for building mounted system and 1.4 ROCs/MWh generated by ground-mounted system. During the following financial years (2015-16 and 2016-17), the ROCs will be reduced by 0.1 every year for both PV categories [110]. Afterwards, "Contracts for Difference" for large scale PV plants will replace the RO mechanism. This scheme is in the design stage at the moment [111].

4.2 LCOE and PV economic evaluation

As the PV technology penetration in the global market increases [87], the cost-effectiveness of PV projects needs to be periodically evaluated. The common parameter used to evaluate the economic feasibility of PV system is the levelized cost of energy. LCOE is also commonly used to compare several different energy sources, so allowing photovoltaic technologies to be compared to other electricity generation technologies [112]. Normally, the photovoltaic LCOE is compared to the retail electricity cost or the wholesale cost of the conventional energy technology, depending on the size and connection details of the PV system. For residential PV systems, a sensible judgment is to compare the LCOE value to the retail electricity cost, which the consumer pays while for large scale PV systems this comparison may be done to the wholesale cost of fossil fuels generators [113]. At this point it should be stated that there are hidden costs associated with the conventional sources of energy such as pollution and impacts on climate change, which are rarely included in this comparison [112,114]. As was mentioned in the introductory chapter of this research, LCOE is the average cost paid to generate 1 kWh of electricity during a given period under the financial parameters valid for PV system operation in that period. Specifically, the average cost per kWh is the amount needed to be paid in order to compensate all the expenditure within the project lifetime.

In general, a PV system can be considered financially viable when it reaches grid parity. The term grid parity, for a domestic PV system, refers to the point at which the PV LCOE is equal to the cost of retail electricity. Although the LCOE value is an

average cost over the lifetime of a project, it is often contrasted with the current electricity cost, which is characterised by volatility [115]. Since the electricity cost has escalated while the PV system cost has dropped, grid parity has already been achieved in some locations in Europe and the USA [113,115].

Individuals may be attracted to invest in a domestic PV system for different reasons based on the expected return on investment. However, in order to make a decision to invest they would have to weigh the climate benefits and the substantial cost of electricity generated by the PV system. Moreover, it should be pointed out that there is a level of inertia in all investments since, even if all the economic indicators support this investment, individuals would have to feel comfortable regarding the stability of the investment and transaction cost. Transaction cost includes all the processes required for the completion of an investment. Hence, there are two criteria, considered in this research, by which an individual can determine viability in installing a PV system. The first criterion examines viability from the point of view of cost of electricity (i.e. if the PV energy cost is lower than the retail electricity cost) while the second takes an economic investment perspective (i.e. whether the investment will be repaid and what will be the return on the investment).

From an economic point of view, grid parity might not be sufficient to influence individuals to invest in a PV system. As with any other investment, there is some level of risk. According to an IEA report, PV plants have low risk characteristics based on their low operation and maintenance cost, short lead times and absence of fuel costs and emissions [116]. However, prospective investors will need to evaluate economic factors other than grid parity before making an investment decision. Two main parameters, which are taken into account for the economic evaluation of a PV system investment, are the Net Present Value (NPV) and the Pay-Back Period of the investment. The NPV defines the suitability of the investment and shows if the benefits would be greater than the costs. Hence, NPV should be as large as possible and always positive in order to invest in a project. Furthermore, the Pay-Back Period is the length of time needed to recover all the project expenditure [117]. Numerical examples of these economic factors are presented in this study in order to demonstrate their connection to the LCOE value of a PV system.

4.2.1 Near-term economic benefits

The near-term economic benefits of a PV system are not analysed in this research, since they are already analysed in the thesis of another PhD student (Mr. Gobind Pillai), whose research is a part of the STAPP project. However, a basic outline is presented and the difference of the near-term economic benefits methodology to the LCOE methodology is stated since it was a collaborative work.

Near-term economic benefits analysis has been made for residential PV systems in India and the UK. It considers the Prosumer Electricity Unit Cost (PEUC) in £/kWh or Rs/kWh that a PV system can have and is defined as:

$$\text{PEUC (£/kWh or Rs/kWh)} = \frac{(TASC + E3 * Elect.C - FIT1 * E1 - FIT2 * E2)}{TEC} \quad (4.1)$$

where TASC= Total annualised system cost, E1= Local PV energy consumed annually (kWh), E2= PV energy exported into the grid annually (kWh), E3= Energy imported from the grid annually (kWh), FIT1= Feed in tariff for local consumption (£ or Rs), FIT2= Feed in tariff for energy exported into the grid (£ or Rs), TEC= Total energy consumed. Hence, the total consumed energy equals to E1+E3, and the total annualised cost of the system equals to annualised capital cost + annualised inverter replacement cost + annual operation cost + annual maintenance cost.

Whereas the annualised cost of a PV system can be found by the combination of the following equations:

Capital recovery factor: $CRF(IR, N) = \frac{IR(1+IR)^N}{(1+IR)^N - 1}$ (4.2)

Annualised cost: $AC = C * CRF$ (4.3)

where N=Project lifetime (yrs), IR= Annual interest rate, and C= Cost.

The PEUC for energy generated by a grid-connected PV system mainly depends on the owner's (customer's) load profile, the PV system's energy generation, the finance of the system, and the grid electricity cost. A PV system could be considered as viable in the near-term when its PEUC is lower than or equal to the grid electricity cost. As many factors (such as capital cost, retail electricity cost, interest rate etc.) influence the viability of a PV system, in the near-term benefits analysis the capital cost and the interest rate are considered as the most important variables and therefore a sensitivity analysis was performed on them in order to express their impact on PEUC values [118].

In the near-term benefits study, the PEUC is expressed as the average cost per 1 kWh of useful energy produced by the system during its first year of operation. At this point, it should be stated that when a system is considered as viable it does not mean that the investment in this system gives profits. A viability study, using PEUC, indicates what a customer with a grid-connected PV system has to pay for a unit of electricity consumed. On the other hand, LCOE expresses the average cost that the consumer has to pay for a unit of electricity generated during the PV system's lifetime. PEUC should not be confused with the levelized cost of energy. LCOE is a metric used to compare different energy technologies by examining the lifetime energy output and the lifetime finance of a generation system.

4.3 LCOE formulae analysis

As was stated in Chapter 1, LCOE is defined as the ratio of the lifetime cost of a project to the lifetime energy production.

$$LCOE = \frac{Total\ Life\ Cycle\ Cost}{Total\ Lifetime\ Energy\ Production} \tag{4.4}$$

There are many types of formula depending on the parameters included in the calculations. In accordance with the "Investment in electricity generation: the role of costs, incentives and risks" report made by the Imperial College on behalf of the UK Energy Research Centre, there are two main methods used for the LCOE calculation.

The first is the “discounting” method and the second is the “annuity’’ method. In the “discounting” method, all the lifetime costs and energy outputs are discounted back to the present value (eq.4.5).

$$LCOE = \frac{\sum_{n=0}^{N} \frac{C_n}{(1+d)^n}}{\sum_{n=0}^{N} \frac{E_n}{(1+d)^n}} \quad (4.5)$$

Where C_n is the costs of the system in year n. When n=0 the cost is equivalent to the initial capital cost. E_n is the energy produced by the system in year n. N is the project lifetime, and d is the discount rate. Regarding this method, the discount of non-financial parameters is a controversial matter [119]. However, in the literature it is reported for the LCOE definition that: “The sum of the present value of LCOE multiplied by the energy generated should be equal to the present valued net costs” (eq.4.6) [115]. Hence, this part of the literature argues that even though it appears that the lifetime energy is being discounted, in reality this result is given by rearranging equation 4.6 [115].

$$\sum_{n=0}^{N} \left[\frac{LCOE_n}{(1+d)^n} \times E_n\right] = \sum_{n=0}^{N} \frac{C_n}{(1+d)^n} \quad (4.6)$$

The equation 4.6 is originated by an NREL document published in 1995 [120]. It actually expresses the net present value of the LCOE while in this study the methodology used for the development of the PV LCOE equation (Section 4.3.1) was based on expressing the average cost of the generated energy throughout the system’s lifetime.

In the “annuity’’ method, the present values of the costs are calculated, and then by the use of an annuity formula, they are converted to an equivalent annual cost. Furthermore, the denominator of this equation is the average annual energy output over the lifetime of the project (eq.4.7).

$$LCOE = \frac{\sum_{n=0}^{N} \frac{C_n}{(1+d)^n} \times \frac{d}{[1-(1+d)^{-N}]}}{\frac{\sum_{n=1}^{N} E_n}{N}} \quad (4.7)$$

According to the Imperial College report, the two methods stated above should give the same LCOE values when they use the same inputs. However, an investigation of these two formulas proved that the LCOE would be the same only if the annual output of the energy source is constant over its lifetime. This is not the case for renewable energy sources and consequently for the PV systems, since their energy output varies continuously [119,114]. Additionally, the implementation of these two methods considering a 3 kW domestic PV system located in the city of Newcastle resulted in LCOE values that are equal to 0.1808 £/kWh for the "discounting" method and 0.1824 £/kWh for the "annuity" method. Even though these methods do not have the same LCOE values, after the conduction of an uncertainty calculation, the two values do not appear to have a significant difference. For the case of Newcastle, if the LCOE was calculated without discounting the lifetime energy (eq.4.8), it would be equal to 0.1203 £/kWh (using the same inputs as in the other two equations). These three numbers reveal the differences in the LCOE values only by using different types of formulas. Analytical calculations using the different LCOE formulae are presented in Appendix I.

$$LCOE = \frac{\sum_{n=0}^{N} \frac{C_n}{(1+d)^n}}{\sum_{n=0}^{N} E_n} \quad (4.8)$$

Finally, apart from the various formulas that can be formed in order to compute the LCOE, there are simulation software packages such as the System Advisor Model (SAM) [121], RETScreen [34] and HOMER [122] that can calculate the levelized cost of energy or provide PV system economic analysis based on the given inputs. All of them make an economic assessment of renewable energy projects by using financial models. Hence, from the aforementioned discussion it is obvious that by acquiring an LCOE value for a system cannot provide enough information if the calculation method is not known. Further, the LCOE for a PV system in a specific location can be computed as a single number, a range of numbers or a statistical distribution [112, 113, 115]. The LCOE formula includes several variables, which may be subject to uncertainties given that these variables would be assumed for the lifetime of the project. Hence, it would be more appropriate for the LCOE values not to be treated as

a single number and a sensitivity analysis to be conducted in order to account for these uncertainties [115].

4.3.1 LCOE formula development

The LCOE parameters are strongly dependent on the location and size of the PV system and current market policies and prices. There are two main categories: the lifetime finance and the lifetime energy production. For lifetime finance, the parameters include the system installation cost, financial factors (inflation and discount rates), operation and maintenance costs, support mechanisms, insurance, taxes, loans (equity/debt ratio), credits, depreciation, carbon credits, etc. For lifetime energy production the parameters include the irradiation and temperature values, PV system conversion efficiency (dependent on selected technology), PV system electrical and mechanical design, PV system degradation rate, reliability and operational issues (e.g. shading) etc. These parameters may not all be included in the LCOE formula, but those incorporated should be clearly stated [115]. The formula used to calculate the LCOE values for domestic PV systems in the UK is the following:

$$LCOE = \frac{\sum_{n=0}^{N}[C_n \times (\frac{1+i}{1+d})^n]}{\sum_{n=0}^{N}[E_n \times (1-D)^n]} \quad (4.9)$$

where C_n is the cost of the system (expressed in £ sterling) (installation, module, electrical equipment, inverter, finance, operation and maintenance (*O&M*) etc.) in year *n*. When *n*=0 the cost is equivalent to the investment cost (C_0). E_n is the energy produced by the system (expressed in kWh) in year *n* and E_0 is energy production in the first year when no degradation is applied. *N* is the system lifetime (expressed in years), *i* and *d* are the inflation and discount rate of the investment (expressed as fractions representing percentage change per annum) and *D* is the annual degradation rate of the system energy output (expressed as a fraction representing percentage change per annum). The equation developed for the LCOE calculations is presented analytically below:

$$LCOE = a - b - c - d \quad (4.10)$$

where

$$a = \frac{C_0 + \sum_{n=0}^{N}[O\&M \times (x)^n] + [Inv.RC \times (x)^{12}]}{\sum_{n=0}^{N}[E_n \times (1-D)^n]} \quad (4.11)$$

$$b = \frac{\sum_{n=0}^{N}[Elect.C \times (x)^n] \times \sum_{n=0}^{N}[\frac{E_n}{2} \times (1-D)^n]}{\sum_{n=0}^{N}[E_n \times (1-D)^n]} \quad (4.12)$$

$$c = \frac{\sum_{n=0}^{N}[Gener.T \times (x)^n] \times \sum_{n=0}^{N}[E_n \times (1-D)^n]}{\sum_{n=0}^{N}[E_n \times (1-D)^n]} \quad (4.13)$$

$$d = \frac{\sum_{n=0}^{N}[Export.T \times (x)^n] \times \sum_{n=0}^{N}[\frac{E_n}{2} \times (1-D)^n]}{\sum_{n=0}^{N}[E_n \times (1-D)^n]} \quad (4.14)$$

The equations 4.11-4.14 express the possible cash flows of the investment divided by the lifetime energy of the system in order to be consistent with the LCOE definition. As a PV system could be considered as an investment, when the costs are calculated, the benefits-returns may also be included. Hence, equation 4.10 separates the cost and the benefits of a PV system investment into four different components explained in more detail below. The variable *x* in equations (4.11-4.14) is equal to *(1+i/1+d)* and represents the nominal discount rate (combination of inflation and discount rates).

$$x = \left(\frac{1+i}{1+d}\right) \quad (4.15)$$

A very important choice for the LCOE calculations is the discount rate since it directly affects all the costs of the LCOE, converting them into their present values. Generally, the real discount rate does not include inflation while the nominal discount rate takes

this into account [112]. The methodology of this study considers both discount and inflation rates resulting in the nominal discount rate (eq.4.15). Increasing the nominal discount rate, while leaving the other parameters steady, the present value of the lifetime costs and financial benefits will increase and vice versa. This will affect the LCOE value, as a high nominal discount rate will result in high lifetime costs and benefits. For the case of PV, the investment cost (C_0), which is the greatest cost for a PV system, is not influenced by the nominal discount rate. Hence, the parameters of the LCOE formula are dominated by the financial benefits. Thus, a high nominal discount rate would be more beneficial for the cost of the generated energy. On the contrary, if the LCOE formula does not account for financial benefits, then the lowest possible nominal discount rate, would offer the lowest LCOE values.

The inverter of the system would have to be replaced at least once during the system's lifetime. Normally, inverters have shorter lifetimes than the PV modules and their lifetime depends on their operating conditions. A realistic assumption that could be used for the inverter lifetime is around 12 years [123]. Hence, the inverter replacement cost (*Inv.RC*) has been calculated for the 12^{th} year of its operation, assuming that the basic cost of the inverter is unchanged. Although it is unlikely the basic cost of the inverter to be the same after 12 years, this is a reasonable assumption as the calculation of the inverter replacement cost includes long-term inflation and discount rates based on the countries examined.

The LCOE formula applies mathematical relationships defined for the case of the UK, since India's residential PV market and policies are not clear yet. However, the formula is slightly modified for the Indian LCOE calculations according to the current Indian status. The modifications are explained in Section 4.5. In equation 4.10, the first term includes all the present values of the lifetime costs of the system divided by the lifetime energy i.e. the net cost/kWh without any benefits. The other three terms are related to the financial benefits that can be gained from a domestic PV system under the current PV supporting policies in the UK. Consistent with the FiT scheme for the grid-connected residential PV systems, half of the energy produced by the system is assumed to be exported into the grid and the other half is consumed in the residence. This means that half of the generated electricity is transformed into energy savings, which reduce the electricity bills of the household based on the retail electricity cost (*Elect.C; eg. 4.12*). Additionally, the FiT scheme for the residential PV systems offers a

generation tariff (*Gener.T; eg. 4.13*) for the generated energy by the PV system and an export tariff (*Export.T; eg. 4.14*) for the exported energy into the grid. Hence, the second term gives the savings from the electricity consumption throughout the lifetime of the system, the third term gives the lifetime income through the generation tariff, and the fourth term gives the lifetime income through the export tariff. The combinations of these terms resulted in the different scenarios used for this study.

4.4 LCOE for domestic PV in the UK

The scope of the methodology presented in this section is the investigation of the domestic PV system economic potential in the UK under the current PV market prices and policies (financial year 2013-14), using LCOE values to explain the outcomes. The results and the methodology of this study have been published in 2014. However, the journal paper was submitted in 2013 and it uses the year 2012 as the base year of the LCOE calculations [124]. The results presented in this thesis are based on the same methodology, but using revised figures for the financial year 2013-14. Moreover, a comparison between the "2012 LCOE" to the "2014 LCOE" is presented along with the revised results in Section 4.4.2.

4.4.1 LCOE methodology for the UK

Optimum LCOE values, based on maximizing energy output, have been calculated for twenty cities around the UK. The optimization sets a lower limit to the LCOE values that can be derived using the different assumptions and methods. The results demonstrate the best-case scenarios for domestic PV systems under realistic assumptions, providing a useful tool that contributes to decision making. The study uses the revised UK solar data (irradiation and temperature; CM-SAF solar database [16, 43]) and the annual energy output of a 3 kW domestic, optimally designed grid-connected PV system acquired by the PVSyst software (Version 5.31) [17] (presented in Chapter 2). An annual degradation rate of PV system performance of 0.5% was used, in accordance with the literature [115]. The cost variables considered are the capital cost of the system, operation and maintenance costs, the inverter replacement cost, the FiT rate for domestic PV systems in the UK, the average retail electricity cost, and the financial factors (discount and inflation rates).

For the “2012 LCOE” study, the installation cost and the O&M cost for the system were taken from the UK Department of Energy and Climate Change (DECC) reports on the average cost of PV systems installed under the FiT scheme, published in 2012 [125, 126]. The installation cost varies with time and, in particular, has been reduced since the time that this study took place [127, 128]. For the O&M cost there has been no updated figure published till the date of writing the thesis, hence the same figure has been kept for the “2014 LCOE” calculations. The FiT has been reduced while the retail electricity cost has increased since 2012.

The installation and O&M costs are UK specific, so they are assumed to account for the system’s soft costs (permitting, labour cost etc.). The inverter cost was taken from the SMA Company, since an SMA inverter model was used for the system simulations [129]. The FiT rates of 15.44 p/kWh-generation tariff and 4.5 p/kWh-export tariff were used in the “2012 LCOE” calculations (valid until 30th of April 2013) while the FiT rates for the “2014 LCOE” were 14.38 p/kWh and 6.38 p/kWh respectively (valid until 30th of June 2014) [130]. The generation tariff has been reduced by 1.06 p/kWh while the retail electricity cost has increased by 0.81 p/kWh from 14.39 p/kWh to 15.20 p/kWh during the period from February 2013 to December 2013 [131, 132].

Generally, in the beginning of 2013, all of six major UK energy suppliers increased their gas and electricity prices by 6% to 11% while at the end of that year four out of the six suppliers announced a further increase in the range of 8.5% to 11.1% [133]. Particularly, in accordance with the Office for National Statistics: Consumer Price Index, the electricity prices rose by 7.1% during the last year (December 2012 to December 2013) while for the year before (December 2011 to December 2012) they had increased by 3.9% [134, 135]. All cost values presented in this study include VAT at the appropriate rate. Table 4.3 summarises the values used in both LCOE calculations, apart from the annual energy output of each city. The starred values and references are for the 2012 base-year.

Table 4.3: Summary of the values used in the 2012 and 2014 LCOE analysis for the UK (*the starred values refer to the 2012 base-year)

project lifetimes in years (*N*): 25, 20, 20+5	installation cost (£): *7692, 6240	Source: Department of Energy and Climate Change [*125, *126], [127, 128]
inflation rates % (*i*): 3, 6	annual O&M cost (£): 45	
discount rates % (*d*): 3.5, 0.5, 7	inverter cost (£): *970, 755	Source: SMA Inverters [129]
annual degradation rate % (*D*): 0.5	electricity cost (£/kWh): *0.1439,0.1520	Source: Energy Saving Trust and [*131], [132]
generation tariff (£/kWh): *0.1544,0.1438	export tariff (£/kWh): *0.045,0.0638	*Costs Base Year: 2012 Costs Base Year: 2013-14

This study considers three different values for the discount rate and two different values for the inflation rate, i.e. six different values for the nominal discount rate (*x*). The choices of the discount rates have been made according to the UK market standards. Their values are 3.5%, 0.5% and 7% per annum. The 3.5% discount rate represents the social time preference rate for long-term investments according to the HM Treasury [136]. The 0.5% discount rate represents the annual interest rate in a regular bank account while the 7% discount rate represents a significantly higher interest rate than the currently existing ones. This 7% discount rate was chosen in order to show its effect on the results. Moreover, the choices of the inflation rates are 3% and 6% per annum. The value of the 3% was chosen because historically, from 1989 to 2014, the United Kingdom average inflation rate was 2.78% [137]. The 6% inflation rate is an assumption based on the escalation of the retail electricity costs in the UK [133-135]. The financial parameters have been kept steady in both LCOE calculations.

The sensitivity analysis of this work focuses on the financial factors and the project lifetime. The inflation and discount rates influence all the costs while the project lifetime influences the lifetime energy production. Six scenarios were considered with eighteen numerical combinations, using different values of discount rate, inflation rate and project lifetime. Table 4.4 summarises all the scenarios and their cases.

Table 4.4: Summary of the LCOE scenarios and cases for the UK

Scenarios:	
A	LCOE with FiT and savings from the electricity consumption for both 20 and 25 years (the generation tariff is paid for the 100% of the PV generated electricity while 50% of the PV generated electricity is consumed domestically and the other 50% is paid with the export tariff)
B	LCOE without FiT or savings from the electricity consumption for both 20 and 25 years (Net PV cost)
C	LCOE with exporting half of the generated PV energy and consuming the other half for both 20 and 25 years (no generation tariff is applied while 50% of the PV generated electricity is consumed domestically and the other 50% is paid with the export tariff)
D	LCOE 20 years FiT & electricity savings + 5 years export tariff and electricity savings (same as A for the 20 years but for the 5 remaining years only 50% of the PV generated electricity is consumed domestically and the other 50% is paid with the export tariff)
E	LCOE 20 years FiT and electricity savings + 5 years with no benefits (same as A for the 20 years but for the 5 remaining years only net PV cost is considered)
F	LCOE 20 years FiT and electricity savings + 5 years electricity savings (same as A for the 20 years but for the 5 remaining years only 50% of the PV generated electricity is consumed domestically)

Cases:		
	Inflation rate	Discount rate
1	i=3%	d=3.5%
2	i=3%	d=0.5%
3	i=3%	d=7%
4	i=6%	d=3.5%
5	i=6%	d=0.5%
6	i=6%	d=7%

In Scenario A, LCOE values are calculated for both 20 and 25 years of lifetime including the FiT payments and the savings from reduced electricity purchases. Scenario A presents the situation where the PV system operates for either 20 or 25 years under the FIT scheme. Scenario B represents LCOE values without including either FiT payments or savings from electricity purchase, i.e. the net cost of the generated energy. Scenario B was chosen in order to demonstrate the net cost of a PV system investment as a source of energy. Scenario C assumes no FiT payment but includes the benefits of exporting 50% of the generated energy and consuming the

other 50%. Scenario C presents the situation where the generation tariff is stopped but the owner receives benefits from both use and sale of the electricity generated. Respectively, Scenarios D, E and F concern the 20+5 years of the project lifetime, where the current FiT duration is considered but the system continues to operate for another 5 years without FiT payments. Scenario D includes the benefits of exporting 50% of the generated energy and consuming the other 50% after 20 years of the operation. Scenario E does not include any benefits for the last 5 years while the Scenario F includes only the savings from the electricity purchase. Furthermore, the PV system may operate more than 25 years, although this option has not been considered in this analysis, as its performance after the 25 years differs from case to case and cannot be easily predicted.

4.4.2 Results and discussion for the UK LCOE

This section presents and discusses the LCOE results for 20 UK cities based on the scenarios and the sensitivity analysis made. A negative bias in the LCOE values means that for every kWh generated by the PV system, there is a profit of the stated amount. A positive bias represents the cost that has to be paid for the generation of one kWh by the PV system. If the LCOE value equals zero, it shows that there are neither profits nor costs of the PV generation. In economic terms, a zero LCOE equates the project lifetime with the payback period to recoup the investment.

As might be expected, the 25-year cases are more beneficial than those for 20-year FiT payments. Figures 4.1 and 4.2 show the LCOE ranges for Scenario A for 25-year and 20-year lifetimes. All other parameters, including the annual irradiation levels for each site, are unchanged. For Scenario A, Glasgow has the highest LCOE value occurring for the 3rd case (i=0.03, d=0.07) for the 20-year lifetime. From an economic perspective, this would mean that it is unprofitable to install a domestic PV system in Glasgow under the current FiT scheme because the investor would not receive benefits from the generated electricity (LCOE= -0.02≈ 0 £/kWh). This indicates that the payback period of the investment would be slightly lower than the project lifetime. It is around 24 years accounting for the export tariff and the savings from the electricity consumption for every year that the system operates after the 20-year period. In the initial analysis for the base-year 2012, specifically for Glasgow and for the 3rd case in Scenario A, the investor would have to pay 1.15 p/kWh. Hence, it is obvious that the 1.17 p/kWh

reduction in the LCOE between 2012 and 2014 base-years is attributed to the installation cost reduction, since the FiT rates have been reduced. Nevertheless, Glasgow still benefits from an energy cost point of view in both base-years. The FiT and export payments reduce the overall cost of the energy from the PV system to below the retail cost. On the other hand, Brighton has the lowest LCOE value in the 5th case (i=0.06, d=0.05) for the 25 years of project lifetime (Figure 4.1). In this case, the investor's benefit would be 37.81 p for each kWh generated by the PV system while for the base-year 2012 it was 34.84 p.

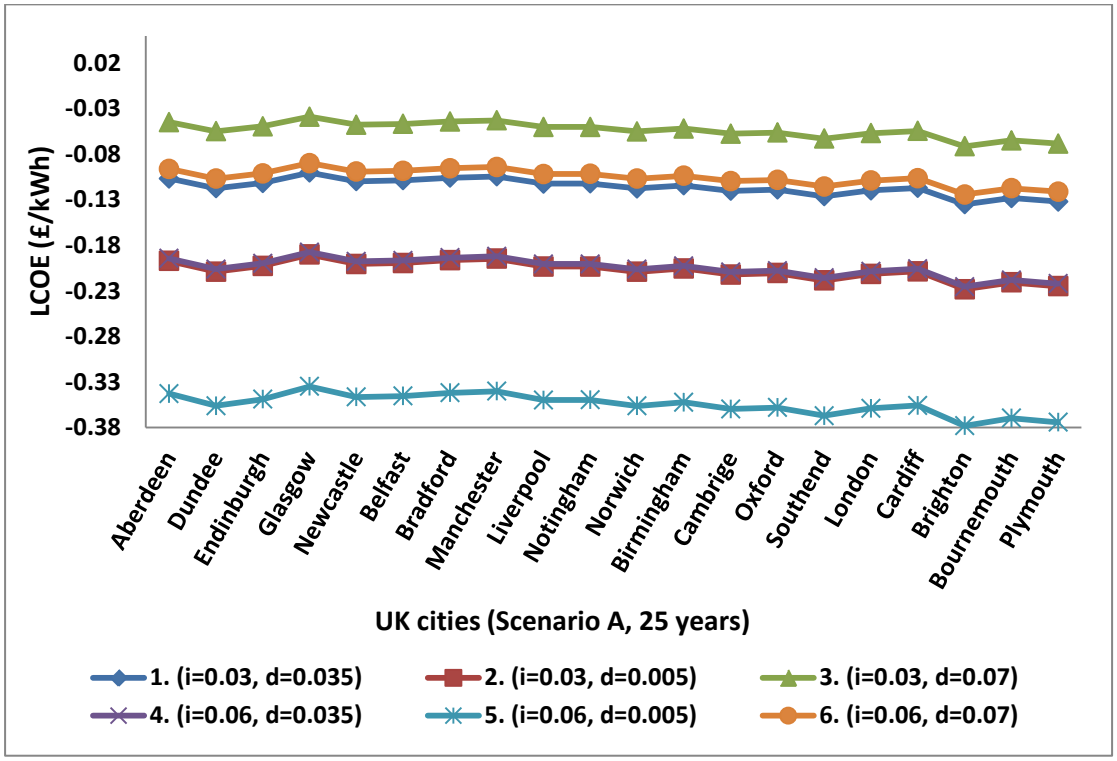

Figure 4.1: LCOE with FIT and Electricity Savings (N=25 yrs)

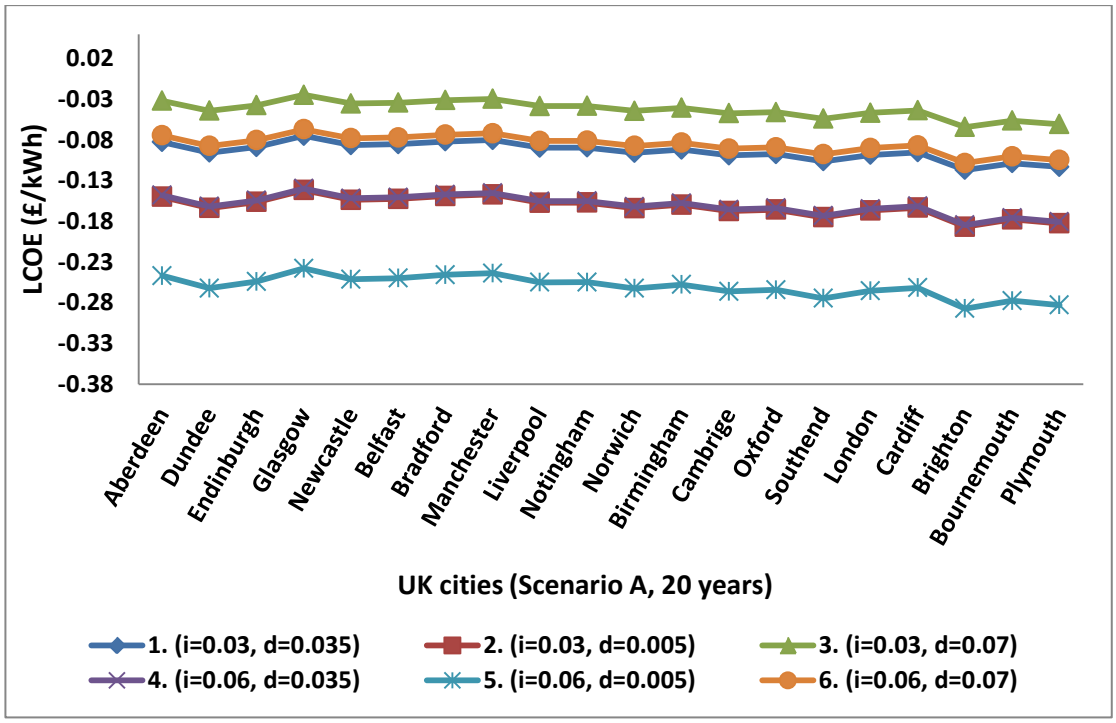

Figure 4.2: LCOE with FIT and Electricity Savings (N=20 yrs)

Figures 4.3 and 4.4 present the LCOE values for Scenario B for 25-year and 20-year lifetimes. As has been discussed, Scenario B depicts the net cost per kWh without considering any supporting mechanisms. According to this scenario and for 25 years lifetime, all the cities can achieve grid parity for all the cases apart from the 5th case where 10 out of 20 UK cities can achieve grid parity. If the PV system operates for 20 years, the number of cities, which can reach grid parity, varies among the different cases and it is obvious that the southern cities can reach grid parity in more cases than the northern cities (Figure 4.4). In contrast, for the base-year 2012 and for 20 years lifetime, only Brighton could reach grid parity and only for the 3rd case. Apart from the installation cost difference of the two base-years, this is also attributed to the increment of the retail electricity cost, which contributes to the LCOE value by the electricity savings benefits and also raises the grid parity limit (from 14.39 p to 15.2 p) by its increment.

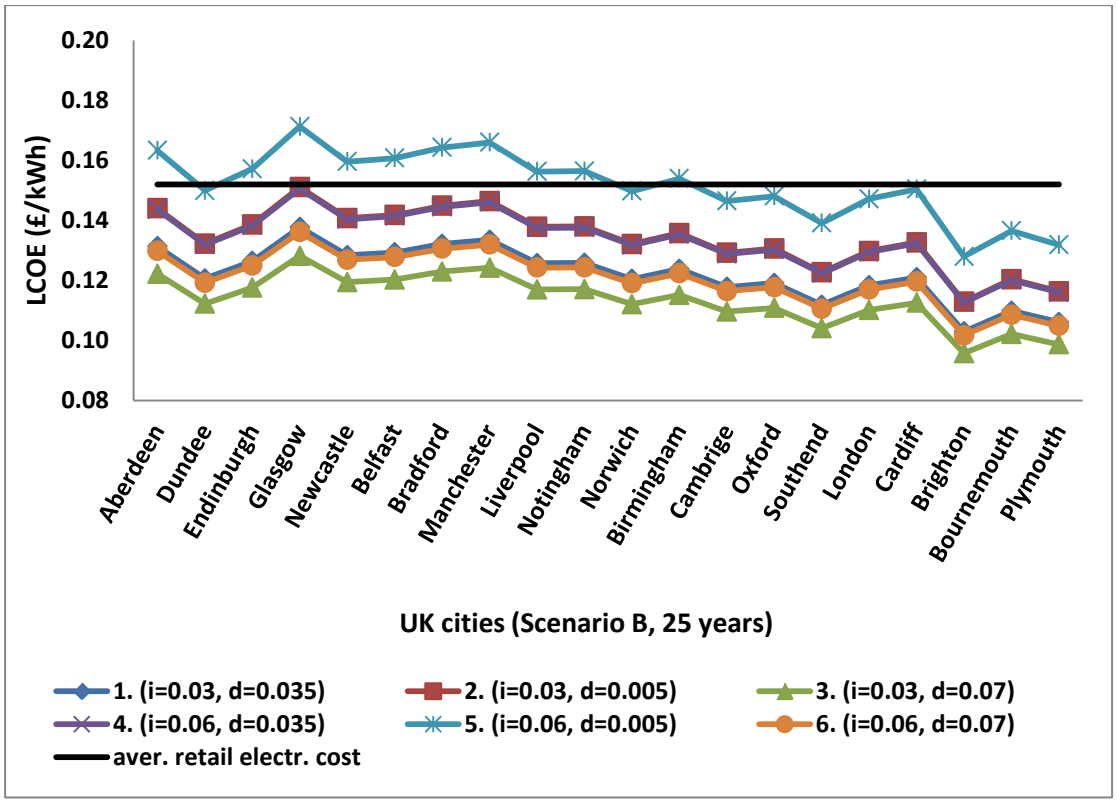

Figure 4.3: LCOE without both FIT and Electricity Savings (N=25 yrs)

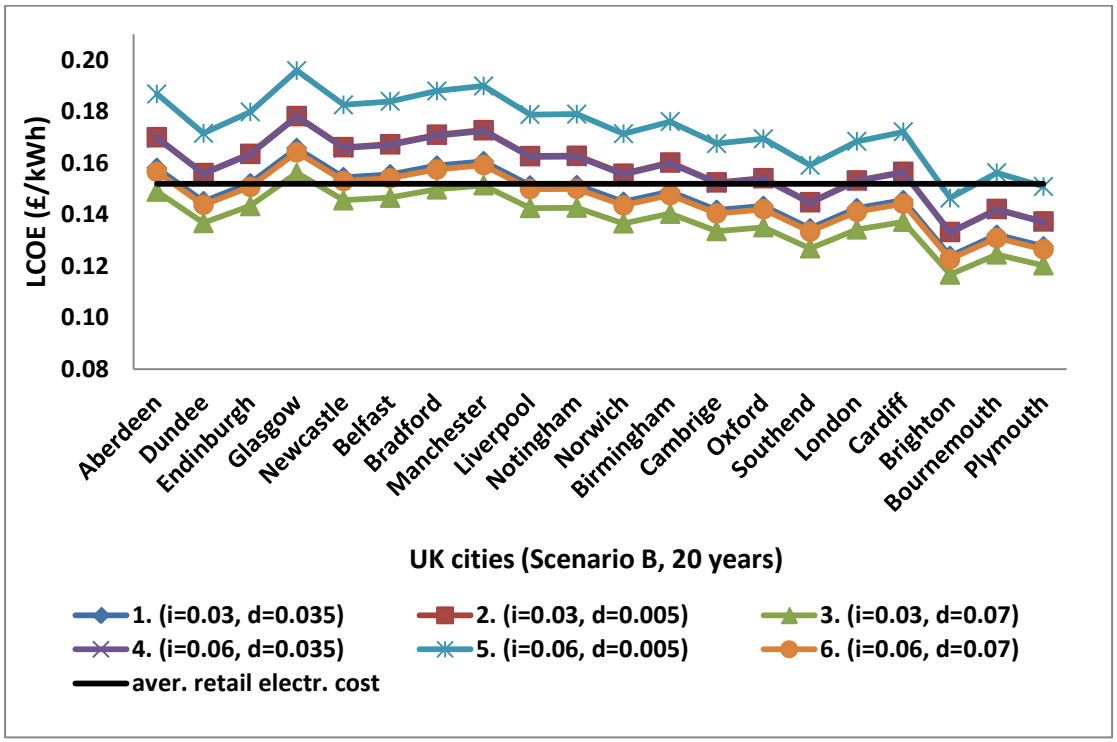

Figure 4.4: LCOE without both FIT and Electricity Savings (N=20 yrs)

Scenario C assumes that the only benefits throughout the system lifetime would be the export tariff for the half of the generated energy and the electricity savings for the other half. In this scenario, grid parity could be achieved for all the cities; however, from the 12 cases (6 for 25 years and 6 for 20 years of lifetime) only the 5th case for the 25 years gives LCOE values below zero and not around or above zero (shown in Figure 4.5). Thus, only this case could be deemed beneficial from an economic viewpoint. However, from an energy cost of electricity perspective, Scenario C constitutes an attractive solution.

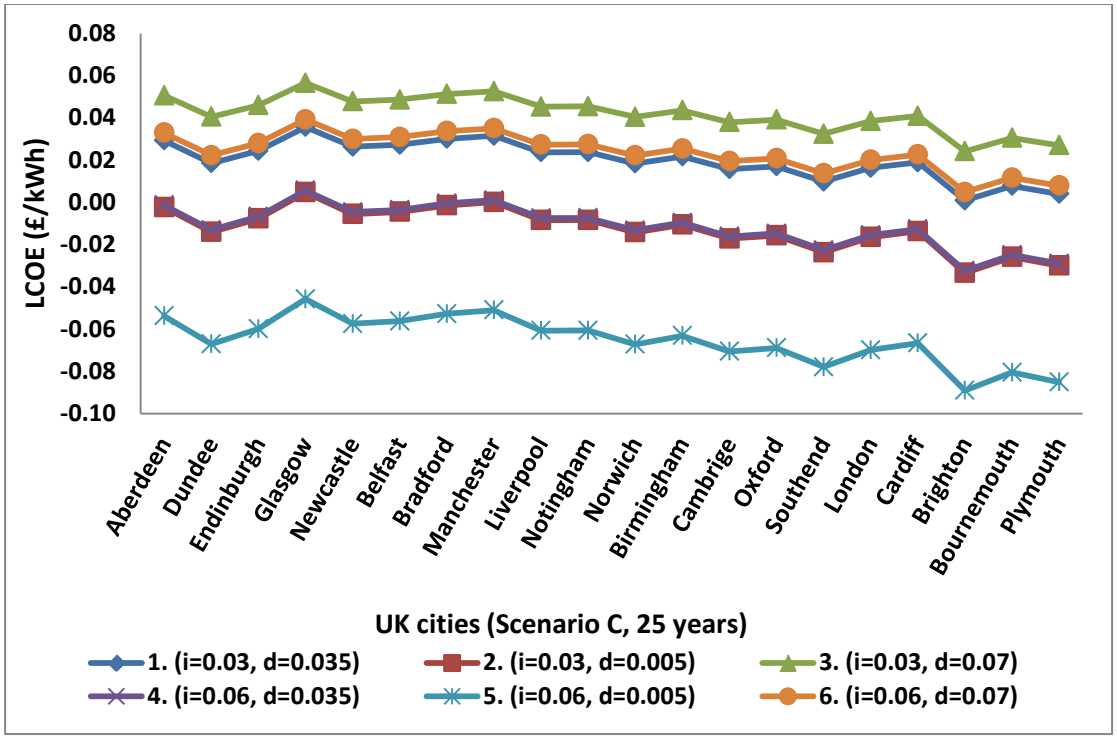

Figure 4.5: LCOE with Export Tariff and Electricity Savings (N=25 yrs)

Scenarios D, E and F reflect the current situation in the UK. All consider 20 years of FiT payments and they differ only for the last 5 years of system operation. The LCOE range for the three scenarios is between -0.0181 £/kWh to -0.2897 £/kWh. As an example, for Scenario F (Figure 4.6), which gives values intermediate between the other two scenarios, the mean LCOE value for all cities is -0.0858 £/kWh for the 1st case (i=0.03, d=0.035). Considering the mean lifetime energy production of 66,000 kWh for 25 years, the net income for the entire lifetime of the system would be £5,663. The present value of the costs has been calculated for the 1st case to be £8,015. The annual income is £(5,663+8,015)/25 yrs=£547 and the payback period is £8015/£547

$\simeq$14.6 yrs. Table 4.5 gives examples of the 1st and 5th cases for Scenario F and demonstrates how the discount and inflation rates influence the payback period of the investment and its relationship with LCOE and NPV. The starred values in Table 4.5 are referred to the 2012 base-year. The results indicate that the current FiT scheme is not very attractive for investors, as it gives a long payback period and is not greatly profitable (excluding the optimum case). However, from an energy cost of electricity perspective, the current FiT scheme could be beneficial.

Table 4.5: Correlation between LCOE, NPV and Payback Period
(*the starred values are referred to the 2012 base-year)

Scenario F, 20+5 yrs Project Lifetime		
Mean Lifetime Energy Production: 65890 kWh		
	1st case (i=0.03, d=0.035)	**5th case (i=0.06, d=0.005)**
Mean LCOE Value	-0.0574*/-0.8580 £/kWh	-0.2111*/-0.2462 £/kWh
Costs Present Value	£9669*/8015	£11823*/9964
NPV	£3782*/5663	£13909*/16249
Payback Period	18*/14.6 yrs	11.5*/9.5 yrs

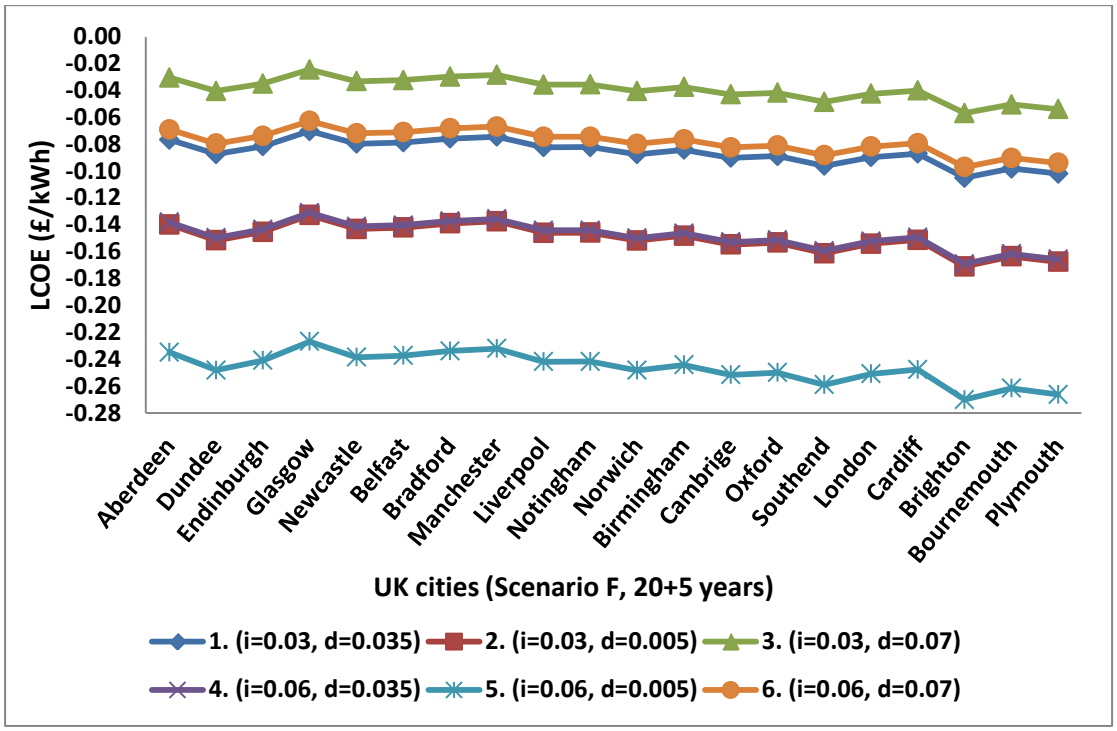

Figure 4.6: LCOE with FIT and Electricity Savings for 20 yrs and Electricity Savings for 5 yrs (N=20+5 yrs)

Table 4.6 summarises the LCOE ranges for all scenarios for Cardiff. This location is close to the mean and the median of the UK cities in respect to annual energy output from the PV system. Therefore, it provides an overall view of the LCOE ranges for all the scenarios and project lifetimes.

Table 4.6: LCOE range summary for Cardiff

LCOE (£/kWh)	A. LCOE with FiT & Electricity Savings		B. LCOE without FiT & Electricity Savings		C. LCOE with Export, FiT & Electricity Savings	
	Highest	Lowest	Highest	Lowest	Highest	Lowest
25 years	-0.0545	-0.3557	0.1504	0.1126	0.0410	-0.0666
20 years	-0.0435	-0.2616	0.1722	0.1372	0.0597	-0.0138
LCOE (£/kWh)	**D. LCOE 20 yrs FiT& Electricity Savings + 5 yrs Export, FiT & Electricity Savings**		**E. LCOE 20 yrs FiT & Electricity Savings + 5 yrs no benefits**		**F. LCOE 20 yrs FiT & Electricity Savings + 5 yrs Electricity Savings**	
	Highest	Lowest	Highest	Lowest	Highest	Lowest
20+5 years	-0.0426	-0.2672	-0.0337	-0.2009	-0.0400	-0.2476

This study demonstrates the lowest cost of produced energy that domestic PV systems can achieve in the UK with the support policies and system costs based on current values at the time of writing. Since all scenarios were based on the optimization of lifetime energy, the influence of the discount and inflation rates and the lifetime of the project on the LCOE were analysed. It is observed that the LCOE range, using the current support policies in the UK, could vary between -0.24 £/kWh to -0.04 £/kWh for the different financial cases (Scenario F) while two years ago it was varying from 0.20 £/kWh to 0.00 £/kWh. Considering Case 2 (i=3% and d=0.5%) of Scenario F as the most realistic assumption under the current financial situation, it can be said that the domestic PV LCOE is around 0.15 £/kWh in the UK for the installation cost assumed in the study. This leads to the result that the payback period for a residential PV system investment would be around 11.8 years (while in 2012 was 14.3 years) with the NPV equals to £9,900. However, the above statements are presented as an example as they are based on the assumption that the system will operate for 25 years minimum and that the current financial parameters (inflation and discount rates) will not change throughout the system's lifetime. Moreover, it is clearly stated in this research that the LCOE value should not be treated as a single number due to the uncertainties included in the calculation parameters.

4.5 LCOE for domestic PV in India

As described in Section 4.1.1, the domestic PV market in India is under development. There are no clear state and/or government policies yet regarding the PV incentives in the domestic sector. However, a few states have announced plans for the domestic PV deployment and specifically two states provide FiT for the PV domestic installations. These states are Uttarakhand and Gujurat, which offer an export and a generation tariff respectively. Uttarakhand considers a net metering policy for the PV installation and gives a FiT of 9.2 Rs/kWh (0.09 £/kWh) for the exported energy into the grid while Gujurat considers a gross metering policy and provides a FiT of 11.78 Rs/kWh (0.115 £/kWh) for every generated kWh by the PV system [93] (exchange rate of 1 Rs= £0.0098, as per September 2014 [96]).

For the LCOE calculations for India the same formula (eq.4.10) as for the case of the UK is used but the four terms of this formula are not being used together in any scenario, as there is not such a policy in India at the moment. Moreover, the same logic as for the UK LCOE calculations is considered. Hence, optimum LCOE values, based on maximizing energy output, have been calculated for thirty-six cities around India. An annual degradation rate of PV system performance of 1% was used, in accordance with the literature for the case of harsh environmental conditions in order to comply with the Indian climates [138]. Both UK and India LCOE formulae use an exponential degradation for the lifetime energy calculations, this is further explained in Chapter 5 Section 5.5.1. The cost variables considered are the capital cost of the system, operation and maintenance costs, the inverter replacement cost, the FiT rate for domestic PV systems (when applicable), the average retail electricity cost, and the financial factors (discount and inflation rates).

The scenarios used for the analysis in India have been modified in order to capture the Indian PV market conditions. Scenario A expresses the LCOE values of the 3 kW domestic PV system in the Indian cities (presented in Chapter 2) by considering only the savings from consuming half of the PV generated energy for both 20 and 25 years of project lifetime (i.e. lifetime savings from the electricity consumption). The decision to assume that half of the PV generated energy is consumed in the residence is because all the Indian states (apart from Gujurat) that have make announcements for domestic PV incentive plans consider a net metering policy. This means that the FiT will apply

only to the amount of energy exported to the grid. Hence, for Scenario A the value of the PV electricity to the consumer is that of the displaced energy from the grid (electricity savings). In reality, there might be higher or lower consumption of energy in some cases. However, there are insufficient data on domestic load profiles to allow us to investigate this situation. Scenario A expresses the current status of the Indian domestic PV market except for the states of Uttarakhand and Gujurat, which have already applied their PV incentive policies. Scenario B is the same as the Scenario B for the UK. It expresses the net cost of the produced PV energy in the various Indian locations for 20 and 25 years of the PV system operation. Finally, Scenario C refers only to the states of Uttarakhand and Gujurat and expresses the LCOE values considering the current PV policies in these two states.

Table 4.7: Summary of the LCOE scenarios and cases for India

Scenarios:		
A	LCOE with consumption of half of the PV generated energy (savings only from the 50% electricity consumption) for both 20 and 25 years	
B	LCOE without FiT or savings from the electricity consumption for both 20 and 25 years (Net PV cost)	
C	LCOE for the states of Uttarakhand and Gujurat using an exportation and a generation tariff respectively for both 20 and 25 years (savings from the 50% electricity consumption is considered in both states)	
Cases:		
	Inflation rate	Discount rate
1	i=9.5%	d=6.65%
2	i=9.5%	d=8%
3	i=8.2%	d=6.65%
4	i=8.2%	d=8%

Regarding the sensitivity analysis of the LCOE values for India, the project lifetime and the financial parameters are included as for the UK case. For India two project lifetimes are consider for 20 and 25 years and four different values of the nominal discount rate (x). Hence, there are eight numerical combinations presented (four for the 20 years and four for the 25 years of project lifetime) for three different scenarios. Table 4.7 presents all the cases and the scenarios for the Indian LCOE analysis.

Two inflation and two discount rates have been chosen for the Indian LCOE calculations. The inflation rates of 9.5% and 8.2% present the long-term average (from 2000-2014) and the current (2014) inflation rates respectively [139].The same stands for the two discount rates of 6.65% (long-term average) and 8% (current-2014) [140]. India's inflation rates are greater than the discount rates due to the country's financial status in the past years (from 2000 onwards). In industrialized countries like India this kind of status occurs sometimes as it encourages investments and shows that it is more beneficial to invest in the present rather than in the future. The installation cost, the operation and maintenance cost and the inverter replacement cost have been obtained from a PV installation company in India [141], specified for a 3 kW multi-crystalline PV system and an SMA inverter in order to capture the PV costs in the Indian market. All the costs include VAT and they are expressed in pounds by using an exchange rate of 1 Rs= £0.0098 (as per September 2014) [96]. Table 4.8 summarises all the values used in the Indian LCOE calculations except for the annual energy output of each city and the domestic retail electricity cost, which differs for each state. Two average retail electricity cost values are considered for each state according to the categories of domestic consumption in India. These categories are the 2 kW and 4 kW domestic loads, which correspond to 200 and 400 units/month of domestic consumption respectively (Table 4.9) [142].

Table 4.8: Summary of the values used in the LCOE analysis India

<table>
<tr><td>project lifetimes in years (N): 25, 20</td><td>installation cost (£): 4094</td><td rowspan="3">Source: KotakUrjaPvt. Ltd. [141]</td></tr>
<tr><td>inflation rates % (i): 9.5, 8.2</td><td>annual O&M cost (£): 164</td></tr>
<tr><td>discount rates % (d): 8, 6.65</td><td>inverter cost (£):800</td></tr>
<tr><td>annual degradation rate % (D): 1</td><td>Uttarakhand State exportation tariff (£/kWh): 0.09</td><td>Gujurat State generation tariff (£/kWh): 0.115</td></tr>
<tr><td colspan="3">Costs Base Year: 2013-14
Exchange rate used: 1 Indian Rupee= £0.0098</td></tr>
</table>

Table 4.9: Average domestic electricity cost per Indian state for 2 kW and 4 kW loads

Indian States and Territories	Indian Cities	Electricity Cost (£/kWh)	Electricity Cost (£/kWh)	Indian States and Territories	Indian Cities	Electricity Cost (£/kWh)	Electricity Cost (£/kWh)
		2 kW	4 kW			2 kW	4 kW
Jammu and Kashmir	**Srinagar**	0.02	0.03	**Mizoram**	**Aizawl**	0.03	0.04
Punjab	**Nangal**	0.06	0.07	**Jharkhand**	**Ranchi**	0.03	0.03
Himachal Pradesh	**Shimla**	0.02	0.03	**Madhya Pradesh**	**Bhopal**	0.06	0.06
Chandigarh	**Chandigarh**	0.03	0.04	**Gujarat**	**Ahmadabad**	0.04	0.05
Uttarakhand	**Dehradun**	0.03	0.03	**West Bengal**	**Kolkata**	0.06	0.07
Haryana	**Hissar**	0.04	0.05	**Chhattisgarh**	**Raipur**	0.03	0.03
Delhi	**New Delhi**	0.04	0.05	**Daman and Diu**	**Daman**	0.02	0.02
Assam	**Dibrugarh**	0.05	0.05	**Odisha**	**Bhubaneswar**	0.04	0.04
Sikkim	**Gangtok**	0.03	0.03	**Dadra and Nagar Haveli**	**Silvassa**	0.02	0.02
Arunachal Pradesh	**Itanagar**	0.04	0.04	**Maharashtra**	**Mumbai**	0.06	0.07
Rajasthan	**Jaipur**	0.06	0.06	**Andhra Pradesh**	**Hyderabad**	0.03	0.06
Uttar Pradesh	**Lucknow**	0.05	0.05	**Goa**	**Panjim**	0.02	0.02
Uttar Pradesh	**Kanpur**	0.05	0.05	**Tamil Nadu**	**Chennai**	0.05	0.06
Nagaland	**Kohima**	0.04	0.05	**Karnataka**	**Bangalore**	0.03	0.04
Bihar	**Patna**	0.04	0.04	**Pondicherry**	**Pondicherry**	0.01	0.02
Meghalaya	**Shillong**	0.03	0.04	**Andaman and Nicobar Islands**	**Port Blair**	0.03	0.04
Manipur	**Imphal**	0.04	0.04	**Lakshadweep**	**Kavaratti**	0.02	0.03
Tripura	**Agartala**	0.05	0.07	**Kerala**	**Trivandrum**	0.04	0.06

4.5.1 Results and discussion for the Indian LCOE

This section presents and discusses the LCOE results for 36 Indian cities based on the scenarios and the sensitivity analysis made. The first four graphs, which are presented below, concern Scenario A for both 20 and 25 years of the system lifetime and for both low and high consumption. As expected and as per the UK analysis, the LCOE values for the 25-year lifetime cases are lower than for the 20-year cases. Moreover, the LCOE for the 25-year case and high consumption tariff is lower than for the low consumption tariff since the value of the displaced electricity is higher resulting in higher lifetime energy savings. This is also the case for the 20-year lifetime value. In Figure 4.7, it is observed that four Indian cities have already reached grid parity while Kolkata is very close to reaching it for the 25-year lifetime and low consumption tariff. For the high consumption tariff, eight cities have reached grid parity while four are close to reaching it (Figure 4.8). When the PV system operates for 20 years with the low consumption tariff, only Nangal reaches grid parity while for the high consumption tariff, five cities reach it (Figures 4.9 and 4.10).

The city of Nangal, which has the lowest LCOE values in Scenario A, has an LCOE range from 4.8 p/kWh to 6.4 p/kWh according to the project lifetime and the consumption tariffs. Nangal also reaches grid parity in almost all cases in this scenario. Hence, from an energy cost of electricity perspective, a PV owner in Nangal could have a small benefit in energy costs in the long term. However, because of the small difference between the retail electricity cost and the LCOE value, a PV system might not constitute an attractive investment under these conditions. All the LCOE values for Scenario A have a positive bias, which means that the investment cannot be recouped. Scenario A shows the present need for PV incentive policies in India, as the current situation does not favour the deployment of domestic PV. Dehradun and Ahmadabad have implemented some PV incentive policies, which are discussed in Scenario C.

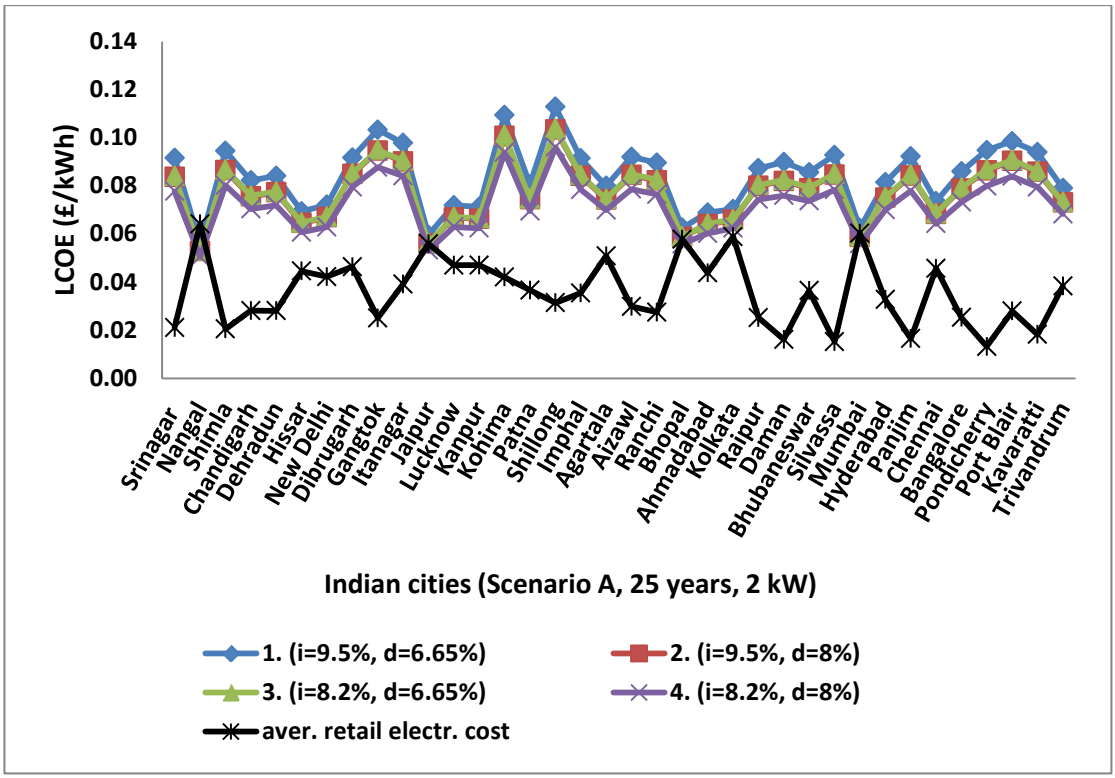

Figure 4.7: LCOE with Electricity Savings for 2 kW load (N=25 yrs)

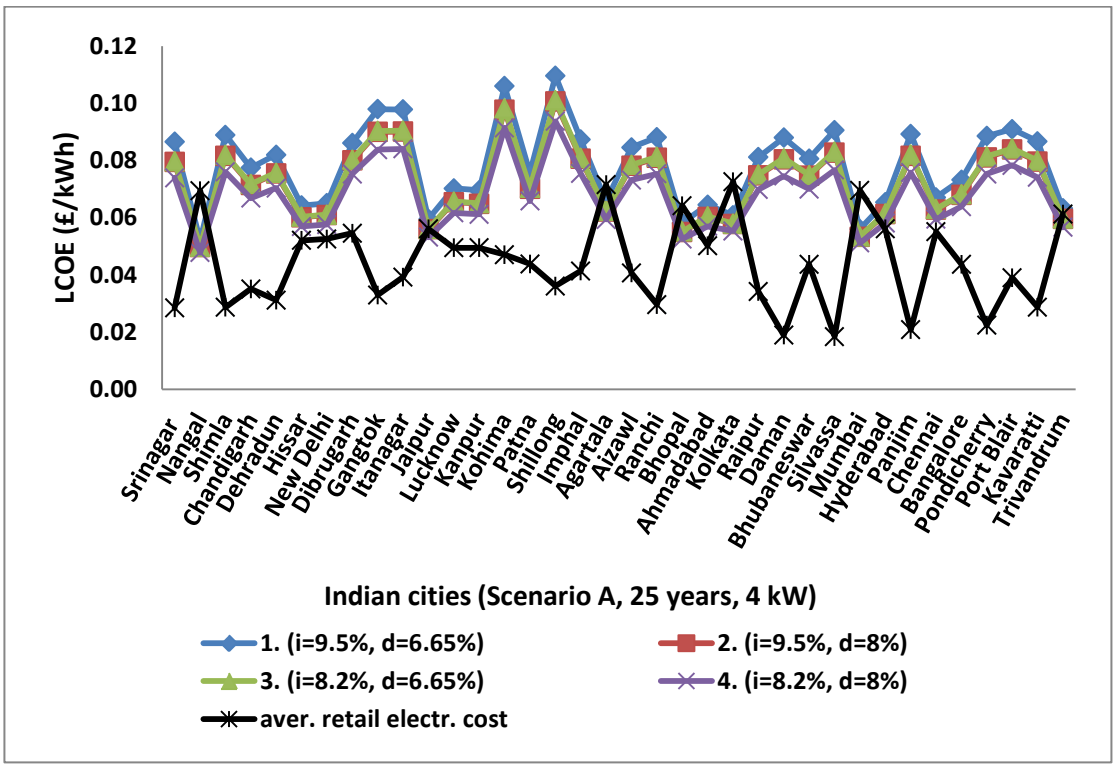

Figure 4.8: LCOE with Electricity Savings for 4 kW load (N=25 yrs)

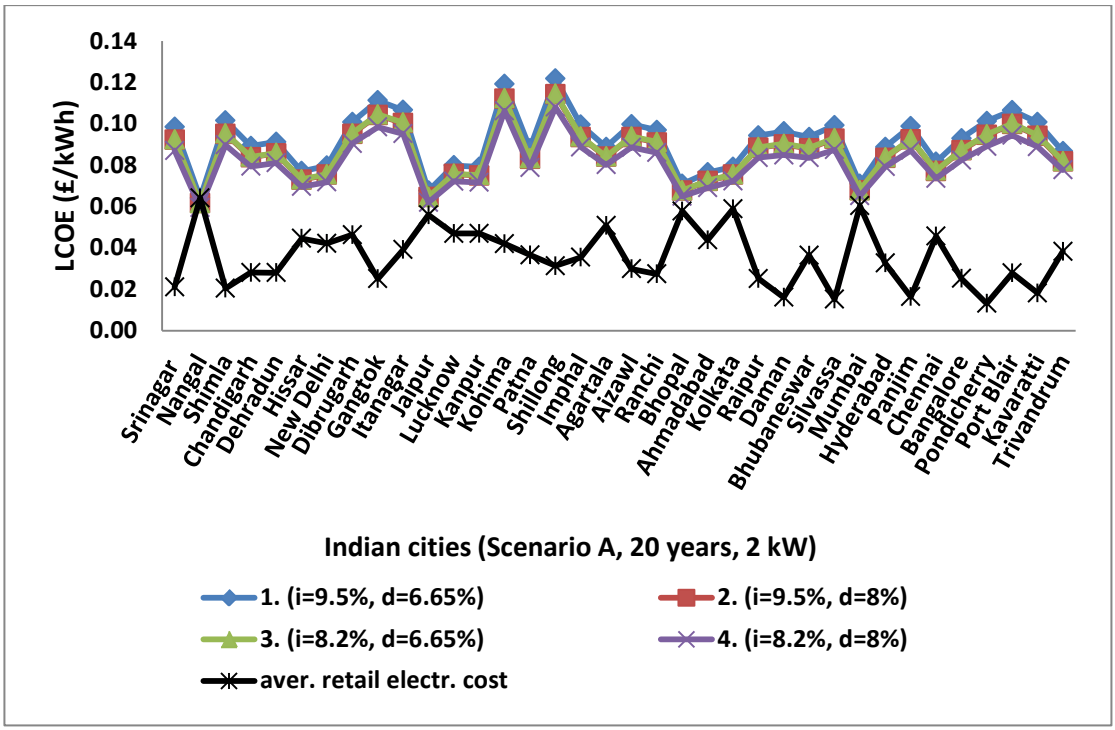

Figure 4.9: LCOE with Electricity Savings for 2 kW load (N=20 yrs)

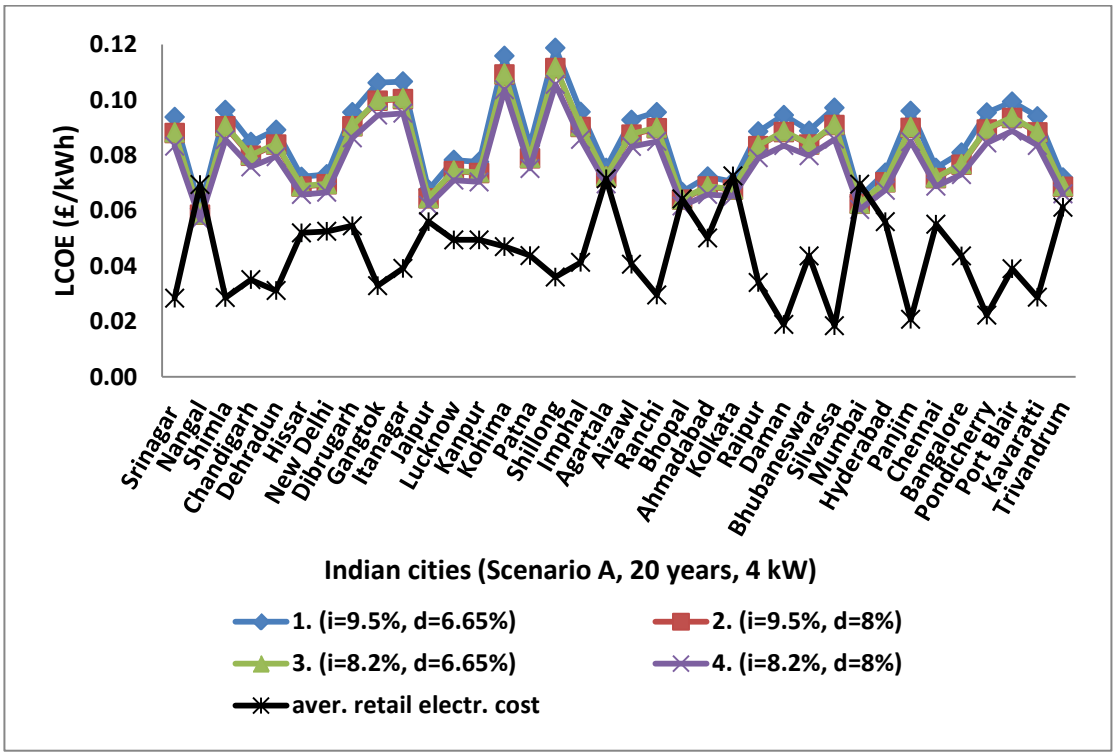

Figure 4.10: LCOE with Electricity Savings for 4 kW load (N=20 yrs)

Scenario B (Figures 4.11 and 4.12) shows how much the average cost per kWh is generated by a 3 kW PV system when this system operates for both 25 and 20 years and for the various financial cases. For the 25-year of lifetime, the LCOE value ranges from 8.2 p/kWh (Jaipur) to 13.8 p/kWh (Kohima) while for the 20-year they range from 9 p/kWh (Jaipur) to 14.6 p/kWh (Kohima). This scenario acts as a reference for any future PV domestic incentive policies as it shows the cost per kWh that has to be met in order to recoup the investment. It could be considered as the minimum incentive, since even if this cost is met, there will be no extra financial benefits for the investors apart from the fact that it would be beneficial from an energy cost of electricity perspective.

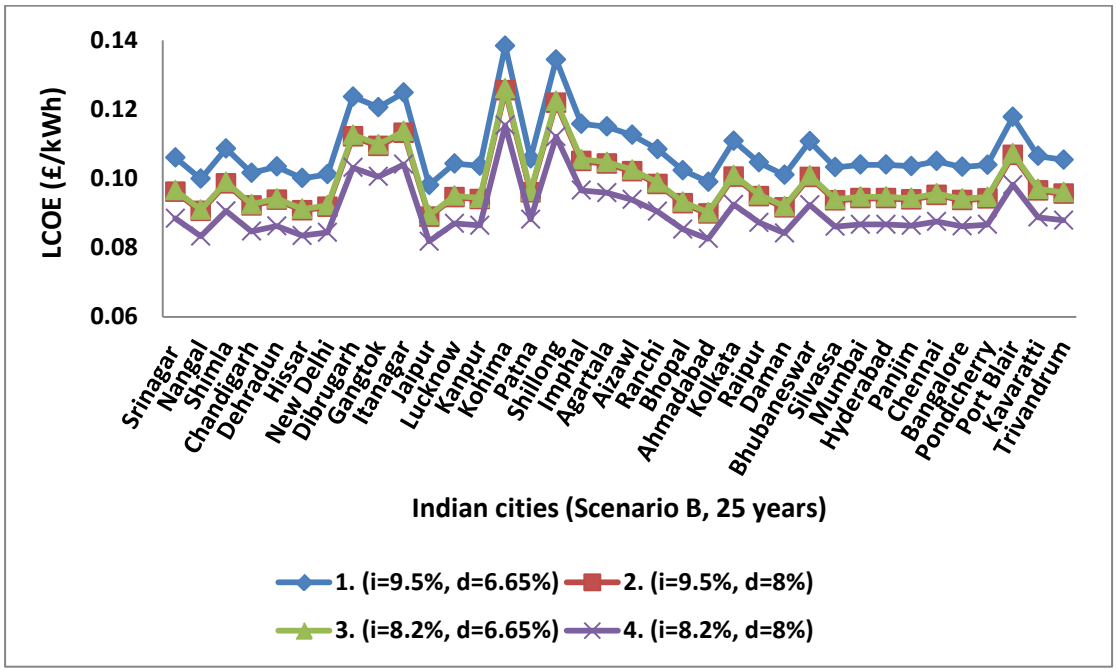

Figure 4.11: LCOE without both FIT and Electricity Savings (N=25 yrs)

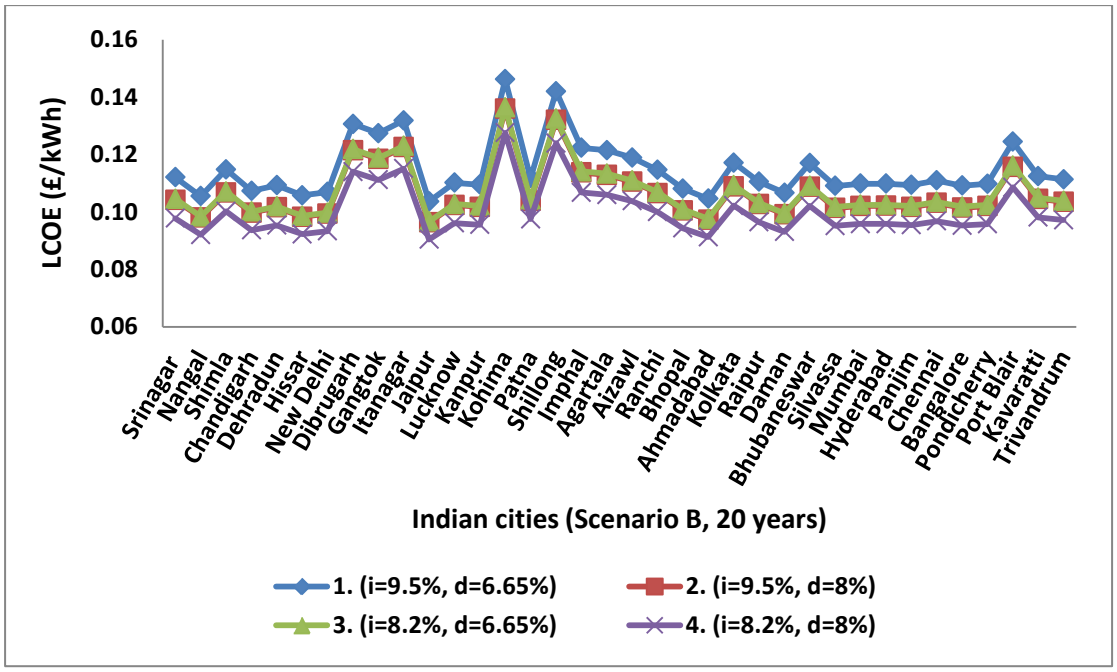

Figure 4.12: LCOE without both FIT and Electricity Savings (N=20 yrs)

Scenario C discusses the current situation for the cities of Dehradun and Ahmadabad. Figure 4.13 shows all the cases for these two cities for 25 and 20 years lifetime and for low and high consumption tariffs. The state of Gujurat, where Ahmadabad is located, has announced a generation tariff of 11.5 p/kWh. Accounting for the electricity savings by consuming half of the PV generated energy plus the generation tariff, Ahmadabad LCOE values give a negative bias, which means extra financial benefits for the investor. Ahmadabad LCOE range in Scenario B is between 8.3 p/kWh to 10.5 p/kWh, so Gujurat state PV policy could be deemed more or less beneficial from an economic viewpoint according to the financial case. Specifically, Case 4 (20 years, low consumption tariff) is the least beneficial offering 4.8 p/kWh while the most beneficial is Case 1 (25 years, high consumption tariff) offering 9.5 p/kWh. Hence, the net lifetime income for a domestic PV investment in Ahmadabad would be between £4330 and £10460. This income is valid only if the generation tariff is paid for all the assumed system lifetime (20 or 25 years).

In contrast, Uttarakhand state, where Dehradun is located, has announced a net metering policy with an export tariff of 9 p/kWh. With the assumption of 50% export of the PV electricity and 50% consumed in the residence (electricity savings), the LCOE value ranges from 1.9 p/kWh to 3.5 p/kWh. The average retail electricity cost for Uttarakhand is 3 p/kWh. Hence, even using the FiT, the results for the city of Dehradun

are around the grid parity level. This makes the PV investment unattractive and shows that the incentive policy should be re-examined. However, this is only valid with the assumption that the 50% of the generated electricity is exported. If the export is higher, the financial benefits will be greater.

Throughout the analysis, it is shown that there are cities that have reached or are close to the grid parity level by using only the savings from the electricity consumption. However, this is not adequate in order to invest in a domestic PV system since it cannot be considered beneficial either from an energy cost of electricity perspective or an economic viewpoint. At this point, the only benefit for an investor would be the environmental benefits of producing clean energy due to the fact that the same amount of money would be spent in long-term.

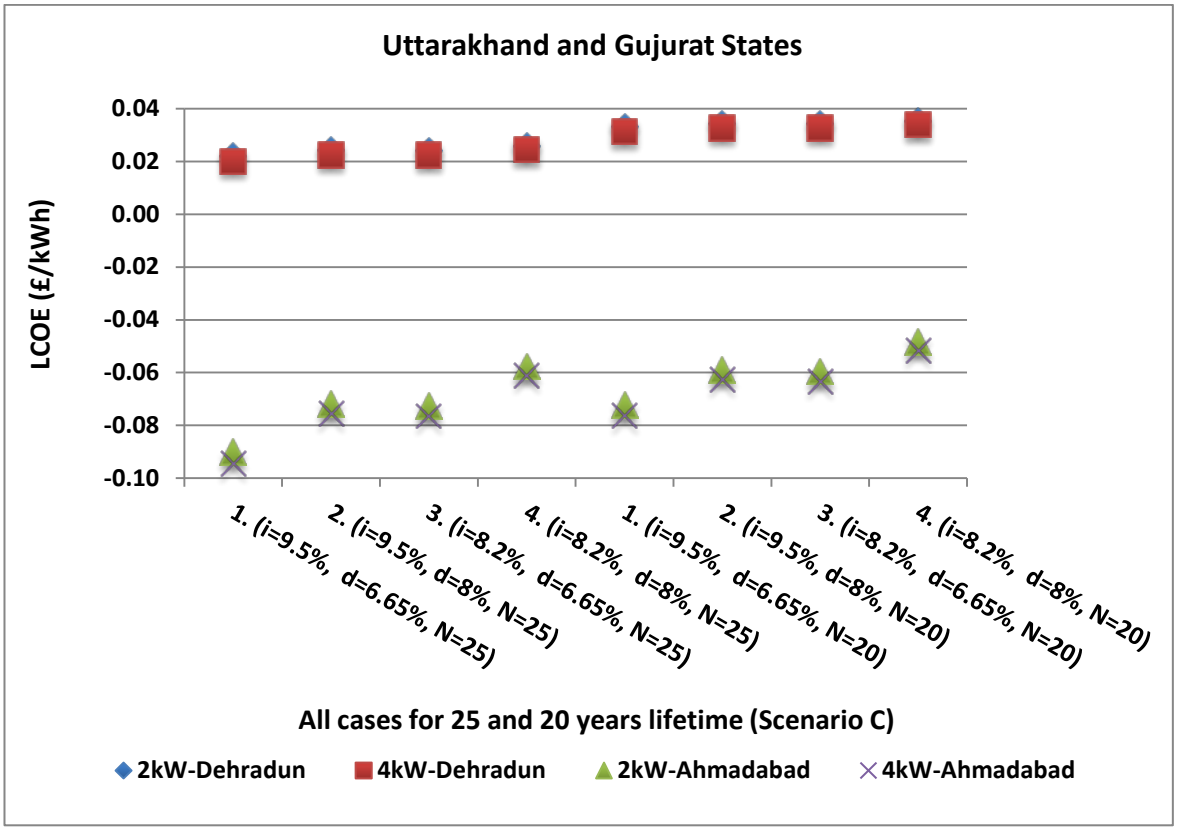

Figure 4.13: LCOE with FIT and Electricity Savings for Dehradun and Ahmadabad (N=20 yrs and 25 yrs)

4.6 Indicative CO_2 emission savings

The United Nations organization created in 1992 the United Nations Framework Convention on Climate Change (UNFCCC). The primary aim of the UNFCCC is the reduction of the greenhouse gas (GHG) emissions [143]. For the aforementioned reason the Kyoto Protocol was formed in 1997. The Kyoto Protocol is a document, which presents an international climate change policy. Its target was to bind the European community and 37 industrialized countries to reduce their GHG emissions by 5% from the 1990 levels during the period 2008 to 2012. The second commitment period (2013-2020) has started, and the Parties have agreed to reduce their GHG emissions by 18% from the 1990 levels. “However, the composition of Parties in the second commitment period is different from the first” [144].

According to the International Energy Agency statistics report published in 2012, electricity and heat generation and transport produced almost two-thirds of the global CO_2 emissions in the year 2010. More analytically, electricity and heat generation was the largest producer of CO_2 emissions (41% of the world’s CO_2 emissions). Furthermore, the IEA report states that India was the third country in the top 10 emitting countries in 2010 while the UK was the 10^{th} [145]. However, with the entry of Saudi Arabia in 2011, the UK was displaced from the top 10 of the emitting countries. The UK’s CO_2 emissions target set by the Kyoto Protocol is a reduction of 12.5% from the 1990 levels and the UK has reached a reduction of 19.3% in 2011. On the other hand, India has almost tripled its CO_2 emissions between 1990 and 2011 [146].

India emitted more than 5% of global CO_2 emissions in 2010, below is presented a graph (Figure 4.14) with India’s CO_2 emissions by sector. Electricity and heat sector produced 54% of CO_2 in 2010 and they have increased up to 40% from 1990 [145]. Hence, the deployment of PV system applications in India, which are a non-emitting energy generation source, would be proved beneficial for the reduction and/or stabilization of CO_2 emission levels [154].

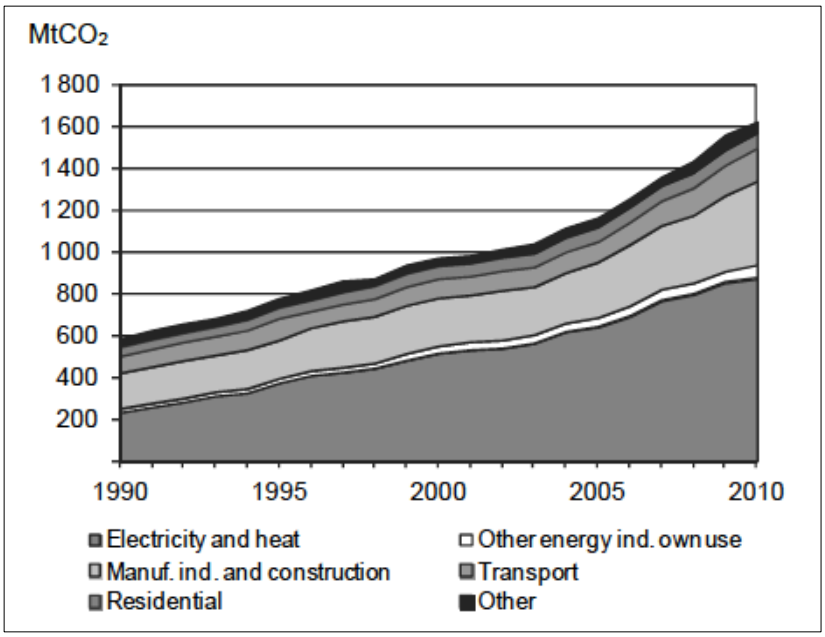

Figure 4.14: India CO_2 emissions by sector [145]

Lifetime CO_2 emission calculations have been made as a part of this research for the 3 kW PV system simulated in the cities of the UK and India. The annual emission factor used in the calculations for the UK is 0.497 tonnes of CO_2 per MWh generated by the system while for India is 0.933 tCO_2/MWh. These values have been taken from the RETScreen software and they originated from the International Panel on Climate Change (IPCC) and industry standard values. Moreover, the specific numbers are referred to all fuel types and they do not account for transmission and distribution (T&D) losses [34]. In addition, even though these values are annual factors, they are not much different from the long-term averaged emission factors for generated electricity that IEA proposes. Hence, for the years of 2000 to 2010, the UK's mean emission factor is 0.486 kCO_2/kWh while India's is 0.927 kCO_2/kWh [145]. Finally, it should be stated that if the T&D losses were included, the emission factors would be higher and the savings of CO_2 would be greater. However, the emission factor for a country could be over or under estimated, since it is referred to all fuel types and every country uses a different mix of fuels for the electricity and heat generation [147].

The table and the graphs below present the CO_2 reduction range of a 3 kW PV system in the UK and Indian cities for 20 and 25 years of lifetime and by using an annual degradation rate of 0.5% for the UK and 1% for India. It is observed that one residential PV system can save up to 104 tCO_2 in India during its lifetime while for the UK it can

save up to 37 tCO_2. Hence, the same PV system can save around two and a half to three times the amount of CO_2 emissions in India than in the UK. The reason for this is the difference in the irradiation and the annual emission factor of the two countries, since the annual degradation rate used for the lifetime energy calculations in India was greater than the one used for the UK. A 3 kW PV system in India produces almost double the annual energy than for the UK and the annual emission factor of UK is almost the half of India's emission factor. It is obvious that the savings from the CO_2 emissions or other air pollutants are not only dependent on the renewable system performance but also on the conventional generator type that it is used in a certain location [148].

Table 4.10: Lifetime CO_2 savings range for a 3 kW PV system

India (tCO_2) for a 3 kW PV system		
Cities Range:	**20 yrs**	**25 yrs**
Min	60.28	73.55
Max	85.03	103.75
UK (tCO_2) for a 3 kW PV system		
Cities Range:	**20 yrs**	**25 yrs**
Min	22.57	27.87
Max	30.20	37.29

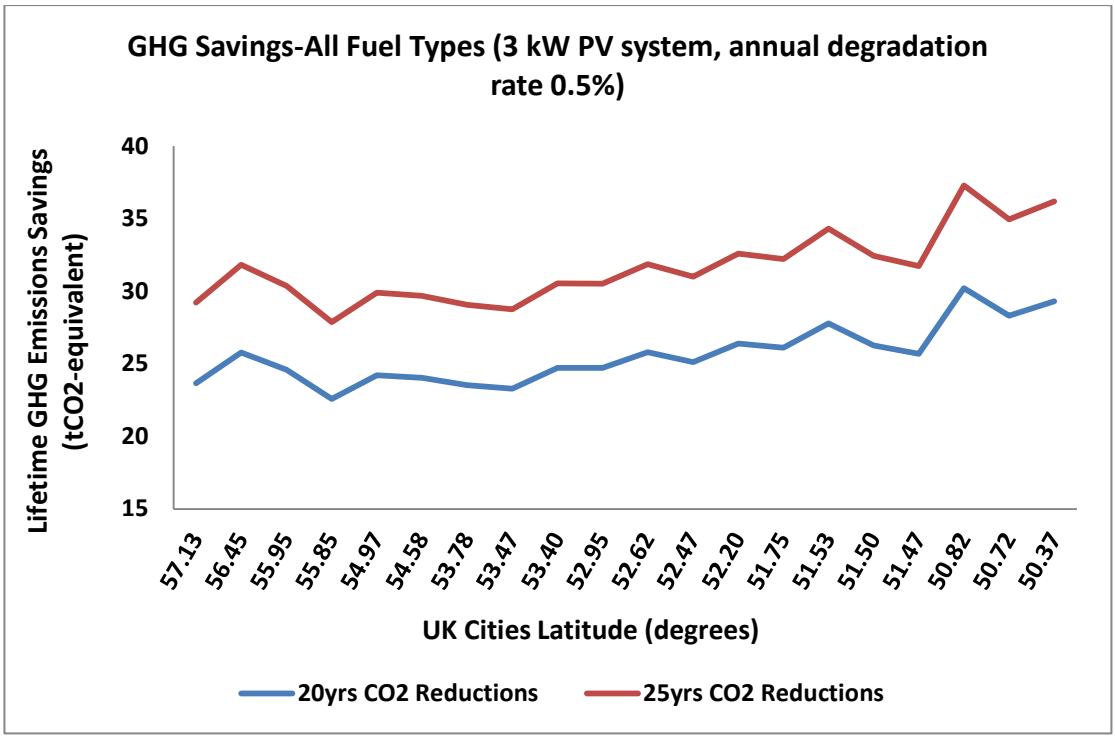

Figure 4.15: Lifetime GHG savings-3 kW PV system in the UK, annual degradation rate 0.5%

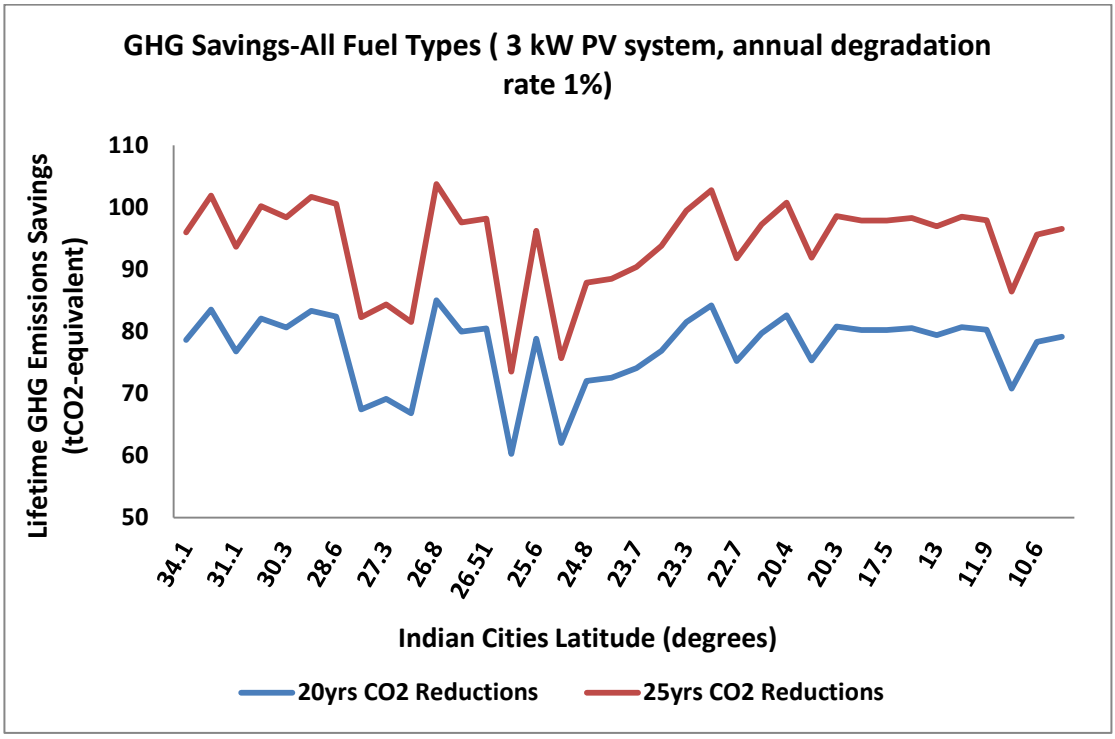

Figure 4.16: Lifetime GHG savings-3 kW PV system in India, annual degradation rate 1%

Chapter 5: PV Potentials in the UK and India

This chapter presents a model for the assessment of the annual and lifetime energy prediction, including uncertainties and degradation factors during a PV system's lifetime. This model has been applied to the chosen locations of the UK and India, which have been presented in Chapter 2. At the beginning of this chapter, brief descriptions of the degradation modes that influence the PV system's lifetime energy yield and the limitations of the main degradation models are given. Further, the results from the lifetime energy prediction model are presented and analysed. Finally, the chapter summarises the technical and economical outputs of this research by expressing the PV potentials in the UK and India.

5.1 Degradation modes and categories

This section presents briefly some degradation modes reported in the literature and mentions the main power loss categories. Till now, temperature, humidity and electrical bias are considered as the most influencing factors for the PV module degradation and they can be identified in most of the degradation modes. The most common degradation modes for crystalline modules are: corrosion, discoloration, delamination, breakage and cracking of cells. The corrosion affects the metallic connections of the module and increases the leakage current, as well as affecting the adhesion between the PV material and the metallic frame [149,150]. In the past, a study conducted for BP solar modules (published in 2005) on the failure modes of the modules found that corrosion was the first failure mode with 45.3% of the total failures considered for the studied sample of modules [151]. Additionally, corrosion might accelerate in hot and humid climates [149]. The delamination is caused by the adhesion loss between the encapsulant and the PV material or the encapsulant and the front glass of the module. It increases light reflection and water penetration in the module [149]. Moreover, it prevents the isothermal operation of cells causing a decrease in the module performance due to higher operating cell temperatures [150]. Delamination can be observed more often in hot and humid climates [149]. The discoloration changes the colour of the encapsulant to yellow or brown mainly due to the UV radiation and affects the transmittance of the light into the PV material. The breakages and cracks in the modules are usually caused during transportation, installation and/or maintenance. They might not influence the PV module performance in the short term but they make

the module more vulnerable to other degradation modes [149]. Further, the breakages and cracks can create safety issues in high voltage systems since the modules cannot offer the required insulation for avoiding electric shock [150].

Generally, a PV module failure is either power degradation higher than the anticipated throughout the years of its operation (as specified in the warranty), or an incident that creates a safety issue. For the first case, the power loss failure is defined by the following equation:

$$P_m + \Delta P_m < P_{max} - \Delta P_{max} \tag{5.1}$$

where P_m is the measured module power according to IEC 60904 standard, P_{max} is the rated power, ΔP_m is the uncertainty of the measurement, and ΔP_{max} is the module tolerance of manufacture. The power loss categories that depict the way in which a module power degrades, are presented in Table 5.1 [152].

Table 5.1: Definition of power loss categories [152]

Power loss category	Description
A	Power loss below detection limit <3%
B	Exponential shaped power loss degradation over time
C	Linear shaped power loss degradation over time
D	Power loss degradation saturates over time
E	Stepwise degradation type over time
F	Special degradation type over time

Other degradation and/or failure modes of the crystalline modules are: back sheet adhesion loss, junction box (j-box) failure, snail tracks, burn marks, potential induced degradation (PID) and defective bypass diodes. Figure 5.1 below presents a diagram that categorises the failure/degradation modes into three groups: infant, midlife and wear-out failure. Further, regarding the diagram, EVA (Ethylene Vinyl Acetate) is the

most common encapsulant type used in c-Si modules, Glass AR deg. is the degradation of the anti-reflective coating of the PV module glass and LID is the light-induced power degradation, which is actually expected for all modules and is usually taken into account in the rated power that is printed on a module [152].

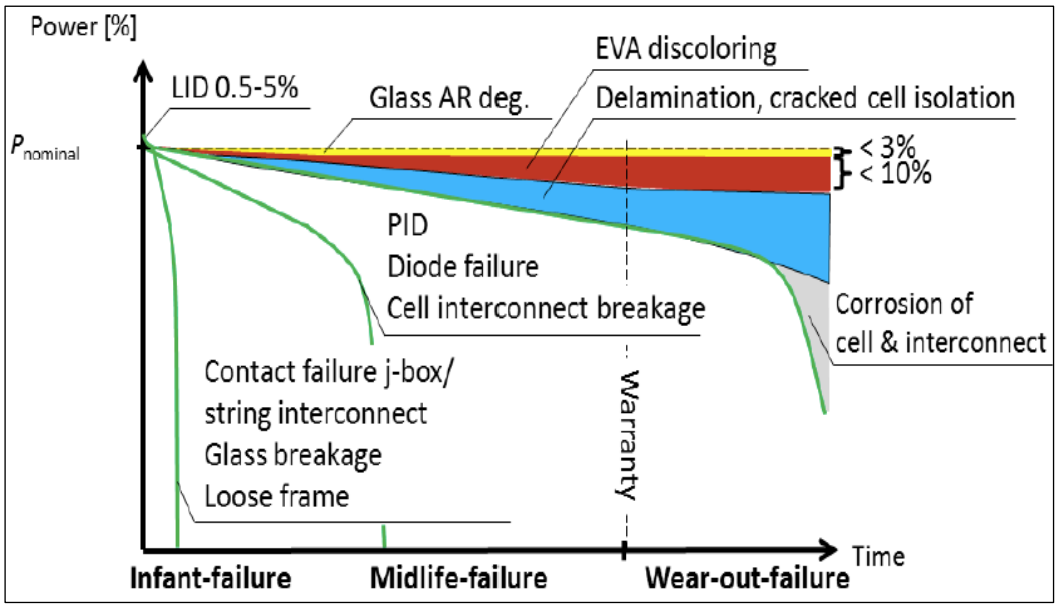

Figure 5.1: Typical failure scenarios for wafer-based crystalline PV modules [152]

Generally, there are accelerated stress tests, which help to qualify the module degradation. However, these tests alone are not adequate to predict the module degradation. As is shown from outdoor field experience, even well qualified modules may fail or degrade more than expected. Table 5.2 summarises the module degradation mechanisms, the stress factors that can cause them and the relevant accelerated tests [150].

Table 5.2: Degradation mechanism, corresponding stress factors and accelerated aging tests [150]

Degradation mechanism	Stress factor					Accelerated stress test
	High temperature	Moisture	Thermal cycling	UV	High voltage	
Broken interconnect	✓	✓			✓	Thermal cycle
Broken cell	✓				✓	
Solder bond failures	✓	✓	✓		✓	
Junction box failure	✓	✓				
Open circuits leading to Arcing	✓				✓	
Corrosion	✓	✓			✓	Damp heat exposure
Delamination of encapsulant	✓	✓	✓	✓	✓	
Encapsulant loss of adhesion and elasticity	✓	✓	✓		✓	Humidity freeze
Encapsulant discoloration	✓			✓		UV test
Hot spots	✓					Hot spot test
Shunts at the scribe lines	✓	✓				
Electrochemical corrosion of TCO	✓	✓			✓	Dry and wet insulation resistance
Ground fault		✓			✓	
Bypass diode failures	✓		✓			bypass diode thermal test

According to the BP Solar study, the observed types of field failures and their percentage are summarised in Table 5.3 [151]. Further, a more recent study by SunPower Corporation (presented in 2011) for midlife PV modules, predicted that around 4% of the studied PV modules would not meet the manufacturer warranty during the first 15 years of their operation [153]. On the other hand, PVPS Task 13 latest report (published in 2014) states that even though the main degradation modes for the c-Si modules used to be delamination, cell part isolation due to cell cracks and the discolouring of the laminate, the modules usually met the manufacturer power warranty. In addition, it states that nowadays the material and the design used in c-Si module manufacturing have been improved. For example, the lamination material that was responsible for the delamination and discoloration is no longer in use [152].

Table 5.3:Types of Field Failures Observed [151]

Types of Failures	% of Total Failures
Corrosion	45.3
Cell or Interconnect Break	40.7
Output Lead Problem	3.9
Junction Box Problem	3.6
Delamination	3.4
Overheated wires, diodes or terminal strip	1.5
Mechanical Damage	1.4
Defective Bypass Diodes	0.2

Finally, a study, which was a part of the PERFORMANCE project (Failure Mode Effect Analysis), has sorted the failure/degradation modes for PV systems. This study was presented in 2009 and showed that in a system level the module related failures/degradation modes were positioned in the second half of the most occurring and/or severe failure modes. In the first half, the failure modes were mostly associated with the inverter and the BOS (balance of system) components [154].

5.2 Energy prediction model background

A way to define the long-term energy yield of a PV system is to identify the degradation rate throughout the years of operation. This could be achieved by making indoor or outdoor experiments, by analysing field data from already installed PV systems or by using a degradation model to predict behaviour. All the aforementioned methods for identifying the PV degradation rate, and for ultimately predicting the lifetime energy, have their limitations. More specifically, regarding the indoor experiments, it is considered difficult to simulate in detail the outdoor operating conditions. On the other hand, the outdoor experiments require a consistent long-term study and their results cannot be easily generalised since they are location specific. For reported field data, there is an uncertainty included in the validity of these data and sometimes the information provided about these data is limited. Finally, the PV degradation models

have constraints due to the assumptions used in the model or factors/parameters determined by a specific experiment and then used in the prediction model.

Below are presented the limitations of the main degradation models in the literature as were stated in Ndiaye et al [149]:

The model of Pan [155]… **"**It is very dependent on the tests determining the degradation parameters. Thus, it will be constrained by the accuracy and testing time. This approach presents some problems because it never occurs in real conditions. Indeed, when PV module has high humidity, temperature is low."

The exponential model [156]… **"**This model gives an indication of the PV module degradation during its lifetime. However, many assumptions are used and therefore the results obtained do not always reflect the reality relating to the real operating conditions."

Model degradation by UV stress… **"**Its use requires knowledge of the intrinsic characteristics of the materials used for the production of PV cells. The measurement of these characteristics requires a rigorous instrumentation without which the model accuracy is compromised."

Model degradation by temperature stress/ Model degradation by temperature and humidity stress [157-159]… **"**The Arrhenius-based model presents some limits. Indeed, the Arrhenius equation can be used to quantify the effect of varying temperature and irradiance on the rate of a property change. However it cannot provide a complete picture of the long-term degradation of PV modules, as other stress factors or combination of stresses are involved."

The various degradation models have their advantages and disadvantages. Especially for the case of the degradation rate prediction, a study has shown that the degradation rate is not only technology and location dependent but methodology dependent as well, as there is the risk of overestimating or underestimating the true degradation rate according to the prediction method used [160]. In this research, the energy prediction model uses reported degradation rates from long-term outdoor studies and does not try to predict the degradation rate. However, an assumption is made for the linear correlation between the annual degradation rate and the annual energy output.

The basic approach to the lifetime energy yield prediction in this study is presented in the block diagram below (Figure 5.2). PV performance is dependent on the PV system design, module technology and climate. The main parameters regarding the “PV system design” can be accounted for in the simulated annual energy output. For the main parameters of “Climate and module material”, only the irradiation and the temperature are routinely included in the simulations and sometimes, if there are available data, wind speed and direction. However comprehensive the inclusion of parameters in the simulation, the performance result is expressed only for the first year of the PV system operation and the lifetime energy production must extend this by considering the operation of the system. Hence, the developed methodology here attempts to take into account the degradation rates and uncertainties included in the energy yield in order to predict the lifetime energy.

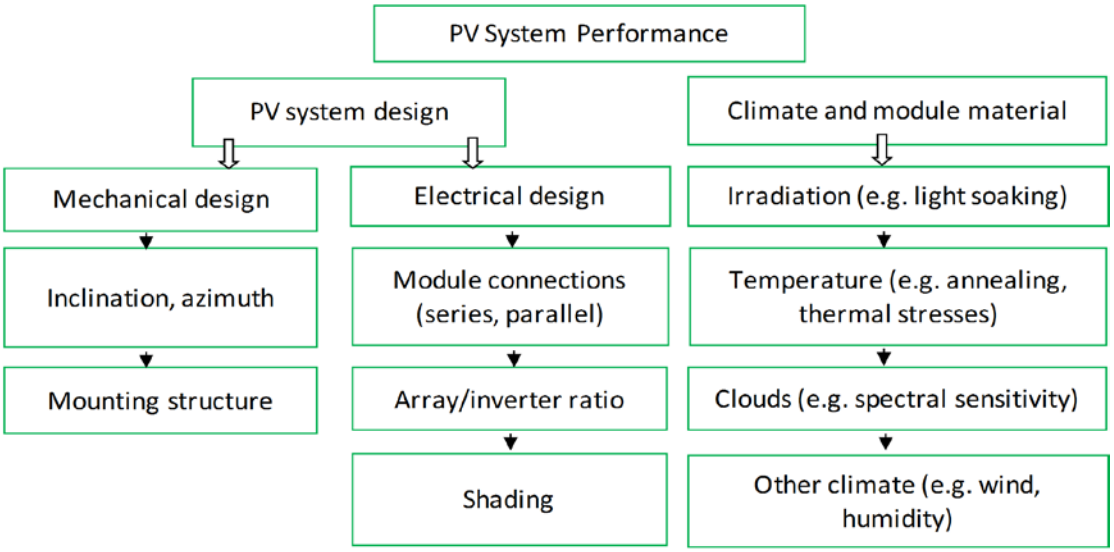

Figure 5.2: PV system performance and influencing parameters

5.2.1 Degradation rates

One of the most important issues is to establish representative degradation rates, but the literature in this regard is diverse and not straightforward to interpret, requiring a careful and thorough analysis. An analytical review on the reported degradation rates for different PV technologies states an average degradation rate for the crystalline silicon technology of 0.7% per year and a median value of 0.5% per year. By considering the reported rates only for the crystalline systems it can be observed that

their median degradation rate does not exceed 1% per year [138]. In addition to this, a study was conducted based on a literature survey (provided by Loughborough University [161]) on the PV system degradation rates, showed very similar results. Calculations have been made based on their provided database and considering only mono and multi-crystalline technologies. The results showed that the median degradation rate for the mono-crystalline PV systems was 0.4%/annum while for the multi-crystalline was 0.64%/annum. Below are presented two graphs with the annual degradation rates of 45 mono and multi-crystalline PV systems installed in various locations (derived from Loughborough University database [161]). The first graph presents the degradation rates reported and the year of the system installation while the second presents the degradation rates according to the years of system operation.

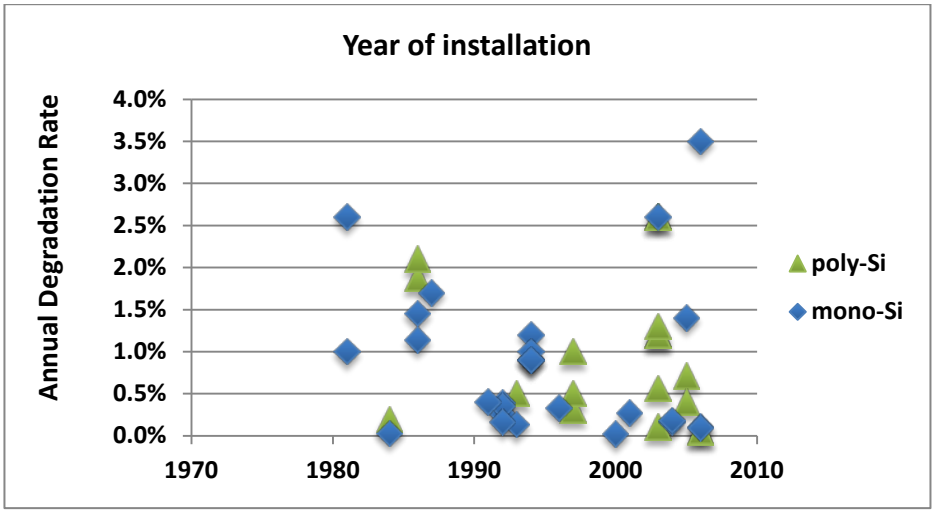

Figure 5.3: Year of PV systems installation and their degradation rates

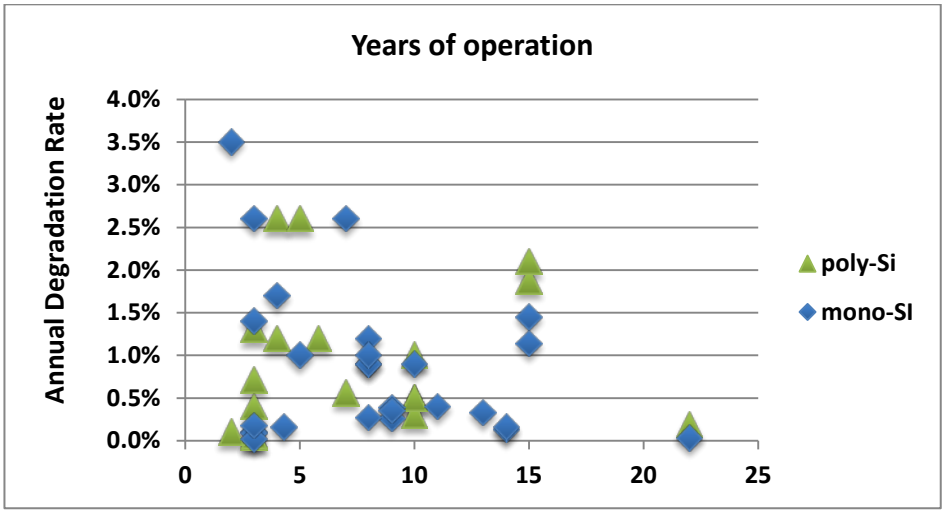

Figure 5.4: Years of PV systems operation and their degradation rates

At this point it should be stated that the average and median values for the degradation rates reported in the literature do not take into account the climatic influence to the PV systems degradation. Regarding India, which has diverse and harsh climates, the National Institute of Solar Energy reported a degradation rate up to 2.8% per year for a 10 year old crystalline PV system installation [162]. In addition, a Loughborough University report concluded that most of the degradation rates reported for all the PV technologies are in the range of 1%-3% per year [161]. It can be said that although the PV system degradation mechanisms are much more complicated to identify and analyse compared to the PV modules, they do not result in much different degradation rates from those of the modules [138]. In this study, 0.5% and 1% degradation rates per year are considered for the sensitivity analysis of the lifetime energy prediction in the UK. However, for the case of India, 1% and 3% degradation rates are included in order to demonstrate the influence of a harsh environment to the lifetime energy yield.

5.2.2 Uncertainties in prediction

According to a report on the uncertainties in long-term photovoltaic yield predictions, these can be divided into three categories [163]. The first category includes the uncertainties of the irradiation computation at a specific location and the year-to-year variability of the annual irradiation. The year-to-year variability uncertainty is not included in this study, as the study considers long-term averaged solar data. Hence, the uncertainty value considered for the irradiance computation is 5% according to the PVGIS CM-SAF database [16]. The second category refers to the uncertainty concerning the transposition model. It has been found that, when only the global irradiance is known, the mean bias error of the transposition model is between 0% and -6% for a south oriented array with optimum tilt angle. In this study, apart from the global irradiance, the diffuse component is also known. Hence, a realistic assumption for this uncertainty could be 3% [163]. The third category includes the uncertainties regarding the PV system performance i.e. module power tolerance, dirt and soiling losses etc. Regarding these uncertainties, PVsyst software accounts for the following factors in the simulations made for this study, as was analysed in Chapter 2:

- Incidence Effect, ASHRAE parameterization (parameter b_0= 0.05)
- Losses due to irradiance level
- Losses due to temperature

- Array soiling losses (loss fraction 3%)
- Module quality loss (loss fraction 1.5%)
- Module mismatch loss (loss fraction 2% at MPP)
- Wiring ohmic loss (loss fraction 1.5% at STC)
- Inverter losses

In addition, there is an uncertainty regarding the accuracy of the PV system simulation. According to PVsyst software, this uncertainty is around 3% [17]. However, due to the discussion that took place in section 3.1.4, the simulation accuracy uncertainty in this study is assumed to be 6%, since, according to a survey by PHOTON magazine in 2011, the maximum difference of the PVsyst yield prediction to the measured yield was 6% [67]. Hence, the uncertainties considered for the calculation of the PV energy output are the following:

- Irradiance computation 5% [16]
- Transposition model 3% [163]
- Simulation accuracy 6% [67]
- Extra module power tolerance 3% (for c-Si array technology)
- Extra soiling uncertainty only for the case of India 4%

Although PVsyst software already accounts for losses due to module power tolerance (module quality loss), an additional allowance has been made to account for a change in tolerance over the system lifetime [156]. Therefore, the combined uncertainty values, which are considered in the sensitivity analysis, are:

Combined Uncertainty 1 (irradiance computation and simulation accuracy):

$$CU1 = \sqrt{5\%^2 + 6\%^2} = 7.81\% \quad (5.2)$$

Combined Uncertainty 2 (as eq.5.2 plus transposition model):

$$CU2 = \sqrt{5\%^2 + 3\%^2 + 6\%^2} = 8.37\% \quad (5.3)$$

Combined Uncertainty 3 (as eq.5.3 plus module power tolerance):

$$CU3 = \sqrt{5\%^2 + 3\%^2 + 3\%^2 + 6\%^2} = 8.89\% \quad (5.4)$$

Combined Uncertainty 4 (as eq.5.4 plus soiling), for extreme cases in India:

$$CU4 = \sqrt{5\%^2 + 3\%^2 + 3\%^2 + 6\%^2 + 4\%^2} = 9.75\% \quad (5.5)$$

5.3 Energy prediction model

The model that was developed and used in this study combines long-term averages of solar data (using the PVGIS CM-SAF database), a commercial PV system simulation package (PVsyst) to predict the first year's annual energy output of the system and a probability density function to express the range of the lifetime energy and the annual energy prediction in different time periods of system operation. Moreover, a sensitivity analysis based on degradation rates and energy output uncertainties is embedded in the lifetime energy prediction calculations.

The model developed in this study was based on a reliability model for a photovoltaic module [156]. Generally, the operation period of a PV system is assumed to be over 25 years since the PV module warranties, provided by the PV manufacturers, are usually around 20-25 years. However, the performance of a system decreases over time due to various degradation mechanisms. The developed model for the lifetime energy prediction is based on statistical formulas and takes into account a range of different degradation rates, from installed PV systems and uncertainties reported in the literature. Even though this model is generic, it can be climate and technology specific since the degradation rates and the uncertainties considered could be changed according to the location and the PV system technology.

PV system annual energy output is the reference parameter to evaluate the system performance. The minimum annual energy for a certain year of system operation can be defined in relation to its first year energy output as follows:

$E_{n,min}$= first year energy output x uncertainty factor for modelled average energy yield over the PV system lifetime x (1 -cumulative annual degradation rate) (5.6)

If, for example, the PV system lifetime is 25 years with an annual degradation rate of 1% and a combined uncertainty of 9%, the minimum energy in the 25th year of the system operation will be:

$$E_{n,min} = E_0 \times 0.75 \times 0.91 \quad (5.7)$$

The value of $E_{n,min}$ in this analysis is equal to the energy value at the point of –σ (x-axis) of the normal distribution graph. In a normal distribution, 68% of the values are in the range of +σ to –σ, about 95% are within two standard deviations (+2σ to –2σ) while 99.7% of the values are in the range of +3σ to –3σ. The PV system energy output, including the uncertainties described above, is assumed to follow a Gaussian distribution. Hence, the probability density function is the following:

$$p(E) = \frac{1}{\sigma\sqrt{2\pi}} \exp\left[-\frac{1}{2}\left(\frac{E-\mu}{\sigma}\right)^2\right] \quad (5.8)$$

where E denotes the system energy output (in kWh), μ is the mean annual energy (in kWh) and σ is the standard deviation of the annual energy (in kWh). Both the mean annual energy and the standard deviation of the annual energy are time dependent variables. The mean annual energy decreases over the years of the PV system operation while the standard deviation of the energy increases as the variability of the module power rating increases due to non-uniform degradation patterns. A linear correlation has been chosen for these two parameters with respect to time. The equations are given below:

$$\mu(t) = E_0 - (DE_0t) \quad (5.9)$$

$$\sigma(t) = \sigma_0 + (bE_0t) \quad (5.10)$$

where E_0 is the first year energy (in kWh), obtained from the system simulation, D is the annual degradation rate, σ_0 is the first year standard deviation and b is the annual variability rate of the standard deviation. Following the Gaussian distribution, the relationship between the combined uncertainty, E_0 and σ_0 is given below:

$$E_0 - 3\sigma_0 = E_0(1 - U) \tag{5.11}$$

where U is the combined uncertainty factor. Since the standard deviation of the system output energy is not known, the annual variability rate (b) is determined in accordance with a study for the standard deviation of the module output power, which was found to double after 10 years of field operation [156]. Hence, b is assumed to be equal to:

$$b = \frac{\sigma_0}{E_0} \times \frac{1}{10} \Rightarrow \frac{U}{3} \times \frac{1}{10} \tag{5.12}$$

Figures 5.5-5.7 are presented as an example of this model. They demonstrate the distributions for the annual and lifetime energy production of 3 kW PV systems in London and in New Delhi. It is observed that the lifetime energy prediction for a residential PV system in London is between 47,800 kWh (–3σ) and 77,200 kWh (+3σ), while in New Delhi is between 80,700 kWh and 130,300 kWh, for the case of 1% annual degradation rate and 8.89% combined uncertainty (Figure 5.5). Note that the whole range of the output probability is being considered here. Since both distributions have been calculated based on the same uncertainty and degradation values, the percentage difference of their distribution range is the same as the percentage difference of their first year energy (E_0). Hence, the normal distribution of the lifetime energy prediction for New Delhi is 40% wider than the normal distribution for London. Moreover, Figures 5.6 and 5.7 show the variations in the annual energy output through different times of the system operation. It can be seen that, as the range of the annual energy output increases over time, it becomes more difficult to assess the annual energy production of the system.

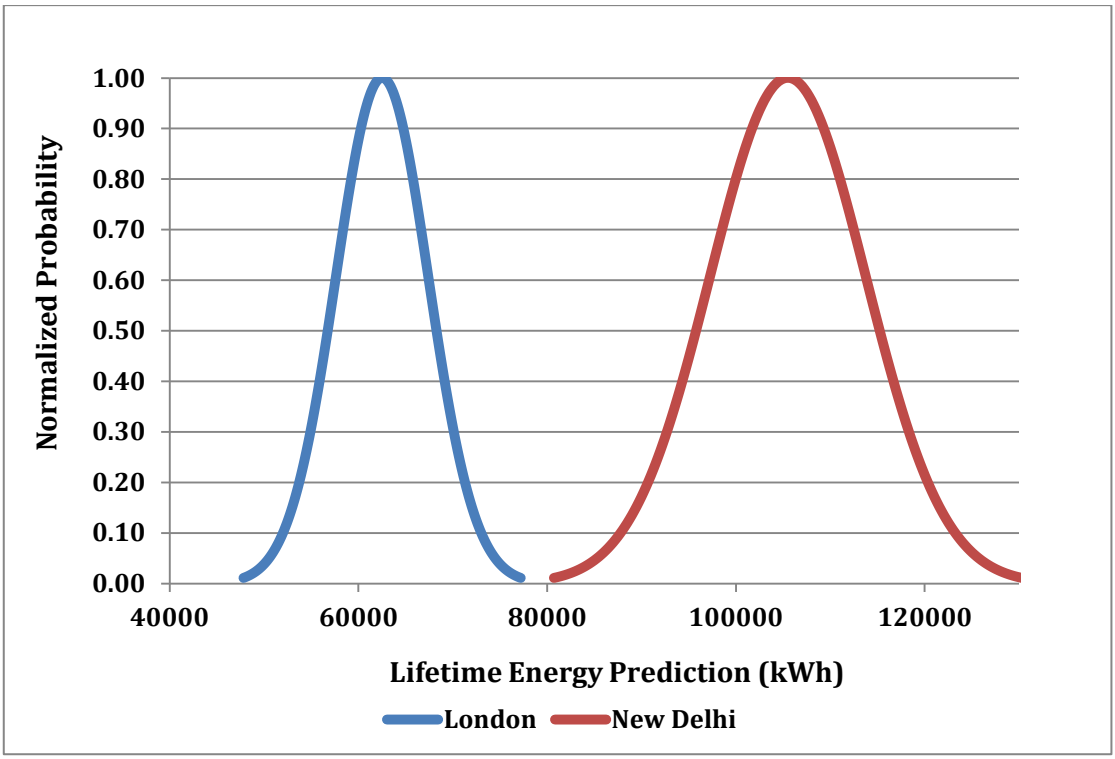

Figure 5.5: Normal distribution for the lifetime energy of a 3 kW PV system in London and in New Delhi
(annual degradation rate 1%, combined uncertainty 8.89%, project lifetime 25 years)

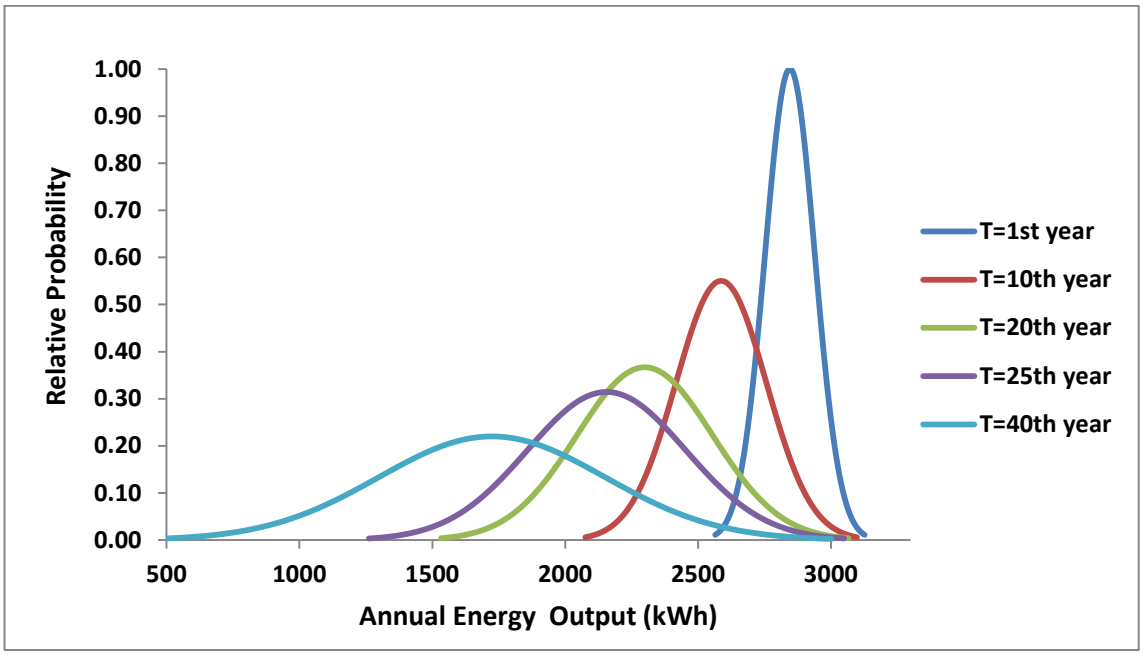

Figure 5.6: Normal distribution for the annual energy of a 3 kW PV system in London
(annual degradation rate 1%, combined uncertainty 8.89%)

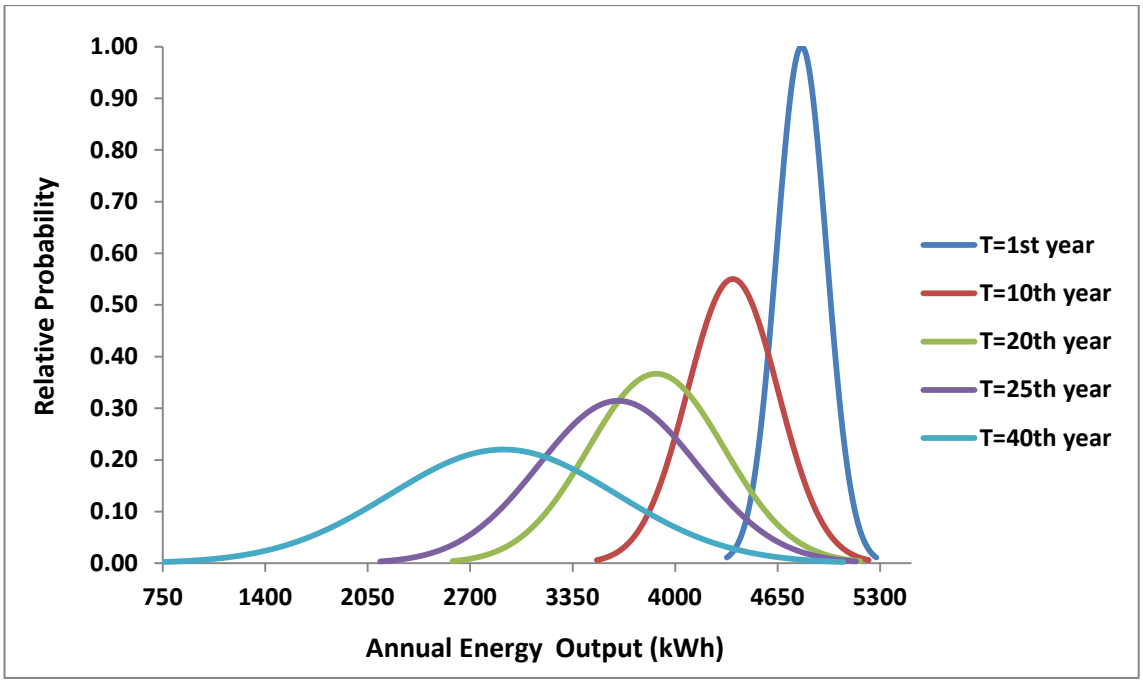

Figure 5.7: Normal distribution for the annual energy of a 3 kW PV system in New Delhi (annual degradation rate 1%, combined uncertainty 8.89%)

5.4 Lifetime energy prediction in the UK and India

This section presents and discusses the results of the energy prediction model and the sensitivity analysis that is embedded in the model. Two annual degradation rates and three uncertainty values were considered for each country. Hence, there are 6 ranges of lifetime energy predictions (scenarios) for each country. Table 5.4 summarises the degradation and uncertainty values for each scenario.

Table 5.4: Degradation and uncertainty values for the UK and India

Scenario	UK	India
1	D=0.5%, U=8.89%	D=1%, U=9.75%
2	D=0.5%, U=8.37%	D=1%, U=8.89%
3	D=0.5%, U=7.81%	D=1%, U=8.37%
4	D=1%, U=8.89%	D=3%, U=9.75%
5	D=1%, U=8.37%	D=3%, U=8.89%
6	D=1%, U=7.81%	D=3%, U=8.37%

The value of 7.81% is the minimum combined uncertainty where only the two main uncertainties are included (irradiance computation and simulation accuracy) and it is used only for the UK calculations. The 8.37% uncertainty includes the transposition model uncertainty, the simulation accuracy uncertainty and the irradiance computation uncertainty. The other two uncertainty values also include the extra module power tolerance uncertainty (combined uncertainty: 8.89%) and the extra soiling loss uncertainty (combined uncertainty: 9.75%). The first three are considered for the case of the UK while the last three are considered for India. Regarding the chosen degradation rates, the 0.5% and 1% degradation rates have been chosen for the UK in accordance with the literature for c-Si modules and/or systems, while for India, 1% and 3% of annual degradation rates have been chosen because of its harsh environmental conditions. Field studies, which were conducted in harsh environments reported annual degradation rates of around 1.1% [164] and up to 2.96% [165]. Kahoul et al, discusses a study conducted in Sahara region over a period of 11 years for mono-Si modules. The region is characterised by high ambient temperatures while the monthly maximum ambient temperature was more than 40°C during 10 out of the 12 months of the year [164]. Ndiaye et al, discusses a study conducted at Dakar in Senegal, which has a tropical environment. Two mono-Si and two multi-Si modules were examined for the first few years of their operation. Three out of four modules had an annual degradation rate of more than 1.5% for the examined period [165]. Hence, by considering the 1% and 3% annual degradation rates for India, it can be said that it is a realistic assumption and can actually express the PV potentials of a harsh environment.

The deviation of the normal distribution of this model is dependent on the combined uncertainty value while the energy values are dependent on the annual degradation rate. Hence, Figures 5.5-5.7, in Section 5.3, offer a comparison between the capital cities of the two countries under the same conditions and consequently of the difference in their solar resource (i.e. theoretical energy potentials). For the continuation of the analysis, the city of Patna in the state of Bihar in India and the city of Cardiff in the UK have been chosen in order to capture the diversity of the conditions between the two countries. These cities have been chosen as representatives for the UK and India because their first year annual energy output is very close to the mean and median values of the examined cities around the UK and India.

In Figure 5.8 the comparison of the lifetime energy ranges for the UK and India is shown. For the case of India, both degradation rates have been considered using the highest uncertainty value (9.75%). Similarly for the UK, the highest uncertainty value (8.89%) is used together with the relevant degradation rates. It is clear that the deviation for Patna is larger as the uncertainty value used is higher than that for Cardiff. Moreover, the lifetime energy ranges do not differ much for Cardiff while they differ greatly for Patna. This illustrates that if the system does not have a good operation and maintenance environment, the uncertainty of its economic viability increases regardless of the solar resource potential of the location. For example, the perceived economic viability for a system installed in Patna will depend on the chosen value of its lifetime energy prediction. By considering only the degradation rate, the mean value for the 25 years of system operation would be expected to be around 101,000 kWh for a 1% annual degradation rate while it would be around 70,800 kWh for a 3% annual degradation rate. This alone is a 30% difference in the lifetime energy prediction. If the uncertainty is also included, for a combined uncertainty of 9.75%, the deviation would be ± 17,300 kWh for ± 2σ and ±8,700 kWh for ±σ. Depending on the chosen mean value of the lifetime energy, these deviations could give a difference in lifetime energy prediction of between 9% and 24%. Note that the ±σ and ± 2σ were selected instead of ±3σ for the above example because they offer a narrower lifetime energy range and a sufficient probability percentage, both of which provide a more realistic prediction for an investor.

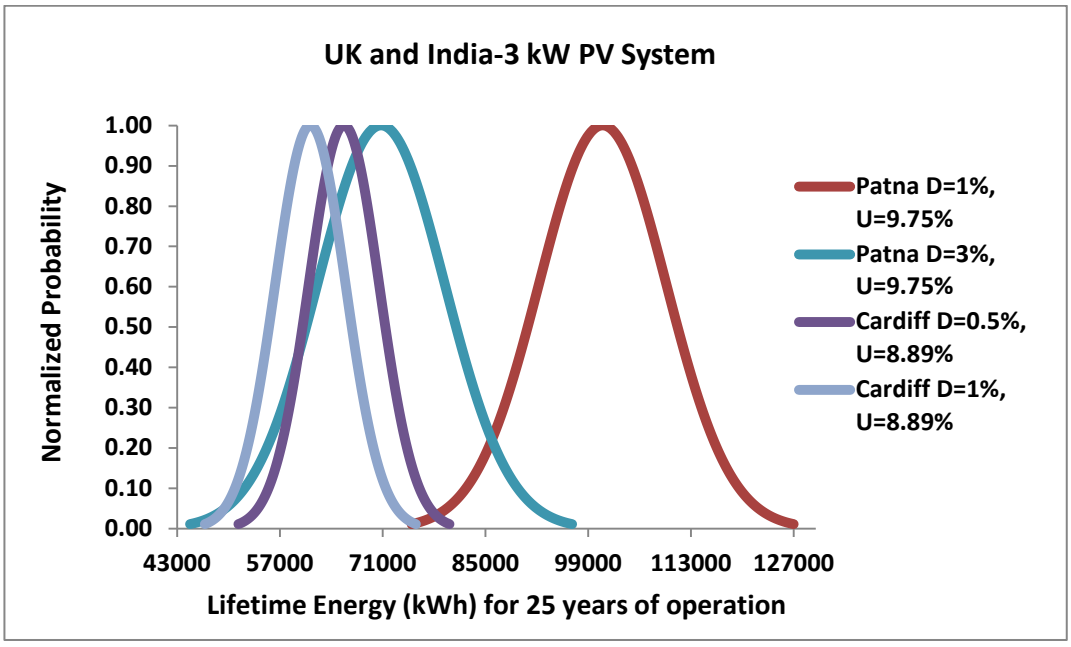

Figure 5.8: Normal distribution for the lifetime energy of a 3 kW PV system in Cardiff (UK) and Patna (Bihar-India)

Table 5.5 presents the lifetime ranges for a ± 2σ deviation for all the scenarios for Cardiff and Patna as representative ranges for the UK and India. However, for a more analytical view on the lifetime ranges (± 2σ) in the UK and India, Scenario 2 has been chosen for each country and the results are presented in Figures 5.9 and 5.10. Scenario 2 excludes the extreme degradation rates and considers the medium uncertainty values for each country in this analysis. Further, Appendix J provides tables with the lifetime ranges for all the cities and all the scenarios.

Table 5.5: Lifetime energy ranges for all the scenarios for Cardiff and Patna

Lifetime energy ranges-Cardiff UK (kWh, ± 2σ)					
D=0.5%, U=7.81%		D=0.5%, U=8.37%		D=0.5%, U=8.89%	
74150	57310	74750	56710	75310	56150
D=1%, U=7.81%		D=1%, U=8.37%		D=1%, U=8.89%	
69580	52740	70180	52140	70740	51580
Lifetime energy ranges-Patna Bihar India (kWh, ± 2σ)					
D=1%, U=8.37%		D=1%, U=8.89%		D=1%, U=9.75%	
115850	86080	116780	85150	118310	83620
D=3%, U=8.37%		D=3%, U=8.89%		D=3%, U=9.75%	
85680	55900	86610	54970	88130	53450

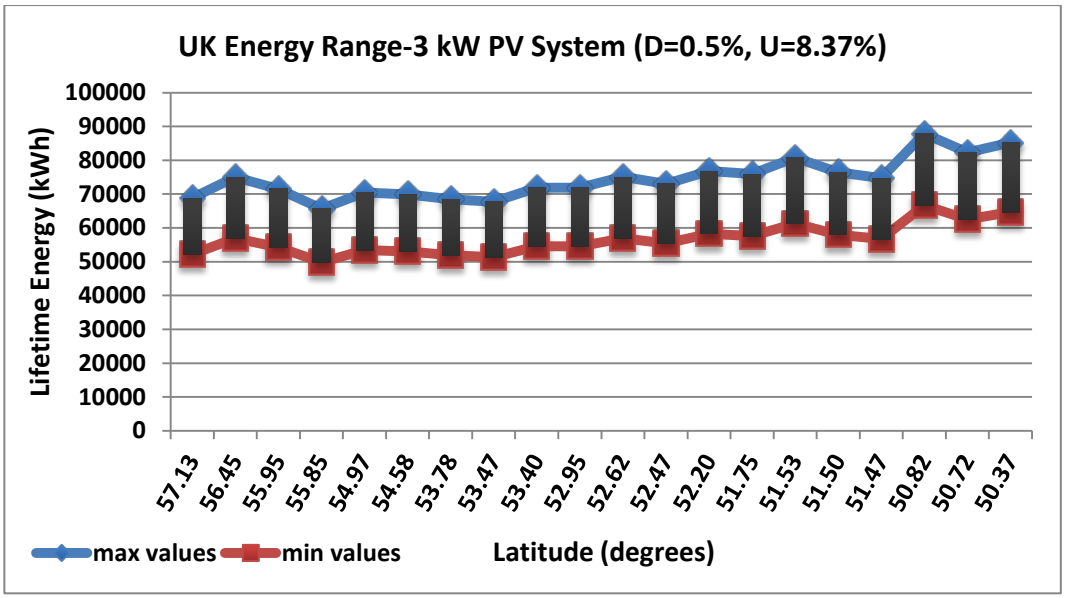

Figure 5.9: Lifetime energy range in the UK for 0.5% degradation rate and 8.37% combined uncertainty
(the black lines depict the range)

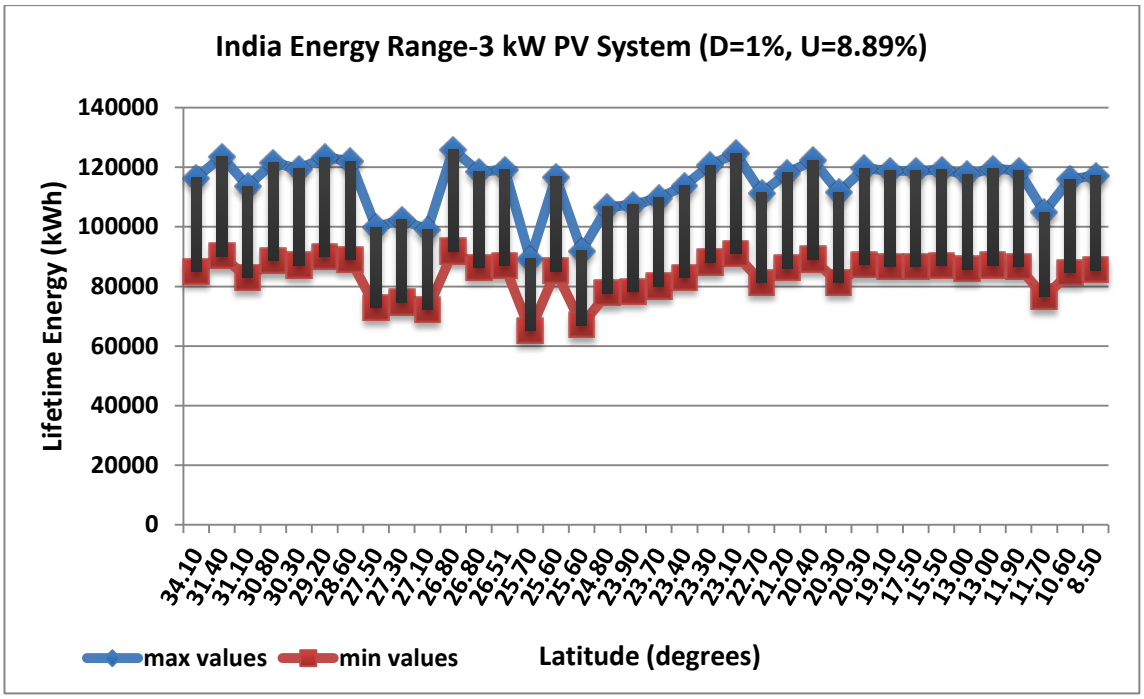

Figure 5.10: Lifetime energy range in India for 1% degradation rate and 8.89% combined uncertainty
(the black lines depict the range)

Finally, Figures 5.11 and 5.12 present the ranges for the lifetime energy prediction for all 6 scenarios for each country. These ranges refer to a 3 kW PV system and they have a 95% probability of occurrence as they account from –2σ to +2σ of the probability density function. For the UK cities it can be observed that most of the lifetime energy prediction ranges lie between 60,000 to 70,000 kWh. In the southern cities of the UK, this range could be raised to 70,000 - 80,000 kWh while in the northern cities it could be decrease to 50,000 - 60,000 kWh (Figure 5.11). For India the variation in the ranges is larger since the degradation rates used have a much greater difference between them. Hence, it can be observed that most of the lifetime energy prediction ranges lie between 75,000 to 105,000 kWh, although in certain scenarios there are areas with lifetime energy production less than 75,000 kWh (Figure 5.12). In addition, because India is a large country and is characterised by various climates, there is not a straightforward correlation between the solar resource and the latitude.

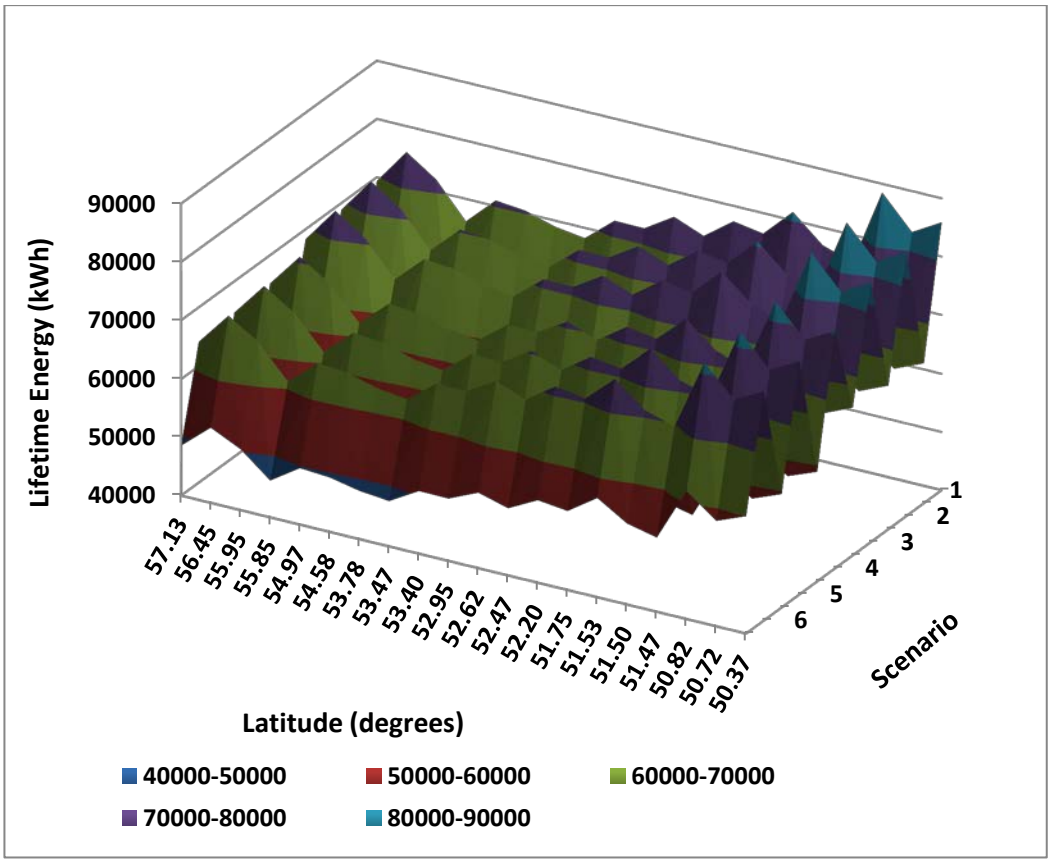

Figure 5.11: Lifetime energy range (all the scenarios) in the UK-small scale PV potentials

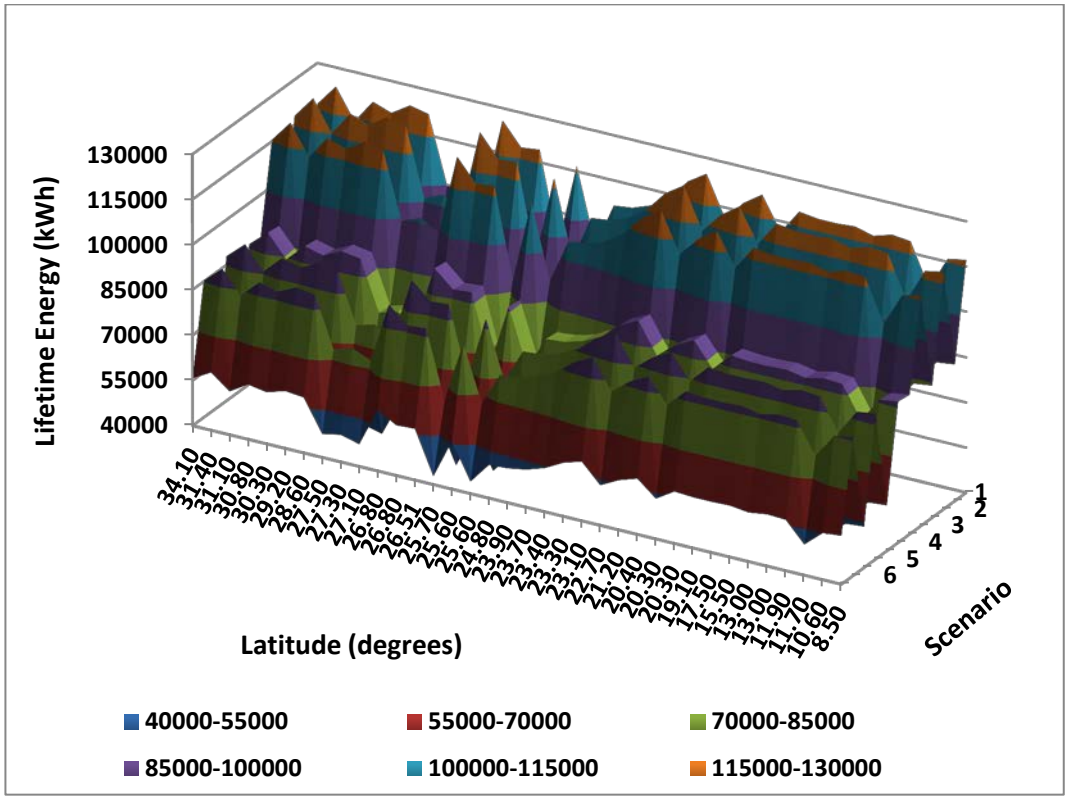

Figure 5.12: Lifetime energy range (all the scenarios) in India-small scale PV potentials

The analysis has shown that while it is expected in India that the PV system during its lifetime will produce much more energy compared to the UK, due to its greater solar resource, the environmental stresses might reduce this possibility. A study regarding the potential of PV systems in countries with high solar insolation clearly demonstrated the advantage of installing a PV system in such locations [166]. However, the examined location was Nicosia in Cyprus, which has a Mediterranean climate with different characteristics from the Indian climates. Hence, this might not be the case for some locations in India where high solar irradiation is available but the environment is harsh.

5.5 PV economical and technical potentials

This section combines the economic analysis and the lifetime energy prediction model in order to assess the PV potentials in the UK and India by considering the average net PV cost per generated kWh. Hence, LCOE ranges based on Scenario B (Chapter 4) for both countries are provided by using lifetime energy prediction ranges from the energy prediction model.

5.5.1 Net PV cost methodology

The power loss categories, which are described in Table 5.1, allow prediction of the expected power over time. Here it should be stated that apart from the category (e.g. mathematical model), the reference power value (i.e. measured module power or rated power) also plays an important role in the power prediction. Regarding the energy prediction model for PV systems, developed in this research and presented in Section 5.3, the linear shaped energy loss degradation over time (C) has been chosen while the reference energy value is the first year's annual energy obtained by the PVSyst simulation software. Moreover, the exponential shape energy loss degradation over time (B) has been used in the LCOE calculations for the UK and India. The two specific categories have been examined and they did not give much difference in their annual energy output throughout the system lifetime. This is mainly due to the fact that the annual degradation rates used in the calculations have a relatively small percentage (i.e. 0.5%, 1%), and that the examined PV systems are small scale PV systems and consequently do not produce large amounts of energy. From all the studied locations,

the one with the highest annual energy yield (Jaipur in Rajasthan in India) has been chosen in order to demonstrate the aforementioned statement. The exponential and linear degradations have been drawn for annual degradation rates of 1% and 3% (Figure 5.13). For the case of India the annual degradation rate considered in this study for c-Si systems is 1%. From Figure 5.13 it is clear that the difference between the exponential and linear degradation for the 1% case is well within the uncertainty prediction limits. On the other hand, if a 3% degradation rate is applied, which is the extreme case only for India in this study, then at the 25th year of the system operation, the two categories give up to 1000 kWh annual energy difference (around 40%) for a 3 kW PV system. So, for the energy prediction model, the linear approach has been chosen in order to account for the worst-case scenario. However, this was not required for the LCOE calculations, as the sensitivity analysis focuses on the financial factors and 1% exponential degradation rate was used in the calculations (Section 4.5).

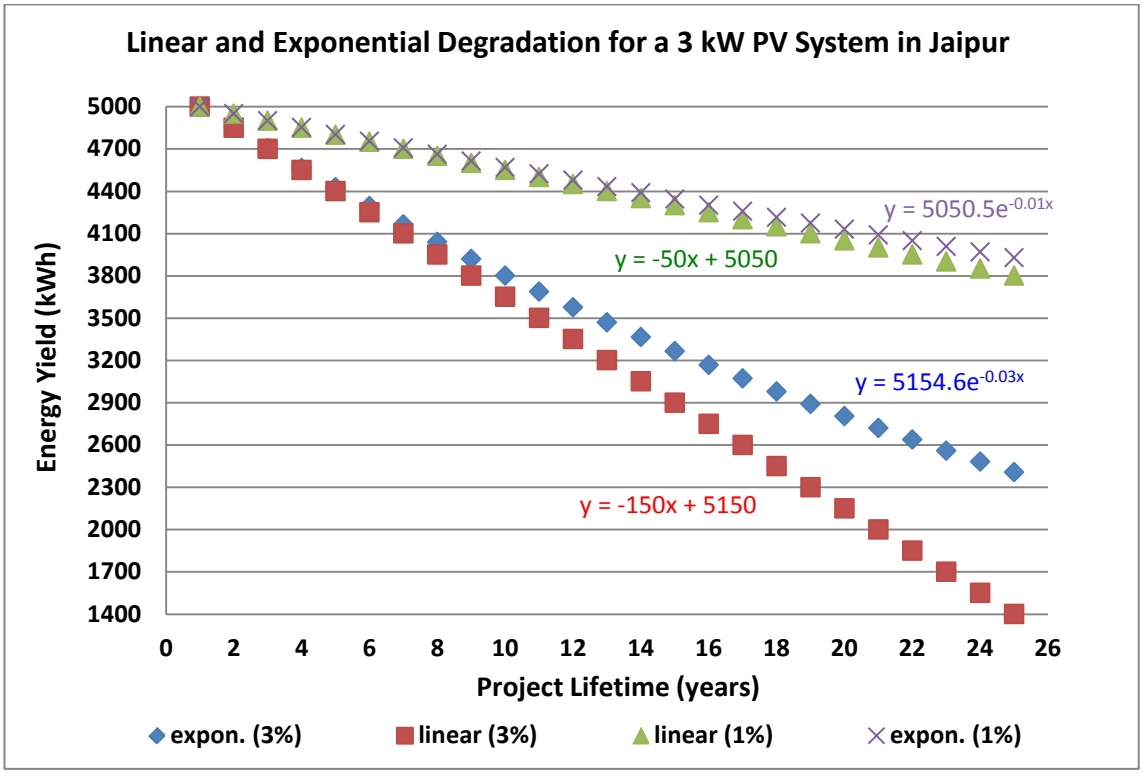

Figure 5.13: Linear and Exponential Degradation for a 3 kW PV System in Jaipur-Annual Degradation Rates 1% and 3%
(trend line equations for each series are displayed in the respective series colour)

The reason for presenting the average net PV cost per kWh is to combine the financial factors with the lifetime prediction uncertainties by excluding the volatility of both the electricity cost and PV incentive policies. Hence, a clear view of the existing PV potentials of the two countries is given based on their current PV costs and their

climatic conditions. Scenario B from Chapter 4 is re-calculated for both countries by embedding the lifetime energy ranges. Table 5.6 summarises all the values used in Scenario B for the UK and India apart from the first year energy (E_0) and the first year standard deviation (σ_0) for each city. Further, the equation used for the re-calculation is the following:

$$LCOE_{(min,\max)} = \frac{C_0+\sum_{n=0}^{N}[O\&M\times(x)^n]+[Inv.RC\times(x)^{12}]}{\sum_{n=0}^{N}[E_0\times(1-n\times D)]\pm\sum_{n=0}^{N}[\sigma_0+n\times B)]} \quad (5.13)$$

where $B = E_0 \times b$ (5.14)

The equation 5.13 provides a range of LCOE values according to the range of lifetime energy chosen for every researched city. Scenarios 2 and 5 from the energy prediction model are used for both the UK and India resulting in two LCOE ranges from each country. Moreover, each LCOE range is divided into sub-ranges according to the financial cases used for each country. Three financial cases are used for the case of India and five for the case of the UK resulting in six LCOE sub-ranges for India and ten for the UK. The lifetime energy ranges used for the calculations of the LCOE ranges have a ± 2σ deviation. Finally, Scenarios 2 and 5 have been selected in order to examine the degradation rates for each country by keeping the medium uncertainty value.

Table 5.6: Summary of the values used for the net PV cost calculations

Scenario B (input values)	**India**	**UK**
installation cost (£) (C_0):	4094	6240
inverter cost (£) (Inv.RC):	800	755
annual O&M cost (£):	164	45
nominal discount rate (*x*): (LCOE financial case number)	1.03, 1.01, 1.00 (1, 3, 4)	1.00, 1.02, 0.96, 1.05, 0.99 (1, 2, 3, 5, 6)
uncertainty factor % (U)	8.89	8.37
annual degradation rate % (*D*):	1, 3	0.5, 1
project lifetimes in years (*N*): 25 Costs Base Year: 2013-14		

5.5.2 Net PV cost results

This section presents the net PV cost results in the UK and India. Figures 5.14 and 5.15 show the LCOE range in India for Scenarios 2 and 5 respectively. Similarly, Figures 5.16 and 5.17 show the LCOE range in the UK for these scenarios. As was mentioned, the cases depicted in the four graphs are the financial cases considered in the economic evaluation of the PV systems in Chapter 4 (LCOE sub-ranges). The financial Case 2 for India and the financial Case 4 for the UK have been excluded from the graphs as they give very similar results to the financial Case 3 and to the financial Case 2 respectively. This decision has been made for the clearer representation of the results. Moreover, for the same reason the financial cases in the UK graphs are not in a numerical order but they are ordered from the lowest to the highest LCOE sub-range. Finally, the colour-bands in the graphs have been divided into 3 p/kWh interims.

The net PV cost presented in Figure 5.14 considers a degradation rate of 1% and an uncertainty factor of 8.89%. It is shown that most of the LCOE values for Case 4 are between 0.07-0.10 £/kWh while in the other two cases are between 0.10-0.13 £/kWh with some locations to be between 0.13-0.16 £/kWh and only Kohima and Shillong to be over 0.16 £/kWh for Case 1 at their upper limit.

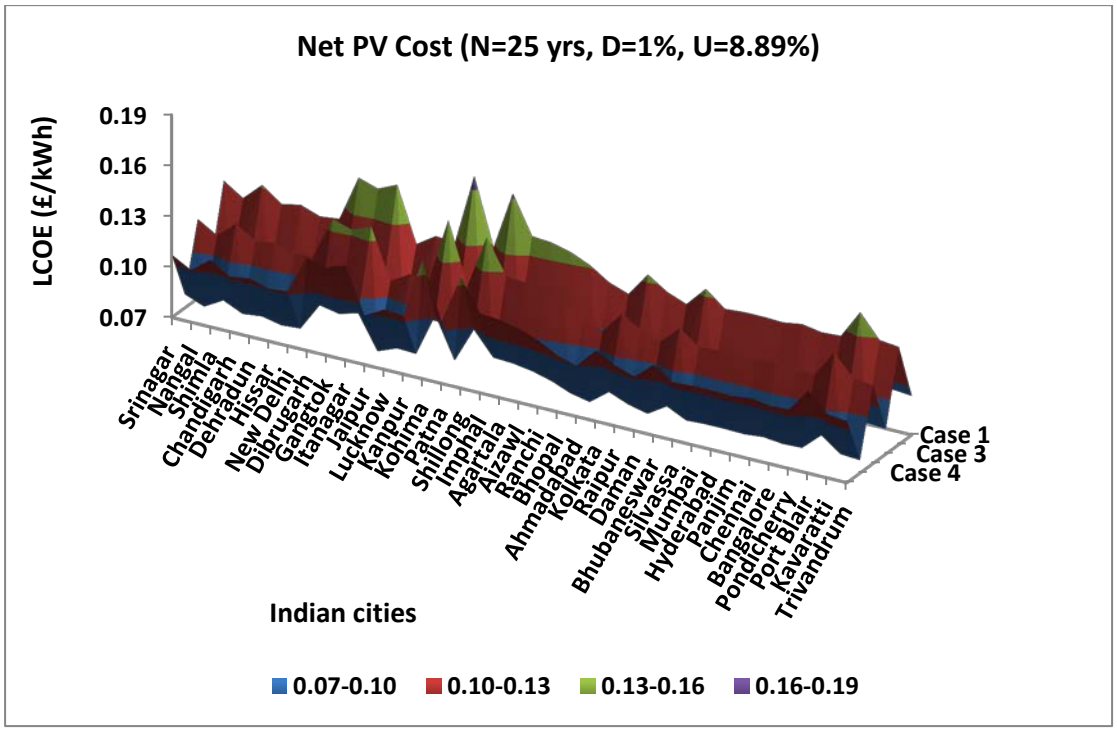

Figure 5.14: LCOE range (scenario 2, financial cases 1, 3 and 4) in India-small scale PV potentials

The results presented in Figure 5.15 consider the same uncertainty value using a degradation rate of 3%. The distribution of the LCOE values is wider than in the previous graph. There are six colour-bands of 3 p/kWh each, compare to four in the previous graph. This is normal as the degradation rate used is triple the previous value and influences the denominator of Equation 5.11. Hence, the difference between the lowest and the highest LCOE value in Scenario 2 is 0.0954 £/kWh while it becomes 0.1623 £/kWh in Scenario 5. The majority of the LCOE values in Figure 5.15 are between 0.12-0.15 £/kWh and 0.15-0.18 £/kWh for all the cases. For India, Case 4 is the one resulting in the lowest LCOE sub-range as it has the lowest nominal discount rate compared to the other two cases. Dibrugarh, Gangtok, Itanagar, Kohima and Shillong are the five cities in India out of the thirty-six that have been analysed with the highest LCOE values due to their relatively lower solar irradiation.

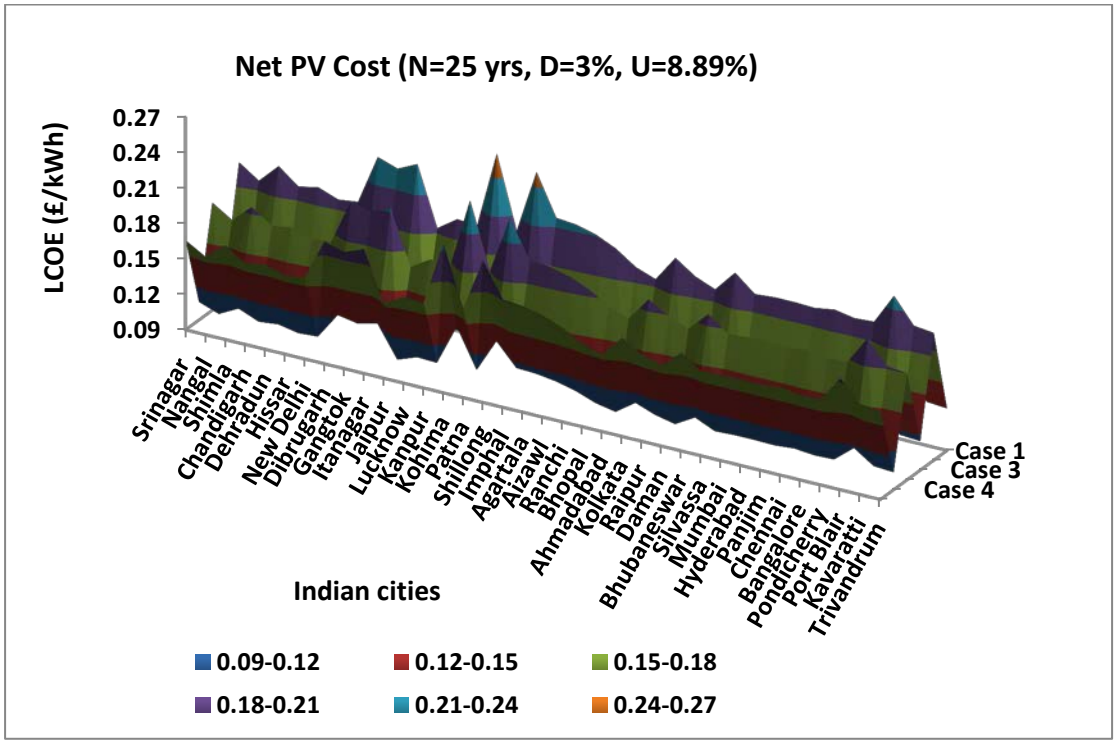

Figure 5.15: LCOE range (scenario 5, financial cases 1, 3 and 4) in India-small scale PV potentials

Regarding the net PV cost in the UK, the difference in the LCOE values between the two scenarios is smaller than India as the degradation rate has been doubled and not tripled (from 0.5% to 1%). So, the difference for the UK scenarios between the lowest and the highest LCOE value is 0.1151 £/kWh in Scenario 2 while it becomes 0.1271 £/kWh in Scenario 5. Around 75% of the LCOE values are between 0.10-0.16 £/kWh in

Figure 5.16 while in Figure 5.17 are between 0.11-0.17 £/kWh. Further, Case 3 provides the lowest LCOE sub-range in the UK.

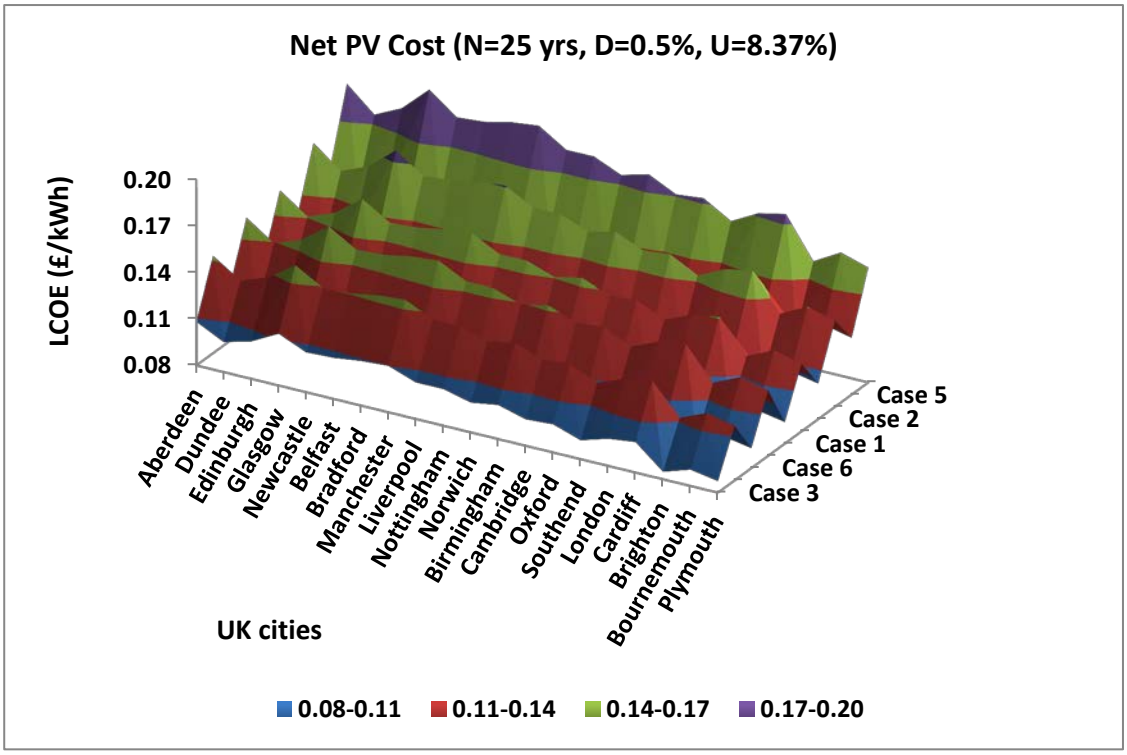

Figure 5.16: LCOE range (scenario 2, financial cases 1, 2, 3, 5, and 6) in the UK-small scale PV potentials

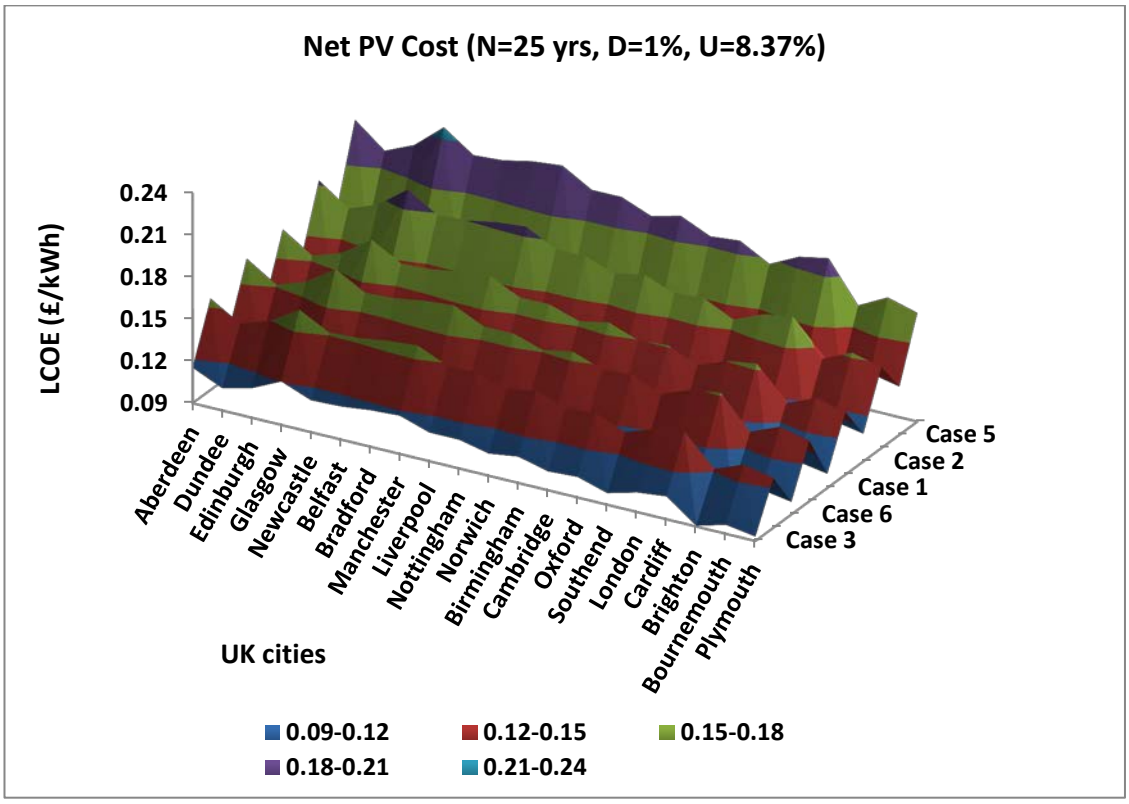

Figure 5.17: LCOE range (scenario 5, financial cases 1, 2, 3, 5, and 6) in the UK-small scale PV potentials

Finally, the cities of Patna and Cardiff have been chosen again to represent the LCOE ranges for the different scenarios and cases in India and the UK as they are close to the mean and median values of the results (Table 5.7). However, Appendix K includes analytically all the LCOE ranges for all the cities of this research. In Table 5.7 it is shown that, when the same nominal discount value is considered, the average net PV cost in India is lower than the one in the UK for Scenario 2 (India LCOE range: 0.0779-0.1069 £/kWh, UK LCOE range: 0.1072-0.1413 £/kWh). However, this changes in Scenario 5 where a higher degradation rate is used for India and the two LCOE ranges become similar (India LCOE range: 0.1051-0.1655 £/kWh, UK LCOE range: 0.1142-0.1537 £/kWh).

Table 5.7: LCOE ranges for the different scenarios and cases in Cardiff and Patna

LCOE range (£/kWh), Cardiff UK					
	Nominal Discount	Scenario 2		Scenario 5	
Financial Case	x	D=0.5%, U=8.37%		D=1%, U=8.37%	
Case 1	1.00	0.1072	0.1413	0.1142	0.1537
Case 2	1.02	0.1176	0.1550	0.1252	0.1685
Case 3	0.96	0.0998	0.1315	0.1063	0.1430
Case 5	1.05	0.1333	0.1757	0.1420	0.1911
Case 6	0.99	0.1060	0.1397	0.1129	0.1519
LCOE range (£/kWh), Patna Bihar India					
Financial Case	x	D=1%, U=8.89%		D=3%, U=8.89%	
Case 1	1.03	0.0934	0.1282	0.1260	0.1985
Case 3	1.01	0.0851	0.1167	0.1148	0.1808
Case 4	1.00	0.0779	0.1069	0.1051	0.1655

Chapter 6: Conclusions and Recommendations

Chapter 6 presents the main conclusions that have been drawn and further recommendations for research. It also expresses the originality of this work and evaluates the results in relation to different target groups (i.e. investors, governments, customers, scientists).

6.1 Main conclusions of the research

Chapter 2 was the basis of this research, as it investigated the available solar data sources and provided annual simulated results for crystalline silicon domestic PV system in various locations in India and the UK. The importance of the choice of the solar database was clearly demonstrated. It was shown that the difference of the annual energy prediction by using the same simulation software could reach around 15% only by changing the solar data in the input parameters. Hence, for comparing the simulated energy output in different locations, the same solar database must be used. It was also observed that this percentage difference is mostly attributed to the different irradiation values rather than to the temperature values for a specific location. This conclusion also appeared in Chapter 3 in the short-term investigation between the measured and the simulated data. It is shown that the differences in the PR and/or energy output values were mostly due to the difference in the irradiation values. This leads to two results; first, that the simulation package used for this research could give results close to the actual values if the on-site measured irradiation values are used as an input and second, that the methodology used in Chapter 5 for the uncertainty of the energy prediction is essential in order to place this prediction between some limits.

In addition, Chapter 2 has revealed that the two simulation packages examined in this research do not give much difference in their annual energy prediction when they consider an optimally designed PV system. This could strengthen the results presented in Chapter 5 for the PV potentials of the two countries. Finally, it was observed that the same optimally designed 3 kW PV system produces almost double the annual energy in India compared to the UK (for the UK is in the range of 2500-3300 kWh while for India is 3500-5000 kWh), which is not the case for the lifetime energy when degradation and uncertainty factors are applied in the prediction.

Chapter 3 presented the short-term performance analysis of three different PV technologies at an Indian site under harsh environmental conditions. The importance of the regular cleaning of the PV modules in such sites was demonstrated. Some performance mismatch was identified between the parallel-connected strings of the examined systems. A possible explanation could be the relative heavier soiling of some strings. Because of the harsh Indian environment, an extra soiling loss factor for the case of India was used in the lifetime energy prediction model, despite the fact that the results from PVsyst already take into account an annual soiling loss factor. However, especially for the examined site and after conducting a further investigation for a single string of the mono-Si array, the frequency of cleaning the systems on alternate days was concluded as adequate (through the experiment) for dusty environments like the one examined here.

Another important factor, which was demonstrated in Chapter 3 through the case study in Kanpur, is the influence of the module power tolerance to the PV system energy yield. It is shown that the mean energy gain between the fixed and tracking system for the examined period could vary by around 12% due to the module power tolerance. Hence, an extra uncertainty factor was considered for the module power tolerance in the lifetime energy model presented in Chapter 5.

Regarding the short-term performance variations of the three technologies, the effect of temperature on the performance ratio is observed for multi-Si at high irradiation levels and inverter threshold and shading issues have been revealed for the CIGS fixed system. Nevertheless, the multi-Si system was the most stable technology in terms of performance during the examined period since it provides a good match between the expected and the calculated results. Hence, it is sensible to examine the PV economic and technical potential by considering a stable PV technology. Finally, the performance variation analysis revealed the need of monitoring in the Indian sites and the need to develop their experience in the case of sensors and data acquisition system installations.

Regarding the economic evaluation presented in Chapter 4, it is observed that in almost all cases (apart from Case 5) a domestic PV system in the UK can reach grid parity without using any supporting mechanism if it operates for 25 years minimum. On

the other hand, in order for some Indian cities to reach the grid parity level, the electricity savings have to be included in the calculations since the domestic electricity cost in India is very low compared to the UK. Hence, it is much more difficult to reach grid parity in India due to the low electricity cost, although the system produces a greater amount of energy. The advantage offered by reaching grid parity is to equal or reduce the cost of energy compared to the retail electricity cost. Nevertheless, this may not be a sufficient stimulus to invest in a PV system, given the length of the payback period. Therefore, the analysis stresses the importance of the incentive scheme policies in both countries. Moreover, it shows the correlation between the LCOE and two main economic parameters (NPV and payback period). Clearly, a reduction in cost will lead to lower LCOE values under all scenarios and so would make the investment more attractive in a larger number of cities and this has also been demonstrated by comparing the 2012 to 2014 LCOE values for the UK. The installation cost depends on a range of market factors but is expected to reduce consistently over time.

Further, the analysis has assumed a maximum system lifetime of 25 years, with costs and benefits associated with that lifetime. Whilst a reduction in output is expected over this period, the useful system lifetime may be much longer than this depending on the economic benefits of replacement of modules at 25 years. Any extension of lifetime would reduce the effective LCOE accordingly, but may not affect the initial investment decision if this is made on the basis of a payback period well below the system lifetime. The ranges of the LCOE values presented could be considered as a snapshot of the mobile situation of the UK and Indian PV market prices and policies.

It should be repeated that LCOE calculations are also influenced by the energy prediction. Hence, using a different energy prediction will provide different LCOE ranges accordingly with the change in energy. This is the reason why in Chapter 5 when the net PV cost for the two countries is presented, the methodology included ranges of lifetime energy prediction and thus ranges of LCOE values. It can be concluded that the accuracy of the energy prediction plays a key role in the LCOE calculations and hence in the cost-effectiveness of the system.

Finally, Chapter 4 presented indicative lifetime CO_2 emission savings for a 3 kW PV system. It was concluded through the results that the same PV system could save

around two and a half to three times the amount of CO_2 emissions in India than in the UK during its lifetime. This was partly attributed to India's emission factor and demonstrates the environmental benefits of the PV systems, whose deployment could contribute in the reduction of this factor.

The analysis in Chapter 5 demonstrates the importance of the operation and maintenance conditions of a domestic PV system and presents a model for the annual energy assessment and lifetime energy prediction. It clearly shows that even for these two countries, which are significantly different in respect to their solar resource, the PV systems may produce similar amounts of energy during their lifetime for reasonable assumptions of degradation rates and uncertainty levels. An uncertainty in the energy output makes the economic viability uncertain. As has been demonstrated for the city of Patna in India, depending on the chosen mean lifetime energy prediction and for a combined uncertainty of 9.75%, the chosen deviations (i.e. ±σ and ±2σ) could give a difference in the lifetime energy prediction between 9% and 24%. Hence, the investor should be aware of the energy prediction risks (i.e. calculation method of the lifetime energy, chosen lifetime energy mean value, combined uncertainty value and deviation), especially in investments where a minimum rate of return is specified.

In addition, the lifetime energy potentials of domestic PV system have been presented, for realistic assumptions and an optimum system design. The results have shown an intermediate lifetime energy range of 60,000-70,000 kWh for the UK while for India it was between 70,000-100,000 kWh. Finally, the majority of the net PV cost values for the UK is in the range of 0.11-0.17 £/kWh for 0.5% degradation rate and 0.12-0.18 £/kWh for 1% degradation rate. Similarly, for India they are in the range of 0.07-0.13 £/kWh for 1% degradation rate and 0.12-0.18 £/kWh for 3% degradation rate. This results in two main conclusions: firstly, that the installation of domestic PV system is cheaper in India than in the UK apart from the extreme case of the 3% annual degradation. Also, even in the extreme degradation case for India the net cost per kWh of installing a PV system in the two countries is similar. Secondly, by combining this result with the economic analysis in Chapter 4, it is shown that it is more profitable with the current policies to install a domestic PV system in the UK rather than India. Hence, it is shown that India has to reconsider its incentive policies for the domestic PV system deployment.

Note that the aforementioned values are valid based on the assumptions and prices considered in the methodologies and models formed for the investigation of the domestic PV potential in the UK and India.

6.2 Originality and Recommendations

As was written in the introductory chapter, the originality of this research is based on four main parts:

- The assessment of the performance variations of different PV system technologies in a harsh Indian environment.
- The calculation of the LCOE parameter for the domestic PV system deployment and cost-effective planning, especially in India.
- The development of a generic model on the lifetime energy prediction and annual energy assessment.
- The expression of the combined PV potential (technical, economic and environmental) as a function of the location within and between the two countries

Chapter-wise the contributions are:

The original contribution from Chapter 2 is the collective annual energy prediction for various locations in the UK and India combined with the investigation of the solar databases, two simulation packages and their loss mechanisms.

The original contribution from Chapter 3 is based on the case study made for the installed PV site at SERE in Kanpur. As was mentioned in Chapter 3, the site is one of the first PV installations in India with a detailed monitoring system. The conclusions drawn for this short-term analysis are important for both the knowledge of the performance variation of three different PV technologies in a harsh Indian environment and for realizing how important is to acquire solid measurements. Moreover, this analysis offered the opportunity to validate the simulated results of this research.

The original contribution from Chapter 4 is the development and the adjustment of the LCOE formula to the UK and India specific PV market policies and prices. Moreover,

the sensitivity analysis, which is embedded in the LCOE results, provides realistic LCOE ranges for all the examined locations. Finally, the formula that has been formed in can be easily combined with two economic indicators: the Net Present Value and Payback Period of an investment.

Chapter 5 combines the knowledge acquired from the research in the previous Chapters. Its original contribution is the lifetime energy prediction and energy assessment model, which is generic but it has the flexibility to evolve to a location specific model if certain parameters are known (i.e. specific degradation and uncertainty values). Finally, Chapter 5 expresses the PV potential of the two countries as regards to their lifetime energy prediction and their net PV cost.

This research is based on the simulation results and the literature review. The models that have been developed for the economic and technical evaluation have been built on this basis and expressed the PV system potential in India and the UK. Even though the assumptions used in these models are based on the current PV literature, they can be periodically updated and/or adjusted in order to express the future PV potential of these two countries or any other country. This research can be useful to the PV scientific community and to decision makers (i.e. investors, governments, customers). For the decision makers, it presents a holistic view of the domestic potential (technical and economic) of these two countries. It contributes to the better understanding of the technical potential and the transformation of this potential into economic terms and values. For the scientific community, the models presented in this research could be adapted and further developed into location specific models taken into account the special characteristics that a location might have. Further recommendation for research could be the analysis of the technical and economic potential for large scale PV systems in these two countries. Moreover, future research could examine in more depth the environmental benefits that they may be added and/or incorporated to the economic and technical potential of a certain location. Finally, this research has shown that a general climate classification is not sufficient to provide a correlation between the PV system energy yield and the climate. However, the categorisation of the influences that the microclimates have (regional categorisation) on the photovoltaic technologies is still an on-going process, which can contribute to the better understanding of the degradation mechanisms and subsequently the energy yield of the systems.

References

[1] Engineering and Physical Sciences Research Council (2010) *UK and India collaborate on cheaper and more efficient solar cells*, Available at: http://www.epsrc.ac.uk/newsevents/news/2010/Pages/solarcells.aspx (Accessed: 11 May 2013).

[2] Stability and Performance of Photovoltaic (STAPP) (2012) *About STAPP*, Available at: http://www.ese.iitb.ac.in/~STAPP/index.html (Accessed: 11 May 2013).

[3] Huld, T. (2014) E-mail to Tatiani Georgitsioti, 16 February. Solar Data for India.

[4] Renew India Campaign (2012) *Renewable Energy Installed Capacity in India Reaches 26,368.36 MW*, Available at: http://www.renewindians.com/2012/12/Renewable-Energy-Installed-Capacity-in-India.html (Accessed: 19 May 2013).

[5] Ministry of New & Renewable Energy (2012) 'JNNSM Phase-II, Policy Document – WORKING DRAFT', Available at: http://mnre.gov.in/file-manager/UserFiles/draft-jnnsmpd-2.pdf (Accessed: 11 May 2013).

[6] Department of Energy & Climate Change (2012) 'UK Renewable Energy Roadmap', Available at: https://www.gov.uk/government/uploads/system/uploads/attachment_data/file/80246/11-02-13_UK_Renewable_Energy_Roadmap_Update_FINAL_DRAFT.pdf (Accessed: 19 May 2013).

[7] Department of Energy & Climate Change (2010) 'National Renewable Energy Action Plan for the United Kingdom', Available at: https://www.gov.uk/government/uploads/system/uploads/attachment_data/file/47871/25-nat-ren-energy-action-plan.pdf (Accessed: 11 May 2013).

[8] Solar Power Portal (2014) *UK solar industry installs massive 1.1GW in first quarter of 2014*, Available at: http://www.solarpowerportal.co.uk/guest_blog/uk_solar_industry_installs_massive_1.1_gw_in_first_quarter_of_2014_2356 (Accessed: 11 May 2014).

[9] The Guardian (2015) *Solar power in the UK almost doubled in 2014*, Available at: http://www.theguardian.com/environment/2015/jan/29/solar-power-in-the-uk-almost-doubled-in-2014 (Accessed: 11 February 2015).

[10] Burton, T. & Mason, N. (2012) 'The potential for PV in the UK', *PVSAT-8*. Northumbria University, Newcastle upon Tyne 2-4 April. Abingdon: The Solar Energy Society, pp.73-76.

[11] Green Word Investor (2011) *Solar Power in India*, Available at: http://www.greenworldinvestor.com/2011/04/07/solar-power-in-india-all-you-wanted-to-know-solar-power-plantssolar-panel-manufacturersinstallersinverter-companiessubsidiesjnnsmtariffsrecrpo-and-technologypvsolar-thermal/ (Accessed: 11 May 2013).

[12] Bridge to India (2013) 'India Solar Compass', Available at: http://bridgetoindia.com/blog/?p=1568 (Accessed: 20 May 2013).

[13] Huld, T. Gottschalg, R. Beyer, H. & Topic, M. (2011) 'Mapping the performance of PV modules, effects of module type and data averaging' *Solar Energy*, 84(2), pp.324-338 *ScienceDirect* [Online]. Available at: http://www.sciencedirect.com (Accessed: 18 May 2013).

[14] Goss, B. Betts, T. & Gottschalg, R. (2012) 'Uncertainty Analysis of Solar Photovoltaic Energy Yield Prediction', *PVSAT-8*. Northumbria University, Newcastle upon Tyne 2-4 April. Abingdon: The Solar Energy Society, pp.157-160.

[15] Brankera, K. Pathaka, M. & Pearcea, J. (2011) 'A review of solar photovoltaic levelized cost of electricity' *Renewable and Sustainable Energy Reviews*, 15(9), pp. 4470-4482 *ScienceDirect* [Online]. Available at: http://www.sciencedirect.com (Accessed: 15 January 2013).

[16] European Commission (2001-2012) *Photovoltaic Geographical Information System (PVGIS)* (Version PVGIS-4) [computer program]. Available at: http://re.jrc.ec.europa.eu/pvgis/ (Accessed: 18 May 2013).

[17] University of Geneva (2010) *PVsyst* (Version 5.3.1) [computer program].

[18] Google Earth (2013) *India* (Version Google Earth 7) [computer program]. Available at: http://earth.google.com/ (Accessed: 10 May 2014).

[19] Google Earth (2013) *United Kingdom* (Version Google Earth 7) [computer program]. Available at: http://earth.google.com/ (Accessed: 10 May 2014).

[20] The World Bank Group (2014) *Land Area (sq. km)*, Available at: http://data.worldbank.org/indicator/AG.LND.TOTL.K2 (Accessed: 10 May 2014).

[21] India Meteorological Department (IMD) (2010) 'Climate Profile of India', Available at: http://www.imd.gov.in (Accessed: 10 May 2014).

[22] India Meteorological Department (IMD) (2014) Available at: http://www.imd.gov.in/doc/regsub.jpg (Accessed: 10 May 2014).

[23] India Meteorological Department (IMD) (2013) 'Climate Diagnostics Bulletin of India' Available at: http://www.imd.gov.in (Accessed: 10 May 2014).

[24] Encyclopedia Britannica (2014) *Köppen climate classification*, Available at: http://www.britannica.com/EBchecked/topic/322068/Koppen-climate-classification(Accessed: 10 May 2014).

[25] Weather Online (1999-2014) *India*, Available at: http://www.weatheronline.co.uk/reports/climate/India.htm(Accessed: 10 May 2014).

[26] Climate (2007) *Köppen classification*, Available at: http://www.meteorologyclimate.com (Accessed: 10 May 2014).

[27] Weather Online (1999-2014) *England and Scotland*, Available at: http://www.weatheronline.co.uk/reports/climate/England-and-Scotland.htm (Accessed: 10 May 2014).

[28] Met office (2014) *Average maps (1981-2010)*, Available at :http://www.metoffice.gov.uk/public/weather/climate/city-of-london-greater-london#?tab=climateMaps (Accessed: 10 May 2014).

[29] Ministry of New and Renewable Energy (MNRE) (2006) 'Chapter 2: Climate and Buildings' Available at: http://mnre.gov.in/solar-energy/ch2.pdf (Accessed: 10 May 2014).

[30] Meteonorm, Available at: http://meteonorm.com/products/meteonorm-software/ (Accessed: 18 May 2014).

[31] World Radiation Data Centre, Available at: http://wrdc.mgo.rssi.ru (Accessed: 18 May 2014).

[32] NASA (2013) *Surface meteorology and Solar Energy*, Available at: https://eosweb.larc.nasa.gov/sse/ (Accessed: 10 May 2014).

[33] Solar GIS (2011) *Database SolarGIS version 1.6 satellite-derived solar radiation and air temperature*, Available at: http://solargis.info/ (Accessed: 11 May 2014).

[34] Natural Resources Canada (2013) *RETScreen* (Version 4) [computer program]. Available at: http://www.retscreen.net/ang/home.php (Accessed: 18 May 2014).

[35] SolarBuzz (2012) *Technologies*, Available at: http://www.solarbuzz.com/going-solar/understanding/technologies (Accessed: 15 May 2013).

[36] Sharp Electronics (2012) *ND-R 250 A5*, Available at: http://www.sharp.co.uk/cps/rde/xchg/gb/hs.xsl/-/html/polycrystalline.htm (Accessed: 30 May 2013).

[37] SMA Solar Technology (2012) *Sunny Boy 2000HF/2500HF/3000HF*, Available at: http://www.sma.de/en/products/solar-inverters-with-transformer/sunny-boy-2000hf-2500hf-3000hf.html (Accessed: 30 May 2013).

[38] SMA Solar Technology (2012) *Sunny Tripower 8000TL/10000TL/12000TL/15000TL/17000TL*, Available at: http://www.sma.de/en/products/solar-inverter-without-transformer.html (Accessed: 30 May 2012).

[39] PVtech (2014) *Top 10 PV module suppliers in 2013*, Available at: http://www.pv-tech.org/guest_blog/top_10_pv_module_suppliers_in_2013 (Accessed: 30 May 2014).

[40] PV Magazine (2013) *Global PV inverter market shakeout and geographical shifts expected, says GTM*, Available at: http://www.pv-magazine.com/news/details/beitrag/global-pv-inverter-market-shakeout-and-geographical-shifts-expected--says-gtm_100010972/#axzz2Ujj4kPp7 (Accessed: 30 May 2013).

[41] Ofgem (2012) 'Feed-in Tariff (FIT): Annual Report 2011-12', Available at: http://www.ofgem.gov.uk/Sustainability/Environment/fits/Documents1/FITs%20Annual%20Report%202011-2012.pdf (Accessed: 15 January 2013).

[42] Šúri, M. Huld, T. Dunlop, E. & Ossenbrink, H. (2007) 'Potential of solar electricity generation in the European Union member states and candidate countries' *Solar Energy*, 81(10), pp.1295–1305 *ScienceDirect* [Online]. Available at: http://www.sciencedirect.com (Accessed: 18 May 2014).

[43] Huld, T. Müller, R. & Gambardella, A. (2012) 'A new solar radiation database for estimating PV performance in Europe and Africa' *Solar Energy*, 86(6), pp.1803–1815 *ScienceDirect* [Online]. Available at: http://www.sciencedirect.com (Accessed: 18 May 2014).

[44] Siraki, A. & Pillay, P. (2012) 'Study of optimum tilt angles for solar panels in different latitudes for urban applications' *Solar Energy*, 86(6), pp.1920–1928 *ScienceDirect* [Online]. Available at: http://www.sciencedirect.com (Accessed: 18 May 2014).

[45] Huld, T. Dunlop, E. Beyer, H. & Gottschalg, R. (2013) 'Data sets for energy rating of photovoltaic modules' *Solar Energy*, 93, pp.267–279 *ScienceDirect* [Online]. Available at: http://www.sciencedirect.com (Accessed: 18 May 2014).

[46] Cape & Islands Self-Reliance (2008) 'A Guide to Grid-Connected Photovoltaic Systems', Available at: http://www.reee.sacities.net/sites/default/files/Tech%20Review/SOLAR/PV/A%20Guide%20to%20Grid-Connected%20Photovoltaic%20Systems.pdf (Accessed: 15 June 2014).

[47] Nordmann, T. & Clavadetscher, L. (2003) 'Understanding Temperature Effects on PV System Performance', *Proceedings of the 3rd World Conference on PV Energy Conversion*. Osaka-Japan, 18 May.

[48] Lenardic, D. (2001-2012) *Photovoltaic Modules*, *PV Recourses*, Available at: http://www.pvresources.com/BalanceofSystem/Modules.aspx (Accessed: 15 June 2014).

[49] National Instruments (2012) *Part II-Photovoltaic Cell I-V Characterization Theory and LabVIEW Analysis Code*, Available at: http://zone.ni.com/devzone/cda/tut/p/id/7230 (Accessed: 15 June 2014).

[50] Bastarrika, M. Kalantzis, C. & Zurutuza, I. (1999) 'Grid Connected Photovoltaics in Buildings', *Department of Mechanical Engineering*, "University of Strathclyde", Available at: http://www.esru.strath.ac.uk/EandE/Web_sites/98-9/grid_connected_pv/index.htm (Accessed: 15 June 2014).

[51] The German Energy Society (2008) *Planning and Installing Photovoltaic Systems-A Guide for Installers, Architectures and Engineers.* 2nd end. London: Earthscan.

[52] Bletterie, B. Bründlinger, R. Häberlin, H. Baumgartner, F. Schmidt, H. Burger, B. Klein, G. & Abella, M. (2008) 'Redefinition of the European Efficiency-Finding the Compromise Between Simplicity and Accuracy'*23rd EU PVSEC*. Valencia Spain, 1-5 September.

[53] Makrides, G. Zinsser, B. Norton, M. & Geroghiou, G. (2012) 'Performance of Photovoltaics Under Actual Operating Conditions' in Fthenakis, G. (ed), *Third Generation Photovoltaics*, InTech, pp. 201-232, Available at: http://www.intechopen.com/books/third-generation-photovoltaics/performance-of-photovoltaics-under-actual-operating-conditions (Accessed: 15 June 2014).

[54] Stein, J. Sutterlüti, J. Ransome, S. Hansen, C. & King, B. (2013) 'Outdoor PV Performance Evaluation of Three Different Models: Single-diode, SAPM and Loss Factor Model', *28th EU PVSEC*. Paris France, 30 September-4 October.

[55] Ransome, S. Sutterlueti, J. & Sellner, S. (2012) 'PV technology differences and discrepancies in modelling between simulation programs and measurements' *38th IEEE PVSC*. Austin TX USA, 3-8 June.

[56] Ransome, S. (2010) 'The present status of kWh/kWp measurements and modelling' *5th World PV Conference*. Valencia Spain, 6-10 September.

[57] Ransome, S. (2010) 'A detailed comparison of measured outdoor performance vs. simulation program predictions for different PV technologies' *PVSAT-6*. Southampton UK, 24-26 March.

[58] Sutterlueti, S. Ransome, S. Kravets, R. & Schreier, L. (2011) 'Characterising PV Modules under Outdoor Conditions: What's Most Important for Energy Yield' *26th EU PVSEC*. Hamburg Germany, 5-9 September.

[59] Marion, B. Adelstein, J. Boyle, K. Hayden, H. Hammond, B. Fletcher, T. Canada, B. Narang, D. Shugar, D. Wenger, H. Kimber, A. Mitchell, L. Rich, G. & Townsend, T. (2005) 'Performance Parameters for Grid-Connected PV Systems', *31st IEEE Photovoltaics Specialists Conference and Exhibition,* Lake Buena Vista Florida, 3-7 January.

[60] Hamidah, I. Sathyajith, M. Aloka, S. Balakrishnan, N. Lim C. & Saiful, H. (2013) 'Comparative Performance of Grid Integrated Solar Photovoltaic Systems under the Tropical Environment' *IEEE ISGT Asia 2013*. Bangalore India, 10-13 November.

[61] Ransome, S. & Wohlgemuth, J. (2005) 'Findings from Worldwide Studies of PV Module and System Performance' *PVSAT-2*. Loughborough UK

[62] Ransome, S. (2010) 'Comparing PV simulation models and methods with outdoor measurements' *PVSC 35*. Hawaii USA, 20-25 June.

[63] Sellner, S. Sutterlüti, J. Ransome, S. Schreier, L. & Allet, N. (2012) 'Understanding Module Performance further: validation of the novel loss factors model and its extension to ac arrays' *27th EU PVSEC*. Frankfurt Germany, 24-28 September.

[64] Ransome, S. (2007) 'How well do PV modelling algorithms really predict performance?' *22nd EU PVSEC*. Milan Italy, 3-7 September.

[65] Ransome, S. (2011) 'Improving and Understanding kWh/kWp Simulations' *26th EU PVSEC*. Hamburg Germany, 5-9 September.

[66] Mermoud, A. & Lejeune, T. (2010) 'Performance assessment of a simulation model for PV modules of any available technology'*25th World EU PVSEC*. Valencia Spain, 6-10 September.

[67] Mermoud, A. (2011) 'Note about the PHOTON simulation Software survey – 2011' *PVsyst software evaluation*, Available at: http://www.pvsyst.com/en/publications (Accessed: 15 June 2014).

[68] Pierro, M. Bucci, F. & Cornaro, C. (2014) 'Full characterization of photovoltaic modules in real operating conditions: theoretical model, measurement method and results', *Progress in Photovoltaics: Research and Applications*, doi: 10.1002/pip.2450, *Wiley Online Library* [Online]. Available at: http://onlinelibrary.wiley.com/ (Accessed: 15 June 2014).

[69] Ueda, Y. Kurokawa, K. Kitamura, K. Yokota, M. Akanuma, K. & Sugihara H. (2009) 'Performance analysis of various system configurations on grid-connected residential PV systems' *Solar Energy Materials & Solar Cells*, 93 (6-7), pp. 945–949 *ScienceDirect* [Online]. Available at: http://www.sciencedirect.com (Accessed: 15 June 2014).

[70] Strobel, M. Betts, T. Friesen, G. Beyer, H. & Gottschalg, R. (2009) 'Uncertainty in Photovoltaic performance parameters- dependence on location and material' *Solar Energy Materials & Solar Cells*, 93 (6-7), pp. 1124–1128 *ScienceDirect* [Online]. Available at: http://www.sciencedirect.com (Accessed: 15 June 2014).

[71] Woyte, A. Richter, M. Moser, D. Mau, S. Reich, N. & Jahn U. (2013) 'Monitoring of photovoltaic systems: good practices and systematic analysis', *28th EU PVSEC*. Paris France, 30 September - 4 October.

[72] Nakada, Y. Fukushige, S. Minemoto T. & Takakura, H. (2009) 'Seasonal variation analysis of the outdoor performance of amorphous Si photovoltaic modules using the contour map' *Solar Energy Materials & Solar Cells*, 93 (3), pp. 334–337 *ScienceDirect* [Online]. Available at: http://www.sciencedirect.com (Accessed: 15 June 2014).

[73] Okullo, W. Munji, M. Vorster, F. & vanDyk, E. (2011) 'Effects of spectral variation on the device performance of copper indium diselenide and multi-crystalline silicon photovoltaic modules' *Solar Energy Materials & Solar Cells,* 95 (2), pp. 759–764 *ScienceDirect* [Online]. Available at: http://www.sciencedirect.com (Accessed: 15 June 2014).

[74] Gottschalg, R. Infield, D. & Kearney, M. (2003) 'Experimental study of variations of the solar spectrum of relevance to thin film solar cells' *Solar Energy Materials & Solar Cells*, 79(4), pp. 527–537 *ScienceDirect* [Online]. Available at: http://www.sciencedirect.com (Accessed: 15 June 2014).

[75] Ghazali, A. & Abdul Malek, A. (2012) 'The performance of three different solar panels for solar electricity applying solar tracking device under the malaysian climate condition', *Energy and Environment Research*, 2 (1), pp. 235-243 Available at: http://www.ccsenet.org/journal/index.php/eer/index (Accessed: 15 June 2014).

[76] Ayompe, L. Duffy, A. McCormack, S. & Conlon, M. (2011) 'Measured performance of a 1.72 kW rooftop grid connected photovoltaic system in Ireland' *Energy Conversion and Management*, 52 (2), pp. 816–825 *ScienceDirect* [Online]. Available at: http://www.sciencedirect.com (Accessed: 15 June 2014).

[77] Firth, S. Lomas, K. & Rees, S. (2010) 'A simple model of PV system performance and its use in fault detection' *Solar Energy*, 84 (4), pp. 624–635 *ScienceDirect* [Online]. Available at: http://www.sciencedirect.com (Accessed: 15 June 2014).

[78] Mani, M. & Pillai, R. (2010) 'Impact of dust on solar photovoltaic (PV) performance: Research status, challenges and recommendations' *Renewable and Sustainable Energy Reviews*, 14 (9), pp. 3124–3131 *ScienceDirect* [Online]. Available at: http://www.sciencedirect.com (Accessed: 15 June 2014).

[79] Ghosh, B. & Roy, S. (2013) 'Performance of a 10MW_p grid-integrated PV system in salty warm and humid ambience in India', *28th EU PVSEC*. Paris France, 30 September - 4 October.

[80] Beattie, N. Moir, R. Chacko, C. Buffoni, G. Roberts, S. & Pearsall, N. (2012) 'Understanding the effects of sand and dust accumulation on photovoltaic modules' *Renewable Energy*, 48, pp. 448-452 *ScienceDirect* [Online]. Available at: http://www.sciencedirect.com (Accessed: 15 June 2014).

[81] Katsumata, N. Nakada, Y. Minemoto, T. & Takakura, H. (2011) 'Estimation of irradiance and outdoor performance of photovoltaic modules by meteorological data' *Solar Energy Materials & Solar Cells*, 95 (1), pp. 199–202 *ScienceDirect* [Online]. Available at: http://www.sciencedirect.com (Accessed: 15 June 2014).

[82] Gottschalg, R. Betts, T. Williams, S. Sauter, D. Infield, D. & Kearney, M. (2004) 'A critical appraisal of the factors affecting energy production from amorphous silicon photovoltaic arrays in a maritime climate' *Solar Energy*, 77 (6), pp. 909-916 *ScienceDirect* [Online]. Available at: http://www.sciencedirect.com (Accessed: 26 August 2014).

[83] Sharma, V. Kumar, A. Sastry, O. & Chandel, S. (2013) 'Performance assessment of different solar photovoltaic technologies under similar outdoor conditions' *Energy*, 58, pp. 511-518 *ScienceDirect* [Online]. Available at: http://www.sciencedirect.com (Accessed: 26 August 2014).

[84] Pavan, A. Mellit, A. De Pieri, D. & Lughi, V. (2012) 'A study on the mismatch effect due to the use of different photovoltaic modules classes in large-scale solar parks' *Progress in Photovoltaics: Research and Applications*, 22 (3), pp.332-345 *Wiley Online Library*[Online]. Available at: http://onlinelibrary.wiley.com/ (Accessed: 15 June 2014).

[85] Villalva, M. Gazoli, J. & Filho, E. (2009) 'Comprehensive Approach to Modeling and Simulation of Photovoltaic Arrays' *Power Electronics IEEE Transactions*, 24(5), pp. 1198–1208 *IEEE Xplore* [Online]. Available at: http://ieeexplore.ieee.org/Xplore/home.jsp (Accessed: 15 June 2014).

[86] Lorenzo, E. Moretón, R. & Luque, I. (2014) 'Dust effects on PV array performance: in field observations with non-uniform patterns' *Progress in Photovoltaics: Research and Applications*, 22(6), pp. 666-670 *Wiley Online Library* [Online]. Available at: http://onlinelibrary.wiley.com/ (Accessed: 15 June 2014).

[87] European Photovoltaic Industry Association (2014) 'Global Market Outlook for Photovoltaic 2014-2018', Available at: http://www.epia.org/news/publications/ (Accessed: 11 July 2014).

[88] European Photovoltaic Industry Association (2013) 'Global Market Outlook for Photovoltaic 2013-2017', Available at: http://www.epia.org/news/publications/ (Accessed: 11 May 2013).

[89] Bridge to India (2014) 'India Solar Compass', Available at: http://bridgetoindia.com/blog/?p=1568 (Accessed: 11 July 2014).

[90] Clean Technica (2014) *India's Installed Solar Power Capacity Crosses 3 GW*, Available at: http://cleantechnica.com/2014/11/26/indias-installed-solar-power-capacity-crosses-3-gw/ (Accessed: 11 February 2015).

[91] ESMAR (2013) 'Paving the Way for a Transformational Future Lessons from Jawaharlal Nehru National Solar Mission Phase I', Available at: http://www.esmap.org/node/3509 (Accessed: 11 July 2014).

[92] X-Rates (2015) *Monthly Average*, Available at: http://www.x-rates.com/average/?from=INR&to=GBP&amount=1&year=2012 (Accessed: 30 October 2015).

[93] Bridge to India (2014) 'India Solar Handbook', Available at: http://bridgetoindia.com/blog/?p=1568 (Accessed: 11 July 2014).

[94] Clean Technica (2014) *India's Solar Power Capacity Tops 2,600 MW*, Available at: http://cleantechnica.com/2014/04/08/indias-solar-power-capacity-tops-2600-mw/ (Accessed: 11 July 2014).

[95] PV Magazine (2014) *India considering tax incentives for solar households*, Available at: http://www.pv-magazine.com/news/details/beitrag/india-considering-tax-incentives-for-solar-households_100015444/#axzz38WHdJKCN (Accessed: 11 July 2014).

[96] XE (1995-2014) *XE Currency Converter*, Available at: http://www.xe.com/currencyconverter/ (Accessed: 6 September 2014).

[97] European Photovoltaic Industry Association (2012) *Global Market Outlook for Photovoltaic until 2016*, Available at: http://www.epia.org/news/publications/global-market-outlook-for-photovoltaics-until-2016/ (Accessed: 15 January 2013).

[98] PV Magazine (2013) *UK hits 2 GW of PV*, Available at: http://www.pv-magazine.com/news/details/beitrag/uk-hits-2-gw-of-pv_100010188/ (Accessed: 11 July 2014).

[99] MCS (2013) *Micro Certification Scheme*, Available at: http://www.microgenerationcertification.org/ (Accessed: 15 January 2013).

[100] Ofgem (2014) *Tariff Tables*, Available at: http://www.ofgem.gov.uk/Sustainability/Environment/fits/tariff-tables/Pages/index.aspx (Accessed: 11 July 2014).

[101] Ofgem (2014) *Feed-in-Tariff (FIT) scheme*, Available at: http://www.ofgem.gov.uk/SUSTAINABILITY/ENVIRONMENT/FITS/Pages/fits.aspx (Accessed: 11 July 2014).

[102] Jäger-Waldau, A. (2013) 'PV Status Report', *JRC/European Commission*

[103] UK Government (2010) 'National Renewable Energy Action Plan for the United Kingdom', *Renewable Energy Directive 2009/28/EC*

[104] Ofgem (2012) 'Feed-in Tariff (FIT): Annual Report 2011-12', Available at: http://www.ofgem.gov.uk/Sustainability/Environment/fits/Documents1/FITs%20Annual%20Report%202011-2012.pdf (Accessed: 4 June 2013).

[105] Renewable Energy Foundation (2013) *Solar Photovoltaic Generation in the United Kingdom*, Available at: http://www.ref.org.uk/publications/297-solar-photovoltaic-generation-in-the-united-kingdom (Accessed: 11 July 2014).

[106] Department of Energy & Climate Change (2015) *Solar Photovoltaics Deployment*, Available at: https://www.gov.uk/government/statistics/solar-photovoltaics-deployment (Accessed: 28 February 2015).

[107] UK Government (2013) *Increasing the use of low-carbon technologies*, Available at: https://www.gov.uk/government/policies/increasing-the-use-of-low-carbon-technologies/supporting-pages/the-renewables-obligation-ro (Accessed: 11 July 2014).

[108] Energy Saving Trust (2013) *Feed-In Tariffs scheme (FITs)*, Available at: http://www.energysavingtrust.org.uk/Generating-energy/Getting-money-back/Feed-In-Tariffs-scheme-FITs (Accessed: 11 July 2014).

[109] Ofgem (2014), Available at: https://www.ofgem.gov.uk (Accessed: 11 July 2014).

[110] UK Government (2013) *Renewables Obligation (RO) banding*, Available at: https://www.gov.uk/calculating-renewable-obligation-certificates-rocs (Accessed: 11 July 2014).

[111] UK Government (2014) *Making Contracts for Difference work for solar*, Available at: https://www.gov.uk/government/speeches/making-contracts-for-difference-work-for-solar (Accessed: 11 July 2014).

[112] Darling, S.You, F. Veselkad, T. & Velosae, A. (2011) 'Assumptions and the levelized cost of energy for photovoltaics' *Energy Environ.Sci.*, 4(9), pp. 3077–3704 *RSC Publishing* [Online]. Available at: http://pubs.rsc.org/en/journals/journalissues/ee (Accessed: 15 January 2013).

[113] Bazilian, M. Onyeji, I. Liebreich, M. MacGill, I. Chase, J. Shah, J. Gielen, D. Arent, D. Landfear, D. & Zhengrong, S. (2013) 'Re-considering the economics of photovoltaic power' *Renewable Energy*, 53, pp. 329-338 *ScienceDirect* [Online]. Available at: http://www.sciencedirect.com (Accessed: 15 January 2013).

[114] Allan, G. Gilmartin, M. McGregor, P. & Swales, K. (2011) 'Levelised costs of Wave and Tidal energy in the UK: Cost competitiveness and the importance of ''banded'' Renewables Obligation Certificates' *Energy Policy*, 39(1), pp. 23-39 *ScienceDirect* [Online]. Available at: http://www.sciencedirect.com (Accessed: 15 January 2013).

[115] Brankera, K. Pathaka, M. & Pearcea, J. (2011) 'A review of solar photovoltaic levelized cost of electricity' *Renewable and Sustainable Energy Reviews*, 15(9), pp. 4470-4482 *ScienceDirect* [Online]. Available at: http://www.sciencedirect.com (Accessed: 15 January 2013).

[116] NEA & IEA (2005) 'Projected costs of generating electricity', Paris: OECD/IEA [Online]. Available at: http://horabsurda.org/wp-content/plugins/downloads-manager/upload/costs_electricity.pdf (Accessed: 15 January 2013).

[117] Brealey, R. Myers, S. & Marcus, A. (2007) *Fundamental of Corporate Finance.*5th edn. New York: McGraw-Hill.

[118] Pillai, G. Putrus, G. Georgitsioti, T. & Pearsall, N. (2014) 'Near-term economic benefits from grid-connected residential PV (photovoltaic) systems', *Energy*, 68, pp.832-843 *ScienceDirect* [Online]. Available at: http://www.sciencedirect.com (Accessed: 11 July 2014).

[119] Gross, R. Heptonstall, P. & Blyth, W. (2007) 'Investment in electricity generation: the role of costs, incentives and risks', *UK Energy Research Centre* [Online]. Available at: http://seg.fsu.edu/Library/Investment%20in%20Electricity%20Generation_%20The%20Role%20of%20Costs,%20Incentives,%20and%20Risks.pdf (Accessed: 15 January 2013).

[120] Short, W. Packey, D. & Holt, T. (1995) 'A Manual for the Economic Evaluation of Energy Efficiency and Renewable Energy Technologies', *National Renewable Energy Laboratory*

[121] National Renewable Energy Laboratory (NREL) (2012) *System Advisor Model (SAM)* (Version 2012.5.11) [computer program]. Available at: https://sam.nrel.gov/ (Accessed: 15 January 2013).

[122] Homer Energy LLC (2014) *Homer Pro* (Version 3.0.X) [computer program]. Available at: http://www.homerenergy.com/HOMER_pro.html (Accessed: 15 September 2014).

[123] Dhere, N. (2005) 'Reliability of PV modules and balance of system components' *Photovoltaic Specialists Conference*, *Conference Record of the 31st IEEE*. Florida, USA, 3-7 January, pp. 1570 – 1576 *IEEE Xplore* [Online]. Available at: http://ieeexplore.ieee.org/Xplore/home.jsp (Accessed: 15 June 2014).

[124] Georgitsioti, T. Pearsall, N. & Forbes, I. (2014) 'Simplified levelised cost of the domestic photovoltaic energy in the UK: the importance of the feed-in tariff scheme' *IET Renewable Power Generation*, 8(5), pp.451-458 *IET Digital Library* [Online]. Available at: http://digital-library.theiet.org (Accessed: 11 July 2014).

[125] Parsons Brinckerhoff (2012) 'Solar PV cost update May 2012', *Department of Energy & Climate Change*, Available at: https://www.gov.uk/government/uploads/system/uploads/attachment_data/file/43083/5381-solar-pv-cost-update.pdf (Accessed: 15 January 2013).

[126] Parsons Brinckerhoff (2012) ‘Solar PV cost update January 2012’, *Department of Energy & Climate Change* Available at: http://www.photon-international.com/newsletter/document/60573.pdf (Accessed: 15 January 2013).

[127] UK Government (2014) *Solar PV Cost Data*, Available at: https://www.gov.uk/government/statistics/solar-pv-cost-data (Accessed: 11 July 2014).

[128] UK Government (2013) *Energy Trends: December 2013, special feature article - Small scale solar PV cost data*, Available at: https://www.gov.uk/government/statistics/energy-trends-december-2013-special-feature-article-small-scale-solar-pv-cost-data (Accessed: 11 July 2014).

[129] Swithenbanks (2014) *SMA Sunny Boy SB-2500HF-30*, Available at: http://www.swithenbanks.co.uk/Solar_Photovoltaic_Equipment/11299/SMA_Sunny_Boy_SB-2500HF-30_Grid_Tie_Inverter.html (Accessed: 11 July 2014).

[130] Ofgem (2014) *Tariff Tables*, Available at: https://www.ofgem.gov.uk/environmental-programmes/feed-tariff-fit-scheme/tariff-tables (Accessed: 11 July 2014).

[131] Energy Saving Trust (2013) *Our Calculations*, Available at: http://www.energysavingtrust.org.uk/Energy-Saving-Trust/Our-calculations (Accessed: 11 July 2014).

[132] UK Government (2014) ‘Revisions to DECC domestic energy bill estimates’, *Domestic energy price statistics*, Available at: https://www.gov.uk/government/statistics/energy-trends-march-2014-special-feature-articles-revisions-to-decc-domestic-energy-bill-estimates (Accessed: 11 July 2014).

[133] Great Britain. Parliament. House of Commons. (2014) *Energy Prices*, (Standard note SN/SG/4153) [Online]. Available at: http://www.parliament.uk/briefing-papers/SN04153/energy-prices (Accessed: 11 July 2014).

[134] Office for National Statistics (2013) ‘Consumer Price Indices, December 2012’ Available at: http://www.ons.gov.uk/ons/rel/cpi/consumer-price-indices/december-2012/index.html (Accessed: 6 February 2013).

[135] Office for National Statistics (2014) 'Consumer Price Inflation, December 2013', Available at: http://www.ons.gov.uk/ons/rel/cpi/consumer-price-indices/december-2013/stb---consumer-price-indices---december-2013.html (Accessed: 11 July 2014).

[136] HM Treasury (2003) 'The Green Book' London: TSO [online]. Available at: http://www.hm-treasury.gov.uk/d/green_book_complete.pdf (Accessed: 15 January 2013).

[137] Trading Economics (2014) *United Kingdom Inflation Rate*, Available at: http://www.tradingeconomics.com/united-kingdom/inflation-cpi (Accessed: 6 August 2014).

[138] Jordan, D. & Kurtz, S. (2013) 'Photovoltaic Degradation Rates-an Analytical Review', *Progress in Photovoltaics: Research and Applications*, 21(1), pp. 12-29 *Wiley Online Library* [Online]. Available at: http://onlinelibrary.wiley.com/ (Accessed: 20 February 2014).

[139] The Word Bank Group (2014) *Inflation, consumer prices (annual %)*, Available at: http://data.worldbank.org/indicator/FP.CPI.TOTL.ZG?order=wbapi_data_value_2010+wbapi_data_value+wbapi_data_value-first&sort=asc (Accessed: 6 August 2014).

[140] Trading Economics (2014) *India Interest Rate*, Available at: http://www.tradingeconomics.com/india/interest-rate (Accessed: 6 August 2014).

[141] Perumal, P. (2014) E-mail to Tatiani Georgitsioti, 14 August. Solar Company: KotakUrja Private Limited, Available at: http://kotakurja.com/company.html

[142] Government of India-Ministry of Power (2014) 'Tariff and Duty of Electricity Supply in India-March 2014' *Central Electricity Authority*, Available at: http://cea.nic.in/eandc_wing.html (Accessed: 6 August 2014).

[143] United Nations (1992) 'United Nations Framework Convention on Climate Change', Available at: http://unfccc.int/key_steps/the_convention/items/6036.php (Accessed: 6 August 2014).

[144] United Nations Framework Convention on Climate Change (2014) *Kyoto Protocol*, Available at: http://unfccc.int/kyoto_protocol/items/2830.php (Accessed: 6 August 2014).

[145] International Energy Agency (2012) 'CO_2 Emissions from Fuel Combustion 2012 – Highlights', Available at: http://www.iea.org/co2highlights/co2highlights.pdf (Accessed: 11 May 2013).

[146] International Energy Agency (2013) 'CO_2 Emissions from Fuel Combustion 2013 – Highlights', Available at: http://www.iea.org/publications/freepublications/publication/co2emissionsfromfuelcombustionhighlights2013.pdf (Accessed: 6 August 2014).

[147] Brander, M. Sood, A. Wylie, C. Haughton, A. & Lovell, J. (2011) 'Electricity-specific emission factors for grid electricity', *Ecometrica*, Available at: http://ecometrica.com/white-papers/electricity-specific-emission-factors-for-grid-electricity/ (Accessed: 6 August 2014).

[148] Siler-Evans, K. Azevedo, I. Morgan, M. & Apt, J. (2013) 'Regional variations in the health, environmental, and climate benefits of wind and solar generation' *PNAS*, 110 (29), pp. 11768-11773 Available at: http://www.pnas.org/content/110/29/11768.abstract (Accessed: 26 August 2014)

[149] Ndiaye, A. Charki, A. Kobi, A. Kebe, C. Ndiaye, P. & Sambou, V. (2013) 'Degradations of silicon photovoltaic modules: A literature review' *Solar Energy*, 96, pp. 140-151 *ScienceDirect* [Online]. Available at: http://www.sciencedirect.com (Accessed: 15 August 2014).

[150] Sharma, V. & Chandel, S. (2013) 'Performance and degradation analysis for long term reliability of solar photovoltaic systems: A review' *Renewable and Sustainable Energy Reviews*, 27, pp. 753-767 *ScienceDirect* [Online]. Available at: http://www.sciencedirect.com (Accessed: 26 August 2014).

[151] Wohlgemuth, J. Cunningham, D. Monus, P. Miller J. & Nguyen, A. (2005) 'Long Term Reliability of PV Modules' *20th EU PVSEC*. Barcelona Spain, 6-10 June.

[152] IEA-PVPS (2014) 'Review on Failures of Photovoltaic Modules' *Task 13*, Available at: http://iea-pvps.org/index.php?id=275 (Accessed: 15 August 2014).

[153] DeGraaff, D. Lacerda, R. Campeau, Z. & SunPower Corp. (2011) 'Degradation Mechanisms in Si Module Technologies Observed in the Field; Their Analysis and Statistics' Workshop on Photovoltaic Module Reliability, NREL, Golden, Colorado, USA, 16 February 2011.

[154] Pearsall, N. & Atanasiu, B. (2009) 'Assessment of PV System Monitoring Requirements by Consideration of Failure Mode Probability' *24th EU PVSEC*. Hamburg Germany, 21-25 September.

[155] Pan, R. Kuitche, J. & Tamizhmani, G. (2011) 'Degradation Analysis of Solar Photovoltaic Modules: Influence of Environmental Factor' *Reliability and Maintainability Symposium (RAMS)*, Lake Buena Vista Florida, 24-27 January.

[156] Vázquez, M. & Rey-Stolle, I. (2008) 'Photovoltaic module reliability model based on field degradation studies', *Progress in Photovoltaics: Research and Applications*, 16(5), pp. 419-433 *Wiley Online Library* [Online]. Available at: http://onlinelibrary.wiley.com/ (Accessed: 20 February 2014).

[157] Cocca, M. D'Arienzo, L. & D'Orazio, L. (2011) 'Effects of Different Artificial Agings on Structure and Properties of Whatman Paper Samples' *ISRN Materials Science*, 2011, 7 pages *Hindaw* [Online]. Available at: http://www.hindawi.com (Accessed: 26 August 2014).

[158] Escobar, L. & Meeker, W. (2006) 'A Review of Accelerated Test Models' *Statistical Science*, 21 (4), pp. 552-557 *IMS* [Online]. Available at: http://imstat.org/publications/ (Accessed: 26 August 2014).

[159] Kurtz, S. Whitefield, K. TamizhMani, G. Koehl, M. Miller, D. Joyce, J. Wohlgemuth, J. Bosco, N. Kempe, M. & Zgonena, T. (2011) 'Evaluation of high-temperature exposure of photovoltaic modules' *Progress in Photovoltaics: Research and Applications*, 19(8), pp.954-965 *Wiley Online Library* [Online]. Available at: http://onlinelibrary.wiley.com (Accessed: 26 August 2014).

[160] Phinikarides, A. Kindyni, N. Makrides, M. & Georghiou, G. (2014) 'Review of photovoltaic degradation rate methodologies' *Renewable and Sustainable Energy Reviews*, 40, pp. 143-152 *ScienceDirect* [Online]. Available at: http://www.sciencedirect.com (Accessed: 26 August 2014).

[161] Wu, D. (2013) E-mail to Tatiani Georgitsioti, 5 September. Loughborough University report

[162] Sastry, O. Saurabh, S. Shil, Pant, P. Kumar, R. Kumar, A. & Bandopadhyay, B. (2010) 'Performance analysis of field exposed single crystalline silicon modules' *Solar Energy Materials & Solar Cells,* 94 (9), pp. 1463-1468 *ScienceDirect* [Online]. Available at: http://www.sciencedirect.com (Accessed: 15 June 2014).

[163] Thevenard, D. & Pelland, S. (2013) 'Estimating the uncertainty in long-term photovoltaic yield predictions' *Solar Energy,* 91, pp. 432-445 *ScienceDirect* [Online]. Available at: http://www.sciencedirect.com (Accessed: 20 February 2014).

[164] Kahoul, N. Houabes, M. & Sadok, M. (2014) 'Assessing the early degradation of photovoltaic modules performance in the Saharan region' *Energy Conversion and Management*, 82, pp. 320-326 *ScienceDirect* [Online]. Available at: http://www.sciencedirect.com (Accessed: 26 August 2014).

[165] Ndiaye, A. Kebe, C. Charki, A. Ndiaye, P. Sambou, V. & Kobi, A. (2014) 'Degradation evaluation of crystalline-silicon photovoltaic modules after a few operation years in a tropical environment' *Solar Energy*, 103, pp. 70-77 *ScienceDirect* [Online]. Available at: http://www.sciencedirect.com (Accessed: 26 August 2014).

[166] Makrides, G. Zinsser, B. Norton, M. Georghiou, G. Schubert, M. & Werner, J. (2010) 'Potential of photovoltaic systems in countries with high solar irradiation' *Renewable and Sustainable Energy Reviews*, 14 (2), pp. 754-762 *ScienceDirect* [Online]. Available at: http://www.sciencedirect.com (Accessed: 26 August 2014).

Appendices

Appendix A: Seasonal temperature distribution over India for the months of January, April, July and October [19].

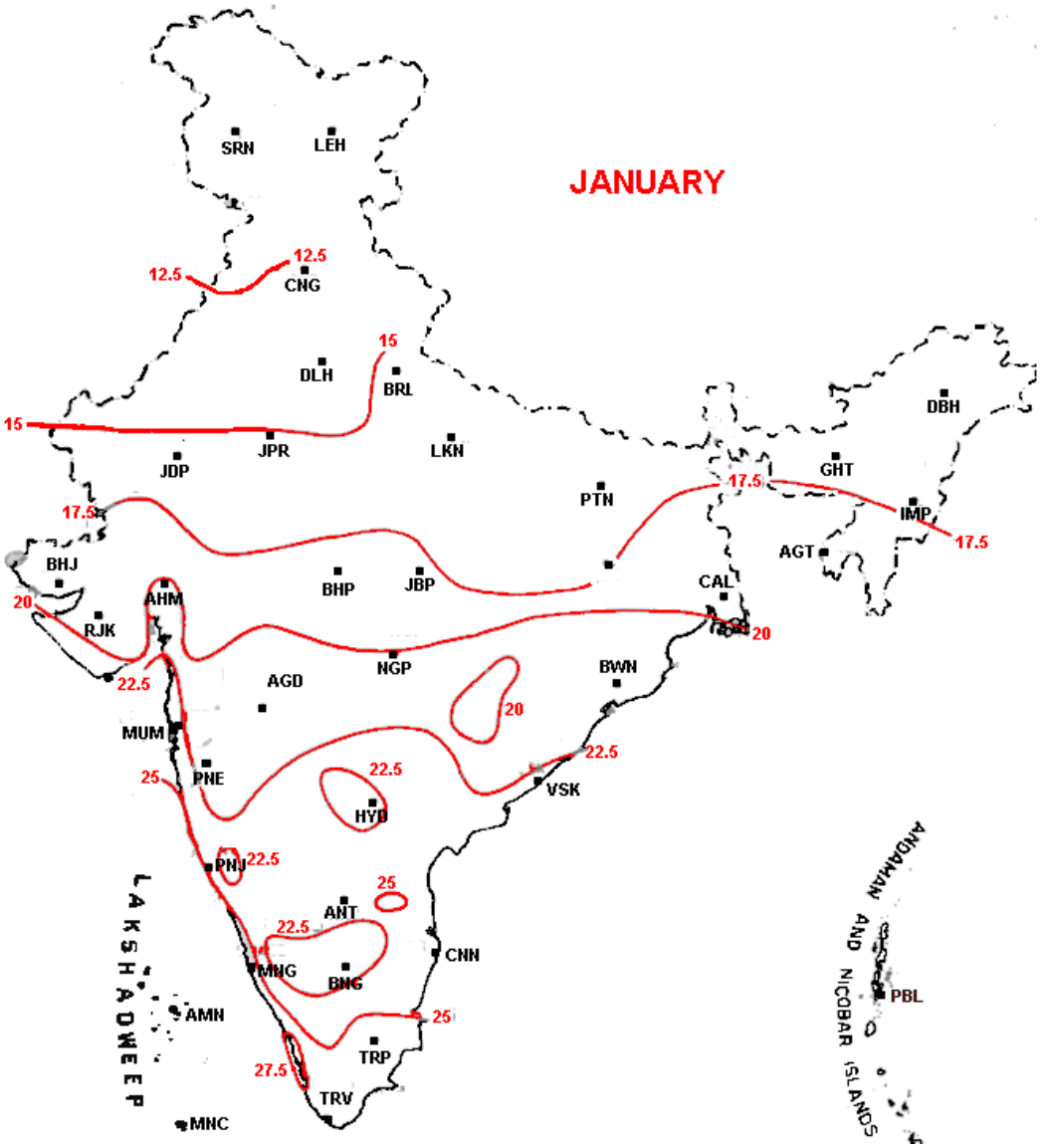

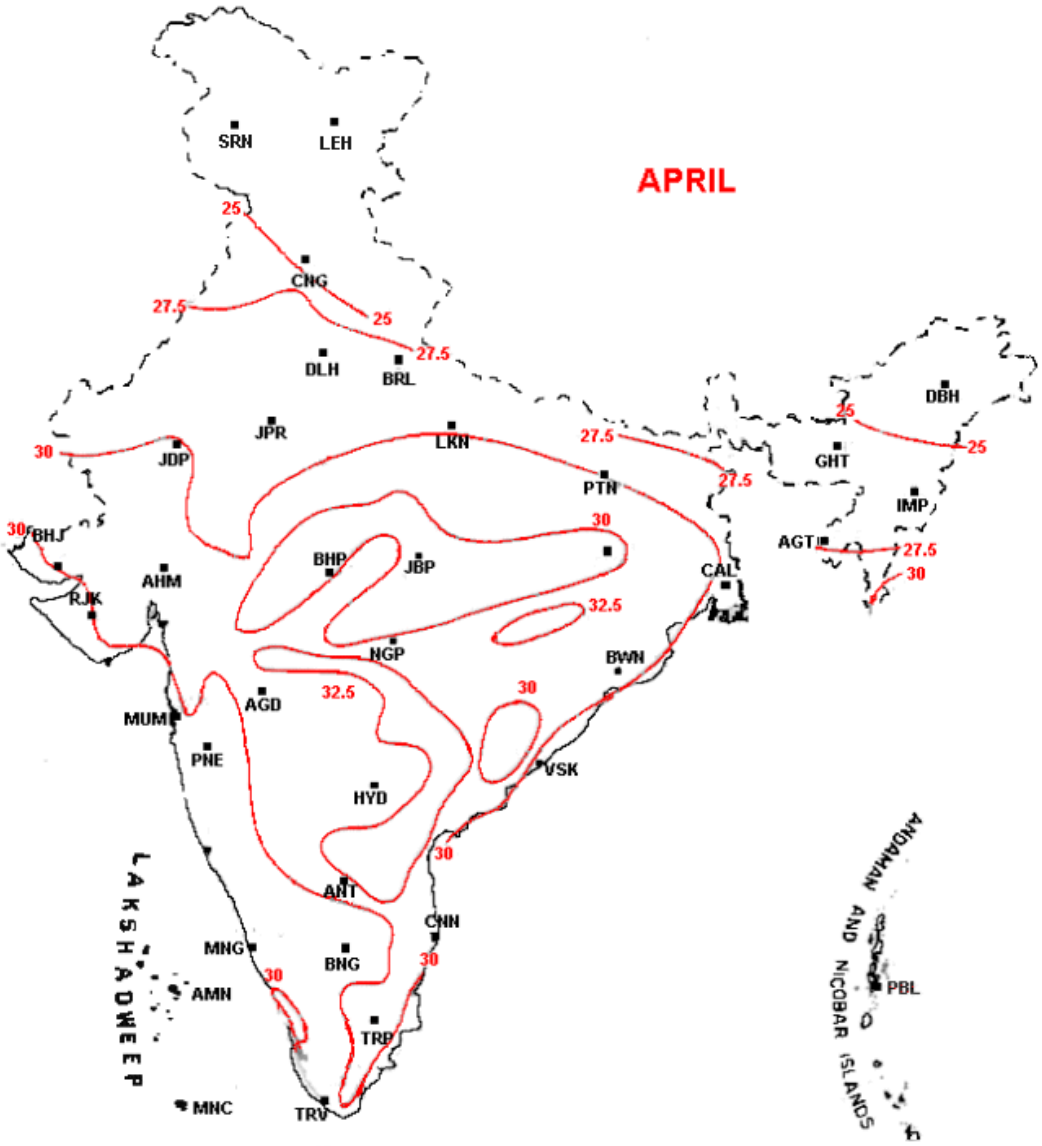
APRIL
SRN
LEH
CNG
DLH
BRL
JPR
JDP
LKN
PTN
DBH
GHT
IMP
AGT
BHJ
AHM
RJK
BHP
JBP
CAL
NGP
BWN
AGD
MUM
PNE
HYD
VSK
ANT
CNN
MNG
BNG
AMN
TRP
MNC
TRV
PBL
25
27.5
30
32.5
LAKSHADWEEP
ANDAMAN AND NICOBAR ISLANDS

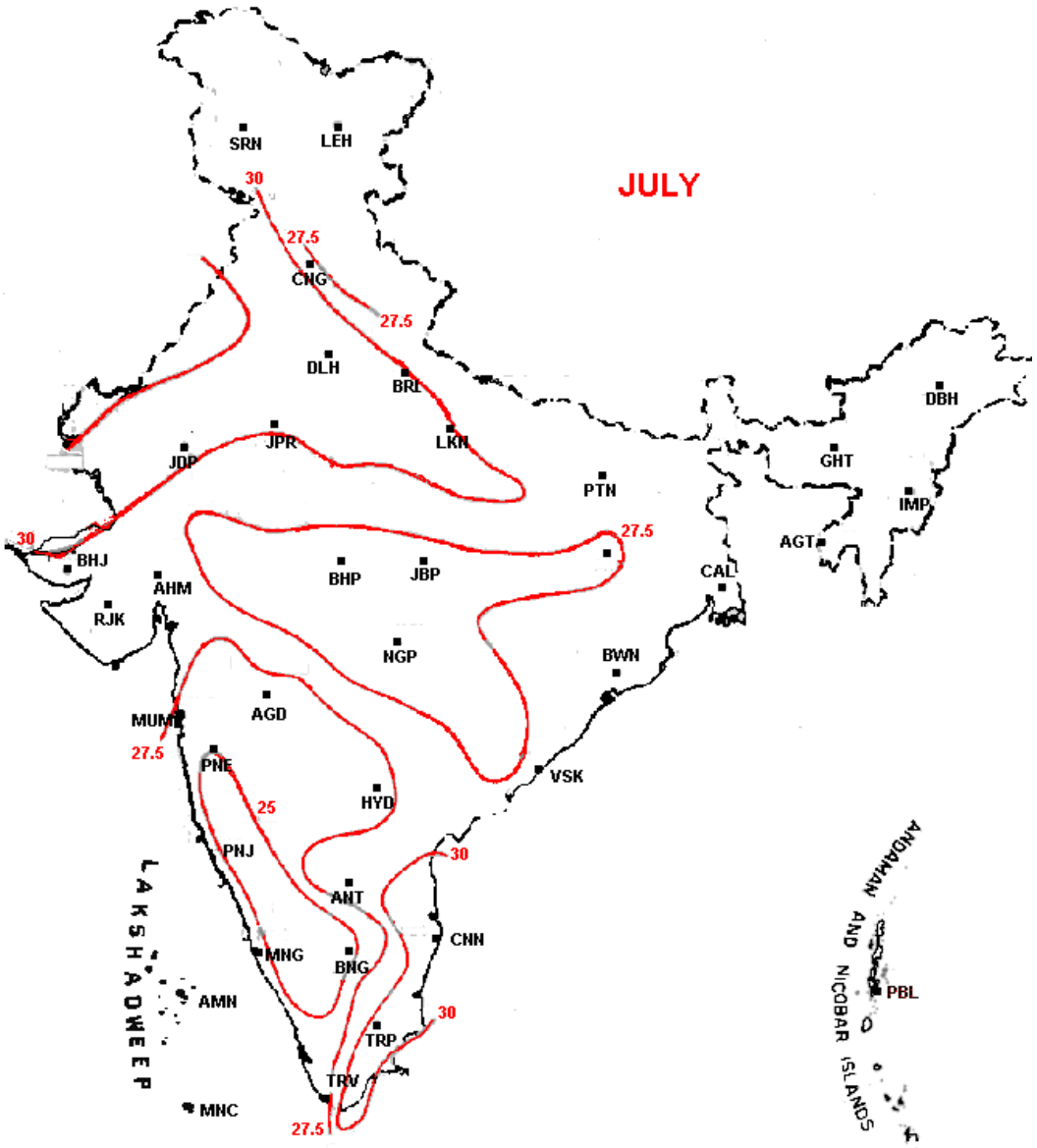
JULY
SRN
LEH
30
27.5
CHG
27.5
DLH
BRL
DBH
JDP
JPR
LKH
GHT
PTN
IMP
30
27.5
AGT
BHJ
BHP
JBP
CAL
AHM
RJK
NGP
BWN
AGD
MUM
27.5
PNE
25
HYD
VSK
PNJ
30
ANT
CNN
MNG
BNG
AMN
30
TRP
TRV
MNC
27.5
LAKSHADWEEP
ANDAMAN AND NICOBAR ISLANDS
PBL

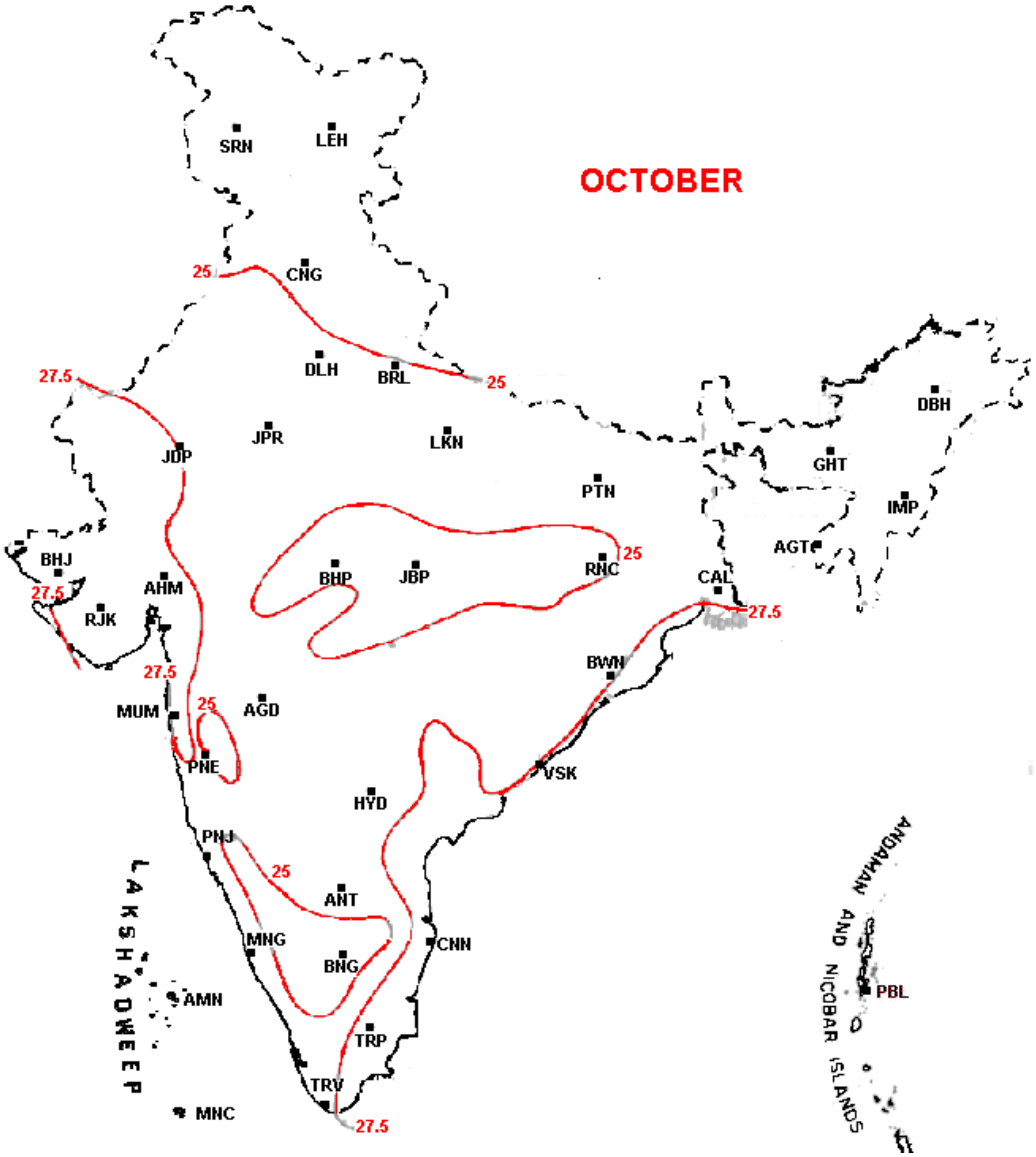
OCTOBER
SRN
LEH
CNG
DLH
BRL
JDP
JPR
LKN
PTN
DBH
GHT
IMP
AGT
BHJ
AHM
RJK
BHP
JBP
RHC
CAL
BWN
MUM
AGD
PNE
VSK
HYD
PNJ
ANT
MNG
BNG
CNN
AMN
TRP
TRV
MNC
PBL
25
27.5
LAKSHADWEEP
ANDAMAN AND NICOBAR ISLANDS

Appendix B: Module and inverter technical characteristics

Table B1: Technical data of the chosen module

Technical Data	Sharp: ND-R 250 A5
Number of cells	60
Type of cells	Multi-crystalline silicon
Maximum power rating (P_{max})	250 W
Open circuit voltage (V_{OC})	37.6 V
Maximum power voltage (V_{MPP})	30.9 V
Short circuit current (I_{SC})	8.68 A
Maximum power current (I_{MPP})	8.1 A
Nominal Operating Cell temperature (NOCT)	47.5°C
Temperature coefficient of I_{SC}	+0.038%/°C
Temperature coefficient of V_{OC}	−0.329%/°C
Temperature coefficient of P_{max}	−0.44%/°C
Maximum system voltage (IEC 61215 rating)	1000 V
Dimensions: length x width x height	1652 x 994 x 46 mm^3
Weight	19 Kg
Bypass diodes:(1 box IP 65 with bypass diodes)	3
Module efficiency (n)	15.2%

Table B2: Technical data of the chosen inverters

Technical data	Sunny Tripower 8000TL	Sunny Boy 2500HF	Sunny Boy 3000HF
For the DC side:			
Maximum dc Power	8200 W	2600 W	3150 W
Operating MPPT Input Voltage Range [V_{dc}]/ Dc Nominal Voltage	320 V – 800 V 600 V	175 V – 560 V 530 V	210 V-560 V 530 V
Maximum Input Voltage	1000 V	700 V	700 V
No of independent MPPT trackers/ No of strings per MPP tracker	2 A: 4, B: 1	1 2	1 2
Maximum DC current at each MPPT/ I_{MPP} per string	A:22 A, B:11 A A:33 A, B:12.5 A	15 A / 15 A	15 A / 15 A
For the AC side:			
AC Nominal Power	8000 W	2500 W	3000 W
AC Grid Connection	3 / N / PE, 230 V / 400 V	220, 230, 240 V	220, 230, 240 V
Maximum AC Voltage Range [V_{ac}]	160 V – 280 V	180 V – 280 V	180 V – 280 V
Nominal AC Frequency/ range	50, 60 Hz / –6 Hz, +5 Hz	50, 60 Hz / ±4.5 Hz	50, 60 Hz / ±4.5 Hz
Maximum AC Line Current	16 A	14.2 A	15 A
Efficiency: Maximum/Euro-eta	98.1%/97.5%	96.3%/95.3%	96.3%/95.4%

Appendix C: Solar irradiation maps of the UK and India

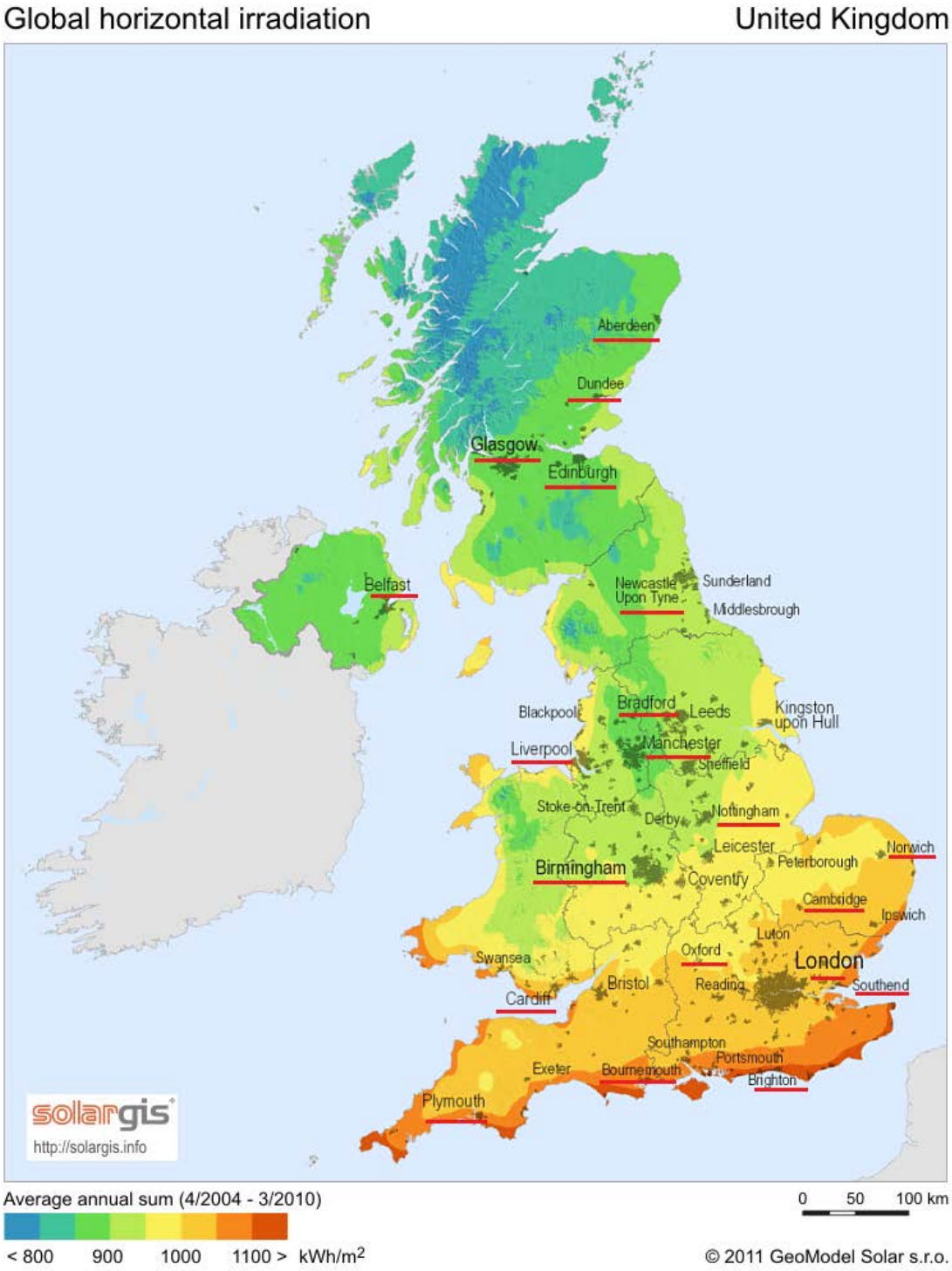

Initial choice of the Indian cities-22 locations

The black lines are roughly depicting the Indian meteorological regions i.e. north, northeast, west, central, east, and south.

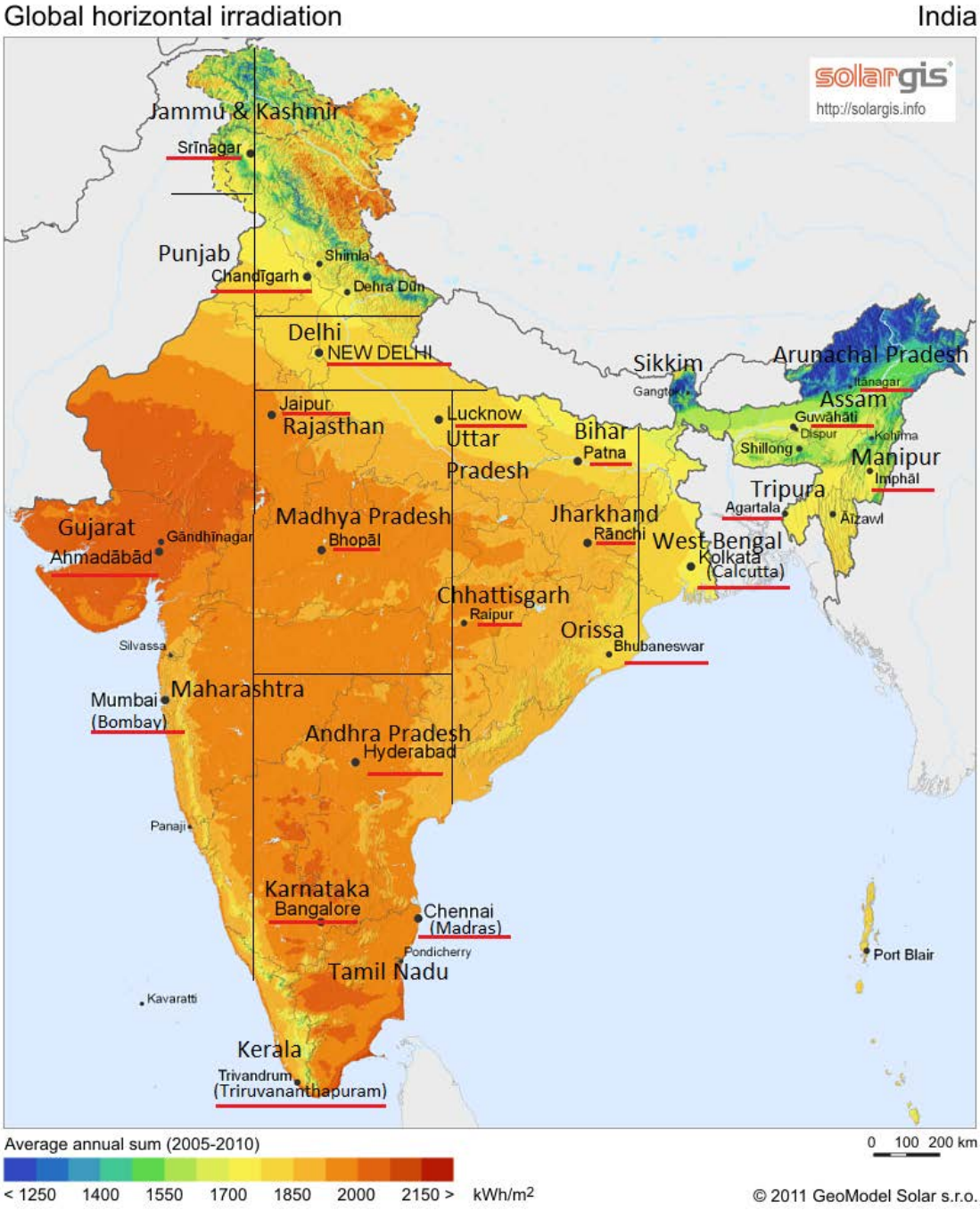

Appendix D: UK cities-Simulation results

Table D1: Irradiation, Energy output, Performance Ratio, Optimum Tilt Angle, and Latitude for 20 locations in the UK (CM-SAF solar data-3 kW PV system)

The colour code in the following tables represents the range of the annual energy production and the global irradiation values. The dark green colour presents the lowest value while the red presents the highest value.

UK cities- PVsyst 20 locations	Inclined Irradiation (kWh/m^2)	Annual Energy (kWh)	PR (%)	Optimum tilt angle (degrees)	Latitude (degrees)
Aberdeen	1119.9	2590	77.1	38	57.13
Dundee	1213.8	2821	77.5	39	56.45
Edinburgh	1161.2	2691	77.2	38	55.95
Glasgow	1072.7	2470	76.8	37	55.85
Newcastle	1146.2	2650	77.1	36	54.97
Belfast	1142.0	2631	76.8	35	54.58
Bradford	1120.2	2575	76.6	35	53.78
Manchester	1108.6	2548	76.6	34	53.47
Liverpool	1174.1	2706	76.8	36	53.40
Nottingham	1176.6	2704	76.6	35	52.95
Norwich	1228.7	2824	76.6	35	52.62
Birmingham	1196.6	2748	76.6	35	52.47
Cambridge	1255.5	2888	76.7	36	52.20
Oxford	1242.5	2856	76.6	35	51.75
Southend	1324.5	3041	76.5	35	51.53
London	1253.6	2874	76.4	35	51.50
Cardiff	1220.5	2812	76.8	35	51.47
Brighton	1439.6	3305	76.5	35	50.82
Bournemouth	1348.1	3098	76.6	35	50.72
Plymouth	1395.8	3207	76.6	35	50.37

Appendix E: Indian cities-Simulation results

Table E1: Irradiation, Energy output, Performance Ratio, Optimum Tilt Angle, Latitude and Climate Classification for 36 locations in India (CM-SAF solar data-3 kW PV system)

Indian cities- PVsyst 36 locations and Climate Classification	Inclined Irradiation (kWh/m^2)	Annual Energy (kWh)	PR (%)	Optimum tilt angle (degrees)	Latitude (degrees)
Srinagar-Cfa	2049.7	4629	75.3	31	34.1
Nangal-Cfa	2215.9	4916	74.0	30	31.4
Shimla-Cfa	2093.2	4519	72.0	32	31.1
Chandigarh-Cfa	2246.5	4833	71.7	30	30.8
Dehradun-Cfa	2162.9	4747	73.2	32	30.3
Hissar-Cfa	2318.0	4905	70.5	28	29.2
New Delhi-BSh	2267.5	4851	71.3	28	28.6
Dibrugarh-Cfa	1820.7	3970	72.7	29	27.5
Gangtok-Cfa	1802.0	4071	75.3	30	27.3
Itanagar-Cfa	1767.6	3934	74.2	28	27.1
Jaipur-BSh	2348.3	5005	71.0	27	26.8
Lucknow-Cfa	2204.5	4708	71.2	26	26.8
Kanpur-Cfa	2222.3	4738	71.1	26	26.51
Kohima-Cfa	1618.9	3548	73.1	29	25.7
Patna-Cfa	2174.2	4642	71.2	25	25.6
Shillong-Cfa	1670.0	3653	72.9	29	25.6
Imphal-Cfa	1939.2	4240	72.9	27	24.8
Agartala-Cfa	1990.7	4270	71.5	25	23.9
Aizawl-Cfa	1997.5	4361	72.8	25	23.7
Ranchi-Cfa	2114.0	4526	71.4	24	23.4
Bhopal-Cfa	2265.0	4798	70.6	26	23.3
Ahmadabad-BSh	2359.7	4958	70.0	24	23.1
Kolkata-Aw	2073.5	4429	71.2	23	22.7
Raipur-Cfa	2220.6	4693	70.4	23	21.2
Daman-BSh	2316.1	4862	70.0	23	20.4
Bhubaneswar-Aw	2103.0	4434	70.3	21	20.3
Silvassa-Aw	2267.0	4756	69.9	23	20.3
Mumbai-Aw	2252.1	4723	69.9	22	19.1
Hyderabad-Aw	2246.3	4722	70.1	19	17.5
Panjim-Am	2257.3	4741	70.0	18	15.5
Chennai-Aw	2230.4	4676	69.9	13	13
Bangalore-BSh	2207.6	4751	71.7	15	13
Pondicherry-Am	2254.5	4725	69.9	11	11.9
Port Blair-Am	1979.7	4169	70.2	14	11.7
Kavaratti-Am	2198.8	4612	69.9	12	10.6
Trivandrum-Am	2220.7	4658	69.9	9	8.5

Appendix F: Module and inverter technical characteristics of the installed PV systems at the IIT Kanpur in India

Table F1: Technical data of the modules at IIT Kanpur

Technical Data	Novergy ATS-O-90	Q.smart UFL	Novergy MCA 205	Tata BP solar TBP3230X
Power tolerance	+5%/-0%	+5%/-0%	+3%/-0%	-3%/+5%
Type of cells	a-Si	CIGS	mono-Si	multi-Si
Maximum power rating (P_{max})	95 W	95 W	205 W	230 W
Open circuit voltage (V_{OC})	137 V	89.0 V	45.74 V	36.7 V
Maximum power voltage (V_{MPP})	100 V	66.4 V	37.56 V	29.1 V
Short circuit current (I_{SC})	1.15 A	1.68 A	5.69 A	8.4 A
Maximum power current (I_{MPP})	0.9 A	1.43 A	5.46 A	7.9 A
Temperature coefficient of I_{SC}	+0.03%/K	−(0.00 ± 0.04)%/K	+0.04%/K	0.065 ± 0.016%/°C
Temperature coefficient of V_{OC}	−0.30%/K	− (0.29 ± 0.04) %/K	−0.30%/K	−(0.36±0.06)%/°C
Temperature coefficient of P_{max}	−0.17%/K	− (0.38 ± 0.04) %/K	−0.37%/K	−(0.5± 0.05)%/°C
Maximum system voltage (IEC 61215 rating)	1000 V	1000 V	1000 V	1000 V
Dimensions: length x width x height	1300 x 1100 x 7 mm	1190x789.5 x 7.3 mm	1580 x 808 x 40 mm	1667 x 1000 x 50 mm
Weight	24 Kg	16.5 Kg	16 Kg	19.4 Kg
Module efficiency (n)	6.6%	10.1%	15.1%	14.2%

Table F2: Technical data of the inverters at IIT Kanpur

Technical data	Sunny Mini Central 5000A	Solivia 5.0 EU G3 TR	Aurora PVI-5000-OUTD-US
For the DC side:			
Maximum dc Power	5750 W	6000 W	5750 W
Operating MPPT Input Voltage Range [V_{dc}]/ Dc Nominal Voltage	246 V - 480 V 270 V	150 V - 450 V N/A	140 V - 530 V 200 V
Maximum Input Voltage	600 V	540 V	600 V
No of independent MPPT trackers/ No of strings per MPP tracker	1 4	1 4	2 2
Maximum DC current at each MPPT/ I_{MPP} per string	26 A / 26 A	32 A / 18 A	18 A / N/A
For the AC side:			
AC Nominal Power	5000 W	5000 W	4600 W
AC Grid Connection	220, 230, 240 V	240 V	230 V
Maximum AC Voltage Range [V_{ac}]	180 V – 260 V	184 V – 264.5 V	180 V – 264 V
Nominal AC Frequency/ range	50, 60 Hz / ±4.5 Hz	47.3-52.7 Hz	50 Hz
Maximum AC Line Current	26 A	22 A	25 A
Efficiency: Maximum/ Euro-eta	96.1%/95.3%	95.6%/94.6%	97%/96.4%

Table F3: Technical data of the pyranometer at IIT Kanpur

Kipp and Zonen (SP LITE2)	
Spectral range	400 to 1100 nm
Sensitivity	60 to 100 (option, 10±0.5) μV/W/m^2
Response time SP LIte2 (95%)	<500 ns
Directional error (up to 80˚ with 1000 W/m^2 beam	<10 W/m^2
Temperature dependence	< -0.15%/°C
Operating temperature range	-30°C to +70°C
Maximum solar irradiance	2000 W/m^2
Field of view	180°

Appendix G: Module and inverter technical characteristics of the simulated PV systems for the IIT Kanpur location plus PVsyst input parameters

Table G1: Technical data of the modules used for simulations

Technical Data	German Solar NH-100AX_3A	Q-Cells Smart UFL95	BP Solar
Power tolerance	+5%/-0%	+5%/-0%	+3%/-0%
Type of cells	a-Si	CIGS	multi-Si
Maximum power rating (P_{max})	95 W	95 W	230 W
Open circuit voltage (V_{OC})	100 V	90.7 V	36.4 V
Maximum power voltage (V_{MPP})	73 V	66.9 V	29.2 V
Short circuit current (I_{SC})	1.62 A	1.63 A	8.7 A
Maximum power current (I_{MPP})	1.3 A	1.42 A	7.9 A
Temperature coefficient of I_{SC}	+0.05%/°C	−0.01 ± 0.04%/°C	+0.06%/°C
Temperature coefficient of V_{OC}	−35 mV/°C	−196 mV/°C	−123 mV/°C
Temperature coefficient of P_{max}	−0.2%/°C	−0.38 ± 0.04%/°C	−0.42%/°C
Maximum system voltage (IEC 61215 rating)	600 V	1000 V	1000 V
Dimensions: length x width x height	1416 x 806 x 35 mm^3	1190x790 x 7 mm^3	1667 x 1000 x 50 mm^3
Weight	24 Kg	16.5 Kg	19 Kg
Module efficiency (n)	8.32%	10.11%	13.84%

Table G2: Technical data of the inverters used for simulations

Technical data	Hefei SG5K	Power One PVI-5000-OUTD-US	Ingetem Sun5
For the DC side:			
Maximum dc Power	6000 W	5300 W	6300 W
Operating MPPT Input Voltage Range [V_{dc}]/ Dc Nominal Voltage	200 V – 780 V N/A	120 V - 580 V 360 V	125 V-450 V 340 V
Maximum Input Voltage	780 V	600 V	450 V
No of independent MPPT trackers/ No of strings per MPP tracker	1 1	2 2	1 4
Maximum PV current	N/A	36 A	33 A
For the AC side:			
AC Nominal Power	5000 W	5000 W	5000 W
AC Grid Connection	230 V	277 V	230 V
Nominal AC Frequency/ range	50 Hz	60 Hz	50 Hz
Maximum AC Line Current	N/A	20 A	25.5 A
Efficiency: Maximum/Euro-eta	94%/92%	97%/96%	95%/94.2%

Table G3: PVsyst input parameters used for the IIT Kanpur simulations

PVsyst Version 5.3.1						
Module Technology	**Thermal loss factor**	**Wiring loss fraction at STC**	**Module efficiency loss**	**Power loss at MPP**	**Loss at fixed voltage**	**Soiling loss**
CIS	20 $(W/m^2)*k$	1.5%	2.5%	1%	1.5%	3%
a-Si	20 $(W/m^2)*k$	1.5%	2.5%	1%	1.5%	3%
multi-Si	20 $(W/m^2)*k$	1.7%	1.5%	2%	4%	3%

Appendix H: Analytical calculation steps for the IIT Kanpur cleaning experiment

Calculations for the string 3 of the mono-Si fixed system installed at the IIT Kanpur.

Table H1: Module technical data

Novergy cells	P_{max} (W)	205	Temperature at NOCT	45±2°C
Model MCA 205	Vmmp (V)	37.56	Temp. Coeff. P_{max}	-0.37%/°C
Mono-crystalline	Immp (A)	5.46	Temp. Coeff. V_{OC}	-0.3%/°C
Dimensions:	V_{OC} (V)	45.74	Temp. Coeff. I_{SC}	0.04%/°C
1580 x 808 x 40 mm^3	I_{SC} (A)	5.69	Maximum system voltage (V)	1000
Cell Number: 72	Module eff. (%)	15.10	Power tolerance (positive)	+3%/-0%

Table H2: Measured values (for one module)

Before		After	
I_b (A)	3.88	I_a (A)	4.15
V_b (V)	33.53*	V_a (V)	35.28*
G_b (W/m^2)	809.88	G_a (W/m^2)	834.4
Ambient Temp. (°C)	23	Ambient Temp. (°C)	23
Module Temp. (°C)	43.87	Module Temp. (°C)	37.17

*Voltage of the 3rd string (before) = 301.79 V, 9 modules connected in series

Therefore, the voltage of one single module (before) = 301.79/9=33.53 V

Similarly, the voltage of the 3rd string (after) = 317.55 V

Voltage of one single module (after) =35.28 V

Table H3: Calculated values (for one module)

Before		After	
I_1 (A)	4.47	I_2 (A)	4.58
V_b (V)	33.53	V_a (V)	35.28
G_1 (W/m^2)	702.03	G_2 (W/m^2)	754.84
Module Temp. (T_1)(°C)	54.37	Module Temp. (T_2)(°C)	41.62

Calculations:

Step 1: calculations for the module temperature before and after cleaning.

Before:

$$V_{mpp}at\ T_1 = V_{mpp}at\ 25\ ℃ + [temp.coeff.of\ voltage \times (T_1 - 25\ ℃)] \Rrightarrow$$

$$33.53\ (V) = 37.56(V) + [-0.137(^{V}/_{℃}) \times (\ (T_1 - 25\ ℃)] \Rrightarrow$$

$$T_1 = 54.37\ ℃$$

where T_1 is the module temperature before cleaning.

After:

$$V_{mpp}at\ T_2 = V_{mpp}at\ 25\ ℃ + [temp.coeff.of\ voltage \times (T_2 - 25\ ℃)] \Rrightarrow$$

$$35.28\ V = 37.56\ V + [-0.137\ ^{V}/_{℃} \times\ (T_2 - 25\ ℃)] \Rrightarrow$$

$$T_2 = 41.62\ ℃$$

where T_2 is the module temperature after cleaning.

Step 2: calculations for the effective irradiance before and after cleaning based on the measured current values.

Before:

$$I_b = [I_{mpp} + (temp.coeff.of\ current \times \Delta T)] \times \frac{G_1}{G_{STC}} \Rrightarrow$$

$$3.88A = [5.46A + \left(0.002\ {}^{A}/_{℃} \times (54.37\ ℃ - 25\ ℃)\right)] \times \frac{G_1}{1000\ {}^{W}/_{m^2}} \Rrightarrow$$

$$G_1 = 702.03\ {}^{W}/_{m^2}$$

where G_1 is the effective irradiance before cleaning.

After:

$$I_a = [I_{mpp} + (temp.coeff.of\ current \times \Delta T)] \times \frac{G_2}{G_{STC}} \Rrightarrow$$

$$4.15A = [5.46A + \left(0.002\ {}^{A}/_{℃} \times (41.62\ ℃ - 25\ ℃)\right)] \times \frac{G_2}{1000\ {}^{W}/_{m^2}} \Rrightarrow$$

$$G_2 = 754.84\ {}^{W}/_{m^2}$$

where G_2 is the effective irradiance after cleaning.

Step 3: calculations for the current values based on the measured irradiance values before and after cleaning (how much would the current have been if there was no dust and mismatch in the string).

Before:

$$I_1 = [I_{mpp} + (temp.coeff.of\ current \times \Delta T)] \times \frac{G_b}{G_{STC}} \Rrightarrow$$

$$I_1 = [5.46A + \left(0.002\ {}^{A}/_{℃} \times (54.37\ ℃ - 25\ ℃)\right)] \times \frac{809.88\ {}^{W}/_{m^2}}{1000\ {}^{W}/_{m^2}} \Rrightarrow$$

$$I_1 = 4.47\ A$$

where I_1 is the current before cleaning, based on the calculated module temperature before cleaning.

After:

$$I_2 = [I_{mpp} + (temp.coeff.of\ current \times \Delta T)] \times \frac{G_a}{G_{STC}} \Rrightarrow$$

$$I_2 = [5.46A + \left(0.002\ {}^{A}/_{℃} \times (41.62\ ℃ - 25\ ℃)\right)] \times \frac{834.4\ {}^{W}/_{m^2}}{1000\ {}^{W}/_{m^2}} \Rrightarrow$$

$$I_2 = 4.58\ A$$

where I_2 is the current after cleaning, based on the calculated module temperature after cleaning.

Step 4: percentage difference of the measured and the calculated string current based on the calculated values (the effect of dust and/or mismatch ≈ 4%).

Table H4: Percentage difference of the measured and the calculated string current

	Measured current (A)	Calculated current (A)	Percentage difference (%)
Before	3.88	4.47	13.20
After	4.15	4.58	9.39

Appendix I: LCOE example calculations for Newcastle

An optimally designed 3 kW PV system at Newcastle was chosen for the LCOE example calculation. The installation cost of the system is £6,240 for the financial year 2013-14 according to the Department of Energy and Climate Change [126]. The operation and maintenance cost is £45 per year [125]. The lifetime of the system is assumed to be 25 years, during which the inverter of the system will be replaced once in the 12th year of its operation. The cost of the inverter is £755 [128], and no benefits or feed-in tariffs are included in the cost calculations. Moreover, the PVSyst annual energy production for this system is 2,650 kWh. Assuming a discount rate of 3.5% [135] and an annual degradation rate of 0.5% [114], the LCOE calculations based on the "discounting" method (eq.4.5) equals to 0.1808 £/kWh while the LCOE of the "annuity" method (eq.4.7) equals to 0.1824 £/kWh.

$$LCOE = \frac{\sum_{n=0}^{N} \frac{C_n}{(1+d)^n}}{\sum_{n=0}^{N} \frac{E_n}{(1+d)^n}} \quad (4.5), \qquad LCOE = \frac{\sum_{n=0}^{N} \frac{C_n}{(1+d)^n} \times \frac{d}{[1-(1+d)^{-N}]}}{\frac{\sum_{n=1}^{N} E_n}{N}} \quad (4.7)$$

Further, without discounting the lifetime energy (eq.4.8) and by using the same inputs the LCOE equals to 0.1203 £/kWh. Considering that the average electricity cost for a typical household in the UK is 0.152 £/kWh [131], it can be concluded that the LCOE prediction of the non-discounting method has already reached grid parity for the case of Newcastle. In this example, it is obvious that the accuracy and the justification of the method used play a key role to the LCOE calculations, which affect the cost-effectiveness of the system.

$$LCOE = \frac{\sum_{n=0}^{N} \frac{C_n}{(1+d)^n}}{\sum_{n=0}^{N} E_n} \quad (4.8)$$

Where C_n is the costs of the system in year n. When n=0 the cost is equivalent to the initial capital cost. E_n is the energy produced by the system in year n including the assumed degradation of 0.5% per year. N is the project's lifetime, and d is the discount rate.

Appendix J: Lifetime ranges for all the cities and all the scenarios

Table J1: Lifetime energy ranges for the UK in kWh (Scenarios 1, 2 and 3)

	Scenario 1		Scenario 2		Scenario 3	
UK cities	**D=0.5%, U=8.89%**		**D=0.5%, U=8.37%**		**D=0.5%, U=7.81%**	
	μ+2σ	**μ-2σ**	**μ+2σ**	**μ-2σ**	**μ+2σ**	**μ-2σ**
Aberdeen	69366	51717	68848	52235	68296	52787
Dundee	75552	56329	74988	56893	74387	57495
Edinburgh	72071	53734	71533	54272	70959	54845
Glasgow	66152	49321	65658	49814	65131	50341
Newcastle	70973	52915	70443	53445	69878	54010
Belfast	70464	52535	69938	53061	69377	53623
Bradford	68964	51417	68449	51932	67900	52481
Manchester	68241	50878	67731	51388	67188	51931
Liverpool	72472	54033	71931	54574	71354	55151
Nottingham	72419	53993	71878	54534	71302	55110
Norwich	75633	56389	75068	56954	74466	57556
Birmingham	73597	54872	73048	55421	72462	56007
Cambridge	77347	57667	76769	58245	76153	58861
Oxford	76490	57028	75919	57599	75310	58208
Southend	81444	60722	80836	61330	80188	61979
London	76972	57388	76397	57962	75784	58575
Cardiff	75311	56150	74749	56712	74149	57312
Brighton	88515	65994	87854	66655	87149	67359
Bournemouth	82971	61860	82352	62480	81691	63141
Plymouth	85890	64037	85249	64678	84565	65362

Table J2: Lifetime energy ranges for the UK in kWh (Scenarios 4, 5 and 6)

	Scenario 4		Scenario 5		Scenario 6	
UK cities	**D=1%, U=8.89%**		**D=1%, U=8.37%**		**D=1%, U=7.81%**	
	μ+2σ	**μ-2σ**	**μ+2σ**	**μ-2σ**	**μ+2σ**	**μ-2σ**
Aberdeen	65157	47508	64639	48026	64087	48578
Dundee	70968	51745	70404	52309	69803	52911
Edinburgh	67698	49361	67160	49899	66586	50473
Glasgow	62138	45307	61644	45801	61118	46327
Newcastle	66666	48609	66137	49138	65571	49704
Belfast	66188	48260	65662	48786	65101	49347
Bradford	64780	47233	64265	47748	63716	48297
Manchester	64100	46738	63591	47247	63048	47790
Liverpool	68075	49636	67534	50177	66957	50754
Nottingham	68025	49599	67484	50140	66908	50716
Norwich	71044	51800	70479	52365	69877	52967
Birmingham	69132	50406	68582	50956	67996	51542
Cambridge	72654	52974	72076	53552	71460	54168
Oxford	71849	52387	71278	52958	70669	53567
Southend	76503	55781	75895	56389	75246	57037
London	72302	52717	71727	53292	71114	53905
Cardiff	70742	51580	70180	52142	69580	52742
Brighton	83144	60623	82484	61284	81779	61989
Bournemouth	77937	56826	77317	57446	76657	58106
Plymouth	80679	58826	80038	59467	79354	60151

Table J3: Lifetime energy ranges for India in kWh (Scenarios 1, 2 and 3)

	Scenario 1		Scenario 2		Scenario 3	
Indian cities	**D=1%, U=9.75%**		**D=1%, U=8.89%**		**D=1%, U=8.37%**	
	μ+2σ	**μ-2σ**	**μ+2σ**	**μ-2σ**	**μ+2σ**	**μ-2σ**
Srinagar	117976	83386	116452	84909	115527	85835
Nangal	125291	88555	123673	90173	122690	91156
Shimla	115172	81404	113685	82891	112782	83795
Chandigarh	123175	87060	121584	88651	120618	89617
Dehradun	120983	85511	119421	87074	118472	88023
Hissar	125010	88357	123396	89972	122415	90952
New Delhi	123634	87385	122037	88981	121067	89951
Dibrugarh	101180	71515	99874	72821	99080	73615
Gangtok	103755	73334	102415	74674	101601	75488
Itanagar	100263	70866	98968	72161	98182	72947
Jaipur	127559	90159	125911	91806	124911	92807
Lucknow	119989	84809	118440	86358	117498	87300
Kanpur	120754	85349	119195	86908	118247	87856
Kohima	90425	63913	89258	65080	88548	65790
Patna	118307	83620	116779	85148	115851	86076
Shillong	93101	65804	91899	67006	91169	67737
Imphal	108062	76378	106666	77774	105819	78621
Agartala	108826	76919	107421	78324	106567	79178
Aizawl	111146	78558	109710	79993	108838	80865
Ranchi	115351	81530	113861	83020	112956	83925
Bhopal	122283	86430	120704	88009	119745	88968
Ahmadabad	126361	89312	124729	90944	123738	91935
Kolkata	112879	79783	111421	81241	110535	82126
Raipur	119607	84538	118062	86083	117124	87021
Daman	123914	87583	122314	89183	121342	90155
Bhubaneswar	113006	79873	111547	81332	110660	82219
Silvassa	121213	85673	119647	87239	118696	88190
Mumbai	120372	85079	118817	86633	117873	87578
Hyderabad	120346	85061	118792	86615	117848	87559
Panjim	120830	85403	119270	86963	118322	87911
Chennai	119174	84232	117635	85771	116700	86706
Bangalore	121085	85583	119522	87147	118572	88097
Pondicherry	120423	85115	118867	86670	117923	87615
Port Blair	106252	75099	104880	76471	104047	77305
Kavaratti	117543	83079	116025	84597	115103	85519
Trivandrum	118715	83908	117182	85441	116251	86372

Table J4: Lifetime energy ranges for India in kWh (Scenarios 4, 5 and 6)

	Scenario 4		Scenario 5		Scenario 6	
Indian cities	**D=3%, U=9.75%**		**D=3%, U=8.89%**		**D=3%, U=8.37%**	
	μ+2σ	**μ-2σ**	**μ+2σ**	**μ-2σ**	**μ+2σ**	**μ-2σ**
Srinagar	87887	53297	86364	54821	85438	55746
Nangal	93337	56601	91719	58219	90736	59202
Shimla	85799	52031	84312	53518	83408	54421
Chandigarh	91761	55646	90170	57237	89204	58203
Dehradun	90128	54656	88565	56218	87616	57167
Hissar	93128	56475	91513	58089	90533	59070
New Delhi	92102	55853	90506	57450	89536	58420
Dibrugarh	75375	45710	74069	47016	73275	47810
Gangtok	77293	46872	75953	48212	75139	49026
Itanagar	74692	45295	73397	46590	72611	47376
Jaipur	95026	57626	93379	59274	92378	60274
Lucknow	89387	54207	87838	55756	86896	56698
Kanpur	89957	54552	88398	56111	87450	57059
Kohima	67363	40851	66196	42018	65486	42728
Patna	88134	53447	86606	54975	85678	55903
Shillong	69357	42060	68155	43262	67424	43992
Imphal	80502	48818	79106	50214	78259	51061
Agartala	81071	49164	79666	50569	78812	51423
Aizawl	82799	50211	81364	51647	80492	52519
Ranchi	85932	52111	84442	53601	83537	54506
Bhopal	91096	55243	89517	56822	88558	57781
Ahmadabad	94134	57085	92502	58717	91511	59708
Kolkata	84090	50994	82632	52452	81747	53338
Raipur	89103	54034	87558	55579	86620	56517
Daman	92311	55980	90711	57580	89739	58552
Bhubaneswar	84185	51052	82726	52511	81839	53398
Silvassa	90299	54759	88733	56325	87782	57276
Mumbai	89672	54379	88118	55934	87173	56878
Hyderabad	89653	54368	88099	55922	87155	56866
Panjim	90014	54587	88454	56147	87506	57095
Chennai	88780	53838	87241	55377	86306	56312
Bangalore	90204	54702	88640	56265	87690	57215
Pondicherry	89710	54402	88155	55958	87210	56902
Port Blair	79154	48001	77782	49373	76948	50206
Kavaratti	87565	53101	86047	54619	85125	55541
Trivandrum	88438	53631	86905	55164	85974	56095

Appendix K: LCOE ranges for all the cities-Net PV cost

Table K1: LCOE ranges for the UK cities-Scenario 2 (Financial Cases 1, 2 and 3)

Net PV Cost for the UK cities						
LCOE ranges (£/kWh), Scenario 2 (D=0.5%, U=8.37%)						
UK cities	Financial Case 1		Financial Case 2		Financial Case 3	
	min	max	min	max	min	max
Aberdeen	0.1164	0.1534	0.1277	0.1683	0.1083	0.1428
Dundee	0.1069	0.1409	0.1172	0.1545	0.0994	0.1311
Edinburgh	0.1120	0.1477	0.1229	0.1619	0.1043	0.1374
Glasgow	0.1221	0.1609	0.1339	0.1764	0.1136	0.1497
Newcastle	0.1138	0.1500	0.1248	0.1644	0.1059	0.1395
Belfast	0.1146	0.1510	0.1257	0.1656	0.1066	0.1405
Bradford	0.1171	0.1543	0.1284	0.1692	0.1089	0.1436
Manchester	0.1183	0.1560	0.1298	0.1710	0.1101	0.1451
Liverpool	0.1114	0.1469	0.1222	0.1610	0.1037	0.1366
Nottingham	0.1115	0.1470	0.1223	0.1612	0.1037	0.1367
Norwich	0.1068	0.1407	0.1171	0.1543	0.0993	0.1309
Birmingham	0.1097	0.1446	0.1203	0.1586	0.1021	0.1346
Cambridge	0.1044	0.1376	0.1145	0.1509	0.0971	0.1280
Oxford	0.1056	0.1391	0.1158	0.1526	0.0982	0.1295
Southend	0.0991	0.1307	0.1087	0.1433	0.0923	0.1216
London	0.1049	0.1383	0.1150	0.1516	0.0976	0.1287
Cardiff	0.1072	0.1413	0.1176	0.1550	0.0998	0.1315
Brighton	0.0912	0.1202	0.1000	0.1319	0.0849	0.1119
Bournemouth	0.0973	0.1283	0.1067	0.1407	0.0906	0.1194
Plymouth	0.0940	0.1239	0.1031	0.1359	0.0875	0.1153

Table K2: LCOE ranges for the UK cities-Scenario 2 (Financial Cases 5 and 6)

Net PV Cost for the UK cities				
LCOE ranges (£/kWh), Scenario 2 (D=0.5%, U=8.37%)				
UK cities	Financial Case 5		Financial Case 6	
	min	max	min	max
Aberdeen	0.1447	0.1908	0.1151	0.1517
Dundee	0.1329	0.1751	0.1056	0.1392
Edinburgh	0.1393	0.1836	0.1107	0.1460
Glasgow	0.1518	0.2000	0.1207	0.1590
Newcastle	0.1414	0.1864	0.1125	0.1482
Belfast	0.1425	0.1878	0.1133	0.1493
Bradford	0.1456	0.1919	0.1157	0.1525
Manchester	0.1471	0.1939	0.1170	0.1542
Liverpool	0.1385	0.1826	0.1101	0.1452
Nottingham	0.1386	0.1827	0.1102	0.1453
Norwich	0.1327	0.1749	0.1055	0.1391
Birmingham	0.1364	0.1798	0.1084	0.1429
Cambridge	0.1298	0.1711	0.1032	0.1360
Oxford	0.1312	0.1730	0.1043	0.1375
Southend	0.1233	0.1625	0.0980	0.1292
London	0.1304	0.1719	0.1037	0.1367
Cardiff	0.1333	0.1757	0.1060	0.1397
Brighton	0.1134	0.1495	0.0902	0.1189
Bournemouth	0.1210	0.1595	0.0962	0.1268
Plymouth	0.1169	0.1541	0.0929	0.1225

Table K3: LCOE ranges for the UK cities-Scenario 5 (Financial Cases 1, 2 and 3)

Net PV Cost for the UK cities						
LCOE ranges (£/kWh), Scenario 5 (D=1%, U=8.37%)						
UK cities	Financial Case 1		Financial Case 2		Financial Case 3	
	min	max	min	max	min	max
Aberdeen	0.1240	0.1669	0.1360	0.1830	0.1154	0.1553
Dundee	0.1138	0.1532	0.1248	0.1680	0.1059	0.1426
Edinburgh	0.1193	0.1606	0.1309	0.1761	0.1110	0.1494
Glasgow	0.1300	0.1750	0.1426	0.1919	0.1210	0.1628
Newcastle	0.1212	0.1631	0.1329	0.1789	0.1128	0.1518
Belfast	0.1221	0.1643	0.1338	0.1801	0.1136	0.1529
Bradford	0.1247	0.1679	0.1368	0.1841	0.1160	0.1562
Manchester	0.1260	0.1696	0.1382	0.1860	0.1173	0.1578
Liverpool	0.1187	0.1597	0.1301	0.1752	0.1104	0.1486
Nottingham	0.1188	0.1598	0.1302	0.1753	0.1105	0.1487
Norwich	0.1137	0.1531	0.1247	0.1678	0.1058	0.1424
Birmingham	0.1169	0.1573	0.1281	0.1725	0.1087	0.1463
Cambridge	0.1112	0.1497	0.1219	0.1641	0.1035	0.1393
Oxford	0.1124	0.1513	0.1233	0.1660	0.1046	0.1408
Southend	0.1056	0.1421	0.1158	0.1559	0.0983	0.1322
London	0.1117	0.1504	0.1225	0.1649	0.1040	0.1399
Cardiff	0.1142	0.1537	0.1252	0.1685	0.1063	0.1430
Brighton	0.0972	0.1308	0.1065	0.1434	0.0904	0.1217
Bournemouth	0.1037	0.1395	0.1137	0.1530	0.0965	0.1298
Plymouth	0.1001	0.1348	0.1098	0.1478	0.0932	0.1254

Table K4: LCOE ranges for the UK cities-Scenario 5 (Financial Cases 5 and 6)

Net PV Cost for the UK cities				
LCOE ranges (£/kWh), Scenario 5 (D=1%, U=8.37%)				
UK cities	Financial Case 5		Financial Case 6	
	min	max	min	max
Aberdeen	0.1541	0.2075	0.1226	0.1650
Dundee	0.1415	0.1905	0.1125	0.1514
Edinburgh	0.1484	0.1997	0.1180	0.1588
Glasgow	0.1616	0.2176	0.1285	0.1730
Newcastle	0.1507	0.2028	0.1198	0.1612
Belfast	0.1517	0.2042	0.1206	0.1624
Bradford	0.1550	0.2087	0.1233	0.1659
Manchester	0.1567	0.2109	0.1246	0.1677
Liverpool	0.1475	0.1986	0.1173	0.1579
Nottingham	0.1477	0.1987	0.1174	0.1580
Norwich	0.1414	0.1903	0.1124	0.1513
Birmingham	0.1453	0.1955	0.1155	0.1555
Cambridge	0.1382	0.1861	0.1099	0.1479
Oxford	0.1398	0.1881	0.1111	0.1496
Southend	0.1313	0.1767	0.1044	0.1405
London	0.1389	0.1870	0.1104	0.1487
Cardiff	0.1420	0.1911	0.1129	0.1519
Brighton	0.1208	0.1626	0.0960	0.1293
Bournemouth	0.1289	0.1735	0.1025	0.1379
Plymouth	0.1245	0.1676	0.0990	0.1332

Table K5: LCOE ranges for the Indian cities-Scenario 2 (Financial Cases 1, 3 and 4)

Net PV Cost for the Indian cities						
LCOE ranges (£/kWh), Scenario 2 (D=1%, U=8.89%)						
Indian cities	**Financial Case 1**		**Financial Case 3**		**Financial Case 4**	
	min	**max**	**min**	**max**	**min**	**max**
Srinagar	0.0937	0.1285	0.0854	0.1171	0.0781	0.1072
Nangal	0.0882	0.1210	0.0804	0.1102	0.0736	0.1009
Shimla	0.0960	0.1316	0.0874	0.1199	0.0800	0.1098
Chandigarh	0.0897	0.1231	0.0818	0.1121	0.0748	0.1026
Dehradun	0.0914	0.1253	0.0832	0.1142	0.0762	0.1045
Hissar	0.0884	0.1213	0.0806	0.1105	0.0737	0.1011
New Delhi	0.0894	0.1226	0.0814	0.1117	0.0746	0.1022
Dibrugarh	0.1093	0.1498	0.0995	0.1365	0.0911	0.1249
Gangtok	0.1065	0.1461	0.0971	0.1331	0.0888	0.1218
Itanagar	0.1103	0.1512	0.1004	0.1377	0.0919	0.1261
Jaipur	0.0867	0.1189	0.0789	0.1083	0.0723	0.0991
Lucknow	0.0921	0.1264	0.0839	0.1151	0.0768	0.1054
Kanpur	0.0915	0.1256	0.0834	0.1144	0.0763	0.1047
Kohima	0.1223	0.1677	0.1114	0.1527	0.1019	0.1398
Patna	0.0934	0.1282	0.0851	0.1167	0.0779	0.1069
Shillong	0.1187	0.1629	0.1082	0.1483	0.0990	0.1358
Imphal	0.1023	0.1403	0.0932	0.1278	0.0853	0.1170
Agartala	0.1016	0.1393	0.0925	0.1269	0.0847	0.1162
Aizawl	0.0995	0.1364	0.0906	0.1243	0.0829	0.1137
Ranchi	0.0958	0.1314	0.0873	0.1197	0.0799	0.1096
Bhopal	0.0904	0.1240	0.0823	0.1129	0.0754	0.1034
Ahmadabad	0.0875	0.1200	0.0797	0.1093	0.0729	0.1000
Kolkata	0.0979	0.1343	0.0892	0.1223	0.0817	0.1120
Raipur	0.0924	0.1268	0.0842	0.1155	0.0771	0.1057
Daman	0.0892	0.1224	0.0813	0.1115	0.0744	0.1020
Bhubaneswar	0.0978	0.1342	0.0891	0.1222	0.0816	0.1119
Silvassa	0.0912	0.1251	0.0831	0.1139	0.0760	0.1043
Mumbai	0.0918	0.1260	0.0837	0.1147	0.0766	0.1050
Hyderabad	0.0919	0.1260	0.0837	0.1148	0.0766	0.1050
Panjim	0.0915	0.1255	0.0833	0.1143	0.0763	0.1046
Chennai	0.0928	0.1272	0.0845	0.1159	0.0773	0.1061
Bangalore	0.0913	0.1252	0.0832	0.1141	0.0761	0.1044
Pondicherry	0.0918	0.1259	0.0836	0.1147	0.0765	0.1050
Port Blair	0.1040	0.1427	0.0948	0.1300	0.0867	0.1190
Kavaratti	0.0940	0.1290	0.0857	0.1175	0.0784	0.1075
Trivandrum	0.0931	0.1277	0.0848	0.1163	0.0776	0.1065

Table K6: LCOE ranges for the Indian cities-Scenario 5 (Financial Cases 1, 3 and 4)

Net PV Cost for the Indian cities						
LCOE ranges (£/kWh), Scenario 5 (D=3%, U=8.89%)						
Indian cities	Financial Case 1		Financial Case 3		Financial Case 4	
	min	max	min	max	min	max
Srinagar	0.1263	0.1990	0.1151	0.1813	0.1053	0.1660
Nangal	0.1190	0.1874	0.1084	0.1707	0.0992	0.1563
Shimla	0.1294	0.2039	0.1179	0.1857	0.1079	0.1700
Chandigarh	0.1210	0.1906	0.1102	0.1737	0.1009	0.1590
Dehradun	0.1232	0.1941	0.1122	0.1768	0.1027	0.1618
Hissar	0.1192	0.1878	0.1086	0.1711	0.0994	0.1566
New Delhi	0.1206	0.1899	0.1098	0.1730	0.1005	0.1584
Dibrugarh	0.1473	0.2321	0.1342	0.2114	0.1228	0.1935
Gangtok	0.1437	0.2263	0.1309	0.2062	0.1198	0.1887
Itanagar	0.1487	0.2342	0.1354	0.2133	0.1240	0.1953
Jaipur	0.1169	0.1841	0.1064	0.1677	0.0974	0.1535
Lucknow	0.1242	0.1957	0.1132	0.1783	0.1036	0.1632
Kanpur	0.1234	0.1945	0.1124	0.1771	0.1029	0.1621
Kohima	0.1648	0.2597	0.1502	0.2366	0.1374	0.2165
Patna	0.1260	0.1985	0.1148	0.1808	0.1051	0.1655
Shillong	0.1601	0.2522	0.1458	0.2298	0.1335	0.2103
Imphal	0.1379	0.2173	0.1256	0.1979	0.1150	0.1812
Agartala	0.1370	0.2158	0.1248	0.1966	0.1142	0.1799
Aizawl	0.1341	0.2113	0.1222	0.1925	0.1118	0.1762
Ranchi	0.1292	0.2036	0.1177	0.1854	0.1077	0.1697
Bhopal	0.1219	0.1920	0.1110	0.1749	0.1016	0.1601
Ahmadabad	0.1180	0.1858	0.1075	0.1693	0.0984	0.1550
Kolkata	0.1321	0.2080	0.1203	0.1895	0.1101	0.1735
Raipur	0.1246	0.1963	0.1135	0.1788	0.1039	0.1637
Daman	0.1203	0.1895	0.1096	0.1726	0.1003	0.1580
Bhubaneswar	0.1319	0.2078	0.1202	0.1893	0.1100	0.1733
Silvassa	0.1230	0.1937	0.1120	0.1765	0.1025	0.1615
Mumbai	0.1238	0.1951	0.1128	0.1777	0.1033	0.1627
Hyderabad	0.1239	0.1951	0.1128	0.1777	0.1033	0.1627
Panjim	0.1234	0.1943	0.1124	0.1770	0.1029	0.1620
Chennai	0.1251	0.1970	0.1139	0.1795	0.1043	0.1643
Bangalore	0.1231	0.1939	0.1121	0.1767	0.1026	0.1617
Pondicherry	0.1238	0.1950	0.1128	0.1776	0.1032	0.1626
Port Blair	0.1403	0.2210	0.1278	0.2013	0.1170	0.1843
Kavaratti	0.1268	0.1998	0.1155	0.1820	0.1057	0.1666
Trivandrum	0.1256	0.1978	0.1144	0.1802	0.1047	0.1649